



8-2000

An Evaluation of Relationships Among Streamflow and Selected Water Quality Parameters in a Forested High-Altitude Watershed

Molly Sarah McCann
University of Tennessee - Knoxville

Follow this and additional works at: https://trace.tennessee.edu/utk_gradthes



Part of the [Engineering Commons](#)

Recommended Citation

McCann, Molly Sarah, "An Evaluation of Relationships Among Streamflow and Selected Water Quality Parameters in a Forested High-Altitude Watershed. " Master's Thesis, University of Tennessee, 2000.
https://trace.tennessee.edu/utk_gradthes/3267

This Thesis is brought to you for free and open access by the Graduate School at TRACE: Tennessee Research and Creative Exchange. It has been accepted for inclusion in Masters Theses by an authorized administrator of TRACE: Tennessee Research and Creative Exchange. For more information, please contact trace@utk.edu.

To the Graduate Council:

I am submitting herewith a thesis written by Molly Sarah McCann entitled "An Evaluation of Relationships Among Streamflow and Selected Water Quality Parameters in a Forested High-Altitude Watershed." I have examined the final electronic copy of this thesis for form and content and recommend that it be accepted in partial fulfillment of the requirements for the degree of Master of Science, with a major in Environmental Engineering.

James L. Smoot, Major Professor

We have read this thesis and recommend its acceptance:

R. Bruce Robinson, Bruce A. Tschantz

Accepted for the Council:

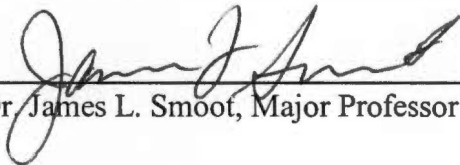
Carolyn R. Hodges

Vice Provost and Dean of the Graduate School

(Original signatures are on file with official student records.)

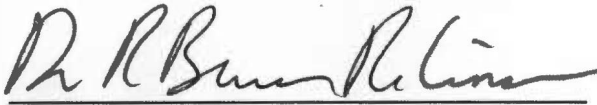
To the Graduate Council:

I am submitting herewith a thesis written by Molly Sarah McCann entitled "An Evaluation of Relationships Among Streamflow and Selected Water Quality Parameters in a Forested, High-Altitude Watershed." I have examined the final copy of this thesis for form and content and recommend that it be accepted in partial fulfillment of the requirements for the degree of Master of Science, with a major in Environmental Engineering.

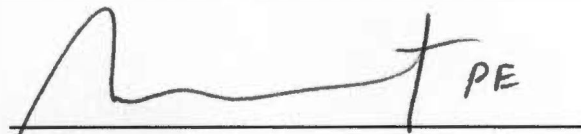


Dr. James L. Smoot, Major Professor

We have read this thesis and recommend its acceptance:

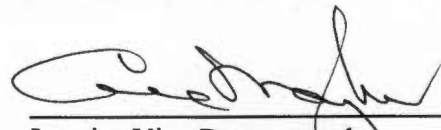


Dr. R. Bruce Robinson



Dr. Bruce A. Tschantz

Accepted for the Council:



Interim Vice Provost and
Dean of The Graduate School

**AN EVALUATION OF RELATIONSHIPS AMONG
STREAMFLOW AND SELECTED WATER QUALITY
PARAMETERS IN A FORESTED, HIGH-ALTITUDE
WATERSHED**

A Thesis
Presented for the
Master of Science
Degree
The University of Tennessee, Knoxville

Molly Sarah McCann
August 2000

ACKNOWLEDGMENTS

I would like to thank the Department of Civil and Environmental Engineering for providing an excellent learning environment for both undergraduate and graduate work. I would also like to thank my master's committee, Drs. James Smoot, Bruce Robinson, and Bruce Tschantz for their guidance and direction. I would particularly like to thank my major advisor, Dr. Smoot, for encouraging me to pursue a master's degree and for providing "real-world" advice.

Further thanks go to my co-workers on the Smoky Mountains Project, John Shubzda and Glenn Harwell, for conducting field and lab work and for sharing information, and to past scientists on this project for their research and data collection. In addition, I would like to thank Bob Muenchen with the Statistical Consulting Center for his assistance with analyzing large data sets.

Principal financial support for this project is provided through a cooperative agreement between the National Park Service and The University of Tennessee, Knoxville (contract number 1443-CA-5460-98-006--Amendment 3). Additional personal financial support was provided by the University of Tennessee, Knoxville, Graduate School Hilton A. Smith Fellowship Fund and the American Society of Civil Engineers Freeman Fellowship Fund and is gratefully acknowledged.

ABSTRACT

A long-term water quality monitoring program has been established at the Noland Divide Watershed (NDW) in the Great Smoky Mountains National Park. The Noland Divide Watershed is a spruce fir-forested catchment which has been shown in previous research to receive some of the largest fluxes of atmospherically-deposited nitrogen and sulfur compounds in the world. Streamwater chemistry data from November 1991 through August 1998 for two streams, the "northeast" (NE) stream and "southwest" (SW) stream, were examined to note results of this deposition on water quality. Automatic monitoring equipment on both streams measure and record pH, conductivity, and temperature readings every 15 minutes, and Stevens recorders in 3-foot H-flumes record stage height which corresponds to a flow rate every 15 minutes. In addition, grab samples were collected weekly and analyzed for pH, conductivity, acid neutralizing capacity (ANC), major anions and cations, aluminum, and silica. Experimental analysis was conducted to describe conditions, detect long-term and/or seasonal trends in water quality, and to relate water quality constituents with the watershed hydrology. In addition, parametric regression models were formed to note influence of several variables such as flow, time, seasonality, pH, and conductivity on analyte loads and concentrations and to test several sampling scenarios that may more-efficiently represent the water quality at NDW. It was determined from the analysis that high flow events are not well represented by the weekly grab samples and therefore water quality during these flow conditions is not fully understood. The SW stream is controlled more by groundwater inputs than is the NE stream, and the water quality characteristics of the two streams are statistically different ($p < 0.05$) with respect to all analyte concentrations except ammonium. Increased sulfate

concentrations (+1.08 $\mu\text{eq/L}$ in SW, +1.32 $\mu\text{eq/L}$ in NE) were observed in the streams for each 1-inch increase of precipitation that occurs since the previous sampling visit. Decreased sulfate concentrations (-0.65 $\mu\text{eq/L}$ in SW and -0.67 $\mu\text{eq/L}$ in NE) were observed in the streams for each 1-day increase in consecutive dry days prior to sampling. Nitrate concentrations observed in the streams were not significantly influenced by precipitation prior to sampling, but decreased concentrations (-0.50 $\mu\text{eq/L}$ in SW and -0.54 $\mu\text{eq/L}$ in NE) were observed for each 1-day increase in consecutive dry days prior to sampling. Parametric regression models show that chloride, sodium, aluminum, and ammonium loads and concentrations are increasing over time, nitrate and silica loads and concentrations are decreasing over time, and sulfate, potassium, and hydrogen ion loads and concentrations are not changing over time. All analyte loads and concentrations except silica are significantly ($p < 0.10$) influenced by seasonality. Parametric regression models also show that grab samples collected on a bi-weekly or tri-weekly frequency would be as statistically adequate for characterizing water quality concentrations and loads as are samples collected on a weekly basis.

TABLE OF CONTENTS

| | <u>Page</u> |
|--|-------------|
| CHAPTER I. Introduction | 1 |
| Background on the Great Smoky Mountains National Park | 1 |
| Development of the Noland Divide Watershed Research Site | 3 |
| Summary of Data Types and Methods of Analysis | 8 |
| Purpose and Scope | 10 |
| CHAPTER II. Review of the Literature | 12 |
| Geochemistry of Natural Waters as a Result of Atmospheric Deposition | 12 |
| Temporal Trends | 15 |
| Hydrologic Influences | 19 |
| Use of Parametric Regression Models | 23 |
| CHAPTER III. Analysis of Flow Data | 28 |
| Data Sources | 28 |
| Methods of Analysis | 28 |
| Results | 30 |
| Continuous Data | 30 |
| Weekly Data | 30 |
| Discussion | 38 |
| Trends | 38 |
| SW vs. NE Stream Conditions | 39 |
| CHAPTER IV. Temporal Variability in Water Quality | 41 |
| Data Sources | 41 |
| Methods of Analysis | 41 |
| Results | 43 |
| Continuous Data | 43 |
| Weekly Data | 55 |
| Discussion | 85 |
| Trends | 85 |
| SW vs. NE Stream Conditions | 91 |
| CHAPTER V. Hydrologic Influences on Water Quality | 93 |
| Data Sources | 93 |
| Methods of Analysis | 93 |
| Results | 95 |
| Statistical and Graphical Analysis of Analytes Versus Flow and Flow Regimes | 95 |

| | |
|---|-----|
| Analyte Responses During a Storm Event, October 31 - November 5, 1995 | 110 |
| Analysis of Relationships between Sulfate and Nitrate Concentrations and Precipitation | 122 |
| Discussion | 127 |
| CHAPTER VI. Parametric Modeling of Water Quality Constituent Concentrations and Loads | 131 |
| Data Sources | 131 |
| Methods of Analysis | 132 |
| Previous Load Calculation Method | 132 |
| Multiple Linear Regression Method, Load Model | 133 |
| 1 st Trial | 133 |
| 2 nd Trial | 135 |
| 3 rd Trial | 136 |
| Multiple Linear Regression Method, Concentration Model | 137 |
| Results | 138 |
| Load Regression Model | 138 |
| Concentration Regression Model | 142 |
| Discussion | 147 |
| CHAPTER VII. Sampling Strategy Testing | 149 |
| Data Sources | 149 |
| Methods of Analysis | 149 |
| Results | 151 |
| Loads Comparison | 151 |
| Concentrations Comparison | 158 |
| Discussion | 161 |
| CHAPTER VIII. Summary of Major Conclusions | 164 |
| CHAPTER IX. Recommendations for Future Research | 171 |
| Sampling | 171 |
| Equipment | 171 |
| Analysis/Research | 172 |
| REFERENCES | 173 |
| APPENDIX | 179 |
| VITA | 198 |

LIST OF TABLES

| <u>Table</u> | <u>Page</u> |
|---|--------------------|
| 1-1. Summary of analyzed data. | 9 |
| 2-1. Proposed ecological consequences of low surface water pH. | 16 |
| 3-1. Descriptive statistics for continuous and weekly streamflow data for both streamlets, 1991-1998. | 31 |
| 4-1. Statistical differences in weekly sample analytes by season for the SW streamlet. | 68 |
| 4-2. Statistical differences in weekly sample analytes by season for the NE streamlet. | 69 |
| 4-3. Coefficients of the concentration regression model with seasonality only and times of the year when seasonality function reaches maximum and minimum values. | 78 |
| 4-4. Coefficients of the load regression model with seasonality only and times of the year when seasonality function reaches maximum and minimum values. | 78 |
| 4-5. Descriptive statistics of weekly sample data for the SW streamlet, 1991-1998. | 82 |
| 4-6. Descriptive statistics of weekly sample data for the NE streamlet, 1991-1998. | 83 |

| <u>Table</u> | <u>Page</u> |
|---|--------------------|
| 4-7. Statistical differences between NE and SW weekly sample streamflow and water quality. | 84 |
| 4-8. Pearson correlation coefficients for weekly sample constituents in the SW streamlet. | 86 |
| 4-9. Pearson correlation coefficients for weekly sample constituents in the NE streamlet. | 87 |
| 5-1. Statistical differences in weekly sample analytes by location on the hydrograph for the SW stream. | 108 |
| 5-2. Statistical differences in weekly sample analytes by location on the hydrograph for the NE stream. | 109 |
| 5-3. Soil solution water quality data from 1992-1998 for three soil horizons. | 111 |
| 5-4. Descriptive statistics for constituents in the NE streamlet during a storm event, October 31 - November 5, 1995. | 121 |
| 5-5. Descriptive statistics for constituents in the SW streamlet during a storm event, October 31 - November 5, 1995. | 121 |
| 6-1. 1 st trial de-transformed regression equations for the SW streamlet based on flow and conductivity. | 139 |
| 6-2. 1 st trial de-transformed regression equations for the SW streamlet based on flow only. | 139 |
| 6-3. Summary of 3 rd trial load regression model for the SW streamlet. | 140 |

| <u>Table</u> | <u>Page</u> |
|---|--------------------|
| 6-4. 3 rd model load regression equations for the SW streamlet. | 141 |
| 6-5. Comparison of mass transport results from the regression and “average” methods for 1993 and 1994. | 143 |
| 6-6. Summary of concentration regression model for the SW streamlet. | 145 |
| 6-7. Concentration regression equations for the SW streamlet. | 146 |
| 7-1. Statistical differences in load results obtained from different sampling schemes in comparison with the weekly scheme, assuming related samples. | 157 |
| 7-2. Statistical differences in load results obtained from different sampling schemes in comparison with the weekly scheme, assuming independent samples. | 157 |
| 7-3. Statistical differences in concentration distributions based on sampling scheme in comparison with the weekly scheme. | 162 |
| A-1. Summary of characteristics of the Noland Divide Watershed. | 180 |
| A-2. Load regression equations for the SW streamlet, bi-weekly sampling strategy. | 192 |
| A-3. Load regression equations for the SW streamlet, tri-weekly sampling strategy. | 193 |
| A-4. Load regression equations for the SW streamlet, monthly sampling strategy. | 194 |

| <u>Table</u> | <u>Page</u> |
|---|--------------------|
| A-5. Concentration regression equations for the SW streamlet, bi-weekly sampling strategy. | 195 |
| A-6. Concentration regression equations for the SW streamlet, tri-weekly sampling strategy. | 196 |
| A-7. Concentration regression equations for the SW streamlet, monthly sampling strategy. | 197 |

LIST OF FIGURES

| <u>Figure</u> | <u>Page</u> |
|---|-------------|
| 1-1. Location of the Great Smoky Mountains on the western edge of the Blue Ridge Physiographic Province. | 2 |
| 1-2. Atmospheric deposition fluxes of S and N across the IFS collection network. | 4 |
| 1-3. Schematic diagram of the Noland Divide Watershed. | 5 |
| 1-4. Schematic diagram of the Noland Divide stream monitoring station. | 7 |
| 3-1. Mean annual streamflow for the SW and NE streamlets from 15-minute data, 1991-1998. | 32 |
| 3-2. Mean monthly streamflow for the SW and NE streamlets from 15-minute data, 1991-1998. | 32 |
| 3-3. Streamflow duration and instantaneous streamflow at time of weekly sampling for the SW and NE streamlets, winter season 1991-1998. | 33 |
| 3-4. Streamflow duration and instantaneous streamflow at time of weekly sampling for the SW and NE streamlets, spring season 1991-1998. | 34 |
| 3-5. Streamflow duration and instantaneous streamflow at time of weekly sampling for the SW and NE streamlets, summer season 1991-1998. | 35 |
| 3-6. Streamflow duration and instantaneous streamflow at time of weekly sampling for the SW and NE streamlets, fall season 1991-1998. | 36 |

| <u>Figure</u> | <u>Page</u> |
|--|--------------------|
| 3-7. Distribution of weekly instantaneous streamflow based on location on hydrograph for the SW streamlet. | 37 |
| 3-8. Distribution of weekly instantaneous streamflow based on location on hydrograph for the NE streamlet. | 37 |
| 4-1. Distributions of continuous pH data by year for the periods 1991-1994 and 1995-1998 for the SW streamlet. | 44 |
| 4-2. Distributions of continuous pH data by season for the periods 1991-1994 and 1995-1998 for the SW streamlet. | 46 |
| 4-3. Distributions of continuous pH data by month for the periods 1991-1994 and 1995-1998 for the SW streamlet. | 47 |
| 4-4. Distributions of continuous conductivity data by year for the periods 1991-1994 and 1995-1998 for the SW streamlet. | 48 |
| 4-5. Distributions of continuous conductivity data by season for the periods 1991-1994 and 1995-1998 for the SW streamlet. | 49 |
| 4-6. Distributions of continuous conductivity data by month for the periods 1991-1994 and 1995-1998 for the SW streamlet. | 50 |
| 4-7. Overall distributions of continuous pH and conductivity data by year for 1998 for the NE streamlet. | 51 |
| 4-8. Distributions of continuous pH and conductivity data by season for 1998 for the NE streamlet. | 52 |

| <u>Figure</u> | <u>Page</u> |
|---|--------------------|
| 4-9. Distributions of continuous pH and conductivity data by month for 1998 for the NE streamlet. | 53 |
| 4-10. Distributions of weekly sample constituent concentrations by year for the SW and NE streamlets, 1991-1998. | 56 |
| 4-11. Distributions of weekly sample constituent concentrations by season for the SW and NE streamlets, 1991-1998. | 62 |
| 4-12. Distributions of weekly sample constituent concentrations by month for the SW and NE streamlets, 1991-1998. | 72 |
| 4-13. Seasonal sine/cosine wave functions for nitrate and hydrogen ion concentration in the SW stream. | 79 |
| 5-1. Distributions of weekly sample constituent concentrations by location on the hydrograph for the SW streamlet, 1991-1998. | 96 |
| 5-2. Distributions of weekly sample constituent concentrations by location on the hydrograph for the NE streamlet, 1991-1998. | 102 |
| 5-3. Precipitation and streamflow response during a storm event, October 31 - November 5, 1995, for the SW and NE streamlets. | 113 |
| 5-4. pH and streamflow response during a storm event, October 31 - November 5, 1995, for the SW and NE streamlets. | 114 |
| 5-5. Conductivity and streamflow response during a storm event, October 31 - November 5, 1995, for the SW and NE streamlets. | 115 |

| <u>Figure</u> | <u>Page</u> |
|--|--------------------|
| 5-6. Acid neutralization capacity response during a storm event, October 31 - November 5, 1995, for the NE streamlet. | 116 |
| 5-7. Nitrate and sulfate response during a storm event, October 31 - November 5, 1995, for the NE streamlet. | 117 |
| 5-8. Ammonium, sodium, chloride, and potassium response during a storm event, October 31 - November 5, 1995, for the NE streamlet. | 118 |
| 5-9. Aluminum and silica response during a storm event, October 31 - November 5, 1995, for the NE streamlet. | 119 |
| 5-10. Relationship between weekly sample sulfate concentrations and precipitation since last sampling period for the SW and NE streams, 1991-1995. | 123 |
| 5-11. Relationship between weekly sample nitrate concentrations and precipitation since last sampling period for the SW and NE streams, 1991-1995. | 124 |
| 5-12. Distributions of weekly sample sulfate concentrations and associated regression equations for the SW and NE streamlets based on number of consecutive dry days preceding sampling. | 125 |
| 5-13. Distributions of weekly sample nitrate concentrations and associated regression equations for the SW and NE streamlets based on number of consecutive dry days preceding sampling. | 126 |
| 7-1. Comparison of monthly chloride loads during a test period (1993-1994) based on weekly, bi-weekly, tri-weekly, and monthly sampling schemes. | 152 |

| <u>Figure</u> | <u>Page</u> |
|---|-------------|
| 7-2. Comparison of monthly nitrate loads during a test period (1993-1994) based on weekly, bi-weekly, tri-weekly, and monthly sampling schemes. | 152 |
| 7-3. Comparison of monthly sulfate loads during a test period (1993-1994) based on weekly, bi-weekly, tri-weekly, and monthly sampling schemes. | 153 |
| 7-4. Comparison of monthly sodium loads during a test period (1993-1994) based on weekly, bi-weekly, tri-weekly, and monthly sampling schemes. | 153 |
| 7-5. Comparison of monthly ammonium loads during a test period (1993-1994) based on weekly, bi-weekly, tri-weekly, and monthly sampling schemes. | 154 |
| 7-6. Comparison of monthly potassium loads during a test period (1993-1994) based on weekly, bi-weekly, tri-weekly, and monthly sampling schemes. | 154 |
| 7-7. Comparison of monthly hydrogen ion loads during a test period (1993-1994) based on weekly, bi-weekly, tri-weekly, and monthly sampling schemes. | 155 |
| 7-8. Comparison of monthly aluminum loads during a test period (1993-1994) based on weekly, bi-weekly, tri-weekly, and monthly sampling schemes. | 155 |
| 7-9. Comparison of monthly silica loads during a test period (1993-1994) based on weekly, bi-weekly, tri-weekly, and monthly sampling schemes. | 156 |
| 7-10. Comparison of constituent concentration distributions based on weekly, bi-weekly, tri-weekly, and monthly sampling schemes. | 159 |
| A-1. Total annual precipitation at Noland Divide Watershed, 1991-1995. | 181 |
| A-2. Mean monthly precipitation at Noland Divide Watershed, 1991-1995. | 181 |

| <u>Figure</u> | <u>Page</u> |
|---|--------------------|
| A-3. Seasonal sine/cosine wave functions for analyte concentrations in the SW stream. | 182 |
| A-4. Seasonal sine/cosine wave functions for analyte instantaneous loads in the SW stream. | 186 |
| A-5. Sample hydrograph and baseflow separation procedure for assigning locations on the hydrograph when weekly samples are taken. | 191 |

CHAPTER I. INTRODUCTION

Background on the Great Smoky Mountains National Park

The Great Smoky Mountains National Park (GRSM) is the second largest National Park in the eastern United States. It comprises more than 220,000 hectares, and is located on the border of Tennessee and North Carolina in the Blue Ridge Physiographic Province (see Figure 1-1). It is the most-visited National Park, with over 9.3 million visitors in 1992 alone (Peine *et al.*, 1995). The GRSM is the largest temperate zone National Park in the southeastern United States, is noted for its biodiversity in plant and animal species. Vegetation types range from virgin areas of hemlock, hardwoods, and spruce-fir forests to areas that have been burned, logged, or farmed prior to establishment of the Park. Approximately 60,000 hectares of the Park have never been disturbed by burning, logging, or settlement, which makes the Park the largest undisturbed deciduous or coniferous forest-dominated landscape in the eastern United States (Delcourt and Delcourt, 1991). In addition, the Park contains approximately 1,200 species of native vascular plants, over 300 lichen species, over 800 species of moths and butterflies, over 2,200 species of macro-fungi, 60 species of mammals, 53 species of fish, 30 species of salamanders, over 325 species of aquatic insects, and numerous species of migratory birds (Ibid., 1991). The Park is also unique because of its extensive elevational range (260 m to 2,025 m) and geographical location. Though direct anthropogenic influences in the Park are limited primarily to automobile traffic and trail and facility use, the Park is affected by boundary encroachment and by air pollution from major population centers and large point-source emissions.

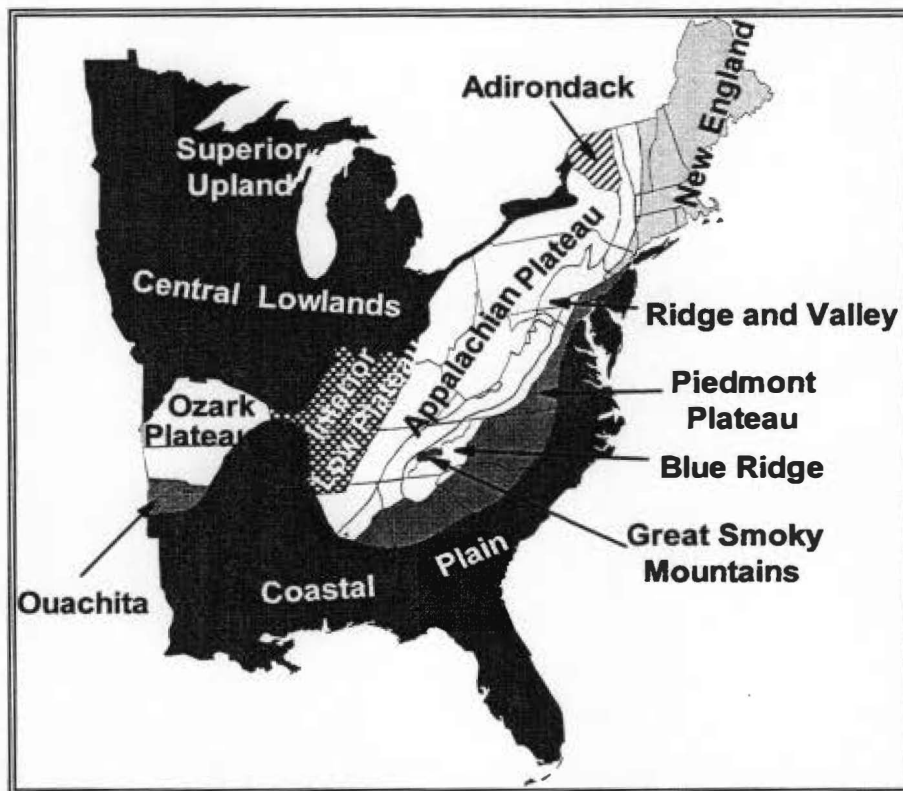


Figure 1-1. Location of the Great Smoky Mountains on the western edge of the Blue Ridge Physiographic Province.

Development of the Noland Divide Watershed Research Site

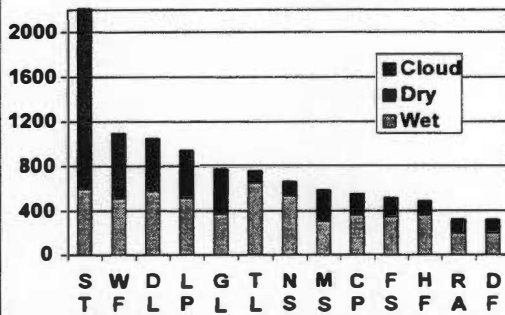
The Noland Divide Watershed (NDW) was chosen as a research site for the Integrated Forest Study (IFS) project from 1986 to 1989, which observed and quantified atmospheric deposition and nutrient cycling in over 17 watersheds internationally (Johnson and Lindberg, 1992). These studies showed that NDW received some of the highest rates of sulfur and nitrogen compound deposition of those watersheds studied (see Figure 1-2). In November 1991, a small watershed research project was established at the same site to examine long-term trends and relationships between atmospheric deposition and water quality. In cooperation with the National Park Service, faculty, staff, and students at the University of Tennessee, Knoxville, have been responsible for monitoring atmospheric deposition rates of acidic compounds, stream water quality and flow, and soil water chemistry.

The Noland Divide Watershed is a spruce fir-forested, high altitude watershed located along the main ridge of the Great Smoky Mountains, near Clingman's Dome (Lat. 35°34'N, Long. 83°28'W). A schematic diagram of the watershed is presented in Figure 1-3. Access to the watershed is possible from the Clingman's Dome Road and the Noland Divide Trail. The watershed comprises approximately 17.4 hectares of terrain with an elevational range of 1695 to 1940 meters. Geology is dominated by the Thunderhead Sandstone of the Great Smoky Group (Upper Proterozoic), which is made up of mainly quartz and potassic feldspar (King *et al.*, 1968). Overstory vegetation includes old-growth red spruce (200-300 years old) and some mature yellow birch, while understory vegetation includes Fraser fir, red spruce, blackberry, witch hobble, blueberry, mountain ash, and rhododendron (Johnson *et al.*, 1991). Soils are primarily Umbric

**Location of Integrated Forest Study Sites;
ST is Great Smokies spruce-fir at Noland Divide Watershed**



**Annual IFS S Deposition
(Eq·Ha⁻¹·Yr⁻¹)**



**Annual IFS N Deposition
(Eq·Ha⁻¹·Yr⁻¹)**

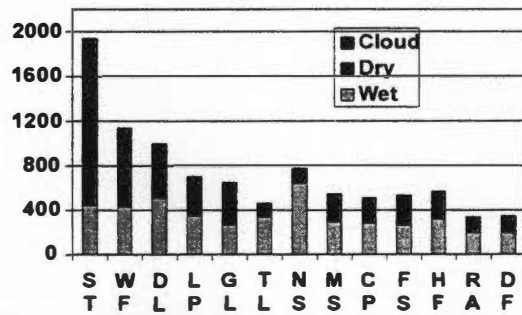


Figure 1-2. Atmospheric deposition fluxes of S and N across the IFS collection network. Data taken from Johnson and Lindberg (1992).

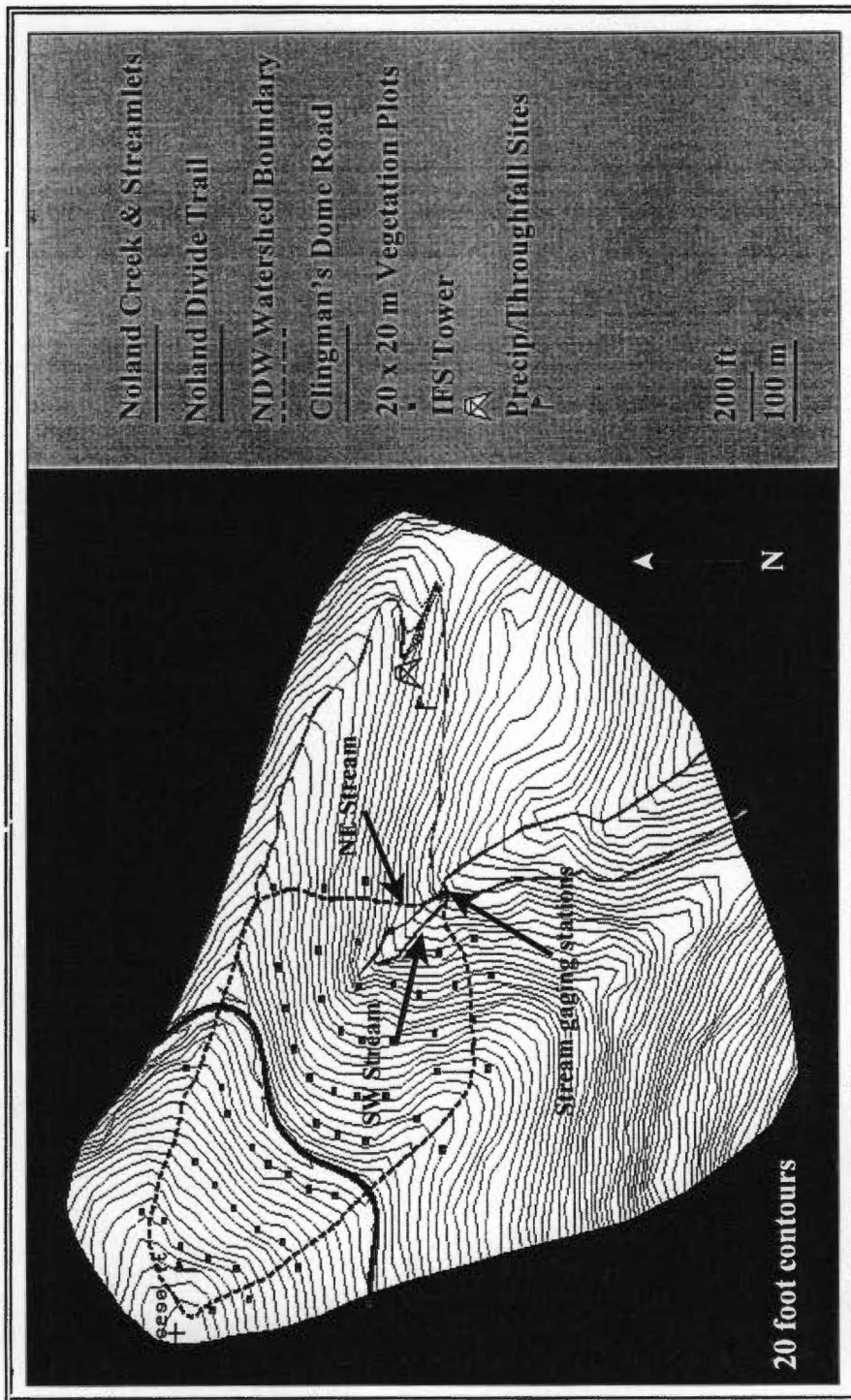


Figure 1-3. Schematic diagram of the Noland Divide Watershed.

Dystrochrepts formed from the Thunderhead Sandstone. The soil profile consists of a 4 cm thick Oi + Oe horizon of needles and leaves, a 4 cm thick Oa horizon of mucky humus, an 8 cm thick A horizon of dark, reddish-brown, mucky loam, a 27 cm thick Bw horizon of dark brown, sandy loam, a 35 cm thick Cb horizon of dark, yellowish-brown loam, a 20+ cm thick C horizon of olive-brown, loamy sand, and underlying sandstone bedrock (Johnson and Lindberg, 1992). A summary table of additional watershed characteristics can be found in the Appendix, Table A-1.

The NDW contains three main monitoring stations: an atmospheric deposition station with an open, wet-only precipitation collector and a throughfall collector (elevation 1740 m), a stream station monitoring two adjacent streams (1720 m), and a soil solution station with soil lysimeters in the A, Bw, and CB horizons (1740 m). Another atmospheric deposition monitoring station existed in the upper portions of the watershed (1920 m) from August 1993 to July 1996; it is no longer used. In addition, several 20 x 20m vegetation plots were established to study stand structure, biomass, and soil nutrient cycling. The focus of this thesis will be on the results of monitoring at the stream station. The stream station monitors stream water quality and flow in two streams, the "southwest" (SW) stream and "northeast" (NE) streams. A schematic diagram of the stream station is presented in Figure 1-4. Each stream is equipped with a 3-foot H-flume and Stevens Type F water level recorder for determining discharge from measured stage height and a Hydrolab unit (model no. 32001 H₂O) to monitor continuous pH, conductivity, and temperature. A Campbell Scientific CR-10 datalogger collects and stores data from both streams at a 15-minute interval; these data can be downloaded onto storage modules and be imported into spreadsheets for storage and analysis. The Hydrolab units are protected from weather and animal damage by

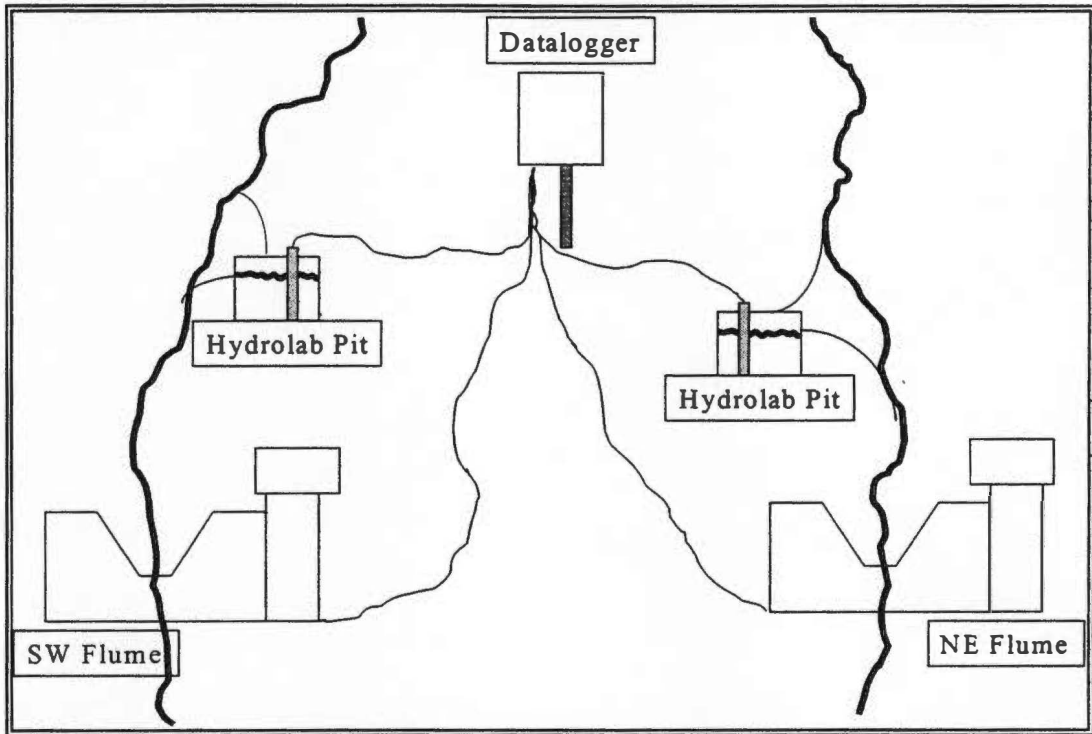


Figure 1-4. Schematic diagram of the Noland Divide stream monitoring station.

diverting stream water through a pipe into an adjacent plastic container or "pit", in which the hydrolab is stored. Stream water circulates in this container and then is channeled back into the stream through another pipe. It should be noted that the SW stream was outfitted with a Hydrolab in November 1991, but the NE stream was not outfitted until April 1998; therefore, a more complete record of continuous data exists for the SW.

Summary of Data Types and Methods of Analysis

Water quality monitoring at NDW is accomplished through continuous data and weekly grab sample data. A summary table of the different data types used in this research is presented in Table 1-1. The Hydrolab units on each stream make readings of pH, conductivity, and temperature every 15 minutes; the datalogger records this data and compiles daily totals throughout the week. The watershed is visited every week to collect four (4) grab samples for each stream. These grab samples are analyzed for pH, conductivity, ANC, chloride, nitrate, sulfate, sodium, ammonium, potassium, magnesium, calcium, aluminum, and silica. Each grab sample has been assigned a flow from the continuous data at the time the sample was taken in order to calculate loads of each water quality constituent out of the watershed. In addition, samples during a storm in 1995 have been collected and analyzed to examine constituent response during an extreme event. Daily precipitation data using a Belfort rain gage were collected from November 1991 through December 1995 and analyzed to detect relationships between nitrate and sulfate concentrations and precipitation prior to sampling.

Chemical analyses of all samples were performed by personnel in the Department of Forestry, Wildlife, and Fisheries at the University of Tennessee, Knoxville, from June 1991 to

Table 1-1. Summary of analyzed data.

| Data Type | Streams Included ? | Parameters Measured | Dates Measured | Sample Size (Data points) |
|--|---------------------------|--|--|--|
| Hydrolab data (15-minute data) | SW and NE | pH, conductivity, temperature | SW: November 1991 - August 1998 NE: April 1998 - August 1998 | SW: 233,473 for each parameter NE: 11,420 for each parameter |
| Weekly grab sample data | SW and NE | pH, conductivity, temperature, ANC, NO ₃ ⁻ , Cl ⁻ , SO ₄ ²⁻ , Ca ²⁺ , Mg ²⁺ , Na ⁺ , K ⁺ , NH ₄ ⁺ , Al, Si | November 1991 - August 1998 Al and Si only: July 1992 - June 1995 | 339 for each parameter for each stream Al and Si only: 167 for each parameter for each stream |
| Stage height/flow data (15-minute data) | SW and NE | stage height converted to streamflow | November 1991 - August 1998 | 233,473 for each stream |
| Storm event data | SW and NE | SW: pH, conductivity, temperature, flow NE: pH, conductivity, temperature, flow, ANC, NO ₃ ⁻ , Cl ⁻ , SO ₄ ²⁻ , Ca ²⁺ , Mg ²⁺ , Na ⁺ , K ⁺ , NH ₄ ⁺ , Al, Si | October 31 - November 5, 1995 | SW: 368 for each parameter NE: 58 for each parameter |
| Precipitation data | N/A | daily rainfall | November 1991 - December 1995 | 1,463 |

December 1998. After that period, the project and all field and analytical services were transferred to the Department of Civil and Environmental Engineering. A summary of procedures and protocols used for collection and analysis of samples can be found in the summary report "Assessment of Stream Water Quality and Atmospheric Deposition Rates at Selected Sites in the Great Smoky Mountains National Park, 1991-1998" by McCann *et al.* (2000).

Purpose and Scope

This thesis focuses on analysis of stream water quality of the SW and NE streams in the NDW. Though a substantial data set has formed since monitoring began in 1991, no extensive analysis on stream water quality had been performed or compared to results in other watersheds. As a result, these water quality data have now been analyzed to detect trends over time and in different flow regimes, to understand relationships between some analytes, precipitation, and dry period prior to sampling, and to formulate load and concentration regression models. The specific objectives of this thesis research are as follows:

1. To summarize trends seen in continuous and weekly stream sample data for the NE and SW streams over time--by month, season, year, and long-term.
2. To summarize trends seen in weekly sample data based on respective flow regimes.
3. To identify chemical "signals" associated with different flowpaths in the watershed (vadose zone, saturated zone, bedrock zone) in different flow regimes.

4. To determine whether there are significant differences in chemistry and flow between the NE and SW streams.
5. To determine whether observed water quality and hydrology fit well with the conceptual/projected watershed response determined from similar studies in other watersheds.
6. To develop multiple linear regression-based models for calculating loads in the SW stream and for understanding influences on constituent concentrations.
7. To evaluate different sampling strategies using regression-based models and propose a more-efficient sampling strategy, if possible.

CHAPTER II. REVIEW OF THE LITERATURE

Geochemistry of Natural Waters as a Result of Atmospheric Deposition

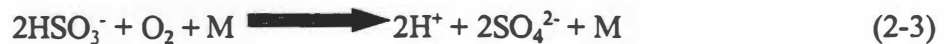
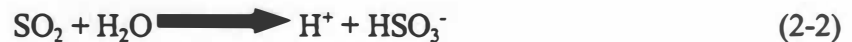
Large areas in North America and Europe have been documented as receiving significant amounts of atmospherically-deposited compounds, particularly sulfuric and nitric acids, as a result of the combustion of fossil fuels, automobile emissions, and the smelting of nonferrous metals (Drever, 1988). The main anionic components of acid deposition are sulfate and nitrate, while the main cationic components are hydrogen and ammonium ions (Church, 1997). The Great Smoky Mountains in the southeastern United States receives some of the highest input rates of sulfur and nitrogen compounds; this in turn affects water quality of streams draining watersheds in the Great Smoky Mountains National Park (Flum and Nodvin, 1995). This is particularly true in the Noland Divide Watershed, where flux rates of nitrate (throughfall flux 911 eq/ha/yr) and sulfate (throughfall flux 2100 eq/ha/yr) rival those in north-central Europe and where there are poorly-buffered soils which are inadequate to counter-act the acid-production processes that accompany deposition (Shubzda *et al.*, 1995; Johnson and Lindberg, 1992). In order to understand and interpret water quality at Noland Divide, one must first understand the basic biological and geochemical interactions that occur within such watersheds.

In many high-elevation watersheds, acid components of sulfur and nitrogen compounds in the atmosphere can be deposited by wet deposition or “acid rain”, dry deposition as particles, or cloudwater deposition (Drever, 1988). Research in Noland Divide has shown that input of these compounds is dominated by dry and cloudwater deposition processes (Nodvin *et al.*, 1995; Shubzda *et al.*, 1995). Once in the watershed, these compounds undergo reactions that can

release excess hydrogen ions, which contribute to acidification of soil and surface waters, and that can mobilize base cations. For example, if nitrogen is deposited to a watershed, nitrification by the biomass will convert it to nitrate; release of this nitrate will generate hydrogen ions, or acidity, to balance the charge (Drever, 1988). This reaction (nitrogen deposited as ammonium) commonly occurs as follows:



Reactions with sulfur compounds are generally much slower than those with nitrogen compounds. In the presence of water, sulfur compounds react to form sulfate and excess hydrogen ions by the following reactions (Schlesinger, 1991):



where M represents a variety of possible catalysts. If the concentration of strong acid anions such as sulfate and nitrate increase in the solution moving through the soil, the concentration of base cations (Ca^{2+} , Mg^{2+} , Na^+ , K^+) must increase accordingly to maintain charge balances. However, if there is low base cation availability, the charge balance will be maintained by the leaching of more hydrogen ions and aluminum (Cosby *et al.*, 1985). The above is true for Noland Divide watershed, as research there has shown a tendency to conserve available base cations and instead

release acid cations (H^+) and aluminum (Johnson and Lindberg, 1992). Research in the Hubbard Brook watershed has shown that wet and dry deposition are the major sources for acid anions and nutrients such as sulfur, nitrogen, and chloride, while weathering is the major source for many base cations such as calcium, magnesium, potassium, and sodium (Likens and Bormann, 1995). Research in the Smoky Mountains and at Noland Divide supports this, yet also has shown that some amounts of base cations are deposited as particulate matter, and that litterfall decomposition and foliar leaching produce significant amounts of potassium, calcium, and magnesium (Johnson and Lindberg, 1992).

Over time, nitrogen inputs can exceed watershed demand, causing various stages of nitrogen saturation. This process can be accelerated if there are large pools of nitrogen in the soil and older-growth forests in the watershed (Stoddard, 1994). Noland Divide Watershed has been shown to be at Stage 2/verge of Stage 3 - nitrogen saturated, which means that the annual nitrogen cycle is dominated by nitrogen loss through leaching and denitrification. As a result, the watershed acts as a net source of nitrate in some periods of the year and there are elevated nitrate concentrations observed during both storm events and baseflow conditions (Nodvin *et al.*, 1995; Stoddard, 1994). Therefore, streams in Noland Divide undergo both chronic and episodic acidification (Nodvin *et al.*, 1995). Studies throughout the United States have shown that increased nitrogen inputs may cause enhanced sulfate retention through adsorption (Nodvin *et al.*, 1995; Flum and Nodvin, 1995; Lynch and Corbett, 1989; Ryan *et al.*, 1989; Clow and Mast, 1999; Herlihy *et al.*, 1991). As a result, further acidification is somewhat buffered. However, once the sulfate adsorption capacity of a soil is reached and then exceeded, release of excess

sulfate will contribute to further chronic and episodic streamwater acidification and base cation export.

Typically, surface waters are considered “acidic” if their acid neutralizing capacity (ANC) becomes zero or negative, which usually causes episodic decreases in pH to below 5, depending on other conditions (Drever, 1988). Surface waters are considered “poorly buffered” against acidity if pH is below 6 and ANC is below 40 $\mu\text{eq/L}$ (Nodvin *et al.*, 1995). The effects of this acidity have been studied, yet there are no widespread conclusions. Research at Hubbard Brook has shown that decreased forest growth may be attributable to the loss of base cations due to soil and surface water acidification (Likens and Bormann, 1995). In the Smoky Mountains, there is evidence that reduced growth and other physical changes in red spruce may be caused by limited availability of calcium and high foliar aluminum levels (Johnson *et al.*, 1991). Other research has shown declines in fish and macroinvertebrate populations due to low pH and toxic levels of aluminum (McAvoy, 1989; Webb *et al.*, 1989; Baker and Schofield, 1982; Swistock *et al.*, 1989). Solubility and mobilization of toxic forms of aluminum are at a minimum at pH 5.5 and increase as pH decreases (Stumm and Morgan, 1981). Table 2-1 shows observed ecological consequences of low pH levels in streams. In addition, mortality of some fish species has been observed in laboratory experiments when aluminum concentrations are as low as 7.5 $\mu\text{mol/L}$ (McAvoy, 1989).

Temporal Trends

Several studies have examined temporal trends of chemical constituents in streams, particularly pH, sulfate, and nitrate, to determine whether conditions are declining or improving over

Table 2-1. Proposed ecological consequences of low surface water pH.

Source: Baker, J.P., J. Van Sickle, C.J. Gagen, D.R. DeWalle, W.E. Sharpe, R.F. Carline, B.P. Baldigo, P.S. Murdoch, D.W. Bath, W.A. Krester, H.A. Simonin, and P.J. Wigington, Jr., Episodic acidification of small streams in the northeastern United States: effects on fish populations, *Ecological Applications*, 6, 422-437, 1996.

| pH Range | Biological Effects |
|-----------------|---|
| 6.5 - 6.0 | Loss of sensitive benthic invertebrates |
| 6.0 - 5.5 | Loss of acid-sensitive fish Reduced reproduction in sensitive fish species Increase in green algae in periphyton |
| 5.5 - 5.0 | Loss of most fish species Green algae dominate periphyton Loss of most mayflies, stoneflies, caddisflies, and shellfish Reduced biomass and productivity |
| < 5.0 | Loss of all fish species Decreased nutrient cycling rates Decline in periphyton species richness Decline in benthic invertebrates Reproductive failure of acid-sensitive amphibians |

time and to detect seasonal patterns. The Northeast U.S. contains by far more extensively-studied watersheds than any other region in the U.S. One of the most notable small watershed studies has been the Hubbard Brook Ecosystem Study in New Hampshire. Scientists have detected strong seasonal cycles in nitrate and other constituents in streamwater; highest concentrations of nitrate, potassium, and hydrogen ion and lowest concentrations of sulfate occur in winter and directly after snowmelt (Likens and Bormann, 1995; Stoddard, 1994). Though there has been no significant long-term trend in streamwater nitrate concentrations after 23 years of study, there has been a significant decrease in sulfate and base cation concentrations, which is believed to be due to decreases in atmospheric deposition of sulfur compounds (Likens and Bormann, 1995; Clow and Mast, 1999). However, there have been no significant changes in pH, and ANC remains negative, indicating the stream has not yet begun to recover from acidification due to sulfate deposition (Ibid., 1999).

Studies in the forested Biscuit Brook Watershed in the Catskills Range show that nitrate is increasing by approximately 1 $\mu\text{eq/L}$ per year, though it is unclear whether this can be attributed to anthropogenic sources of nitrogen (Stoddard, 1994). A significant long-term increase in nitrate has also been observed in the forested Fernow Experimental Watershed in West Virginia, approximately 3 $\mu\text{eq/L}$, yet this trend should be interpreted with caution as analytical methods were changed during the study period (Stoddard, 1994). Clow and Mast (1999) have studied long-term trends in five headwater basins in the northeast U.S. Common characteristics of these watersheds were that they experienced minimal human impact other than atmospheric deposition, all are undeveloped forested areas, logging has occurred in all watersheds at some time, and all have soils

that are acidic, have low base cation saturation, and have low sulfate adsorption capacities (except for one watershed studied). Clow and Mast (1999) found that from 1984 to 1996, all sites showed significant decreases in streamwater sulfate, and many sites showed significant decreases in ANC. In addition, trend analysis of precipitation also showed significant decreases in sulfate, which supports findings and conclusions in the Hubbard Brook Watershed. Research focusing on sulfate has been conducted in another northeast U.S., forested watershed, the Leading Ridge Experimental Watershed in central Pennsylvania. Though a limited record of data does not permit extensive analysis of long-term trends, scientists there have observed strong seasonal patterns, with highest sulfate levels occurring in winter, and lowest levels occurring in the summer and early fall; this pattern is inversely related to sulfate patterns observed in precipitation (Lynch and Corbett, 1989). Significant research has also been conducted in Shenandoah National Park in Virginia; these studies show that sulfate concentrations are in fact increasing over time at an average rate of $2 \mu\text{eq/L}$ per year and that hydrogen ion concentrations are increasing at rates from $0.06 - 0.37 \mu\text{eq/L}$ per year (Ryan *et al.*, 1989). There have also been slightly significant ($p < 0.30$) increasing trends in calcium and magnesium concentrations and decreasing trends in ANC.

Research in the Smoky Mountains has focused mainly on seasonal patterns; no extensive long-term trend analyses have been conducted until now. Streamwater studies throughout the park have shown that nitrate concentrations are highest in the winter and lowest in the summer and fall, conductivity was highest in winter and lowest in summer, pH was highest in fall and lowest in winter, and ANC was highest in fall and lowest in spring and early summer (Silsbee and Larson, 1982).

Hydrologic Influences

Behavior of water quality constituents in forested watersheds can be affected by hydrologic changes, such as storm events and drought periods, and water flowing through different paths within a watershed during those periods can have distinct chemical and isotopic characteristics. Storm events are of particular interest to scientists studying acidification of streams, as it is during these events that the most dramatic fluctuations in pH, ANC, and concentrations of cations and anions occur.

Stormflow in a forested catchment can originate by one or more of the following flowpaths:

1) direct interception of precipitation by the stream channel, 2) overland or surface flow, 3) subsurface flow through soil layers, 4) basin transfer, and 5) groundwater flow (Church, 1997).

Most research has shown that the majority of stormflow is generated in subsurface soil layers and is composed mainly of pre-event or "old" water (Hill *et al.*, 1999; Collins *et al.*, 2000; Swistock *et al.*, 1989; Lynch and Corbett, 1989; McAvoy, 1989). One exception to this is a study in forested catchments in Quebec, in which it was observed that groundwater contributed to 60 - 80% of stormflow, yet researchers there cautioned their conclusions were most likely site-specific (Sklash and Farvolden, 1979). Research in the forested Laurel Hill catchment in the Pennsylvania Appalachians showed that precipitation directly on the stream channel was a noticeable component on the early rising limb of the hydrograph, yet as the storm progressed, older laterally moving or upwelling soil water and groundwater comprised the majority of stormflow. Late in the event, younger soil water was converted to stormflow (Swistock *et al.*, 1989). In addition, Swistock *et al.* (1989) hypothesized that there should be a significant difference in chemical constituents in

streamwater between identical flows on the rising and falling limbs of the hydrograph, and they observed higher inputs of aluminum on the falling limb. The theory of upwelling soil water and groundwater is supported by research by Creed *et al.* (1996), which states that as a storm event progresses, the water table rises and flushes water into the stream from upper soil layers. Researchers in Pennsylvania further hypothesized that groundwater inputs would be the major contributor to stormflow during smaller events, and that "flashy" headwater streams in steeper catchments would be even more likely to receive the vast majority of stormflow from upper soil layers (Swistock *et al.*, 1989).

Since the pathways that water takes through a watershed have significant influence on its composition, many different tracers have been used to detect where streamwater has been. These include temperature, conductivity, calcium, magnesium, chloride, bromide, sulfate, aluminum, and environmental isotopes such as oxygen-18 (^{18}O) and deuterium (^2H) (Church, 1997; Swistock *et al.*, 1989). In addition, isotopes such as radon-222 (^{222}Rn), carbon-13 (^{13}C), and others of strontium, uranium, and thorium have been used in recent studies (Church, 1997; Genereux *et al.*, 1993). Research in the Laurel Hill Catchment included the use of oxygen-18 and aluminum; oxygen-18 was chosen because it is a natural constituent of the water molecule and travels where water travels, yet aluminum was determined to be the most accurate chemical tracer, as its sources could be separated by components of the hydrograph (Swistock *et al.*, 1989).

Many recent stormflow studies have proposed the evidence of three distinct flowpaths: bedrock zone flow, saturated soil zone flow, and unsaturated vadose zone flow. Mulholland (1993) has conducted significant research in the Walker Branch Watershed in Oak Ridge,

Tennessee, using a chemical end-member mixing analysis with calcium and sulfate to separate chemical signals of the three sources. Research showed that the dominant flow path was dependent on watershed antecedent moisture condition (AMC) (Mulholland *et al.*, 1990), a phenomenon which will be discussed in subsequent paragraphs. Generally, both shallow and deep flowpaths were important in generating storm streamflow, but inputs from the vadose zone dominated during peak flow; this resulted in a distinct chemical "signal" of elevated sulfate levels and diminished calcium levels. Sulfate concentrations were high in the vadose zone due to increased concentrations in precipitation and due to pools of available sulfate on the forest floor and upper soil layers from dry deposition. Conversely, calcium concentrations were low in the vadose zone because of low base cation saturation and base exchange capacity of soils. Later in the storm, inputs from the deep saturated soil zone produced chemical signals of low sulfate and low calcium concentrations, while after the stream returned to baseflow conditions, chemical signals from the bedrock zone showed high calcium and low sulfate concentrations (Mulholland, 1993). Other studies in Georgia, Norway, and Sweden have supported this three flowpath theory (Peters, 1994; Lundin, 1995; Collins *et al.*, 2000).

Most research involving water quality changes during storm events has shown that watershed AMC prior to a storm event and intensity of rainfall during the storm can have a significant influence on the physical and chemical characteristics of water moving through the watershed. Research in the Leading Ridge Watershed in Pennsylvania has shown higher sulfate export/input ratios in storms after high AMC periods (Lynch and Corbett, 1989). Findings in the Laurel Hill Watershed in the same state have shown that peak flow, volume of storm runoff, and

the "hydrologic responsiveness" are related to AMC and the intensity of rainfall during the storm (Swistock *et al.*, 1989). In events when the AMC has been low, soil water contributions were observed to be less significant; therefore, lower concentrations of constituents associated with soil water were found in streamwater during these storms than if the AMC had been high. This is supported by research by Mulholland *et al.* (1990), who observed that during high AMC and high rainfall intensity conditions, most storm runoff moved laterally through soil layers to the stream and showed elevated levels of chloride, aluminum, and sulfate and diminished levels of ANC, calcium, and magnesium. However, in storm events after low AMC conditions or with low rainfall intensity, most storm runoff moved through deeper pathways, and thus produced different hydrological and chemical responses. Perhaps one of the most interesting studies conducted on AMC and stormflow characteristics is that of a completely enclosed catchment in Norway as part of the CLIMEX project. This 1200 m² catchment is essentially a greenhouse in which watershed properties can be controlled and altered. In one particular experiment, the AMC of the watershed was brought to saturated conditions, and a storm event was simulated using lithium bromide as a tracer (Collins *et al.*, 2000). Researchers observed that AMC is a fundamental control on the mixing of old and new water during a storm event. That is, at high AMC, there is a higher contribution of old or pre-event water. Similarly, during storms of low rainfall intensity, there is also a higher contribution of old or pre-event water (Ibid., 2000). Therefore, in storms of high intensity or after a low AMC period, streamwater chemistry should be influenced more by the chemistry of the rainfall itself.

Many watersheds influenced by acid deposition undergo episodic acidification before ever

reaching chronic acidification status. Changes in stream chemistry during storm events can have a significant impact on aquatic biota. Storm event studies in the Laurel Hill Watershed showed that aluminum concentrations at peak flows were generally 18 - 28 $\mu\text{mol/L}$, which exceed acute toxicity limits of most indigenous fish species there; these episodic increases were considered the reason for trout mortality and current absence of aquatic life (Swistock *et al.*, 1989). In addition, as flow increased during storm events, pH decreased 0.2 to 0.6 units. In similar studies at the West Wachusett Brook Watershed in Massachusetts, aluminum concentrations ranged from 15 - 22 $\mu\text{mol/L}$, and pH decreased from 5.0 to 4.5 during the storm event (McAvoy, 1989). Episodic acidification has also been documented in brook trout streams in Shenandoah National Park; during a storm event in the White Oak Run Watershed, ANC decreased from 20 $\mu\text{eq/L}$ to 3 $\mu\text{eq/L}$ and pH decreased from 6.2 to 5.5 (Eshleman *et al.*, 1995). In other watersheds at Shenandoah, such as Paine Run, ANC commonly becomes negative during these events (Hyer *et al.*, 1995). Therefore, acidity of streams need not be chronic to cause lasting impact on aquatic biota.

Use of Parametric Regression Models

Many statistical techniques have been used to determine constituent loads in streamwater, detect time and seasonal trends in concentrations and loads, and determine optimal sampling scenarios for representing water quality. In many previous studies, regression models have been used to compute sediment and chemical constituent loads in large rivers (e.g., Smoot *et al.*, 1986; Walling, 1977; Steele, 1980); however, many recent studies have shown their applicability to smaller streams. Regression models have even been used to detect sources, both anthropogenic and natural, of constituents such as chloride in streams (Albek, 1999).

Calculating loads in streams draining small watersheds is often accomplished through an averaging method, which is a simple technique commonly applied for lack of better methods; this has been the method used for calculating loads in all previous research at NDW. Estimates of loads using the average method are made by averaging concentrations and flow over a time period and assigning that average load to that entire period. However, this method assumes that flow, concentration, and load data are independent and identically distributed, which is usually not true (Preston *et al.*, 1989). If these assumptions are not met and if data used for calculating loads do not represent the full range of flow and concentration values, estimation bias and errors can be large (Ferguson, 1987). The two other methods commonly used for determining loads are the ratio estimator and regression estimator methods. The ratio estimator method entails the use of flow as the auxiliary variable and each constituent load as the dependent variable. This linear method has been shown to work best when the relationship between the dependent and independent variables is linear and passes through the origin and when the variance of the dependent variable about the line is proportional to the independent variable (Cochran, 1977). The linear regression or rating curve method often entails the use of log-log relationships between dependent and independent variables, given that flow and constituent concentrations often follow a bivariate lognormal distribution (Preston *et al.*, 1989). Regression models are somewhat flexible; the influence of combinations of several independent variables, such as time or seasonal variability, on the dependent variable can be examined. Some studies have shown that log-log regression methods can be improved through the use of a bias correction factor or a minimum variance unbiased estimator (Cohn *et al.*, 1989), though application of these seems to be necessary only for small

data sets.

Preston *et al.* (1989) conducted an evaluation of the three above methods and attempted to characterize errors associated with each, using Monte Carlo simulations and actual tributary data and a range of constituents. For determining “true” loads with which to compare results from estimation methods, scientists collected data on a daily basis; this frequency was justified by the fact that the tributaries in Preston’s study are not “flashy” or highly event-responsive, and variability within the day is assumed to be negligible. Other studies have cautioned that samples for smaller, more event-responsive streams, such as in NDW, should be collected at a greater frequency in order to determine “true” values (Richards and Holloway, 1987). Preston *et al.* (1989) observed that no one method was consistently superior. The averaging method produced accurate and precise values only when the data set included flow and concentration values from the entire range of actual values, otherwise results were biased. The ratio method often produced less precise but virtually unbiased values than the other methods; this method was more robust than other methods under certain conditions, such as a weak flow-concentration relationship. The regression method produced lower errors and more accurate and precise values than any other method when the relationship between flow and a particular constituent’s concentration was consistent and strong. They also observed that the regression method required a smaller sample size than did the ratio estimator method to gain the same level of precision. It was also noted in this study that not collecting data during high flows or storm events may result in biased estimates when using the averaging or regression method; the ratio estimator method again appears more robust in this case (Ibid., 1989). However, it should be noted that only flow was used in the regression method to

explain variability in loads; some precision may have been lost by not including the influence of other variables.

As was mentioned previously, capturing the full range of flow and concentration values in a stream is key to reducing errors in most load and concentration estimates. Robertson and Roerish (1999) evaluated several sampling scenarios for small streams using a regression approach to determine which strategies produced the least errors. The scientists noted that while continuous, high-frequency sampling produces the most accurate results, this is not often feasible and thus regression methods have been used with some success to produce load estimates for periods when concentration data is not collected. In addition, they chose the regression method in their analyses because it could account for more variability in flow and concentration than did ratio estimator or integration methods. Both flow and seasonality terms were included in the regression equations. They determined that choosing an optimal sampling strategy with least error is highly dependent upon the length of the monitoring period. For example, for 1-year studies, they concluded that samples need only be collected monthly with supplemental samples collected during storm events. For studies of 2 - 3 years, samples need to be collected semimonthly, and for studies of more than 3 years, samples collected on either a monthly or semimonthly basis were statistically adequate. The importance of capturing storm events was debatable for studies of 2 or more years (Ibid., 1999).

Collection of samples during high flow events is usually desirable given that a large percentage of annual mass transport of most constituents occurs during high-flow periods. However, Robertson and Roerish (1999) observed that for longer-term studies, additional samples

from high flow events resulted in a positive bias and less precise overall annual load estimates. However, they placed more importance on random sampling and on representing the average load for each day, which is generally best for low-variability large rivers. They mention that for many small, flashy streams, storm sampling may still be desirable. Interestingly, they observed that the optimal sampling strategy for capturing these events is utilizing storm chasing crews instead of automated equipment. This is because storm chasing crews usually do not respond immediately to storm events and sample later on the hydrograph, when most loads and concentrations are decreasing. This sampling strategy, they claim, will better represent average daily values and reduce the magnitude of bias (Robertson and Roerish, 1999). However, export of most analytes is highest on the rising limb of the hydrograph and during peak flow; therefore, characterizing water quality during this period is integral for understanding total export from the watershed. It should also be noted that only phosphorus and sediment were used as constituents in Robertson's and Roerish's analysis; many other constituents, such as chloride or sodium, are diluted during a storm event, and therefore their collection during storm events may result in negative instead of positive bias. Robertson and Roerish (1999) observed that although the aforementioned sampling strategies were feasible and statistically adequate for representing water quality in small streams, median and average absolute errors were still approximately 30%. However, results can be improved by having longer monitoring periods, and often the regression method is the most accurate and precise approach of feasible approaches for determining loads.

CHAPTER III. ANALYSIS OF FLOW DATA

Characterizing and understanding streamflow patterns in the Noland Divide watershed can be invaluable when trying to understand trends, make predictions of water quality, and calculate constituent loads. The Noland Divide Watershed, because of its high-altitude location, is influenced by a variety of rainfall events. Particularly in summer and fall, flashy convective storm events are difficult to capture, and therefore trends in stream water chemistry at these high flows are virtually unknown. Rainfall events in winter and spring are generally longer-lasting, less flashy, and are generally larger in terms of overall rainfall volume, based on personal observation. The Stevens chart recorders in the H-flumes measure stage height in each stream; the stage height data are converted to flow data using a stage-discharge relationship for the flume. These data are important because they show where on the hydrograph each weekly sample is taken and how much of the hydrograph is not represented by the weekly samples.

Data Sources

Flow values determined from the 15-minute stage height data set measured by the Stevens chart recorders were used in the analysis in this chapter. For each weekly grab sample for each stream, a corresponding flow is read from the continuous data record at the time when the grab sample is taken. The flow data set for each stream includes values from November 1991 through August 1998.

Methods of Analysis

The record of flow data was analyzed graphically and statistically using Excel, Sigmaplot, and SPSS. In order to note flow distributions and probability of exceedence, flow-duration curves

were generated from the 15-minute data, which were divided by season in order to recognize differences among seasonal distributions and because the full data set was too large for any software package to generate a single curve. The instantaneous weekly sample flows were also placed on these curves to note which flow regimes are being represented and to note differences in distributions between the 15-minute and weekly sample data set. Plotting positions for each individual flow were determined from a Weibull probability formula, as follows:

$$\text{Probability of exceedance} = m / (n + 1) \quad (3-1)$$

where: m = rank of each flow value

n = total number of observations

The Weibull plotting position has been used extensively in the United States for plotting flow-duration and flood frequency curves (Helsel and Hirsch, 1992). The record of continuous flow data was ranked from lowest to highest values, the plotting position was calculated for each data point, and then the data were plotted on a log-probability plot. Plotting positions for the weekly sample flow data were computed separately; these values were then superimposed on the continuous data plots.

Throughout this chapter, “seasons” are defined as follows: December, January, and February constitute “winter”; March, April, and May constitute “spring”; June, July, and August constitute “summer”; and September, October, and November constitute “fall.”

Results

Continuous Data

Summary statistics for the 15-minute flow data are shown in Table 3-1. It is apparent that flow in the NE streamlet has a greater range than does flow in the SW streamlet. Percentile values for continuous flow data could not be generated due to the statistical software's inability to process the volume of data. Patterns in mean annual streamflow and mean monthly streamflow for both streams are shown in Figures 3-1 and 3-2, respectively. Similar representations of companion total annual and mean monthly precipitation from available data can be found in the Appendix, Figures A-1 and A-2. The flow duration curves in Figures 3-3 through 3-6 show distributions of the data and what flow regimes occur most often in the watershed. It is evident that flow is consistently higher in the NE stream than in the SW stream during high flows, yet flow is consistently higher in the SW stream than in the NE stream during baseflow conditions.

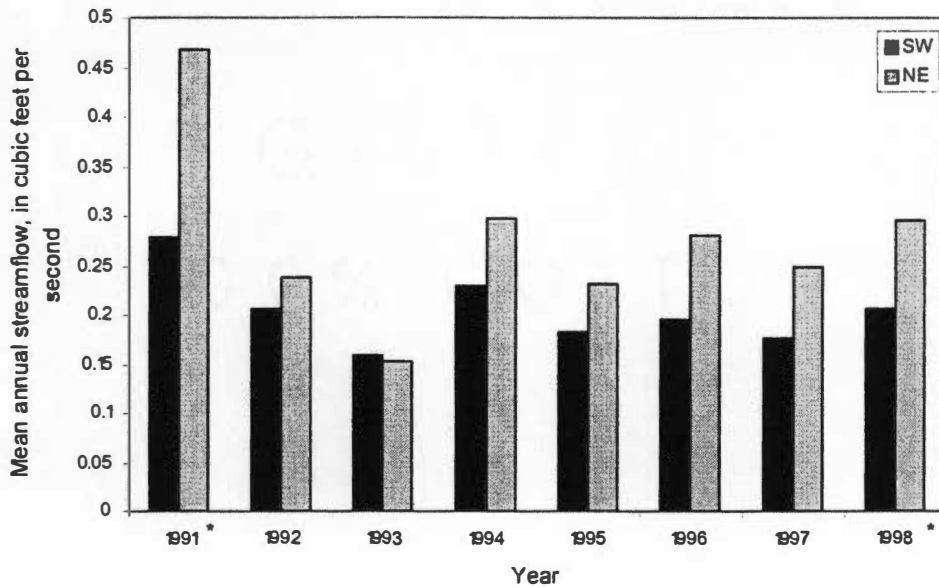
Weekly Data

When samples are collected on a weekly basis, their corresponding flow is read from the 15-minute data at the time at which they are taken. In Figures 3-7 and 3-8, the distributions of these weekly instantaneous flows show that there is great variability in flow when the sample is taken on the rising limb of the hydrograph, but the vast majority of samples (223 out of 339, or 66%) are taken under baseflow conditions, where there is little variability. Figures 3-7 and 3-8 show flow distributions through Tukey box plots. The "box" portion represents the inter-quartile range; the lower end of the box represents the 25th percentile value, the line within the box represents the median, and the upper end of the box represents the 75th percentile value. The

Table 3-1. Descriptive statistics for continuous and weekly streamflow data for both streamlets, 1991-1998.

| Streamflow* Sample Type | Stream | Median | Mean | Standard Deviation | Minimum | Maximum | Percentiles | | | |
|----------------------------|--------|--------|------|-----------------------|---------|---------|-------------|------|------|------|
| | | | | | | | 10th | 25th | 75th | 90th |
| Continuous | SW | 0.12 | 0.20 | 0.31 | 0.01 | 7.80 | N/A | N/A | N/A | N/A |
| | NE | 0.12 | 0.25 | 0.64 | 0.00 | 26.78 | N/A | N/A | N/A | N/A |
| Weekly | SW | 0.12 | 0.18 | 0.25 | 0.01 | 2.73 | 0.04 | 0.07 | 0.20 | 0.34 |
| | NE | 0.12 | 0.22 | 0.45 | 0.01 | 5.02 | 0.03 | 0.06 | 0.22 | 0.39 |

*All streamflow values are in cubic feet per second



*1991 and 1998 are partial years

Figure 3-1. Mean annual streamflow for the SW and NE streamlets from 15-minute data, 1991 - 1998.

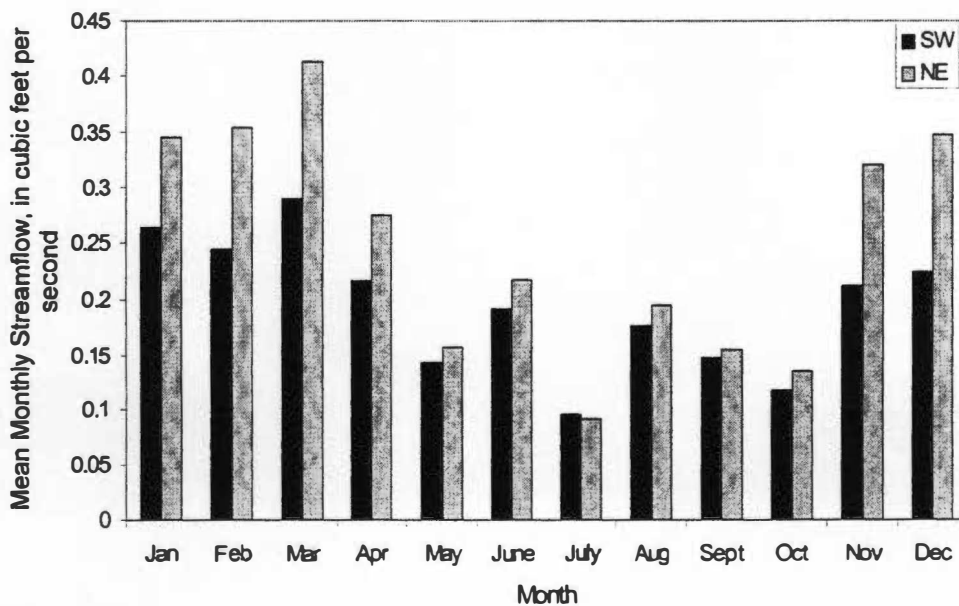


Figure 3-2. Mean monthly streamflow for the SW and NE streamlets from 15-minute data, 1991 - 1998.

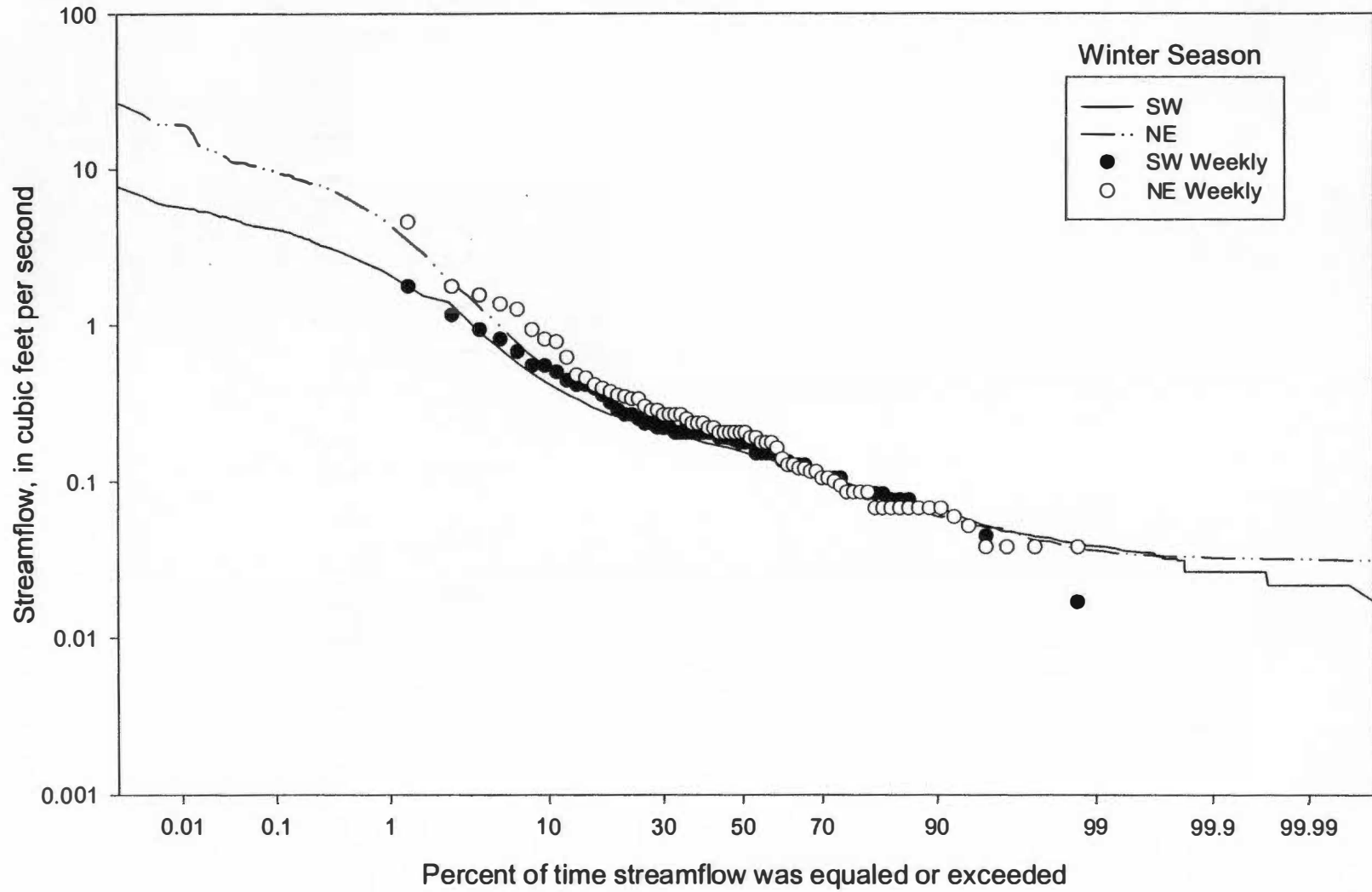


Figure 3-3. Streamflow duration and instantaneous streamflow at time of weekly sampling for the SW and NE streamlets, winter season 1991-1998.

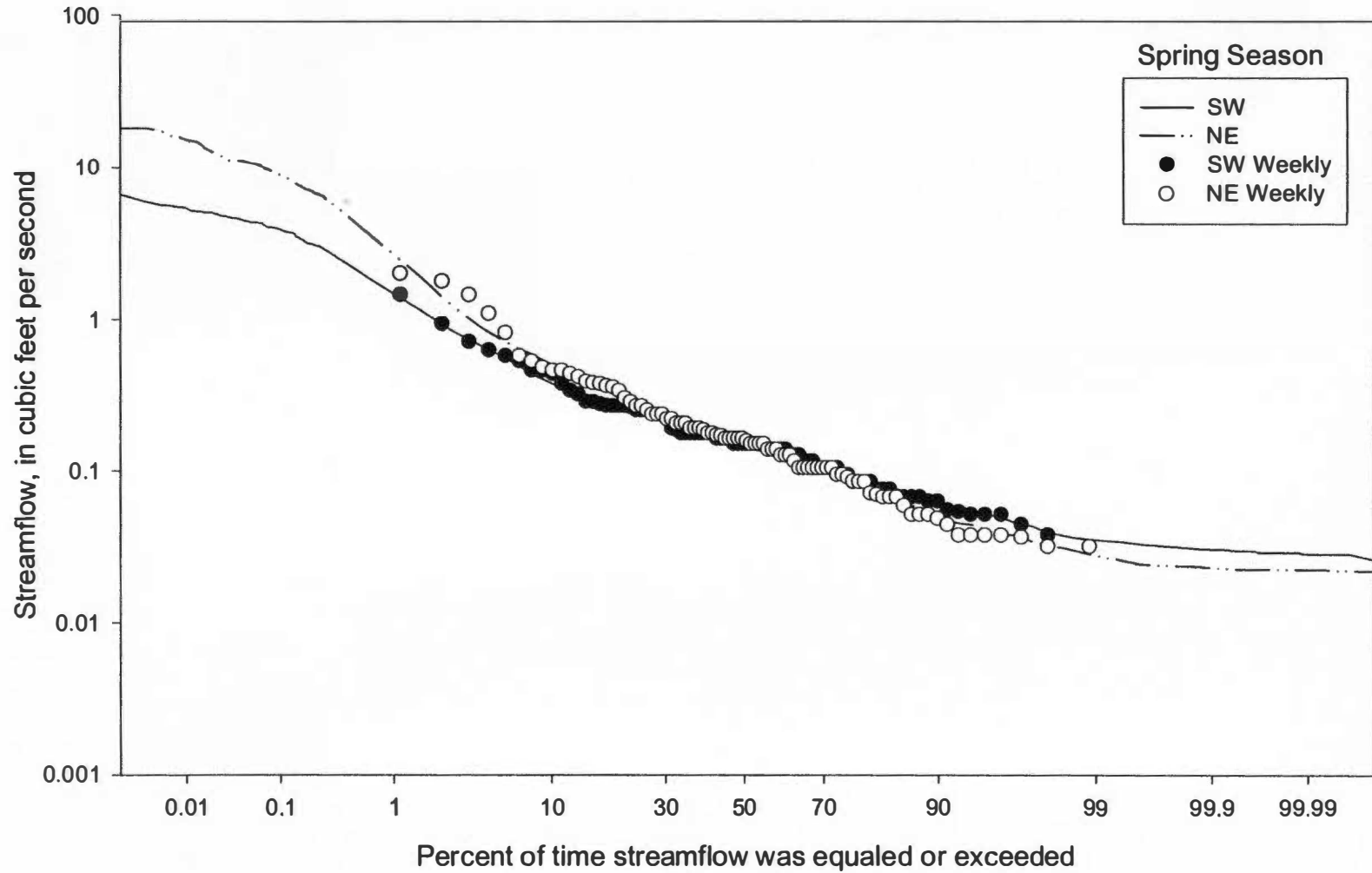


Figure 3-4. Streamflow duration and instantaneous streamflow at time of weekly sampling for the SW and NE streamlets, spring season 1991-1998.

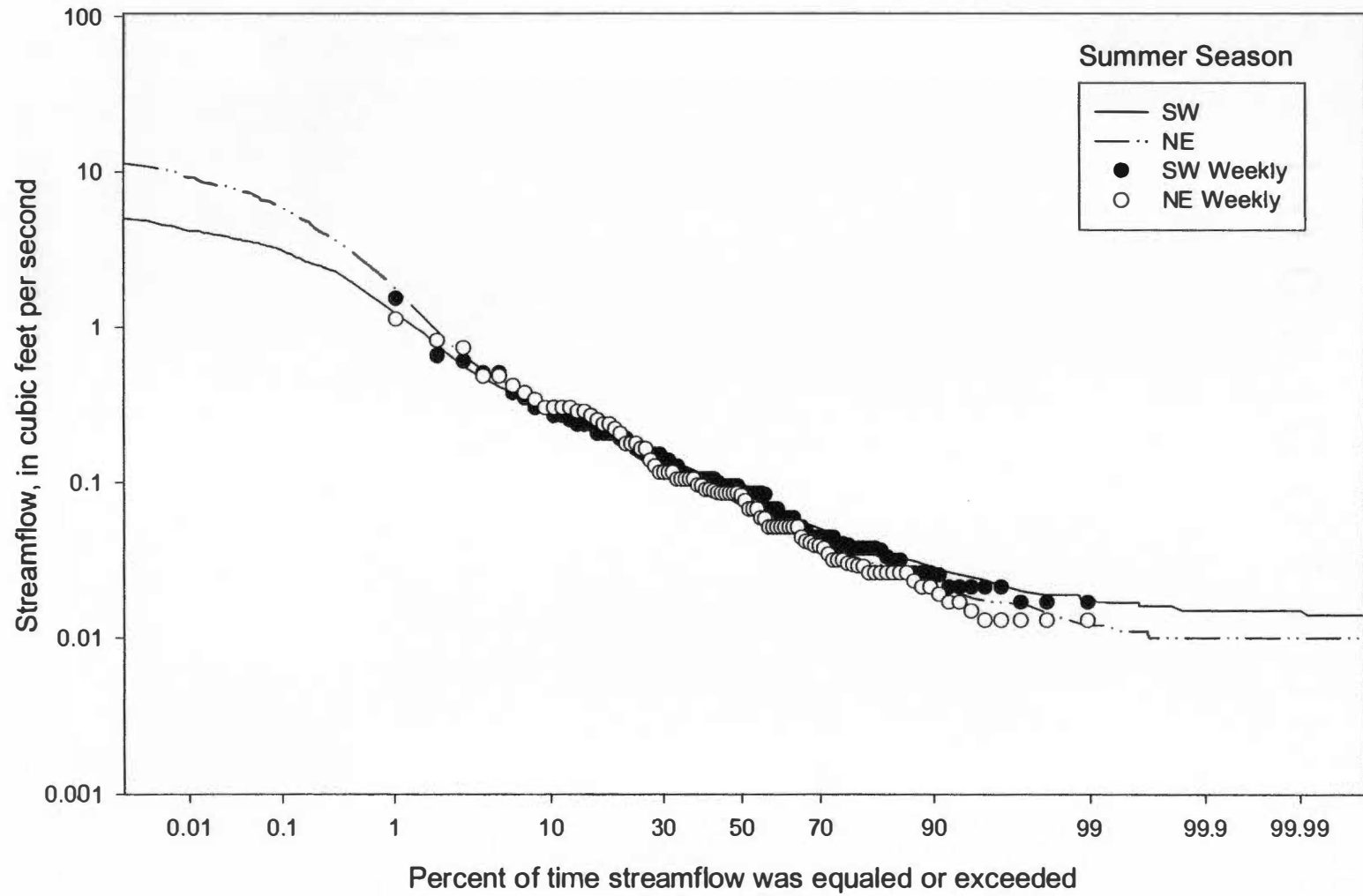


Figure 3-5. Streamflow duration and instantaneous streamflow at time of weekly sampling for the SW and NE streamlets, summer season 1991-1998.

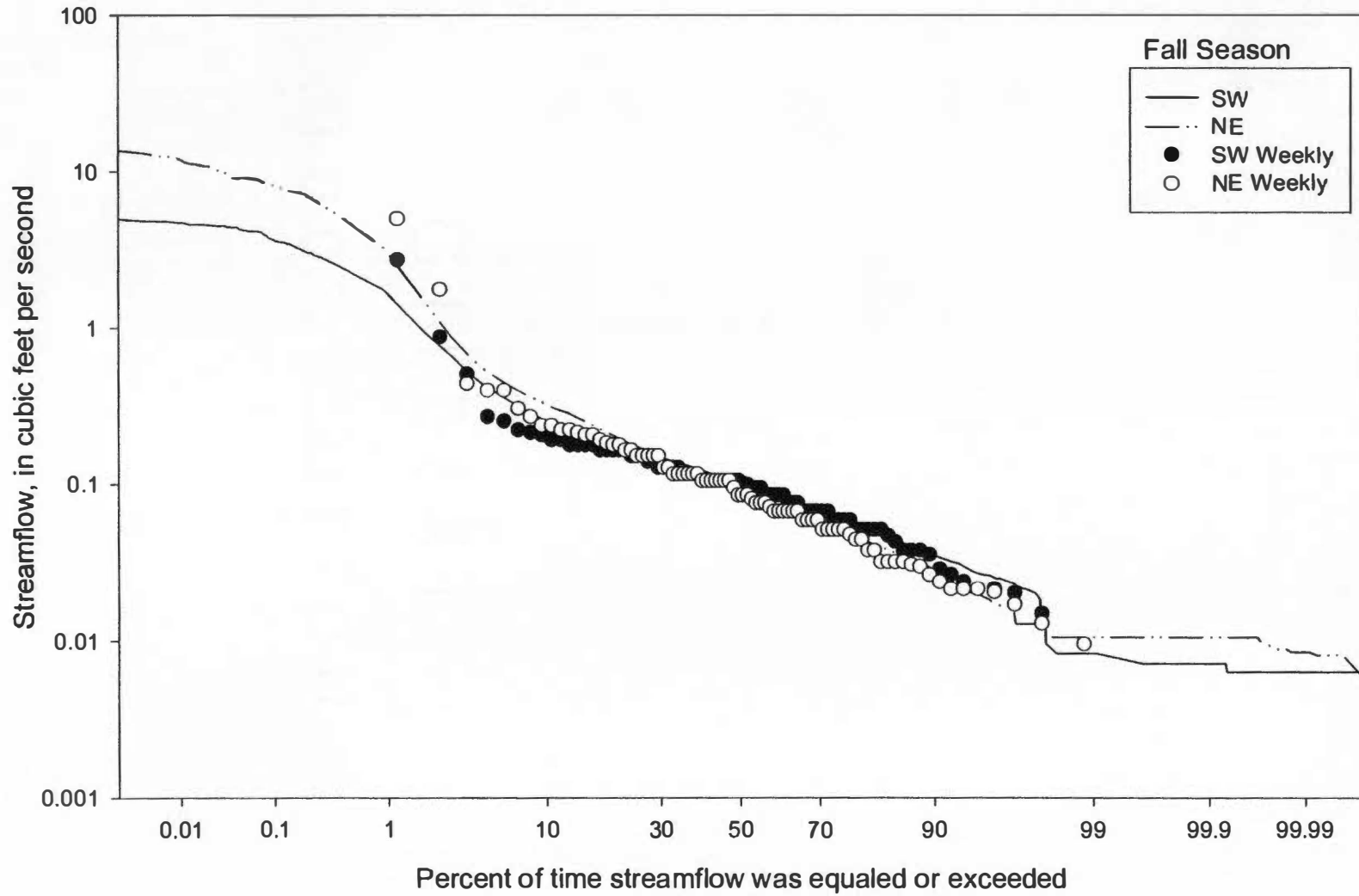


Figure 3-6. Streamflow duration and instantaneous streamflow at time of weekly sampling for the SW and NE streamlets, fall season 1991-1998.

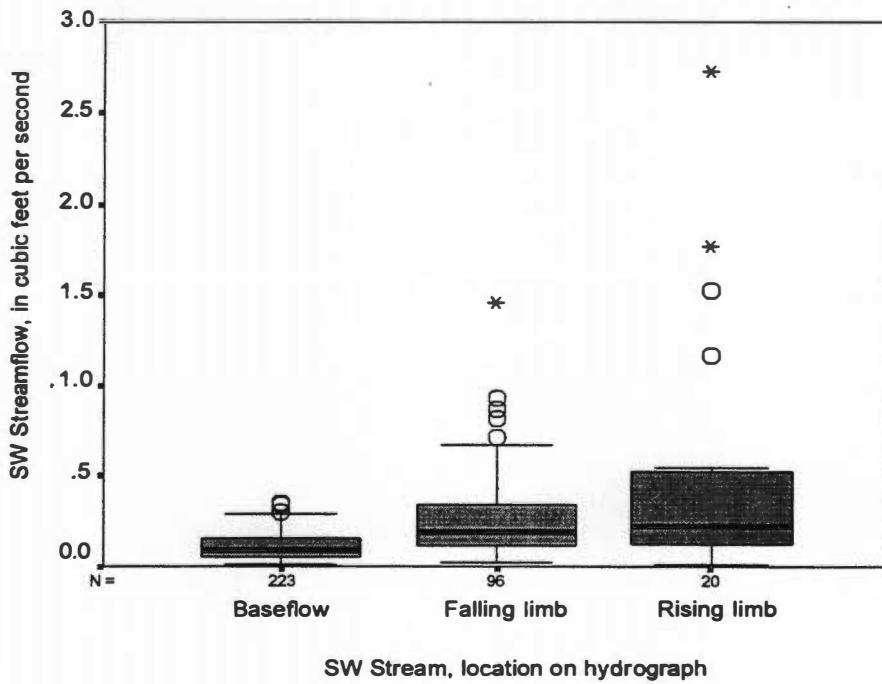


Figure 3-7. Distribution of weekly instantaneous streamflow based on location on hydrograph for the SW streamlet.

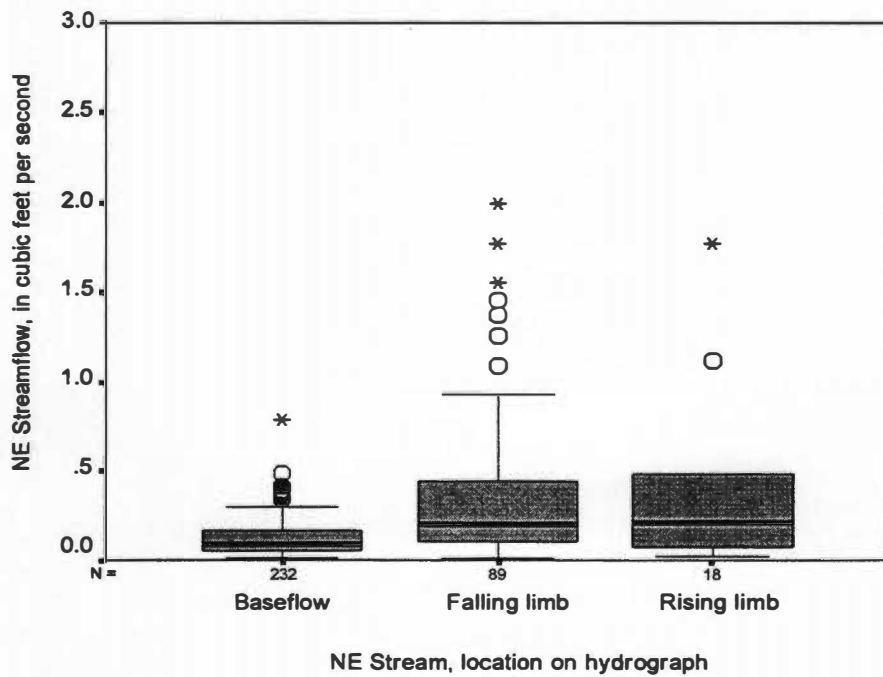


Figure 3-8. Distribution of weekly instantaneous streamflow based on location on hydrograph for the NE streamlet.

“whiskers” extending above and below the box represent the upper and lower adjacent values, respectively. Circles represent mild outliers, and asterisks represent extreme outliers. Outliers are considered “mild” if they lie farther than 1.5 times the inter-quartile range below the 25th percentile or above the 75th percentile. Outliers are considered “extreme” if they lie farther than 3 times the inter-quartile range below the 25th percentile or above the 75th percentile. Wider boxes, or inter-quartile ranges, as in Figure 3-7 for the rising limb of the hydrograph, usually indicate greater variability in the data set.

Summary statistics for the weekly instantaneous flow samples are shown in Table 3-1 along with statistics for the continuous data. Compared to the 15-minute data statistics, the weekly flow maximums are smaller and the minimums are greater. Therefore, both the high and low ends of the flow spectrum at Noland Divide are not fully represented in the weekly samples. This observation is reinforced by the flow-duration curves (see Figures 3-3 - 3-6), in which it is obvious that the high flow or storm events are not being captured, and therefore little is known about stream chemistry during these times.

Discussion

Trends

From Figure 3-1, patterns in the 15-minute flow data show that the highest mean streamflow occurred in 1991, but this is misleading since the data set does not include that entire year. Overall, flow patterns agree with rainfall patterns in that the most rainfall and highest streamflow occurred in 1994 and the least rainfall and lowest streamflow occurred in 1992 and 1993. From Figure 3-2, the highest mean streamflow occurs in March (the spring season), while

the lowest mean streamflow occurs in July (the summer season). In some years, however, the lowest flows occurred in October (the fall season). The flow-duration curves also show seasonal patterns and distributions. Weekly sampling schemes during the summer fit the continuous distribution well; there may have been less variability in the baseflow conditions during summer which allowed the sampling scheme to accurately represent the parent population. For the other seasons, the weekly data distribution deviates from the parent distribution, especially at mid-range on the probability scale. Perhaps the most deviant is the fall distribution; this may be the season that experiences the most “flashy”, rare events that do not endure for long periods and therefore are very difficult to catch with any frequency. In addition, most of these convective storm events tend to occur in the afternoon. Since most weekly samples are taken around 11:00 am - 12:00 pm every time, it is even more unlikely that fall storm events are represented in the weekly samples.

SW vs. NE Stream Conditions

Though both streams lie within the same watershed, differences exist between them with respect to flow and chemistry at any given time. During baseflow conditions, flow in the SW stream is slightly but consistently higher than flow in the NE stream. However, during rainfall events, the NE stream experiences much higher flows than does the SW stream. One explanation for this phenomenon is that at high flows, the SW stream short-circuits its banks, travels through distinct channels, and enters the NE stream upstream of the flume. Other contributing factors may be that the NE stream drains a larger area which captures more overland flow during storm events, or that flow in the SW stream is controlled more by groundwater sources. It would be extremely difficult to isolate drainage areas to each stream given the inter-connectivity of the streams in the

upper elevations of the watershed. The cross-over phenomenon has important implications for water chemistry in this watershed. However, it is unclear whether the effects of this cross-over are being observed at the exact sampling locations in the NE stream. The effects of the largest cross-over may be seen only in the flumes, where flow and stage height are measured, but since several smaller cross-overs occur further upstream of the sampling points, the water chemistry in both streams is most likely inter-related. The cross-over phenomenon, in relation to water chemistry, will be discussed further in later chapters.

CHAPTER IV. TEMPORAL VARIABILITY IN WATER QUALITY

Data Sources

To examine trends of water quality constituents over time, both the continuous (15-minute) and weekly grab sample data were used. The Hydrolab monitoring equipment in the Noland Divide watershed provides valuable information on the continuous behavior of pH, conductivity, and temperature. By having these data on a 15-minute basis, one is able to gain a piece of the total picture of what occurs during storm events and all other flow regimes. The Hydrolab continuous monitoring equipment was installed in November 1991 on the SW stream, but was not installed in the NE stream until April 1998. The data sets for each stream in this analysis extend through August 1998. Therefore, a more complete record exists for the SW stream and thus this record will be the main focus of this section.

Weekly grab samples taken for both streamlets provide a more complete water chemistry profile; grab sample data from November 1991 through August 1998 were used in this analysis. Each weekly sample is analyzed for pH, conductivity, acid neutralizing capacity (ANC), chloride, nitrate, sulfate, sodium, ammonium, potassium, hydrogen ion, calcium, magnesium, aluminum, and silica. In this report, trends in calcium and magnesium concentrations are not presented or discussed due to an ongoing review of quality assurance/quality control procedures.

Methods of Analysis

Fifteen-minute conductivity and pH were analyzed over time-by year, season, and month. The full 1991-1998 record was too large for the statistical software package and/or computer to analyze graphically. For this reason, the full record was split into two periods: 1991-1994 and

1995-1998. As a result, summary statistics for continuous pH, conductivity, and temperature are not provided because the software package would not generate these statistics for the full data set.

Weekly data were also analyzed and represented graphically over time--by year, season, and month. Statistical tests for determining differences between seasons and between the NE and SW streams' constituents were conducted using SPSS statistical software. Data sets were tested for normality through the Kolmogorov-Smirnov test; if data were normal, a parametric t-test was performed to note statistical differences and if data were non-normal, a non-parametric Mann-Whitney U test was performed. These statistical tests could not be performed on the continuous data because the data set was too large.

Further analysis of seasonality in weekly sample constituents was made by fitting load and concentration data with sine/cosine seasonality functions in a linear regression model. The load of each constituent was determined by multiplying concentration by a corresponding streamflow, read from 15-minute flow data at the time each weekly sample is taken. The load is calculated as follows:

$$\text{Flow (L/s)} * \text{Concentration } (\mu\text{eq/L}) * 1\text{eq}/10^6 \mu\text{eq} = \text{Instantaneous Load (eq/sec)} \quad (4-1)$$

The seasonality function was formed by determining the fractional part of the year in which each sample was taken. For example, if a sample was taken on May 1, 1995 (Julian day = 121), the fractional part of the year that had elapsed so far is $121/365 = 0.3315$. This value is then multiplied by 2π to convert it to radians; this term is called θ . The seasonality variable is then introduced into

the regression as $(b_1 \cos \theta + b_2 \sin \theta)$. The regression equations are in the following form:

$$\ln(QC) \text{ or } \ln(C) = I + b_1(\cos \theta) + b_2(\sin \theta) \quad (4-2)$$

where: C is concentration in $\mu\text{eq/L}$
 Q is streamflow in L/s
 I is the regression intercept
 ln is the natural logarithm
 θ is the fractional part of the year, in radians
 b_1, b_2 are the regression coefficients

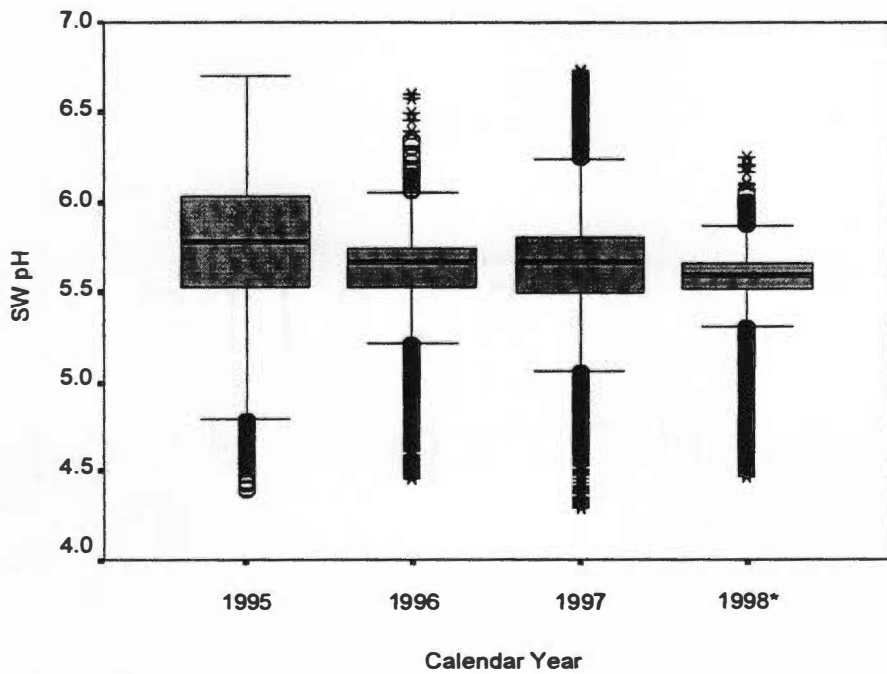
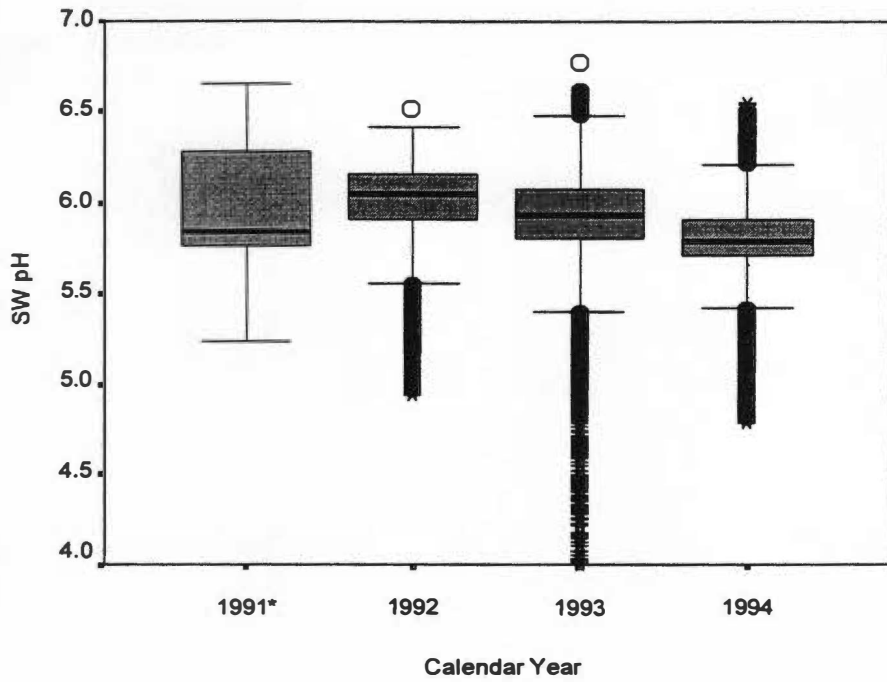
The seasonality function serves to explain the seasonal variability in analyte concentrations or loads by fitting them with a variation of a sine wave. Because these seasonality terms are the only independent variables in the regression, one can isolate the influence of seasonality and determine during which periods of the year analytes reach maximum and minimum concentrations or loads.

Throughout this chapter, seasons are defined as follows: December, January, and February constitute “winter”; March, April, and May constitute “spring”; June, July, and August constitute “summer”; and September, October, and November constitute “fall.” More statistical and quantitative analysis of time and seasonality trends in the weekly data set will be presented in Chapter VI, Parametric Modeling.

Results

Continuous Data

From Figure 4-1, it appears that the SW pH has declined slightly over the period of monitoring, 1991-1998. This trend will be tested for statistical significance in Chapter VI. The distribution during 1993 shows an unusual amount of outliers. It is possible that unusually cold



*Indicates partial year

Figure 4-1. Distributions of continuous pH data by year for the periods 1991-1994 (top) and 1995-1998 (bottom) for the SW streamlet.

weather and blizzards caused malfunctions and erroneous readings in the monitoring equipment during March of that year. In general, pH is higher in the late summer and fall (see Figures 4-2 and 4-3), when the stream is fed more by baseflow, and rainfall events are less frequent (see Figures 3-2 and A-2). pH is lower in the winter and early spring, when streamflow is higher and rainfall events are more frequent. There were wider distributions and greater variabilities for pH during the summer, particularly for the 1995-1998 record. Again, this variability could be due to less frequent, though perhaps more extreme, rainfall events and generally low antecedent moisture condition during the summer. The distribution of overall pH and conductivity data for the NE stream in 1998 is shown in Figure 4-7. From this limited record, it is evident that pH is lower in the summer months than in the late spring (see Figures 4-8 and 4-9); this is surprising given the behavior in the SW stream and given what is known about the frequency of rainfall events and rainfall composition during these seasons. It is difficult, however, to fully analyze this data given the limited period of record.

Figures 4-4, 4-5, and 4-6 show patterns in conductivity over year, season, and month, respectively, for the SW stream. There are few recognizable patterns for stream conductivity. Baseline conductivity is already very low for Noland given the low weathering potential of the sandstone that underlies the site. In general, one would expect that conductivity would be higher in baseflow conditions due to longer groundwater residence times in the bedrock and therefore greater dissolution capacity and higher dissolved mineral content in the water. However, at Noland it appears that higher mineral content and higher conductivity in the stream occur when water is flushed from the vadose zone into the stream, which normally does not occur during baseflow

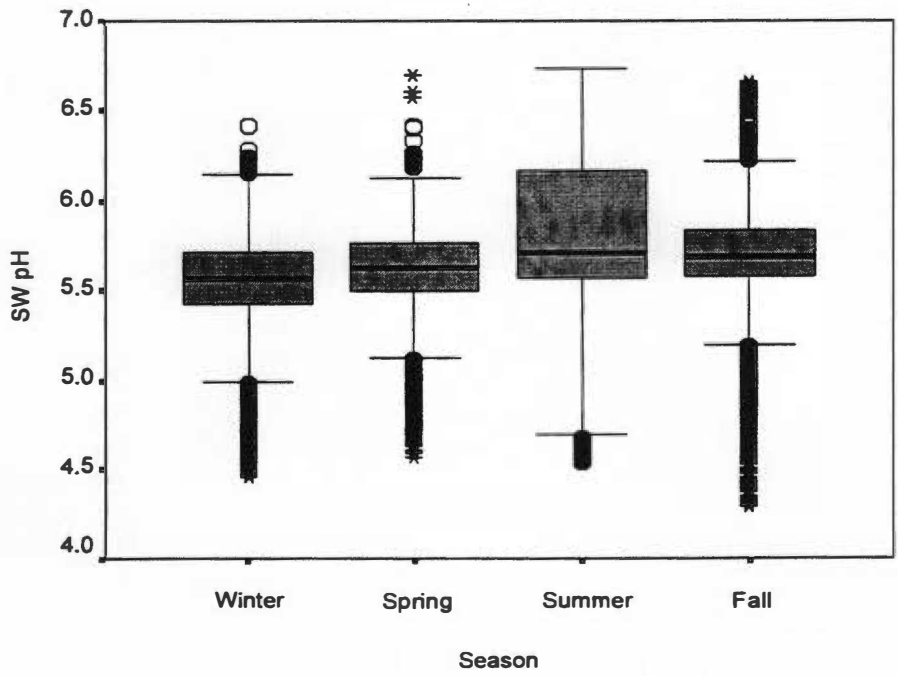
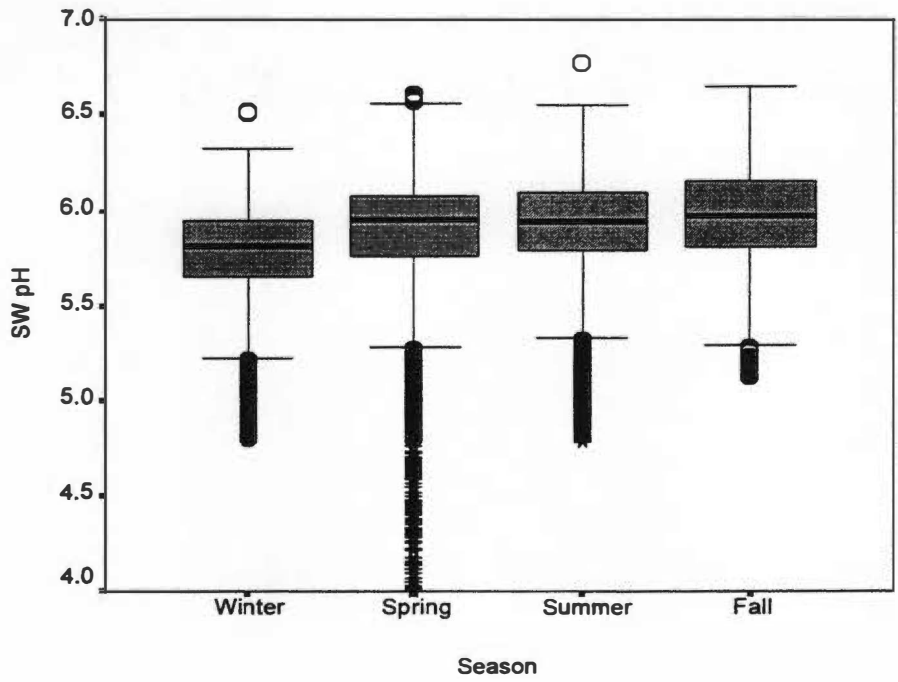


Figure 4-2. Distributions of continuous pH data by season for the periods 1991-1994 (top) and 1995-1998 (bottom) for the SW streamlet.

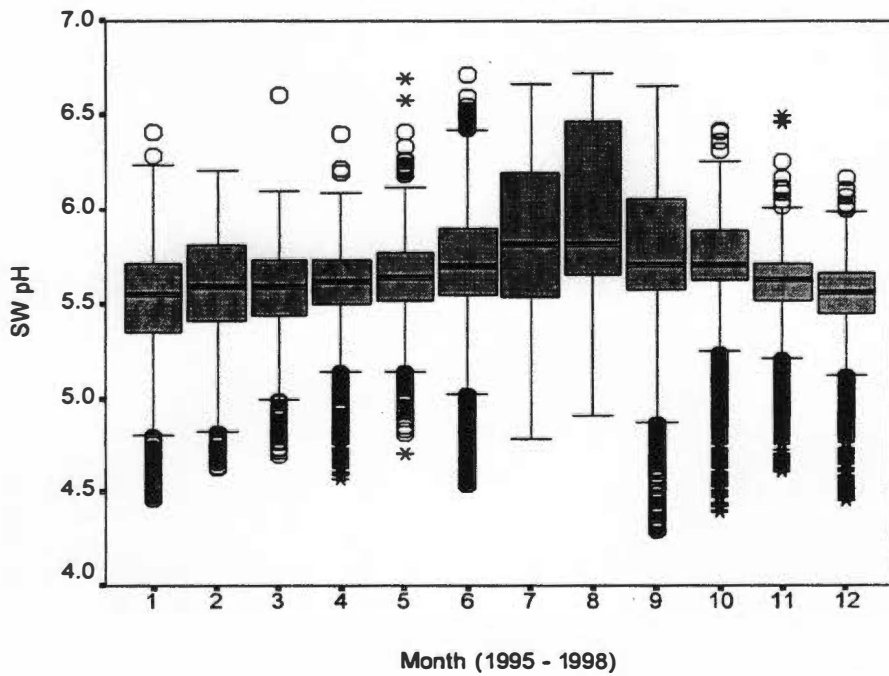
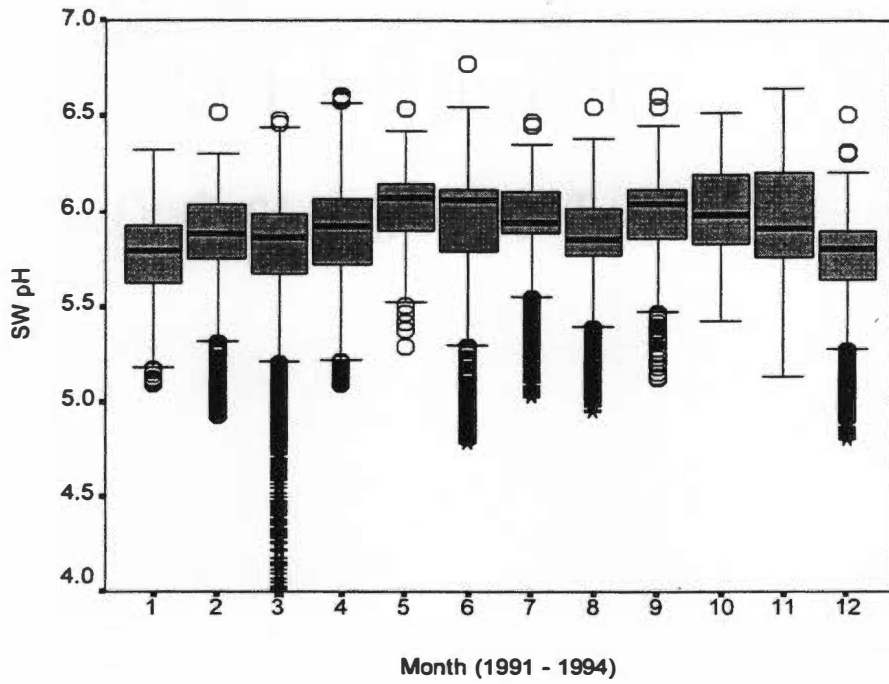
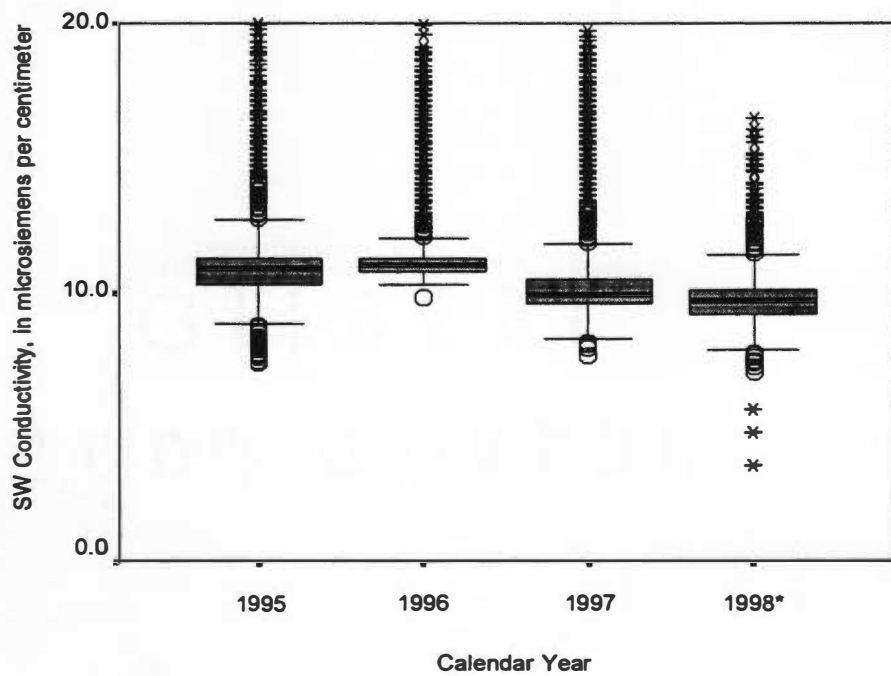
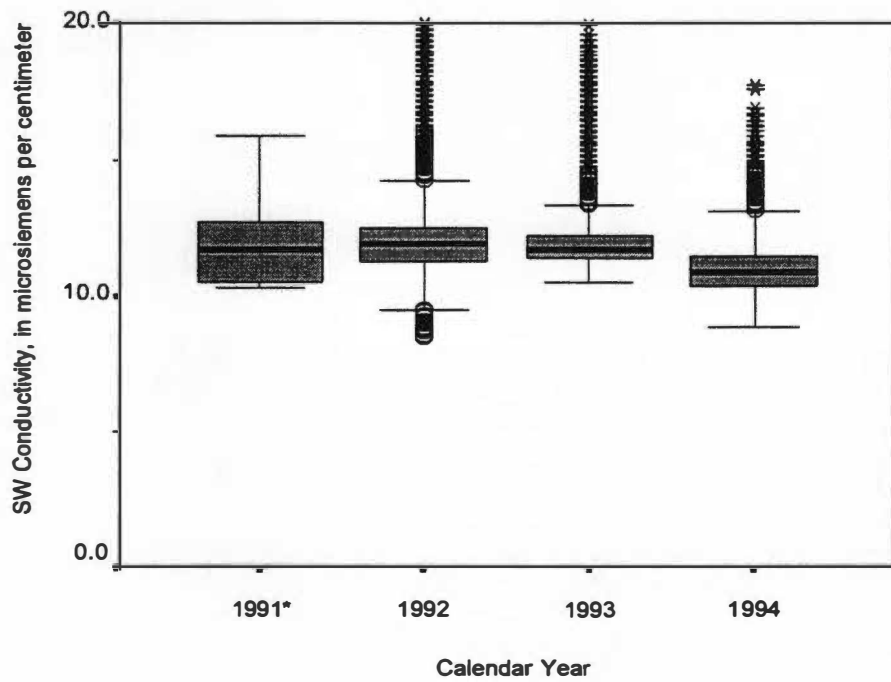


Figure 4-3. Distributions of continuous pH data by month for the periods 1991-1994 (top) and 1995-1998 (bottom) for the SW streamlet.



*Indicates partial year

Figure 4-4. Distributions of continuous conductivity data by year for the periods 1991-1994 (top) and 1995-1998 (bottom) for the SW streamlet.

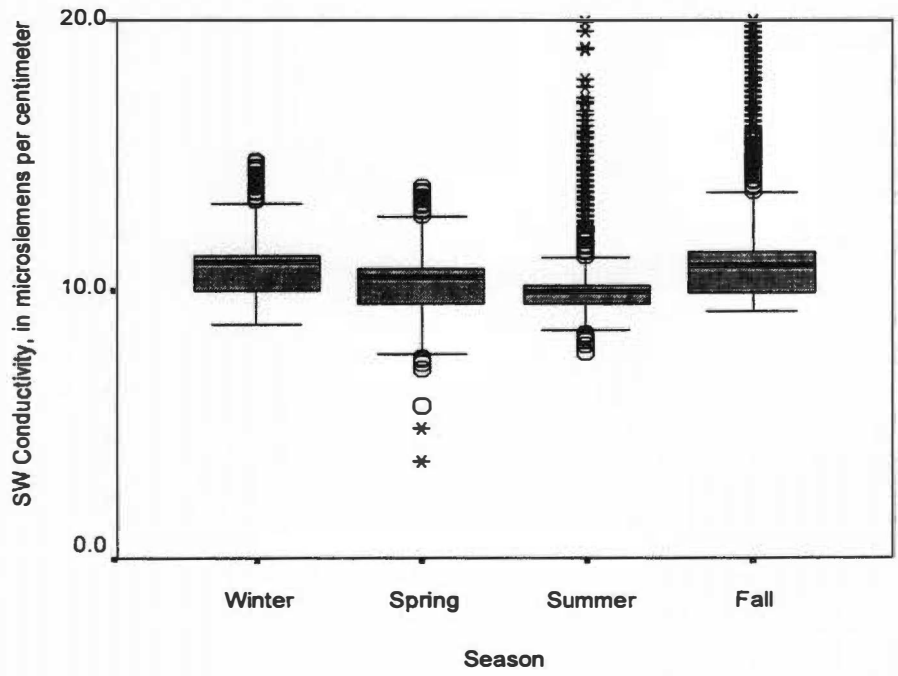
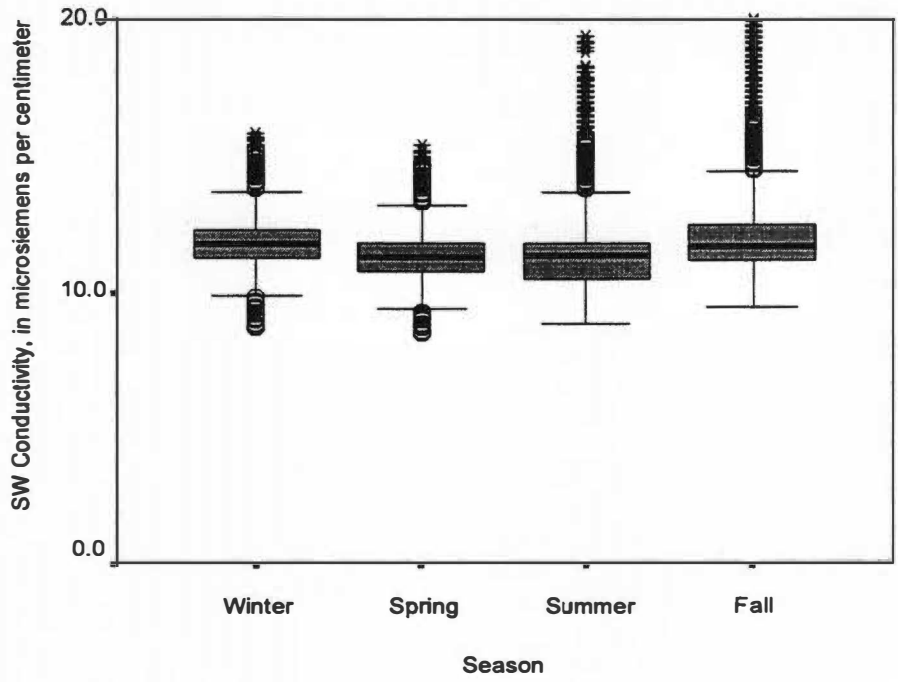


Figure 4-5. Distributions of continuous conductivity data by season for the periods 1991-1994 (top) and 1995-1998 (bottom) for the SW streamlet.

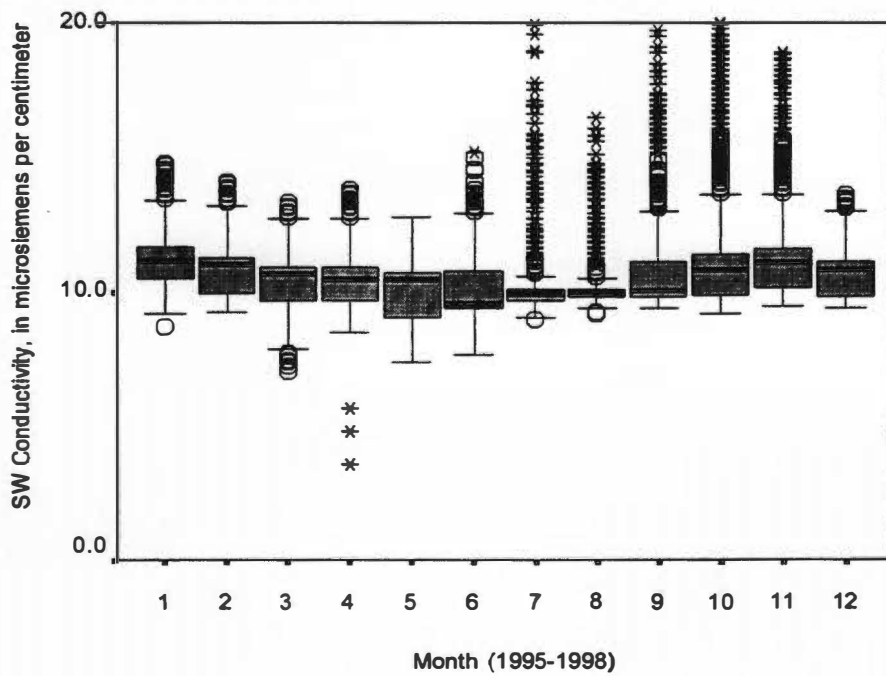
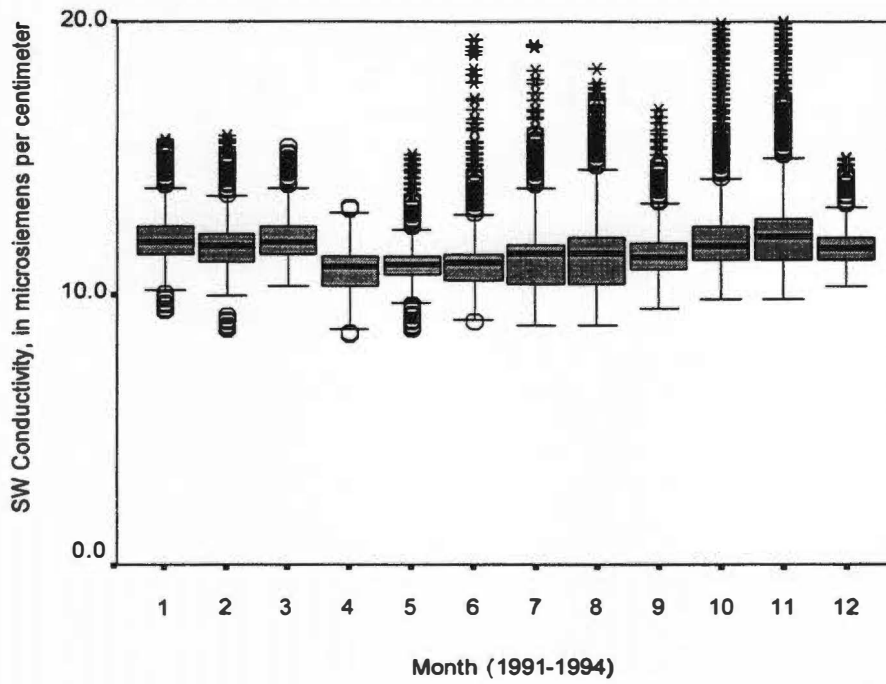


Figure 4-6. Distributions of continuous conductivity data by month for the periods 1991-1994 (top) and 1995-1998 (bottom) for the SW streamlet.

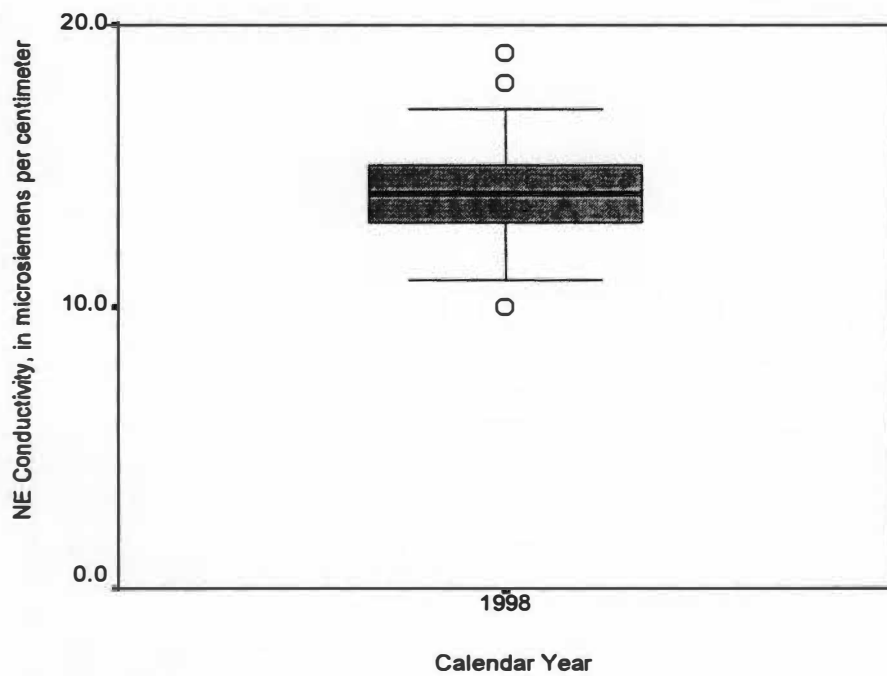
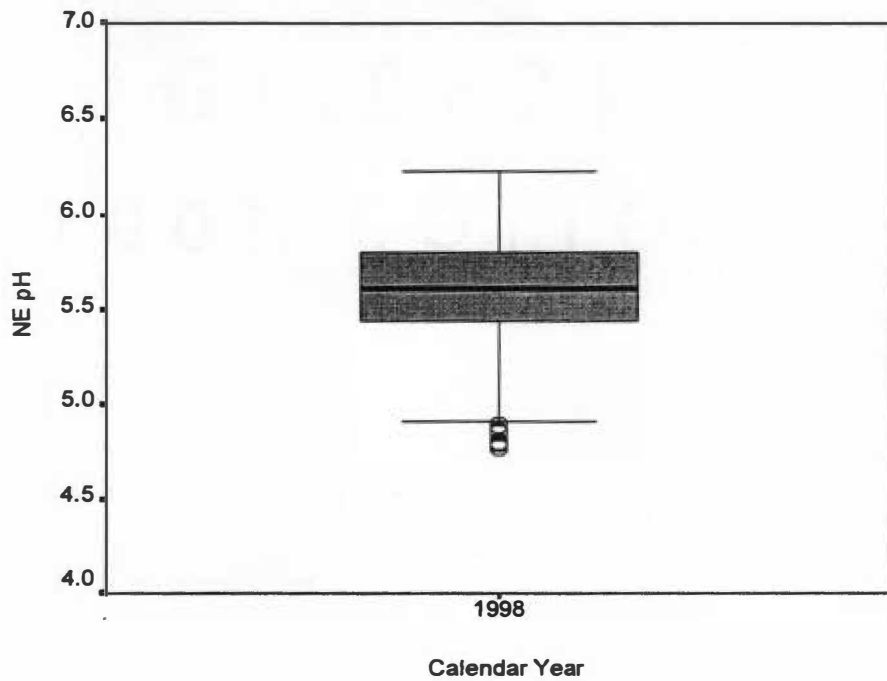
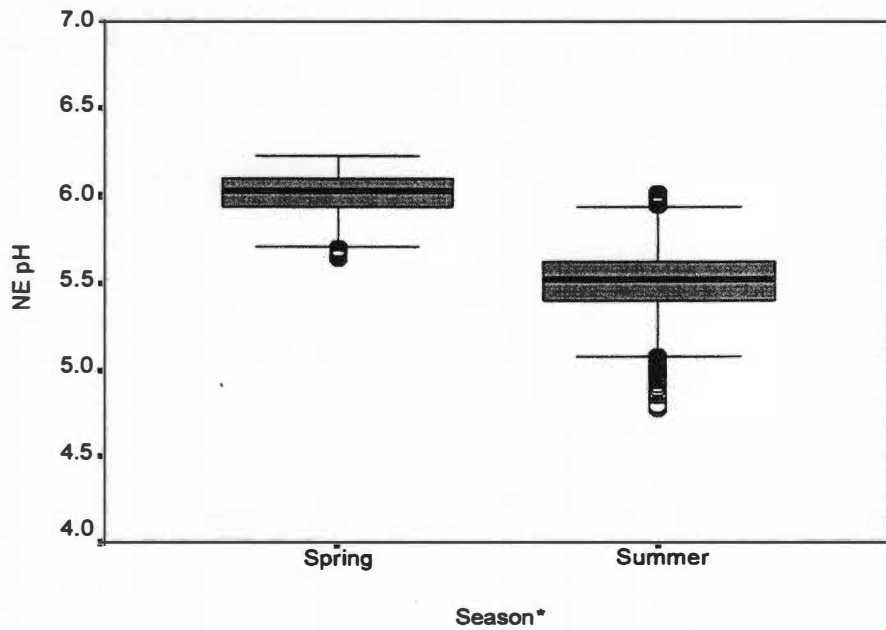
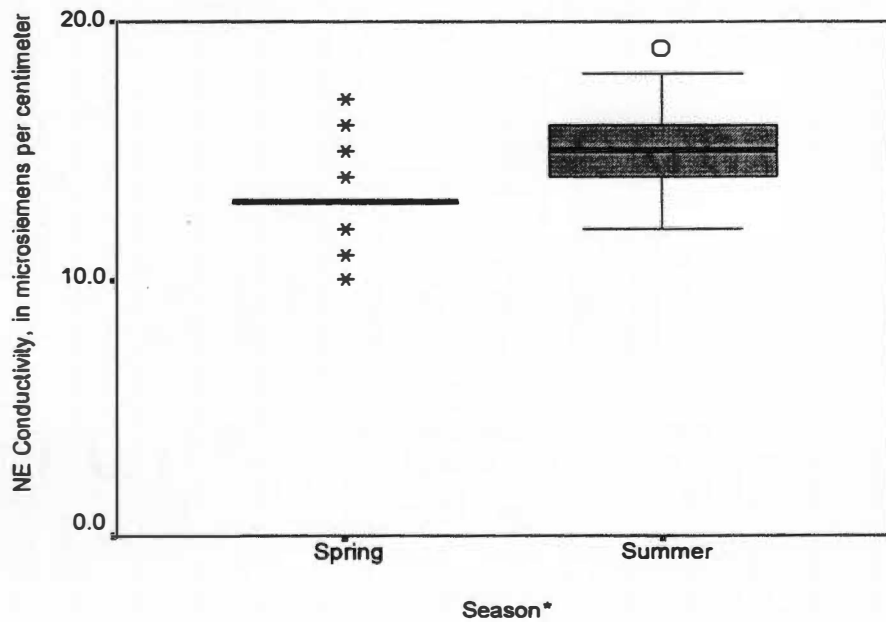


Figure 4-7. Overall distributions of continuous pH and conductivity data by year for 1998 for the NE streamlet.

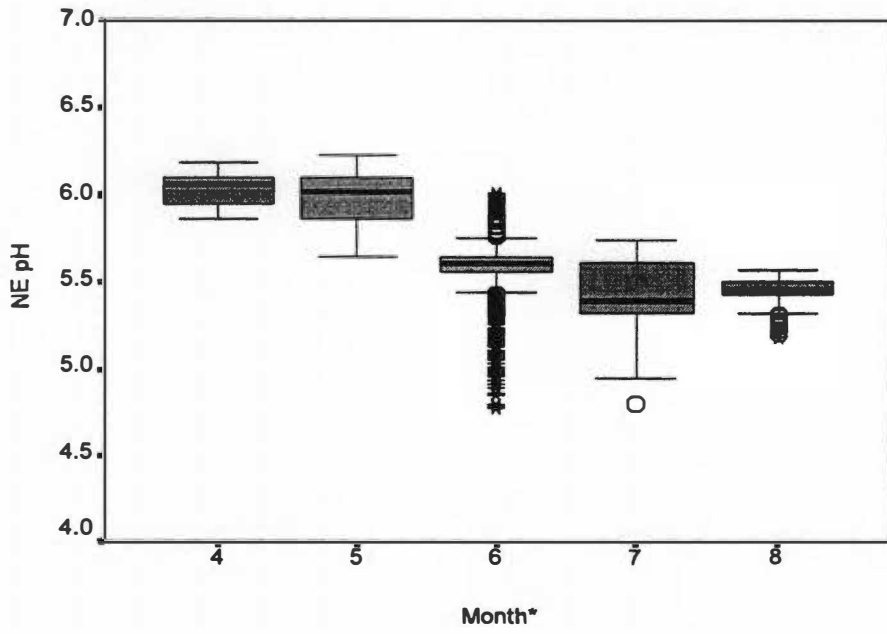


*NE continuous data available for only a portion of 1998

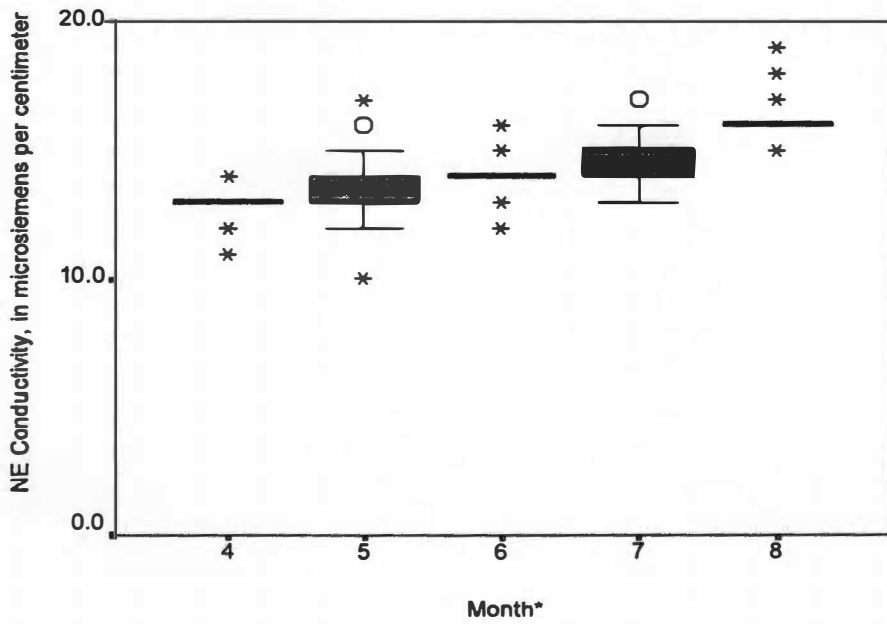


*NE continuous data available for only a portion of 1998

Figure 4-8. Distributions of continuous pH and conductivity data by season for 1998 for the NE streamlet.



*NE continuous data available for only a portion of 1998



*NE continuous data available for only a portion of 1998

Figure 4-9. Distributions of continuous pH and conductivity data by month for 1998 for the NE streamlet.

conditions. Figures 4-5 and 4-6 support this; though all distributions are tight and show little relative difference, it appears that lower conductivity is found in the summer and early fall (baseflow conditions), while higher values are found in the winter (higher flow). As with pH, conductivity appears to have declined slightly over the period of record. Nearly all the distributions, though, have many outliers on the high side, particularly for the summer and fall months. As in the previous paragraph with pH, conductivity in the NE stream exhibits behavior opposite to that of the SW stream. Figures 4-8 and 4-9 show that the NE conductivity is higher in the summer and lower in the spring.

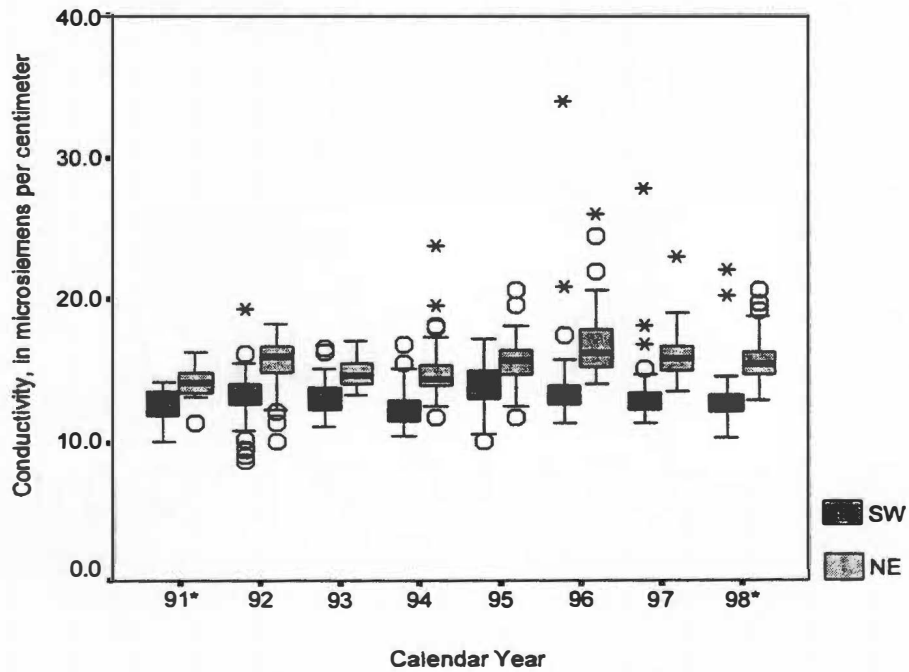
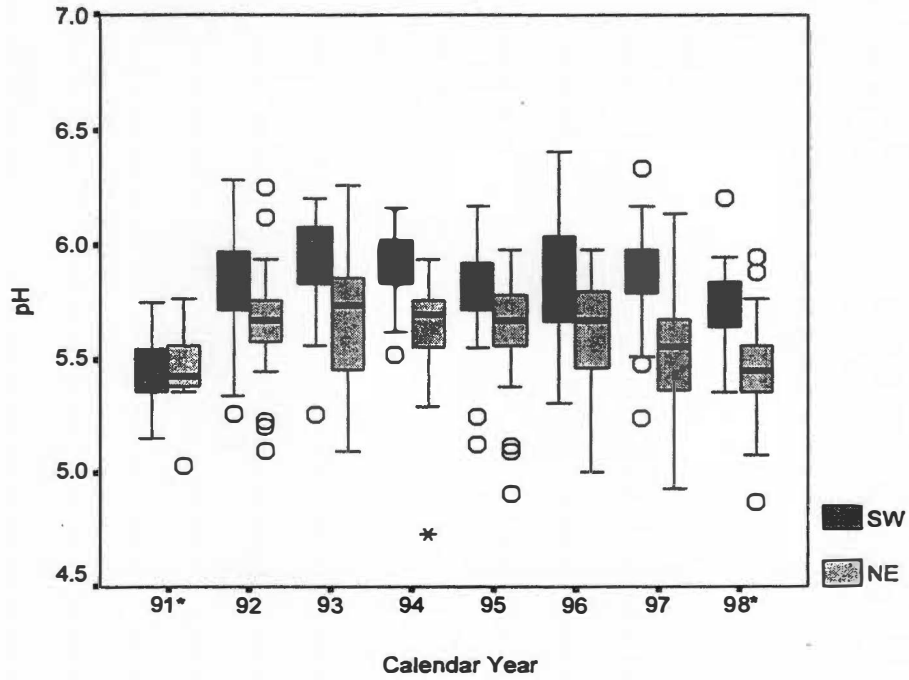
Extensive graphical analysis was not performed for temperature in both streams due to gaps in the record of data. However, from available data, the median stream temperature in the SW stream is about 7° C, while the median for the NE stream is several degrees higher, about 12° C. It should be noted that the conductivity probe on the Hydrolab unit uses the temperature probe to provide temperature-corrected readings. As a result, when the temperature probe is not functioning, which sometimes occurs in very cold weather, conductivity data may not be as reliable. During these times, conductivity readings remain constant at the last value recorded when the temperature probe was functioning. After comparing field conductivity data with lab conductivity data during times when the temperature probe was and was not working, it was determined that the field and lab conductivity differ by about 15-20%, on average, regardless of the status of the temperature probe. Given that conductivity is already relatively low in both streams, is variable regardless of the status of the temperature probe, and that the periods when the temperature probe is not functioning usually last less than one day, continuous conductivity data is still considered

acceptable and is used for forming mass transport models in Chapter VI.

Weekly Data

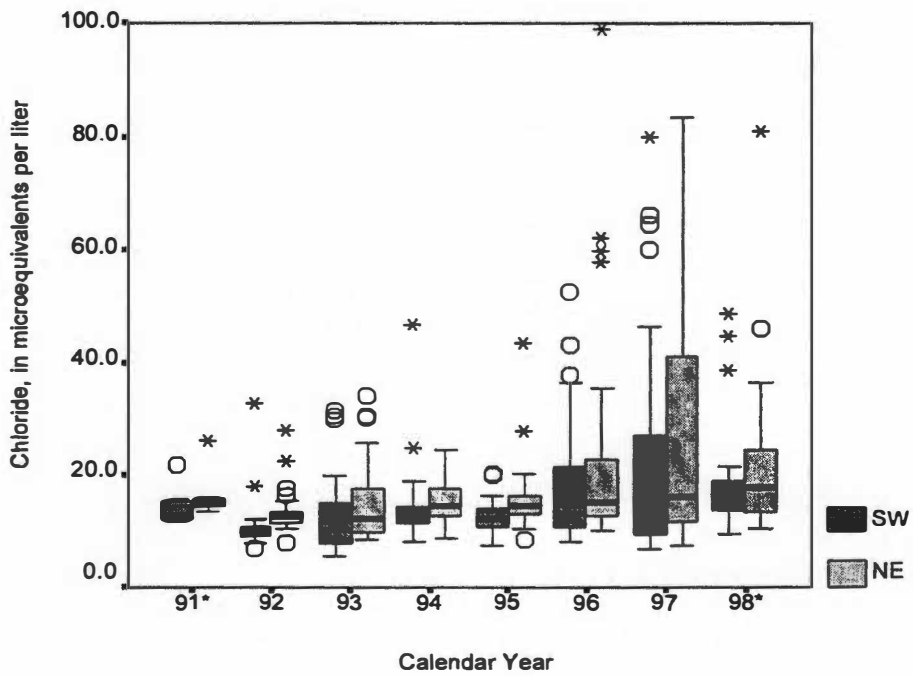
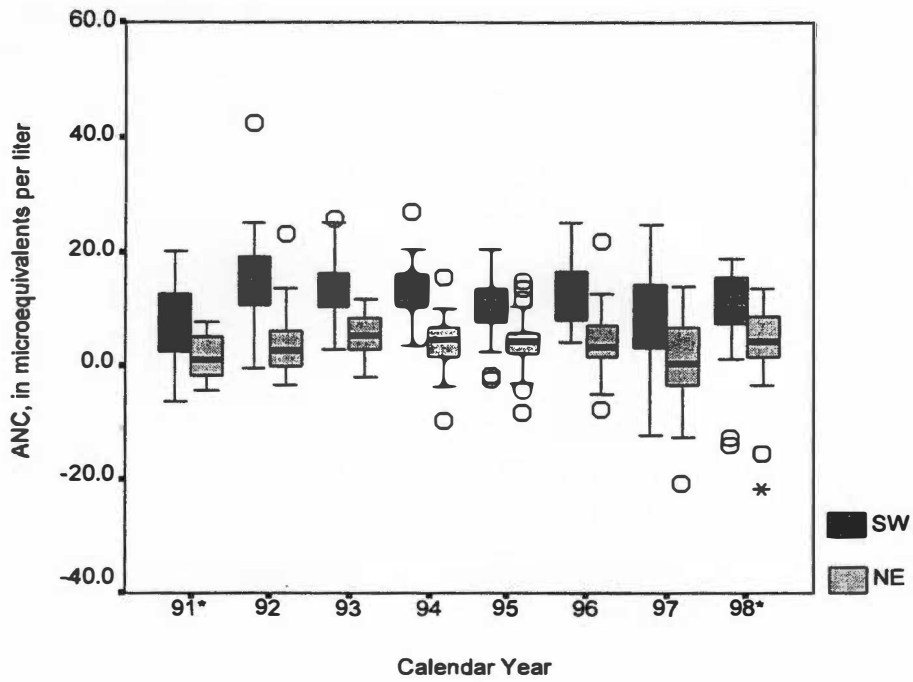
Distributions of weekly samples for each analyte are shown by year in Figure 4-10. It should be noted that only seven samples were collected in 1991; it is difficult to accurately compare analyte distributions for this year with those from other years due to the small sample size. In addition, data for 1998 extend only through August of that year. Therefore, more emphasis will be placed on trends that occur from 1992 to 1997. pH fluctuates slightly over the period of record, with the SW pH being consistently higher than the NE pH. Nitrate exhibits a very interesting overall trend. From 1991 through 1994, there is a distinct drop in stream nitrate levels. A somewhat similar trend is seen for sulfate, for which there was a decreasing trend from 1991 to 1993, then an increase in 1994 and subsequent “leveling” in concentration for the remaining period of record. Sodium shows an increase in concentration during the same early period, 1991-1994, and then levels out. Yearly trends for other constituents can be found in Figure 4-10. Statistical support for these time trends through multiple linear regression is presented in Chapter VI.

Distributions for each weekly sample analyte by season are shown in Figure 4-11. In addition, results of the Mann-Whitney U test to detect statistical differences in constituents among seasons for a given stream are shown in Tables 4-1 and 4-2. These tables report the significance level, or p-value, of the comparison of constituent distributions between any two seasons. The null hypothesis in these tests is that constituent distributions for any two seasons have the same median. If the p-value is greater than the chosen α level of 0.05, the null hypothesis should be accepted,



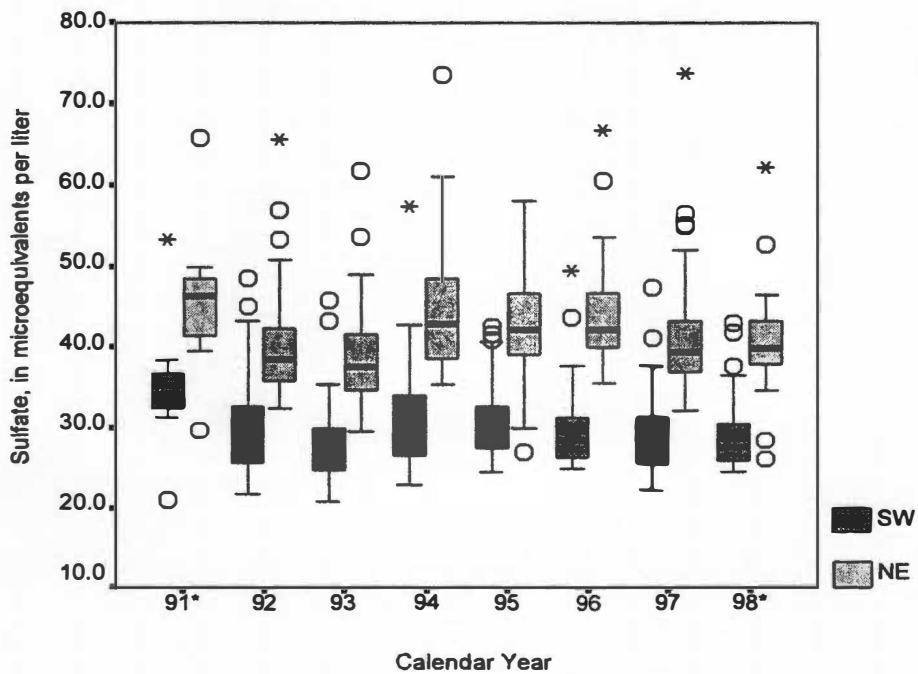
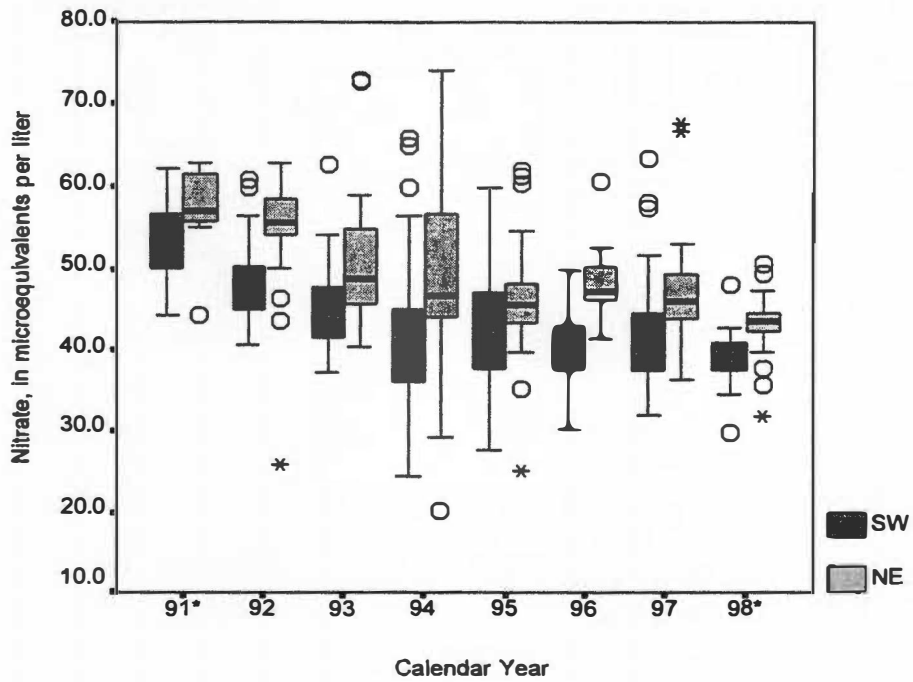
*Indicates partial year

Figure 4-10. Distributions of weekly sample constituent concentrations by year for the SW and NE streamlets, 1991-1998.



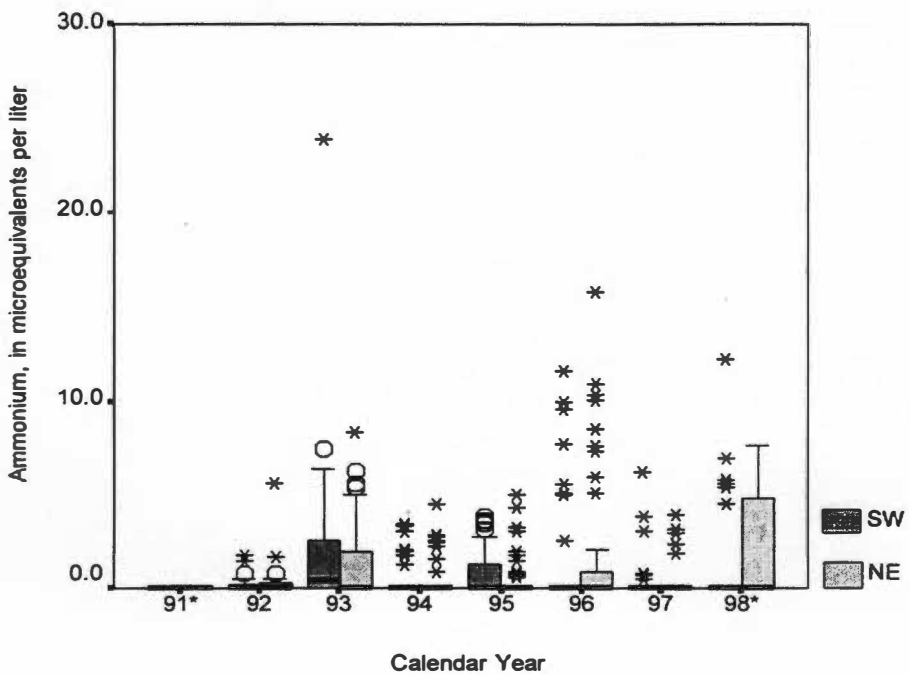
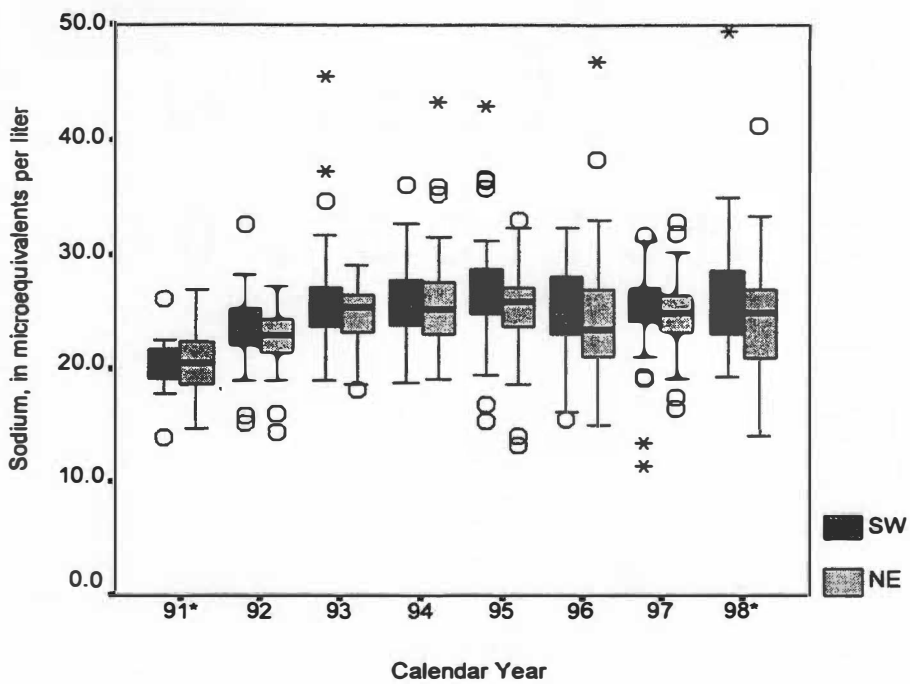
*Indicates partial year

Figure 4-10 (continued). Distributions of weekly sample constituent concentrations by year for the SW and NE streamlets, 1991-1998.



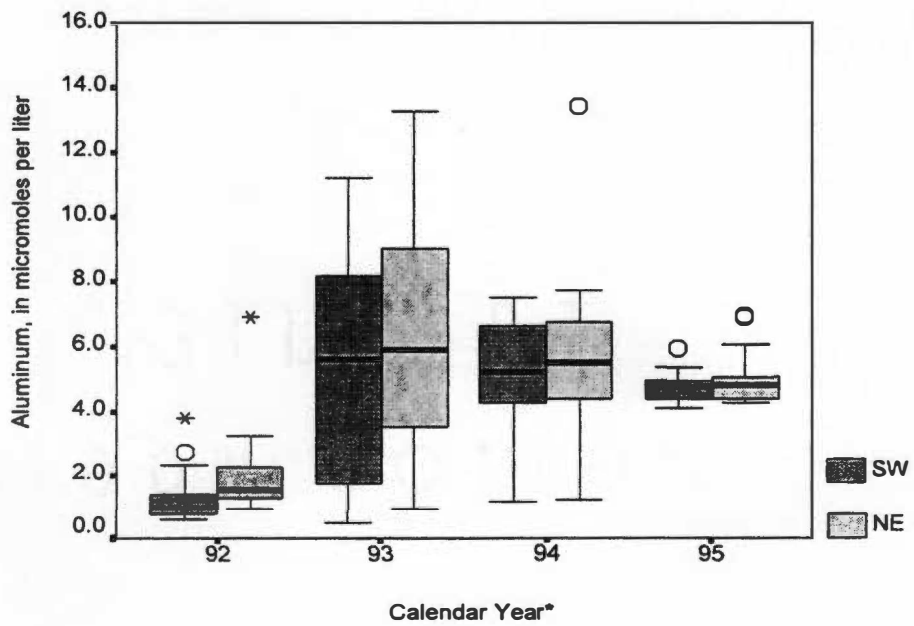
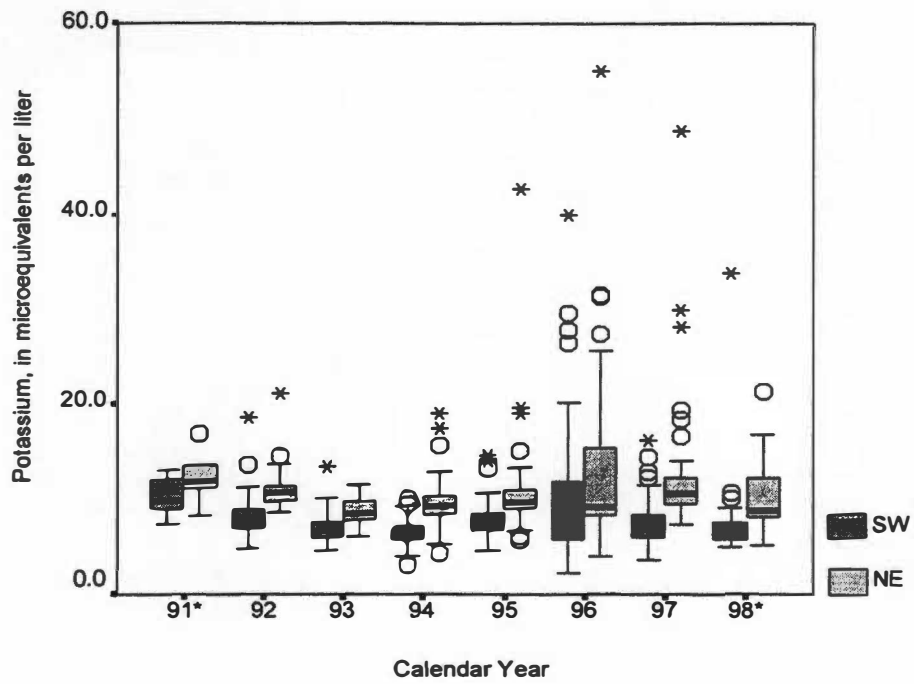
*Indicates partial year

Figure 4-10 (continued). Distributions of weekly sample constituent concentrations by year for the SW and NE streamlets, 1991-1998.



*Indicates partial year

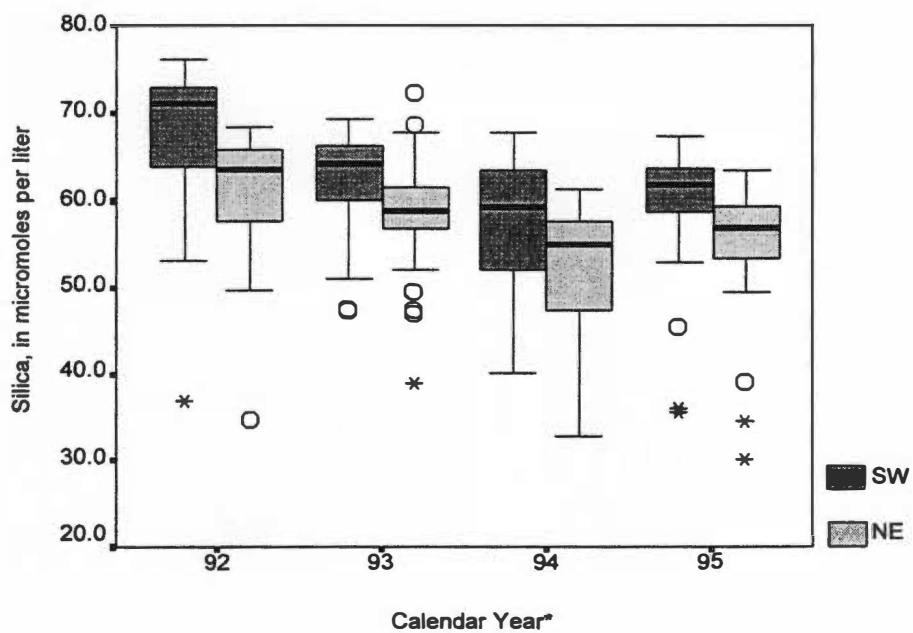
Figure 4-10 (continued). Distributions of weekly sample constituent concentrations by year for the SW and NE streamlets, 1991-1998.



*Aluminum data available only for 1992 - 1995

*Indicates partial year

Figure 4-10 (continued). Distributions of weekly sample constituent concentrations by year for the SW and NE streamlets, 1991-1998.



*Silica data available only for 1992-1995

Figure 4-10 (continued). Distributions of weekly sample constituent concentrations by year for the SW and NE streamlets, 1991-1998.

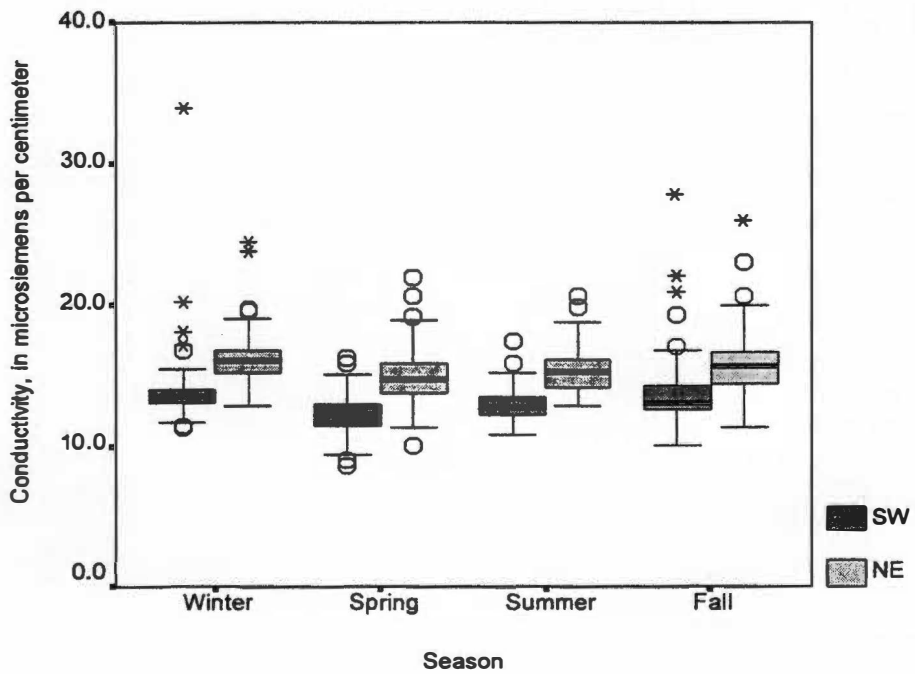
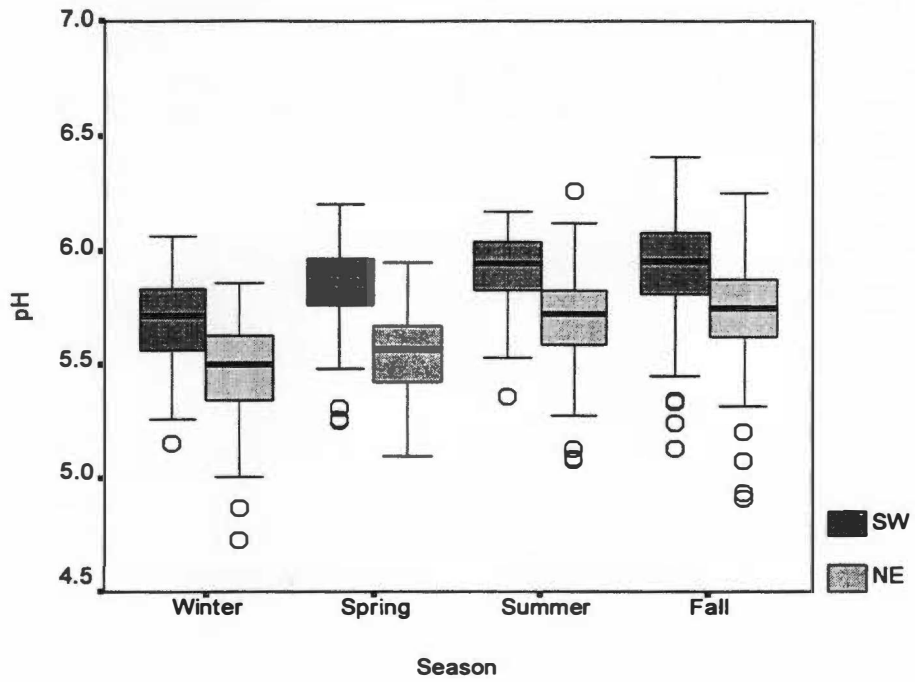


Figure 4-11. Distributions of weekly sample constituent concentrations by season for the SW and NE streamlets, 1991-1998.

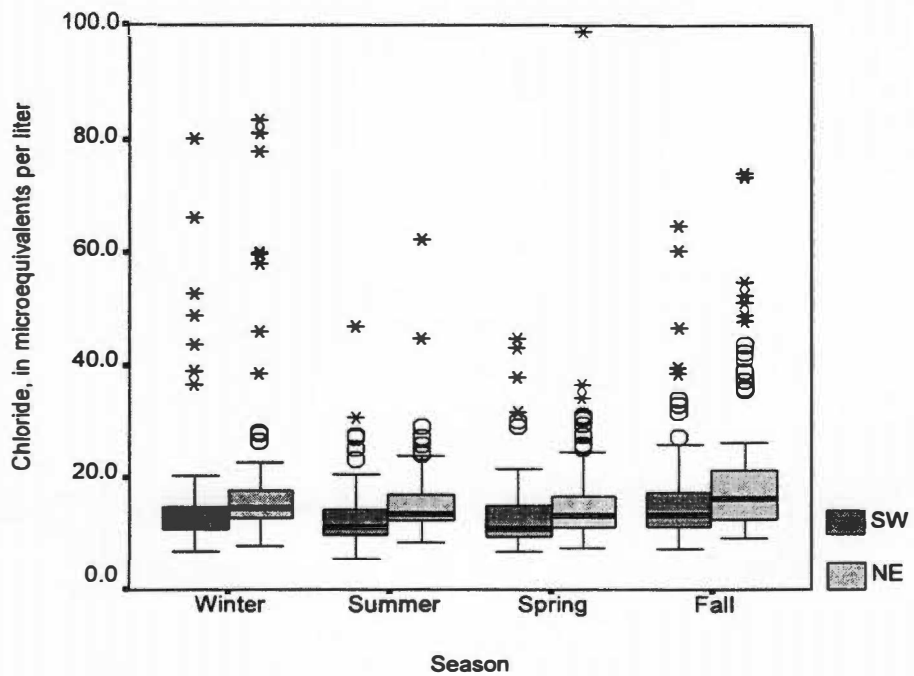
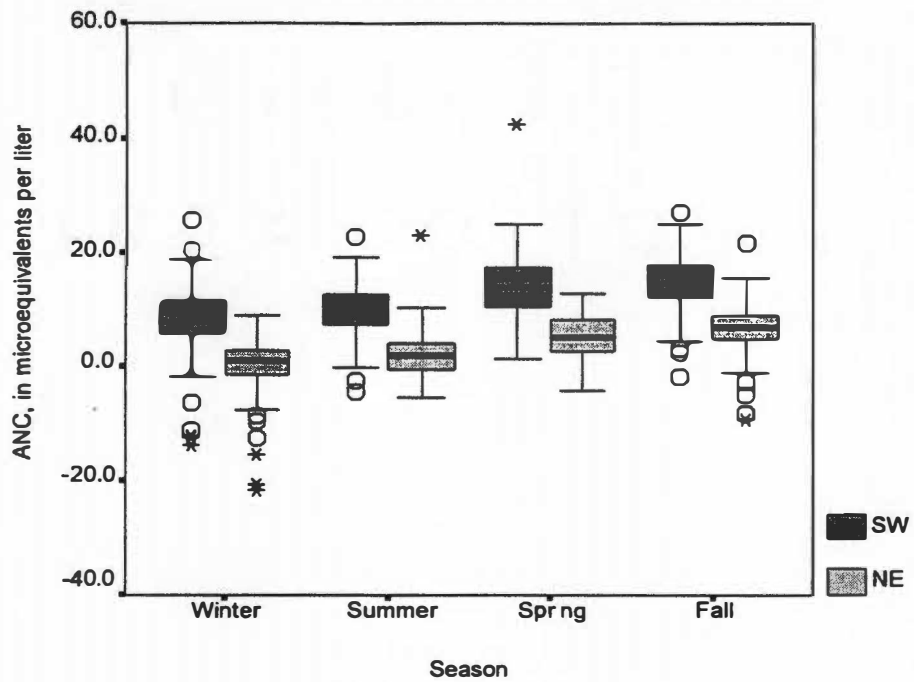


Figure 4-11 (continued). Distributions of weekly sample constituent concentrations by season for the SW and NE streamlets, 1991-1998.

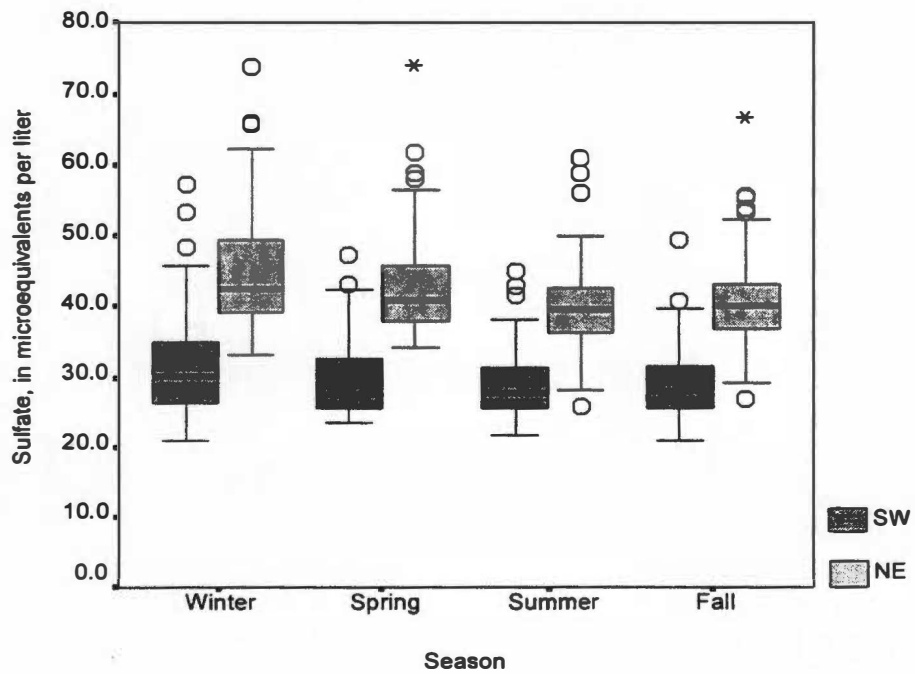
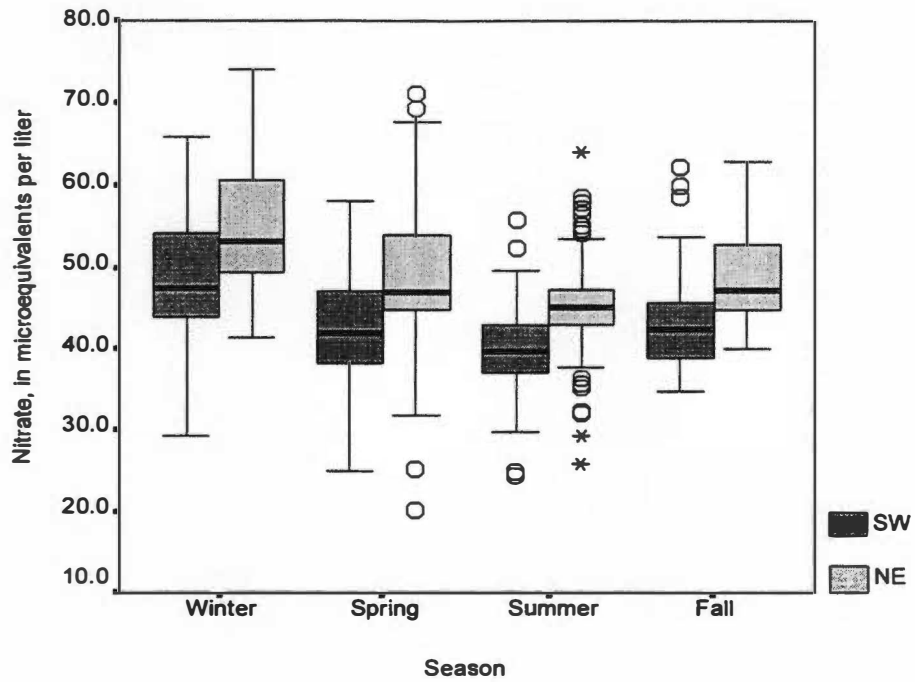


Figure 4-11 (continued). Distributions of weekly sample constituent concentrations by season for the SW and NE streamlets, 1991-1998.

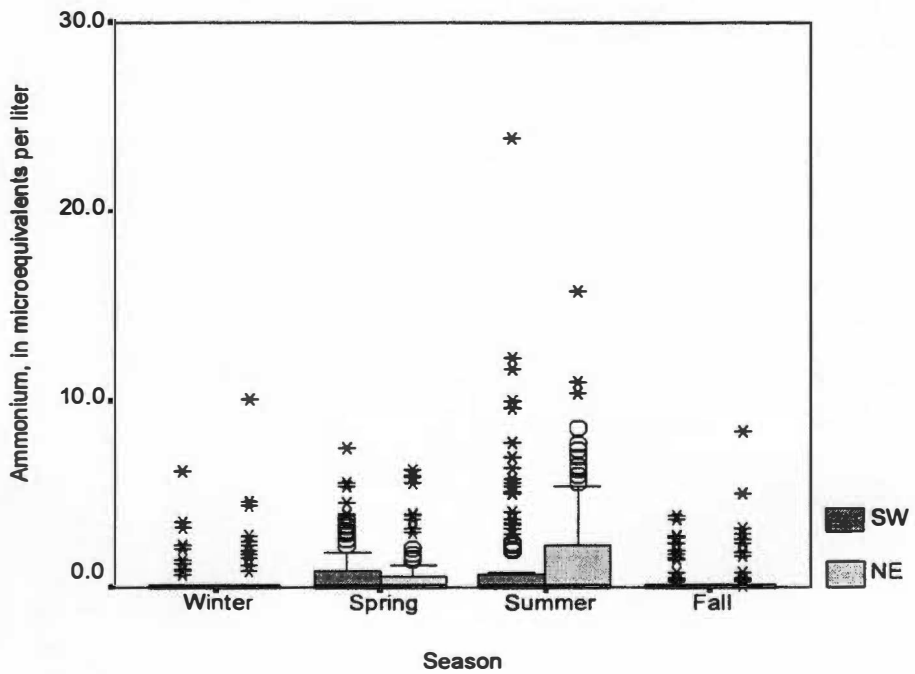
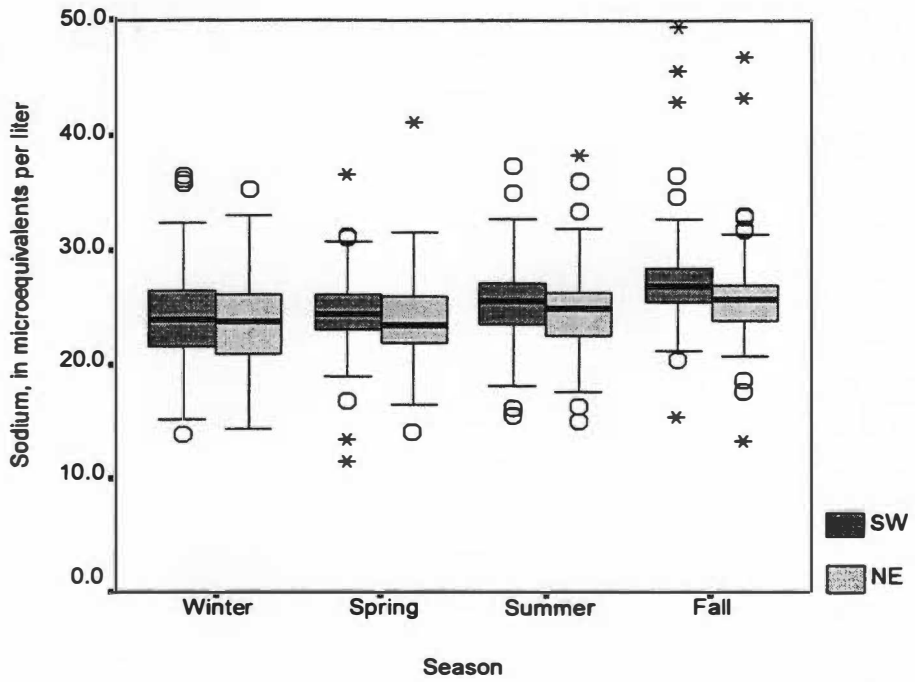


Figure 4-11 (continued). Distributions of weekly sample constituent concentrations by season for the SW and NE streamlets, 1991-1998.

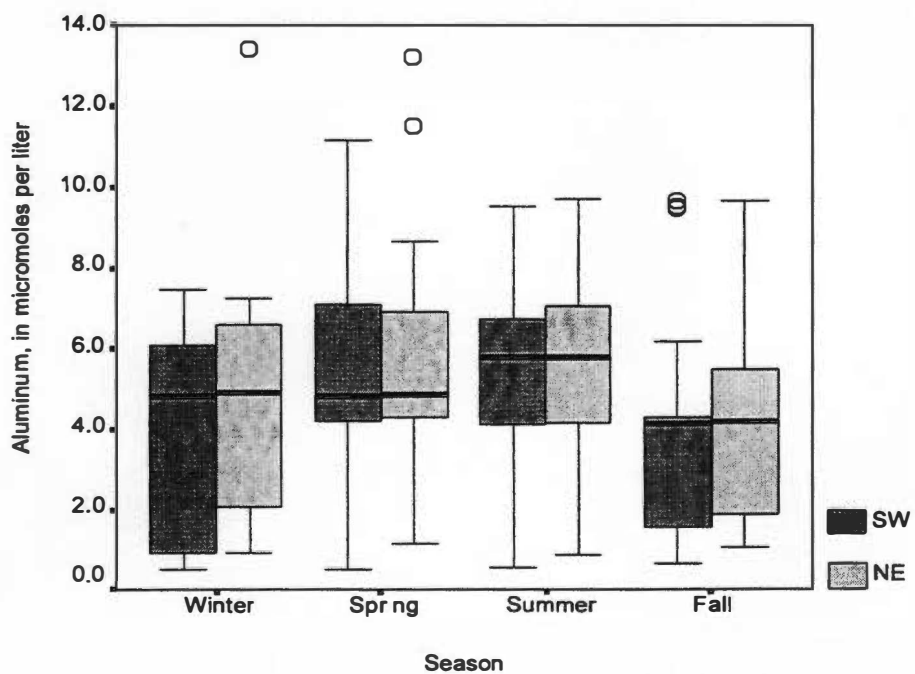
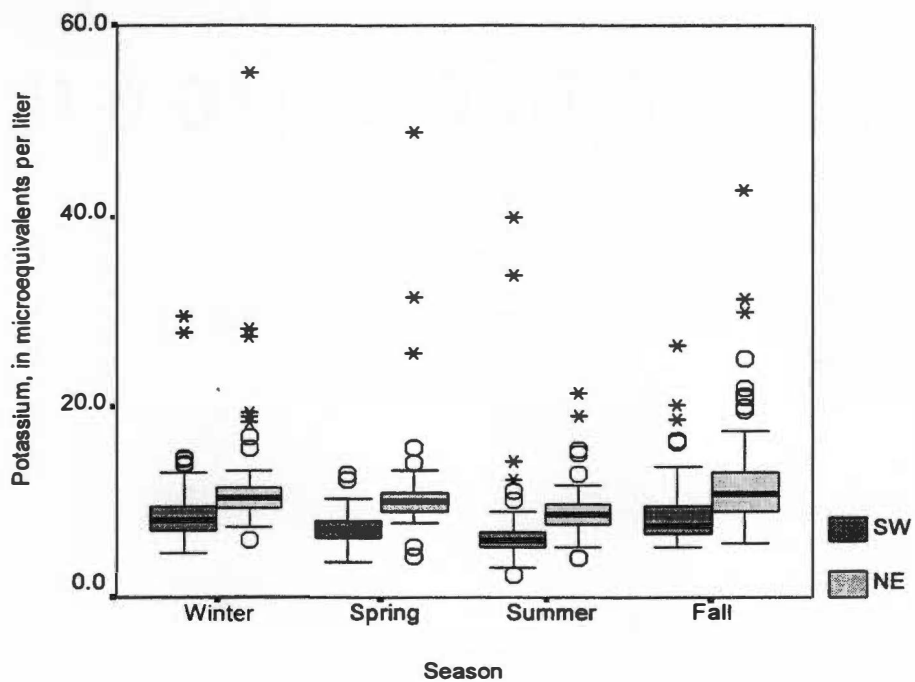


Figure 4-11 (continued). Distributions of weekly sample constituent concentrations by season for the SW and NE streamlets, 1991-1998.

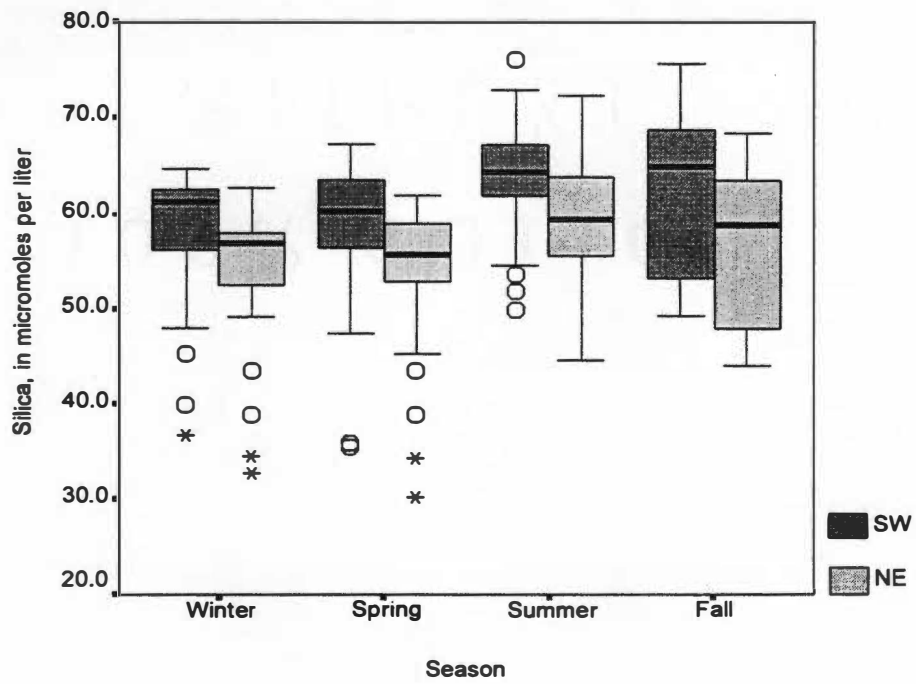


Figure 4-11 (continued). Distributions of weekly sample constituent concentrations by season for the SW and NE streamlets, 1991-1998.

Table 4-1. Statistical differences in weekly sample analytes by season for the SW stream.

| Stream | Constituent | Season Combination | | | | | |
|--------|--------------|--------------------|---------------|------------------|------------------|------------------|------------------|
| | | Winter- Spring | Winter-Summer | Winter-Fall | Spring-Summer | Spring-Fall | Summer-Fall |
| SW | Flow | p = 0.446 | p = 0.000 | p = 0.000 | p = 0.000 | p = 0.000 | p = 0.433 |
| | pH | p = 0.000 | p = 0.000 | p = 0.000 | p = 0.006 | p = 0.002 | p = 0.371 |
| | Conductivity | p = 0.000 | p = 0.000 | p = 0.208 | p = 0.000 | p = 0.000 | p = 0.014 |
| | ANC | p = 0.041 | p = 0.000 | p = 0.000 | p = 0.000 | p = 0.000 | p = 0.271 |
| | Chloride | p = 0.017 | p = 0.011 | p = 0.320 | p = 0.759 | p = 0.002 | p = 0.001 |
| | Nitrate | p = 0.000 | p = 0.000 | p = 0.000 | p = 0.004 | p = 0.689 | p = 0.000 |
| | Sulfate | p = 0.029 | p = 0.017 | p = 0.016 | p = 0.864 | p = 0.991 | p = 0.952 |
| | Sodium | p = 0.730 | p = 0.023 | p = 0.000 | p = 0.014 | p = 0.000 | p = 0.001 |
| | Ammonium | p = 0.077 | p = 0.028 | p = 0.312 | p = 0.539 | p = 0.332 | p = 0.170 |
| | Potassium | p = 0.000 | p = 0.000 | p = 0.389 | p = 0.000 | p = 0.003 | p = 0.000 |
| | Hydrogen Ion | p = 0.000 | p = 0.000 | p = 0.000 | p = 0.001 | p = 0.000 | p = 0.993 |
| | Aluminum | p = 0.068 | p = 0.035 | p = 0.311 | p = 0.868 | p = 0.000 | p = 0.001 |
| | Silica | p = 0.688 | p = 0.000 | p = 0.000 | p = 0.000 | p = 0.001 | p = 0.919 |

Note: P-values are bolded and boxes are shaded if the constituent distributions are statistically equal for the two seasons listed

Table 4-2. Statistical differences in weekly sample analytes by season for the NE stream.

| Stream | Constituent | Season Combination | | | | | |
|--------|--------------|--------------------|------------------|------------------|------------------|------------------|------------------|
| | | Winter-Spring | Winter-Summer | Winter-Fall | Spring-Summer | Spring-Fall | Summer-Fall |
| NE | Flow | p = 0.210 | p = 0.000 | p = 0.000 | p = 0.000 | p = 0.000 | p = 0.329 |
| | pH | p = 0.017 | p = 0.000 | p = 0.000 | p = 0.000 | p = 0.000 | p = 0.191 |
| | Conductivity | p = 0.000 | p = 0.002 | p = 0.140 | p = 0.032 | p = 0.002 | p = 0.157 |
| | ANC | p = 0.081 | p = 0.000 | p = 0.000 | p = 0.000 | p = 0.000 | p = 0.040 |
| | Chloride | p = 0.111 | p = 0.008 | p = 0.352 | p = 0.297 | p = 0.008 | p = 0.000 |
| | Nitrate | p = 0.000 | p = 0.000 | p = 0.000 | p = 0.000 | p = 0.929 | p = 0.000 |
| | Sulfate | p = 0.116 | p = 0.000 | p = 0.002 | p = 0.014 | p = 0.091 | p = 0.566 |
| | Sodium | p = 0.849 | p = 0.065 | p = 0.000 | p = 0.064 | p = 0.000 | p = 0.019 |
| | Ammonium | p = 0.504 | p = 0.030 | p = 0.846 | p = 0.111 | p = 0.296 | p = 0.016 |
| | Potassium | p = 0.155 | p = 0.000 | p = 0.513 | p = 0.000 | p = 0.074 | p = 0.000 |
| | Hydrogen Ion | p = 0.035 | p = 0.000 | p = 0.000 | p = 0.000 | p = 0.000 | p = 0.630 |
| | Aluminum | p = 0.195 | p = 0.127 | p = 0.185 | p = 0.751 | p = 0.003 | p = 0.020 |
| | Silica | p = 0.832 | p = 0.002 | p = 0.014 | p = 0.001 | p = 0.017 | p = 0.311 |

Note: P-values are bolded and boxes are shaded if the constituent distributions are statistically equal for the two seasons listed

and the constituent distributions are statistically similar for the two seasons tested.

In Figure 4-11, the graph of pH shows an increasing trend through the year, with the lowest values in the winter and highest values in the fall; these two seasons are statistically different ($p = 0.000$) with respect to pH. ANC also increases as the year elapses, with the lowest values and the most outliers occurring in the winter. ANC distributions are statistically different for all season combinations except for winter-spring for the NE stream and summer-fall for the SW stream. Conductivity is lowest in the spring and highest in the winter, and conductivity distributions for these two seasons are statistically different ($p = 0.000$). For nitrate, there is greater variability in the winter and spring; concentrations for this analyte are also higher during this period. Nitrate concentrations reach a low in the summer, during the growing season, and then start to rise again in the fall, when vegetation starts to become dormant. Nitrate distributions are statistically different for all seasons except spring and fall, when they are highly similar ($p = 0.929$ for NE stream). Sulfate concentrations are statistically lowest in the summer and highest in the winter, and sulfate distributions are statistically different ($p = 0.000$ for NE stream) for these seasons. Sodium exhibits a slight increasing trend throughout the year. Aluminum and silica both exhibit fairly wide distributions. Aluminum is highest in the summer and lowest in the fall, and these two seasons produce statistically different ($p = 0.001$ for NE stream) aluminum distributions. It is surprising that aluminum does not follow the same statistical patterns as pH, as it is hypothesized that aluminum is mobilized from the soil as pH decreases, usually during rainfall events. Silica increases fairly steadily throughout the year; it follows the same statistical pattern as flow in that distributions are statistically similar for winter-spring and for summer-fall. In most cases, the NE stream receives

the higher analyte concentrations. The SW stream, however, receives higher silica concentrations. Seasonal relationships for other constituents can be found in Figure 4-11 and Tables 4-1 and 4-2.

Distributions for each analyte by month are shown in Figure 4-12. The graph for pH shows that it reaches a high in October, which is one of the periods of least rainfall, and a low in December and January. As expected, ANC also follows this trend. Conductivity is lowest in May and highest in December, though again, there is little overall change throughout the year. Nitrate is highest in December and January, again when most vegetation is dormant and nitrate is allowed to build up in the soil, and is lowest in May, June, and July, which is the growing season. Sulfate is lowest in July and is highest in December. Sodium is highest in October, probably because of predominantly baseflow conditions, and is lowest in December and January. Ammonium shows greater variability and high outliers in June and July. As with the seasonal distributions, aluminum and silica both exhibit wide distributions throughout the year. Aluminum appears to be highest in April and lowest in August and September, while silica is highest in September and the other late summer/early fall months and is lowest in May and the other spring months. No significant monthly trends are observed for potassium.

More support for seasonal trends is made through a regression analysis with seasonality terms (sine θ and cosine θ) only on weekly data loads and concentrations. Tables 4-3 and 4-4 show results of this regression analysis. Results for both loads and concentrations are presented here; however, since this chapter focuses mainly on concentration data, further discussion of trends in loads can be found in Chapter VI. Figure 4-13 shows scatter plots of actual nitrate and hydrogen ion weekly sample concentration data and predicted values from the regression analysis.

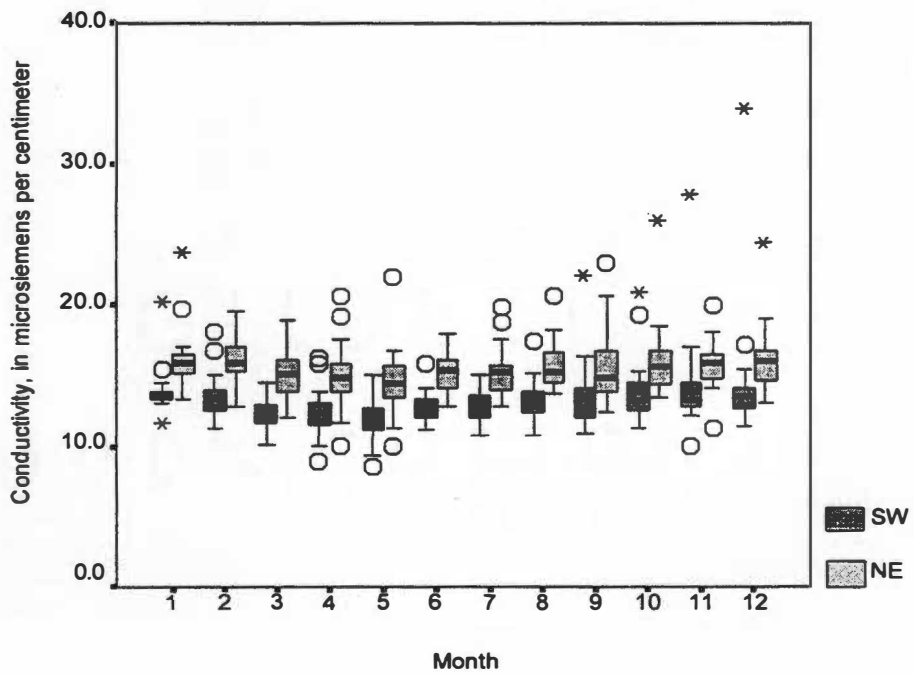
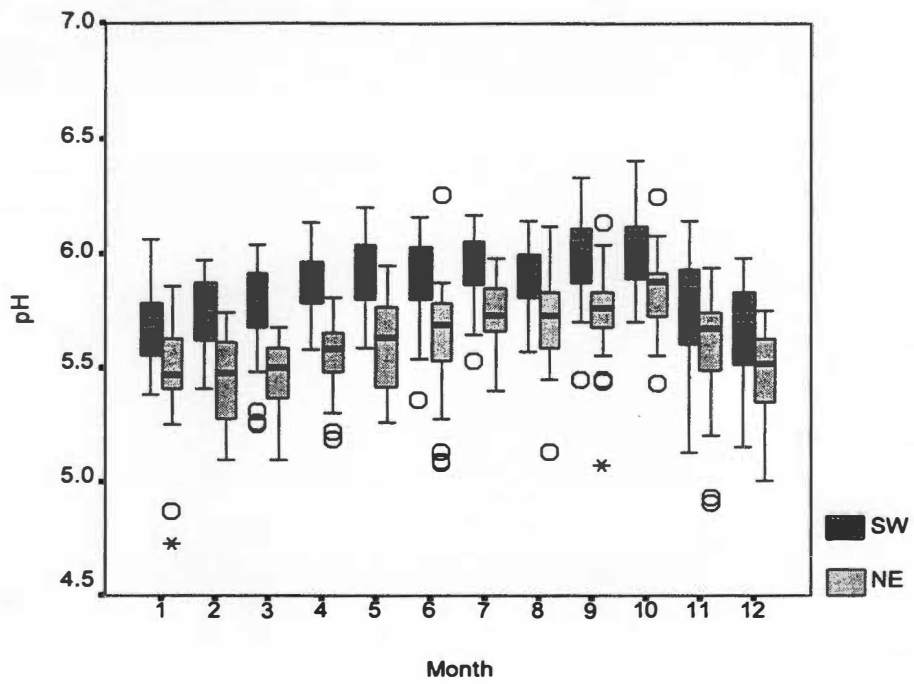


Figure 4-12. Distributions of weekly sample constituent concentrations by month for the SW and NE streamlets, 1991-1998.

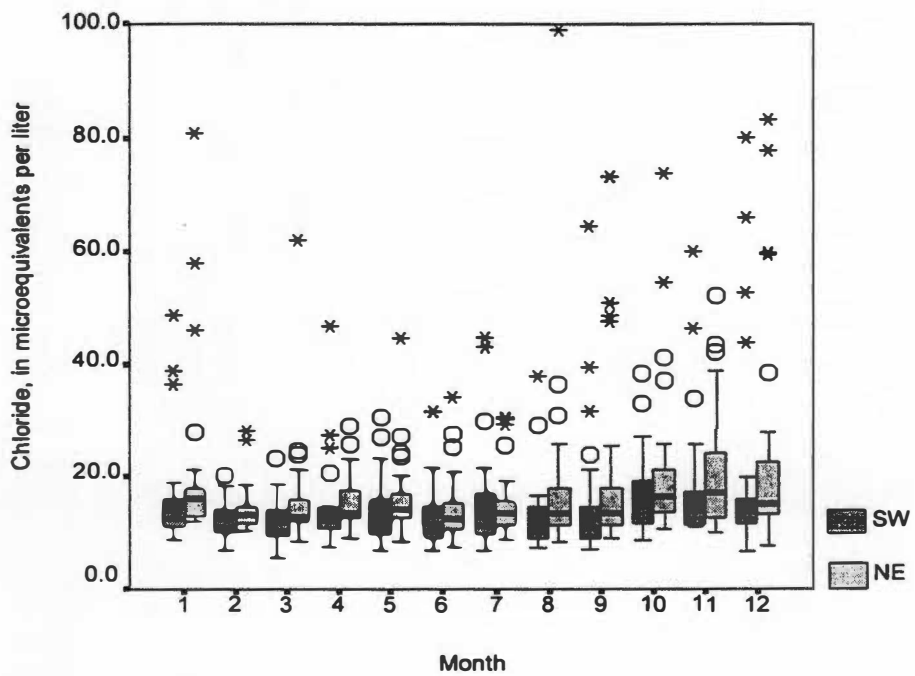
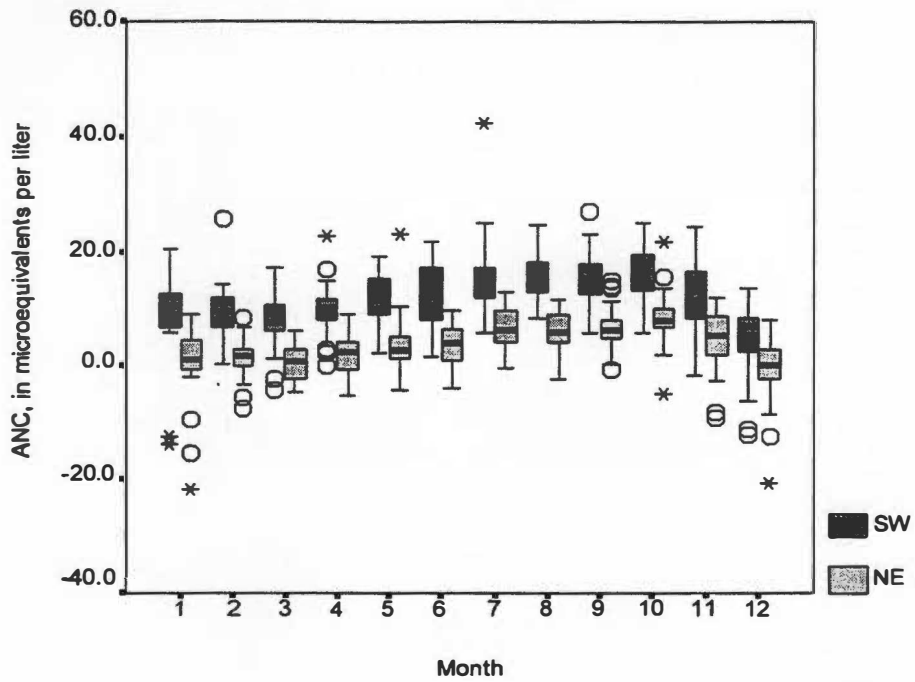


Figure 4-12 (continued). Distributions of weekly sample constituent concentrations by month for the SW and NE streamlets, 1991-1998.

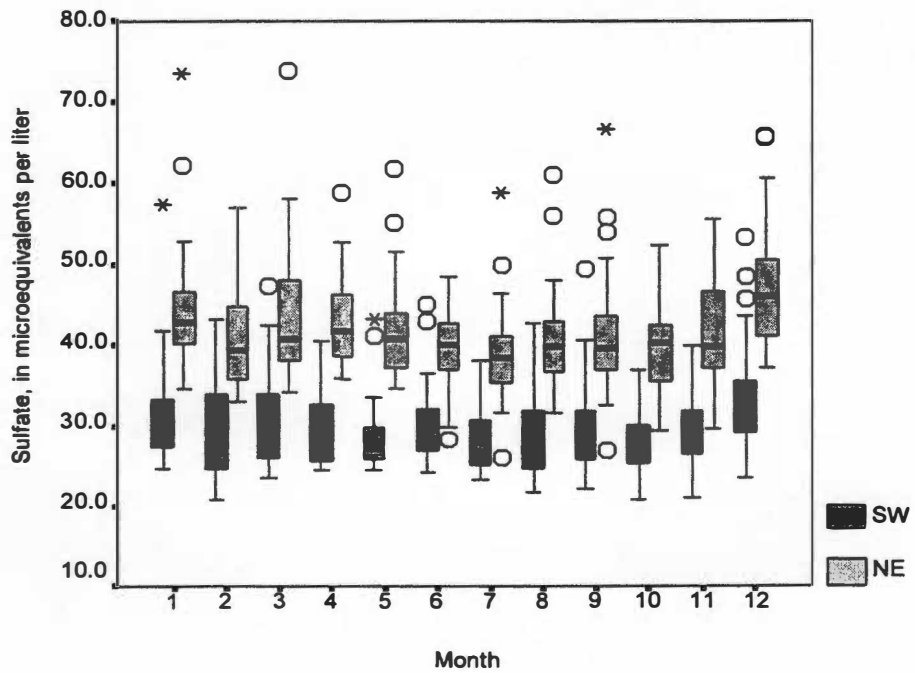
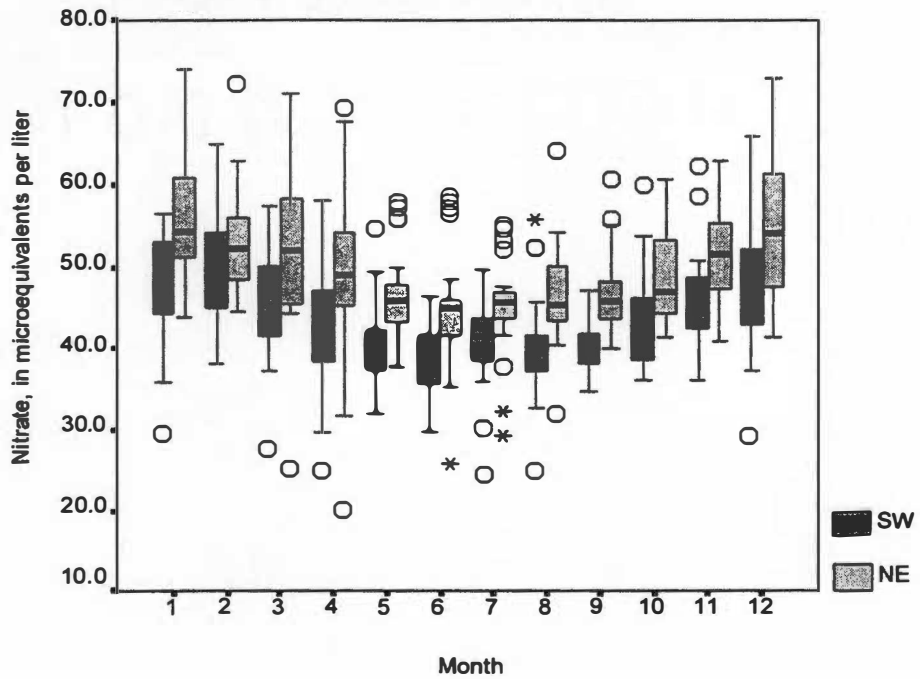


Figure 4-12 (continued). Distributions of weekly sample constituent concentrations by month for the SW and NE streamlets, 1991-1998.

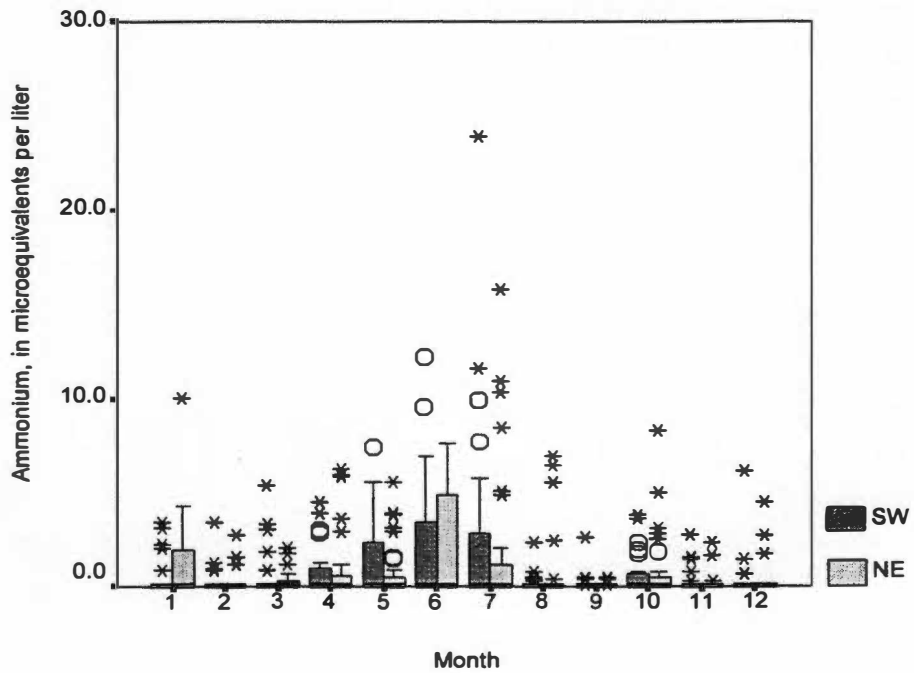
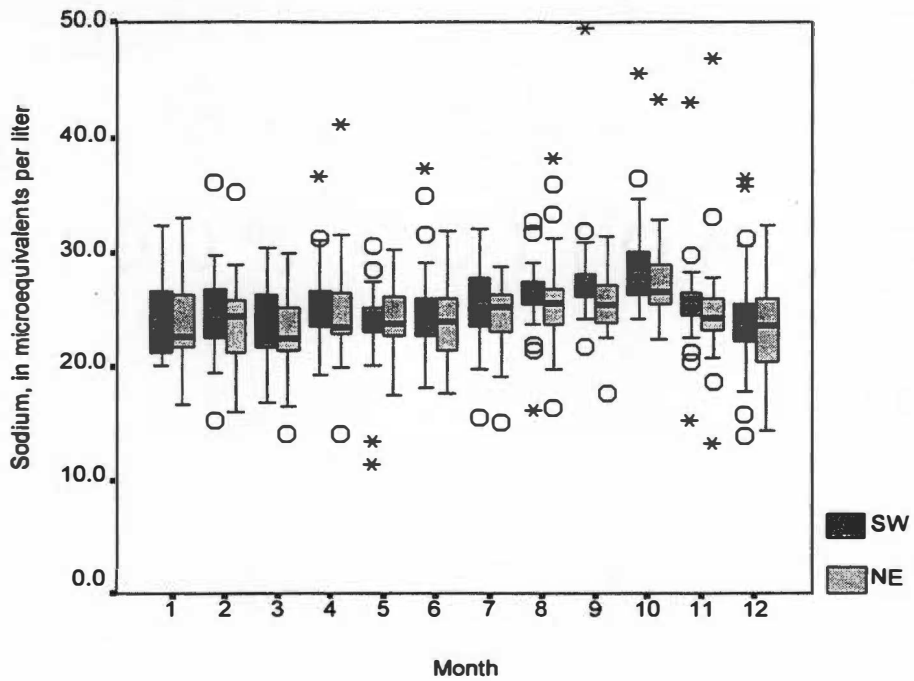


Figure 4-12 (continued). Distributions of weekly sample constituent concentrations by month for the SW and NE streamlets, 1991-1998.

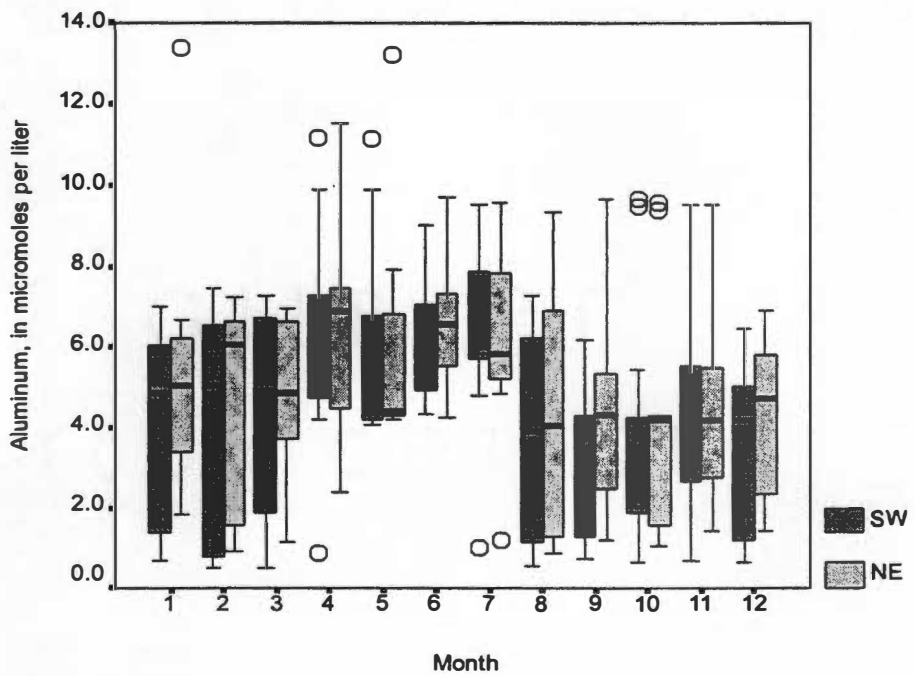
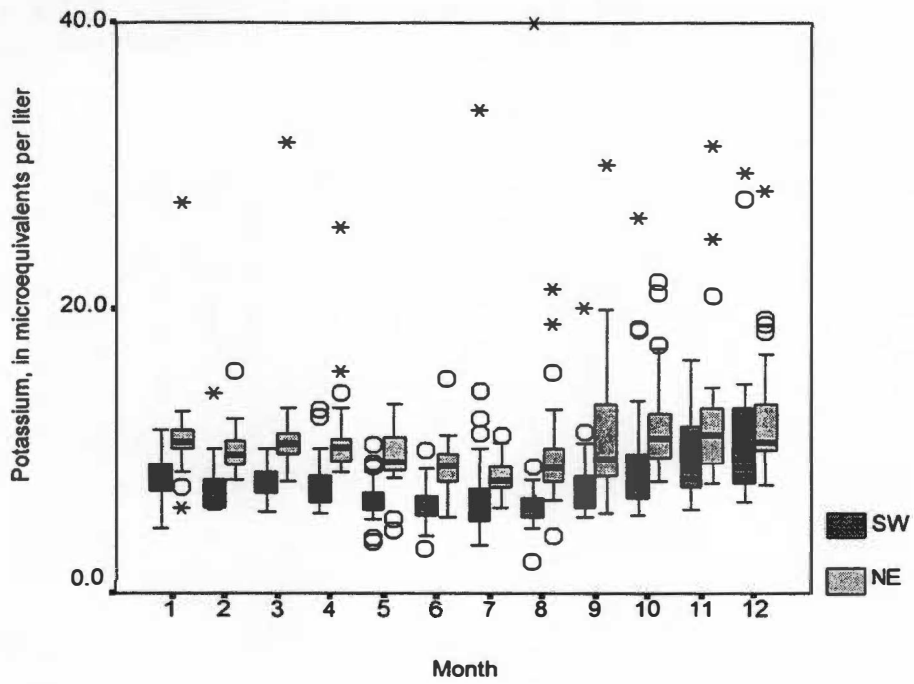


Figure 4-12 (continued). Distributions of weekly sample constituent concentrations by month for the SW and NE streamlets, 1991-1998.

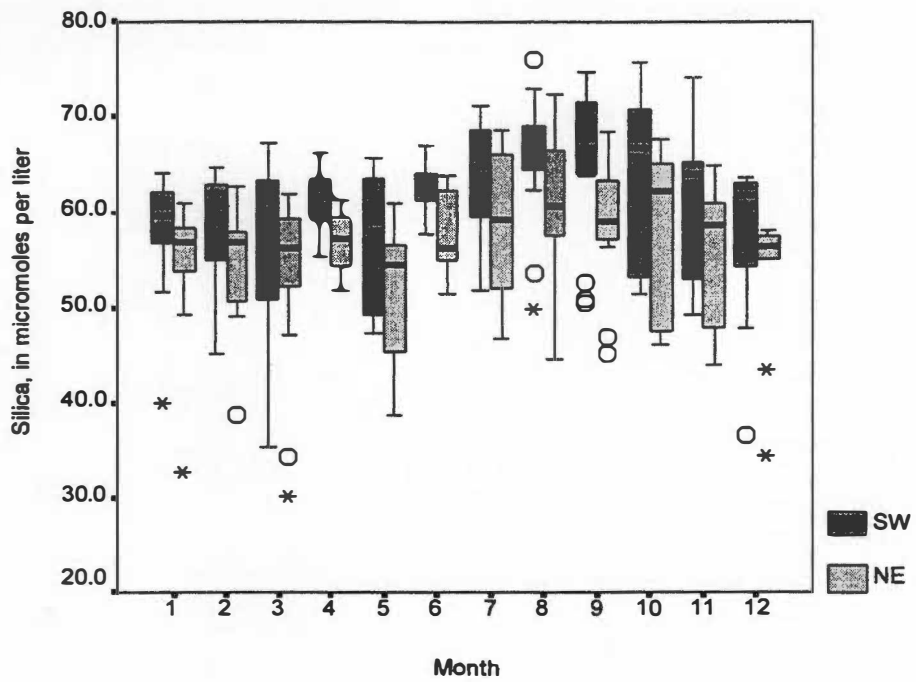


Figure 4-12 (continued). Distributions of weekly sample constituent concentrations by month for the SW and NE streamlets, 1991-1998.

Table 4-3. Coefficients of the concentration regression model with seasonality only and times of year when seasonality function reaches maximum and minimum values.

| Analyte (conc.) | Coeff. on Sin θ (b_2) | Coeff. on Cos θ (b_1) | b_1/b_2 | Approx. Day of Maximum | Approx. Day of Minimum | Amplitude/Range ($\mu\text{eq/L}$) |
|-----------------|----------------------------------|----------------------------------|-----------|------------------------|------------------------|--------------------------------------|
| Chloride | -0.09663 | 0.101 | -1.045 | Nov 16 | May 18 | 3.72 |
| Nitrate | 0.02630 | 0.103 | 3.916 | Jan 15 | July 17 | 9.15 |
| Sulfate | 0.01294 | 0.03477 | 2.687 | Jan 22 | July 21 | 2.17 |
| Sodium | -0.06557 | -0.01169 | 0.178 | Sept 21 | Mar 21 | 3.35 |
| Ammonium | 0.527 | -0.470 | -0.892 | May 14 | Nov 11 | 2.78 |
| Potassium | -0.06147 | 0.189 | -3.075 | Dec 13 | June 13 | 3.03 |
| Hydrogen Ion | 0.155 | 0.266 | 1.716 | Jan 31 | Aug 1 | 0.90 |
| Aluminum | 0.234 | -0.288 | -1.231 | May 23 | Nov 22 | 2.74* |
| Silica | -0.05303 | -0.04463 | 0.842 | Aug 21 | Feb 19 | 8.37* |

*Units of amplitude for aluminum and silica are given in $\mu\text{mol/L}$.

Table 4-4. Coefficients of the load regression model with seasonality only and times of year when seasonality function reaches maximum and minimum values.

| Analyte (load) | Coeff. on Sin θ (b_2) | Coeff. on Cos θ (b_1) | b_1/b_2 | Approx. Day of Maximum | Approx. Day of Minimum | Amplitude/Range (eq/sec) |
|----------------|----------------------------------|----------------------------------|-----------|------------------------|------------------------|--------------------------|
| Chloride | 0.241 | 0.407 | 1.689 | Jan 31 | Aug 1 | 4.42E-5 |
| Nitrate | 0.364 | 0.409 | 1.124 | Feb 10 | Aug 11 | 1.68E-4 |
| Sulfate | 0.351 | 0.340 | 0.969 | Feb 17 | Aug 17 | 1.00E-4 |
| Sodium | 0.272 | 0.293 | 1.077 | Feb 12 | Aug 14 | 7.01E-5 |
| Ammonium | 0.712 | -0.138 | -0.194 | Apr 12 | Oct 12 | 9.40E-6 |
| Potassium | 0.276 | 0.494 | 1.790 | Jan 29 | July 31 | 3.06E-5 |
| Hydrogen Ion | 0.493 | 0.571 | 1.158 | Feb 12 | Aug 12 | 8.06E-6 |
| Aluminum | 0.451 | -0.00956 | -0.0212 | Apr 1 | Oct 2 | 1.11E-5* |
| Silica | 0.170 | 0.206 | 1.212 | Feb 9 | Aug 11 | 1.09E-4* |

*Units of amplitude for aluminum and silica are given in mol/sec.

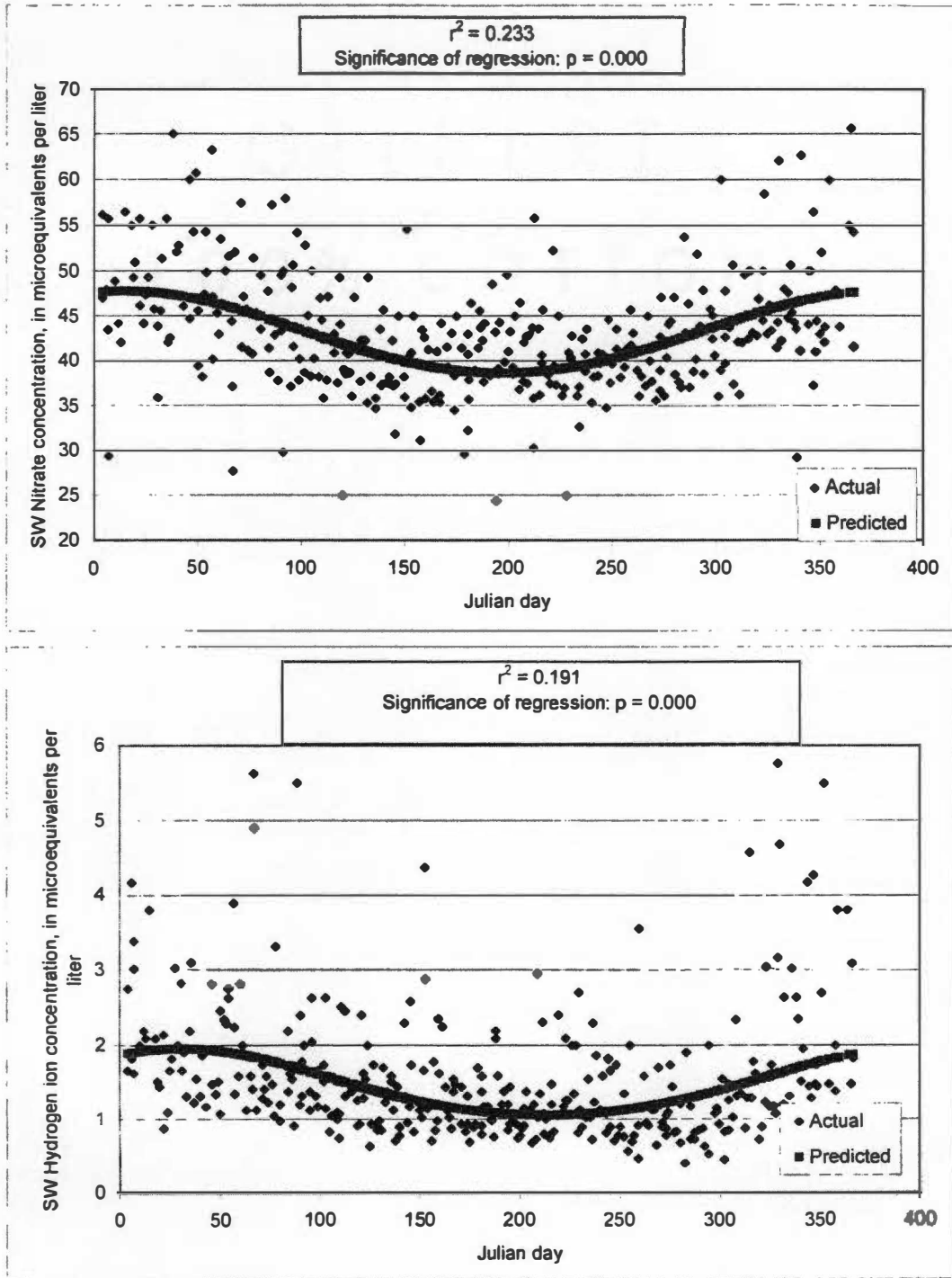


Figure 4-13. Seasonal sine/cosine wave functions for nitrate (top) and hydrogen ion (bottom) concentrations in the SW stream.

These constituents, particularly nitrate, are closely fit with the sine/cosine function and therefore exhibit distinct seasonal trends. These plots are presented for other constituents concentrations and loads in Figures A-3 and A-4 in the Appendix. Plotting the sine/cosine wave allows one to determine at what time of the year each constituent reaches maximum and minimum concentration or load. For example, for nitrate concentrations, the sine/cosine wave reaches a maximum around Julian day 15, or January 15, and reaches a minimum around Julian day 198, or July 17 (see Figure 4-13 and Table 4-3). Hydrogen ion concentrations reach a maximum around Julian day 31, or January 31, and reach a minimum around Julian day 213, or August 1. For all regressions, the overall regression and coefficients on the sine/cosine terms were significant at an α level = 0.05. The significance levels, or p-values, for the overall regressions are noted on each figure. Though r-squared values are low for each regression, this analysis still serves to explain some of the variability in the data. For example, seasonality explains approximately 23.3% of the variability, or a range (determined by the amplitude) of 9.15 $\mu\text{eq/L}$, in nitrate concentrations. Likewise, seasonality explains approximately 19.1% of the variability, or a range of 0.90 $\mu\text{eq/L}$, in hydrogen ion concentrations. Coefficients on the sine/cosine functions in Tables 4-3 and 4-4 can show whether concentration or load data more closely follow a sine wave or a cosine wave. For example, the coefficient ratio (b_1/b_2) for nitrate, 3.916, shows that the seasonal pattern matches a cosine wave four times more closely than it matches a sine wave. Results from the regression analysis agree with comments made earlier based on distribution plots; predicted maximum and minimum concentration values match closely with observed values.

Overall descriptive statistics for weekly sample concentration data are given for the SW

and NE streams in Tables 4-5 and 4-6, respectively. The order in which anions dominate streamwater chemistry at NDW is as follows:



The order in which cations dominate streamwater chemistry at NDW is as follows (excluding calcium and magnesium):



It is apparent that most of these weekly samples are captured during baseflow conditions, for the mean corresponding flow for both streams is very similar, while it is known from continuous data that flow is not always similar. Table 4-7 presents the results of non-parametric Mann-Whitney U tests that were performed on all weekly analyte concentrations and flow to determine whether the SW and NE streams are statistically different. These tests also show that flow corresponding to weekly samples is statistically the same ($p = 0.053$) for both streams. It is thought that the two streams are statistically different in flow during storm events; again, these events are generally not well represented in the weekly samples. With respect to stream chemistry, the SW and NE streams are statistically different for all analyte concentrations except ammonium ($p = 0.593$).

The constituent concentrations captured in the weekly samples are not all independent of

Table 4-5. Descriptive statistics of weekly sample data for the SW streamlet, 1991-1998.

| Constituent | Units | Median | Mean | Standard Deviation | Minimum | Maximum | Percentiles | | | |
|--------------|--------|--------|-------|-----------------------|---------|---------|-------------|-------|-------|-------|
| | | | | | | | 10th | 25th | 75th | 90th |
| Flow | cfs | 0.12 | 0.18 | 0.25 | 0.01 | 2.73 | 0.04 | 0.07 | 0.20 | 0.34 |
| pH | | 5.88 | 5.85 | 0.21 | 5.13 | 6.40 | 5.56 | 5.74 | 6.00 | 6.09 |
| Conductivity | μS/cm | 13.00 | 13.26 | 2.12 | 8.60 | 34.00 | 11.50 | 12.20 | 13.90 | 15.13 |
| ANC | μeq/L | 11.88 | 11.84 | 6.42 | -13.79 | 42.41 | 4.78 | 7.99 | 16.06 | 19.10 |
| Chloride | μeq/L | 11.84 | 14.81 | 9.43 | 5.64 | 79.98 | 8.74 | 10.04 | 15.19 | 23.11 |
| Nitrate | μeq/L | 42.43 | 43.14 | 6.72 | 24.37 | 65.72 | 36.03 | 38.47 | 46.51 | 52.12 |
| Sulfate | μeq/L | 28.27 | 29.66 | 5.54 | 20.79 | 57.36 | 24.37 | 25.72 | 32.66 | 36.70 |
| Sodium | μeq/L | 25.39 | 25.52 | 4.24 | 11.48 | 49.52 | 20.87 | 23.38 | 27.40 | 30.12 |
| Ammonium | μeq/L | 0.00 | 0.81 | 2.21 | 0.00 | 23.96 | 0.00 | 0.00 | 0.14 | 3.17 |
| Potassium | μeq/L | 7.12 | 8.14 | 5.38 | 2.28 | 77.82 | 5.39 | 6.05 | 8.54 | 11.02 |
| Hydrogen Ion | μeq/L | 1.32 | 1.61 | 1.00 | 0.40 | 7.41 | 0.81 | 1.00 | 1.82 | 2.75 |
| Aluminum | μmol/L | 4.74 | 4.61 | 2.57 | 0.48 | 11.18 | 0.79 | 2.80 | 6.23 | 7.36 |
| Silica | μmol/L | 63.06 | 61.03 | 7.79 | 35.54 | 76.06 | 50.57 | 56.78 | 65.57 | 69.32 |

Table 4-6. Descriptive statistics of weekly sample data for the NE streamlet, 1991-1998.

| Constituent | Units | Median | Mean | Standard Deviation | Minimum | Maximum | Percentiles | | | |
|--------------|--------|--------|-------|-----------------------|---------|---------|-------------|-------|-------|-------|
| | | | | | | | 10th | 25th | 75th | 90th |
| Flow | cfs | 0.12 | 0.22 | 0.45 | 0.01 | 5.02 | 0.03 | 0.06 | 0.22 | 0.39 |
| pH | | 5.65 | 5.61 | 0.24 | 4.73 | 6.26 | 5.30 | 5.47 | 5.77 | 5.88 |
| Conductivity | μS/cm | 15.48 | 15.60 | 1.95 | 10.00 | 26.07 | 13.60 | 14.40 | 16.50 | 17.66 |
| ANC | μeq/L | 3.90 | 3.62 | 5.25 | -21.57 | 22.92 | -2.44 | 0.75 | 7.07 | 9.60 |
| Chloride | μeq/L | 14.17 | 18.05 | 12.42 | 7.38 | 99.18 | 10.71 | 12.21 | 17.99 | 28.16 |
| Nitrate | μeq/L | 47.31 | 49.22 | 7.66 | 20.02 | 74.10 | 42.16 | 44.38 | 54.26 | 59.26 |
| Sulfate | μeq/L | 40.58 | 41.92 | 7.04 | 25.99 | 73.91 | 34.99 | 37.29 | 45.06 | 51.48 |
| Sodium | μeq/L | 24.58 | 24.64 | 4.06 | 13.29 | 46.89 | 19.87 | 22.55 | 26.45 | 28.86 |
| Ammonium | μeq/L | 0.00 | 0.85 | 2.07 | 0.00 | 15.74 | 0.00 | 0.00 | 0.28 | 3.11 |
| Potassium | μeq/L | 9.77 | 11.15 | 7.04 | 4.07 | 98.03 | 7.69 | 8.63 | 11.26 | 13.73 |
| Hydrogen Ion | μeq/L | 2.24 | 2.90 | 2.06 | 0.55 | 18.62 | 1.32 | 1.70 | 3.39 | 5.01 |
| Aluminum | μmol/L | 4.84 | 5.06 | 2.56 | 0.89 | 13.40 | 1.41 | 3.74 | 6.77 | 8.87 |
| Silica | μmol/L | 57.70 | 56.38 | 7.46 | 30.13 | 72.31 | 46.29 | 53.34 | 60.92 | 65.03 |

Table 4-7. Statistical differences between NE and SW weekly sample streamflow and water quality.

| Constituent | P-value for NE/SW comparison | NE/SW-Statistically same or different? |
|--------------|------------------------------|--|
| Flow | 0.053 | Same |
| pH | 0.000 | Different |
| Conductivity | 0.000 | Different |
| ANC | 0.000 | Different |
| Chloride | 0.000 | Different |
| Nitrate | 0.000 | Different |
| Sulfate | 0.000 | Different |
| Sodium | 0.000 | Different |
| Ammonium | 0.593 | Same |
| Potassium | 0.000 | Different |
| Hydrogen Ion | 0.000 | Different |
| Aluminum | 0.000 | Different |
| Silica | 0.000 | Different |

one another; in fact, many are directly- or inversely-related. Tables 4-8 and 4-9 show Pearson correlation coefficients for all combinations of constituents in the weekly samples for both the SW and NE streamlets. Values are reported only if they are significant at the $\alpha = 0.05$ confidence level and are bolded and shaded if significant at the $\alpha = 0.01$ level. For both streams, strong correlations exist ($\alpha = 0.01$) between flow and pH, ANC, nitrate, sulfate, sodium, and silica. Nitrate has strong correlations with flow and potassium, while sulfate has strong correlations with flow, pH, ANC, sodium, potassium, and silica. Aluminum and nitrate show no correlation with pH, which again contradicts hypothesized behavior for these analytes. In addition, aluminum and nitrate are negatively correlated, yet they are expected to be positively correlated. On the other hand, aluminum and sulfate are positively correlated, which supports the hypothesis that increased concentrations of acidic anions will mobilize aluminum from the soil. Relationships for other constituents can be found in the tables. Significance among constituents is different for the NE and SW streams; some analytes are significant for one stream but not the other, or are strongly significant ($\alpha = 0.01$) for one but less significant ($\alpha = 0.05$) for the other.

Discussion

Trends

Most of the trends in the continuous data can be explained by seasonality. In general, lower pH and higher conductivity are seen during months with more rainfall, and the opposite is seen during the drier months, under mainly baseflow conditions.

In the weekly data set, nitrate concentrations characterized by year show that from 1991 through 1994, there was a distinct drop in stream nitrate levels. A drop in soil nitrate levels also

Table 4-8. Pearson correlation coefficients for weekly sample constituents in the SW streamlet.

| | Flow (cfs) | pH | Cond. ($\mu\text{S}/\text{cm}$) | ANC | Cl | NO_3 | SO_4 | Na | NH_4 | K | Al ($\mu\text{mol}/\text{L}$) | Si ($\mu\text{mol}/\text{L}$) |
|-----------------------------------|---------------|---------------|-----------------------------------|---------------|--------------|---------------|---------------|--------------|---------------|---------------|---------------------------------|---------------------------------|
| Flow (cfs) | --- | | | | | | | | | | | |
| pH | -0.650 | --- | | | | | | | | | | |
| Cond. ($\mu\text{S}/\text{cm}$) | 0.169 | -0.292 | --- | | | | | | | | | |
| ANC | -0.501 | 0.598 | | --- | | | | | | | | |
| Cl | -0.147 | 0.151 | 0.188 | | --- | | | | | | | |
| NO_3 | -0.333 | | 0.303 | | | --- | | | | | | |
| SO_4 | 0.678 | -0.514 | 0.173 | -0.445 | | | --- | | | | | |
| Na | -0.504 | 0.417 | | 0.432 | 0.287 | 0.170 | -0.438 | --- | | | | |
| NH_4 | | | | | 0.201 | | | | --- | | | |
| K | 0.236 | -0.377 | -0.578 | | 0.187 | 0.339 | 0.245 | | | --- | | |
| Al ($\mu\text{mol}/\text{L}$) | | | -0.334 | | 0.249 | -0.242 | 0.167 | | 0.256 | -0.199 | --- | |
| Si ($\mu\text{mol}/\text{L}$) | -0.601 | 0.465 | | 0.472 | | 0.190 | -0.534 | 0.454 | | | -0.183 | --- |

All constituent concentrations are in $\mu\text{eq}/\text{L}$, unless otherwise noted

Note: Values are reported only if significant at the $\alpha = 0.05$ level; values are bolded and boxes are shaded if significant at the $\alpha = 0.01$ level

Table 4-9. Pearson correlation coefficients for weekly sample constituents in the NE streamlet.

| | Flow (cfs) | pH | Cond. (μS/cm) | ANC | Cl | NO ₃ | SO ₄ | Na | NH ₄ | K | Al (μmol/L) | Si (μmol/L) |
|-----------------|---------------|---------------|---------------|---------------|--------------|-----------------|-----------------|--------------|-----------------|---------------|---------------|-------------|
| Flow (cfs) | --- | | | | | | | | | | | |
| pH | -0.608 | --- | | | | | | | | | | |
| Cond. (μS/cm) | 0.411 | -0.382 | --- | | | | | | | | | |
| ANC | -0.594 | 0.747 | -0.262 | --- | | | | | | | | |
| Cl | -0.165 | 0.259 | | 0.215 | --- | | | | | | | |
| NO ₃ | -0.201 | | 0.166 | -0.185 | 0.276 | --- | | | | | | |
| SO ₄ | 0.663 | -0.545 | 0.365 | -0.536 | | | --- | | | | | |
| Na | -0.488 | 0.379 | -0.199 | 0.380 | 0.362 | 0.287 | -0.335 | --- | | | | |
| NH ₄ | | | | | | 0.168 | | 0.169 | --- | | | |
| K | 0.147 | -0.159 | 0.306 | | | 0.270 | 0.203 | 0.308 | | --- | | |
| Al (μmol/L) | 0.228 | | -0.143 | | 0.178 | -0.137 | 0.257 | | 0.276 | -0.191 | --- | |
| Si (μmol/L) | -0.614 | 0.465 | -0.205 | 0.353 | 0.205 | 0.276 | -0.615 | 0.363 | | | -0.207 | --- |

All constituent concentrations are in μeq/L, unless otherwise noted

Note: Values are reported only if significant at the α = 0.05 level; values are bolded and boxes are shaded if significant at the α = 0.01 level

occurred during this period, after most of the major Fraser fir were inflicted by the woody adelgid (Nodvin *et al.*, 1995). Personal observations show that the death of these trees resulted in a “clearing” of the canopy, which then allowed increased growth in the understory. Many young Fraser fir in the understory grew rapidly during this period, and the woody adelgid inflicted little harm on them because they were not able to land on the smooth, undeveloped bark. Therefore, during this growth period, more nitrate was probably taken up by the trees. The trees’ growth leveled off, causing also a leveling off of nitrate levels in the soil and streams. The trend for sulfate is somewhat similar to that for nitrate, yet the cause is believed to be rain- and flow-related. This is supported by the Pearson correlation coefficients between sulfate and flow in Tables 4-8 and 4-9. Sulfate has a highly significant positive correlation (0.678) with flow; therefore, in years when mean streamflow is decreasing, sulfate concentrations should also be decreasing. From Figure 3-1, it is evident that the mean streamflow dropped steadily from 1991 -1993, then suddenly increased for 1994 and leveled out for the remaining period of record. This trend matches that for sulfate concentrations; thus, more sulfate was both input from the rainfall and flushed from the soil during high-rain, high-flow years. In low-rain, low-flow years, most of the sulfate that was deposited probably remained adsorbed to the soil. Sodium is also linked to flow; the Pearson correlation coefficient shows there is a highly significant negative correlation between these variables. Thus, one would expect higher sodium concentrations under baseflow conditions. In addition, the increase in sodium concentrations from 1991 - 1993 could be explained by the overall decrease in mean streamflow during this period.

In general, pH and ANC are highest in the fall and lowest in the winter because of rainfall

patterns (less rainfall in the fall and more rainfall in winter) and related acid inputs to the watershed. In addition, pH may be highest in the summer and fall because of photosynthesis processes in vegetation in the stream. For example, moss growing on rocks in the stream will undergo more photosynthesis in the growing season; in this process, the moss pulls carbon dioxide from the water which will increase the pH somewhat. As was mentioned previously, higher nitrate concentrations are found in the stream in dormant seasons, when there is less vegetation to take up nitrate from the soil. Aluminum concentrations are expected to follow similar trends as nitrate, yet at times they exhibit opposite behavior. From past research at NDW and other watersheds, it is believed that input of acidic anions and accompanying drop in soil and stream pH causes aluminum to be mobilized from the soil (Cosby *et al.*, 1985; Johnson and Lindberg, 1992). Therefore, seasonal and monthly trends for these analytes should be similar, yet they are not according to this analysis. One explanation for this is that mobilization of aluminum is not well represented in the weekly samples. As was mentioned in Chapter III, Analysis of Flow Data, the high end of the flow spectrum is under-represented in the weekly samples. It is during these high flows that pH is expected to be lowest due to large fluxes of acidic anions from the rain itself and from the soil. Since aluminum is solubilized and mobilized at $\text{pH} < 5.5$, with concentrations increasing as pH decreases (Stumm and Morgan, 1981), clear relationships between acid anions, pH, and aluminum may not be seen in the weekly samples since they do not represent these periods of high mobility. The median pH for the SW and NE streams are 5.92 and 5.68, respectively, and the minimum pH are 5.25 and 4.73, respectively. The continuous data shows lower median and minimum pH for both streams. In addition, the period for which aluminum has been analyzed is shorter than the

period of record for other constituents; therefore, seasonal patterns may not be as easily defined or detected.

Higher sulfate concentrations are higher in periods of more rainfall, generally in the winter, most likely because of the high concentrations present in the rainfall itself. Seasonal and flow-related trends for sodium and silica are similar; they are both clearly found at higher concentrations in baseflow conditions and therefore are most likely present due to dissolution of minerals in the bedrock.

Seasonal trends discussed in this chapter are in agreement with trends observed elsewhere in the Smoky Mountains National Park, particularly at high-elevation sites (e.g., Flum and Nodvin, 1995; Silsbee and Larson, 1982). These trends are also supported by research at other high-elevation watersheds such as the Leading Ridge catchment in Pennsylvania (Lynch and Corbett, 1989), yet research by Likens and Bormann (1995) at the Hubbard Brook Watershed noted opposite seasonal trends for sulfate. This is probably due to very different soil types in this watershed, which influence sulfate retention patterns.

Research by Nodvin *et al.* (1995) at NDW has shown that streams are poorly buffered against acidification, with the standard being a pH less than 6.0 and ANC less than 40 $\mu\text{eq/L}$. Research presented in this chapter supports this conclusion for chronic acidification, as the median pH is 5.92 for the SW stream and 5.68 for the NE stream. ANC of the weekly samples is always below 40 $\mu\text{eq/L}$; the median ANC is 12.34 $\mu\text{eq/L}$ for the SW stream and 4.57 $\mu\text{eq/L}$ for the NE stream. Drever (1988) states that surface waters can be considered acidic if ANC becomes negative and pH drops below 5. The minimum pH recorded by the weekly samples in the NE

stream is 4.73, and the minimum ANC for both streams is negative. Therefore, both chronic and episodic acidification is occurring in these streams.

SW vs. NE Stream Conditions

Though SW stream water quality has been monitored on a 15-minute basis for much longer than has NE stream water quality, data have shown that more dramatic changes in stream chemistry occur in the NE stream because of the greater amount of flow it receives in rainfall events. Therefore, a long-term record of 15-minute water quality data for the NE is invaluable, particularly for developing a complete comparison between the two streams. From the data that are available, it is apparent that the two streams behave differently. In most cases, the NE stream receives the higher analyte concentrations and lower pH and ANC, and it exhibits more dramatic relative changes in analyte concentrations over time and flow regimes. In the case with silica, however, the SW receives the higher analyte concentrations. In addition, the mean temperature of the SW stream is 5° C lower than that of the NE stream. This could mean that the SW is generally controlled more by groundwater, and weathering of the sandstone by groundwater could produce the higher silica concentrations. In addition, as was mentioned previously, the SW stream short-circuits its banks and contributes to higher flows in the NE stream, which probably also contributes to higher analyte concentrations and greater fluctuations in the NE stream. Additional reasons for statistical differences between the two streams could be that the soils surrounding the streams could be of slightly different composition, or depth to bedrock could be greater for the NE stream than the SW stream. Drainage patterns and areas could also be different; groundwater potentiometric gradients may be more directed to the SW stream, yet during storm events, runoff source areas and

gradients may change, directing more flow toward the NE stream. Again, it would be extremely difficult to isolate drainage areas to each stream given the inter-connectivity of the streams in the upper elevations of the watershed. In addition, depositional patterns over the entire watershed and canopy density may vary, which also may explain some of the differences in chemical characteristics of the two stream.

CHAPTER V. HYDROLOGIC INFLUENCES ON WATER QUALITY

Flow data were summarized in Chapter III and related somewhat to temporal trends in water quality in Chapter IV. This chapter focuses further on hydrologic influences on water quality in NDW, including changes in constituent concentrations over the hydrograph and during storm events and possible effects of flow pathways on water quality.

Data Sources

In general, weekly grab sample concentration data and corresponding streamflows from November 1991 through August 1998 were used in the analysis in this chapter. To examine the behavior of analytes during high flow periods, a storm event study was conducted from October 31 through November 5, 1995. Samples were collected in the NE stream using automated sampling equipment and were analyzed for pH, conductivity, ANC, nitrate, sulfate, chloride, sodium, ammonium, potassium, magnesium, and calcium. In addition, the Hydrolab monitoring unit on the SW stream analyzed for pH and conductivity during this period. Relationships between AMC, precipitation, and sulfate and nitrate were examined by using weekly sample concentration data along with daily precipitation readings from a Belfort rain gage from November 1991 through December 1995.

Methods of Analysis

Nearly all analyte concentrations measured in the weekly samples are affected by fluctuations in streamflow. Therefore, it is important to characterize samples according to the flow regime under which they were collected. To accurately characterize location on the hydrograph, the continuous (15-minute) flow record for the entire period was plotted on semi-log scale versus

time. The baseflow component of the hydrograph is shown as linear on this scale; this makes it possible to discern baseflow from the falling limb. A detailed example of this hydrograph separation procedure is provided in Figure A-5 in the Appendix. Because the NE and SW streams experience slightly different flow conditions, there were times that the samples collected at the same time for each stream were collected under different flow regimes. For this reason, distributions of analytes for both streams cannot be shown on the same graphs. Statistical tests for determining differences in constituent concentrations based on location on the hydrograph were conducted using SPSS statistical software. Concentration data were tested for normality through the Kolmogorov-Smirnov test; since data were non-normal, a non-parametric Mann-Whitney U test was performed. Descriptive statistics for all data sets were computed using SPSS.

In the analysis to detect relationships among precipitation, AMC, and sulfate and nitrate concentrations, inches of rainfall that occurred since the last sampling date was computed for each weekly grab sample. In general, the rainfall that was recorded on a given sample date was assumed to have occurred after the sample was taken because it was impossible to know exactly when the rain occurred. The number of consecutive days with no rain was also counted for each weekly sample to establish a rough estimate of AMC; this value at times overlapped with the previous week's value. That is, the total number of consecutive dry days preceding a sampling date was assigned to that sample, not just the number of consecutive dry days since the last sampling period. These relationships were analyzed using simple linear regression.

Results

Statistical and Graphical Analysis of Analytes Versus Flow and Flow Regimes

Full distributions of weekly sample analytes based on location on the hydrograph when collected are shown in Figure 5-1 for the SW stream and in Figure 5-2 for the NE stream. In addition, results of the Mann-Whitney U test to detect statistical differences in constituents among locations on the hydrograph are shown in Table 5-1 for the SW stream and Table 5-2 for the NE stream.

As expected, pH is statistically lower ($p = 0.000$) on the rising and falling limbs of the hydrograph than in baseflow. In addition, pH drops to more critical levels in the NE stream than in the SW stream. Conductivity is statistically higher ($p = 0.034$) on the rising limb than in baseflow. ANC follows much the same pattern as pH. Chloride changes little over the hydrograph; distributions are statistically similar for all components of the hydrograph, except in the NE stream, where distributions for baseflow and the falling limb are different ($p = 0.018$). For nitrate, there appears to be a pronounced “flush” through the stream as the hydrograph rises, then a dilutional effect brings nitrate levels back down, sometimes below baseflow levels, as the hydrograph falls. However, statistical comparisons show that nitrate distributions are similar for all components of the hydrograph. Sulfate is statistically higher ($p = 0.000$) on the rising and falling limbs than in baseflow, and there appears to be no dilutional effect as with nitrate. Though aluminum appears to increase as the hydrograph rises, the difference in aluminum distributions is statistically similar ($p = 0.136$ for NE stream) between baseflow and the rising limb. Silica is statistically lower on the rising and falling limbs than in baseflow. Relationships between the hydrograph and other

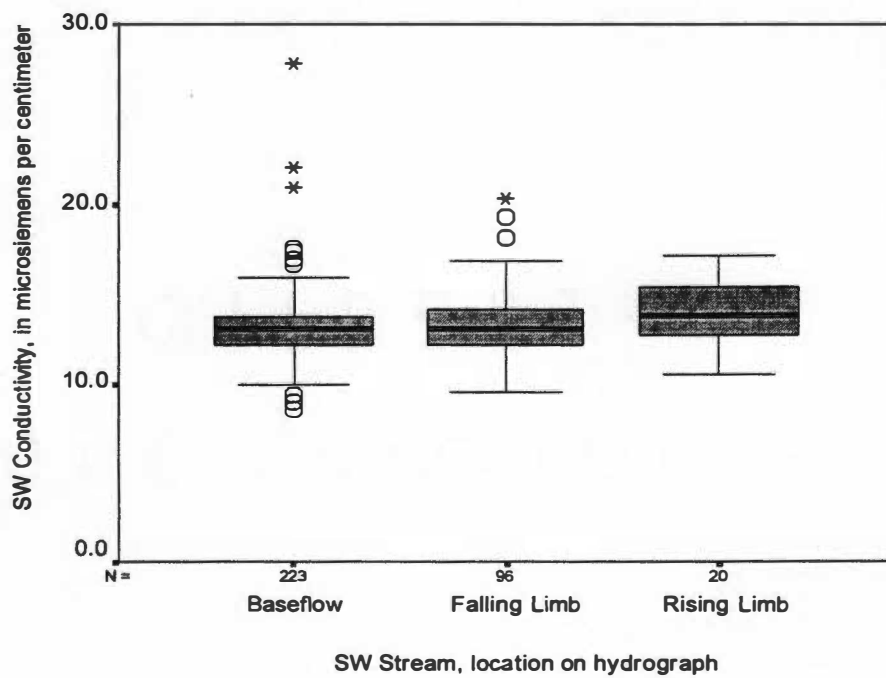
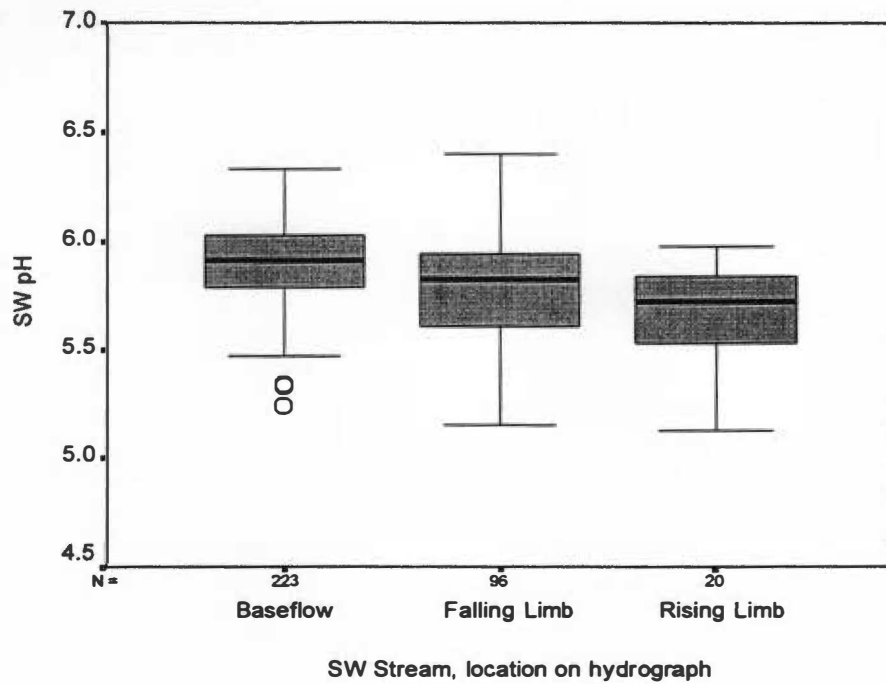


Figure 5-1. Distributions of weekly sample constituent concentrations by location on the hydrograph for the SW streamlet, 1991-1998.

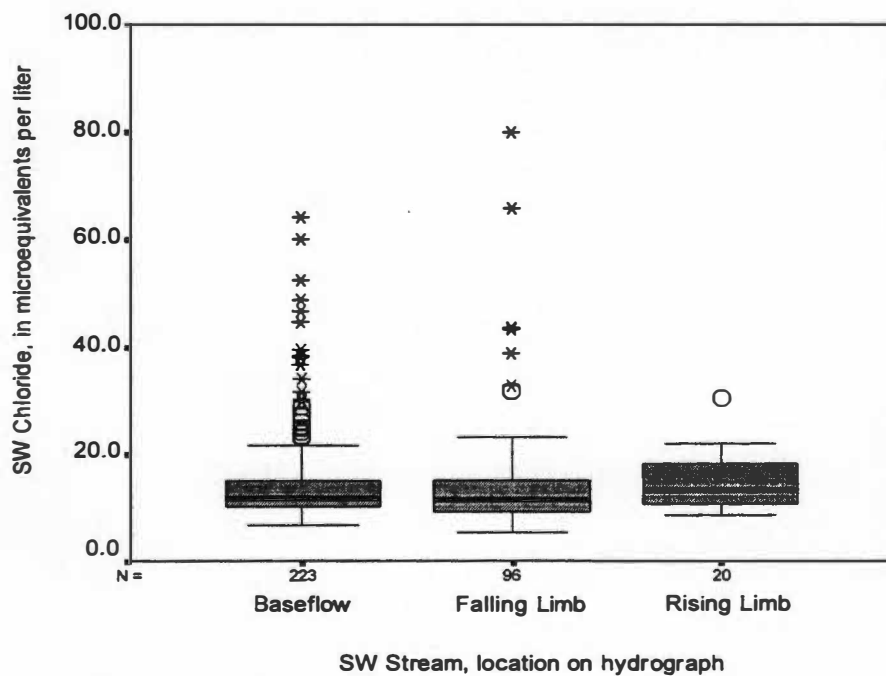
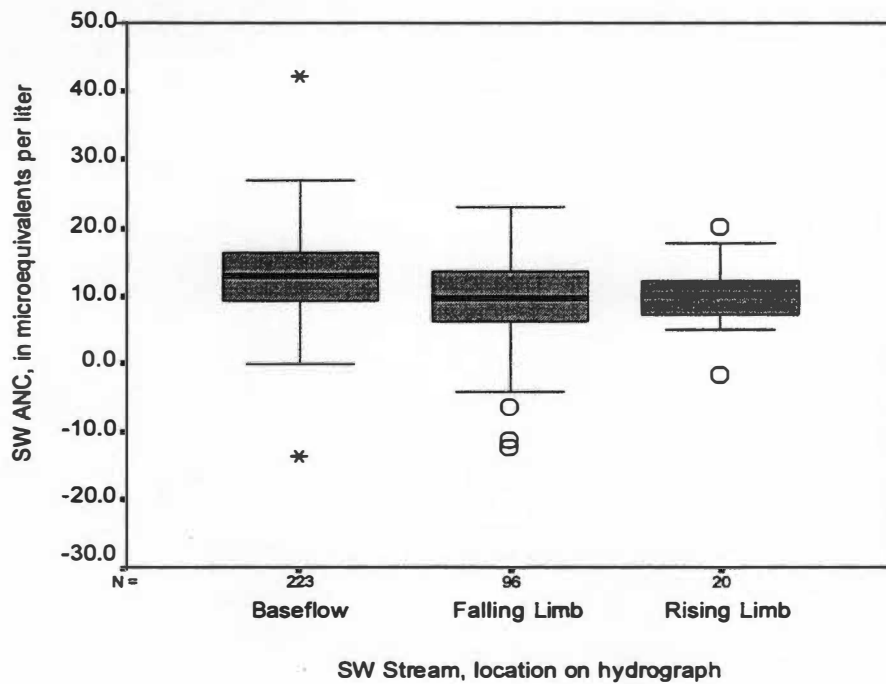


Figure 5-1 (continued). Distributions of weekly sample constituent concentrations by location on the hydrograph for the SW streamlet, 1991-1998.

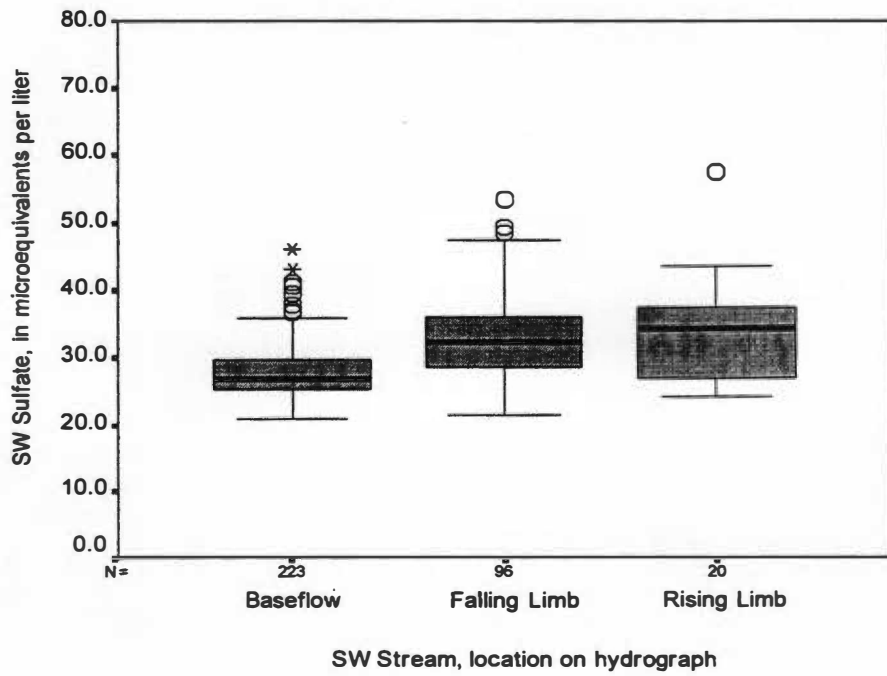
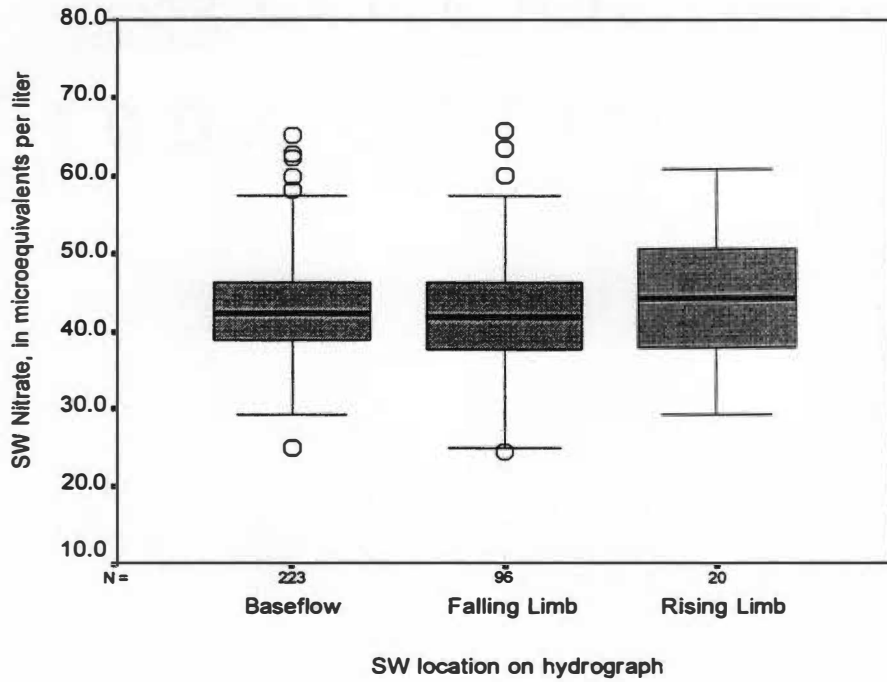


Figure 5-1 (continued). Distributions of weekly sample constituent concentrations by location on the hydrograph for the SW streamlet, 1991-1998.

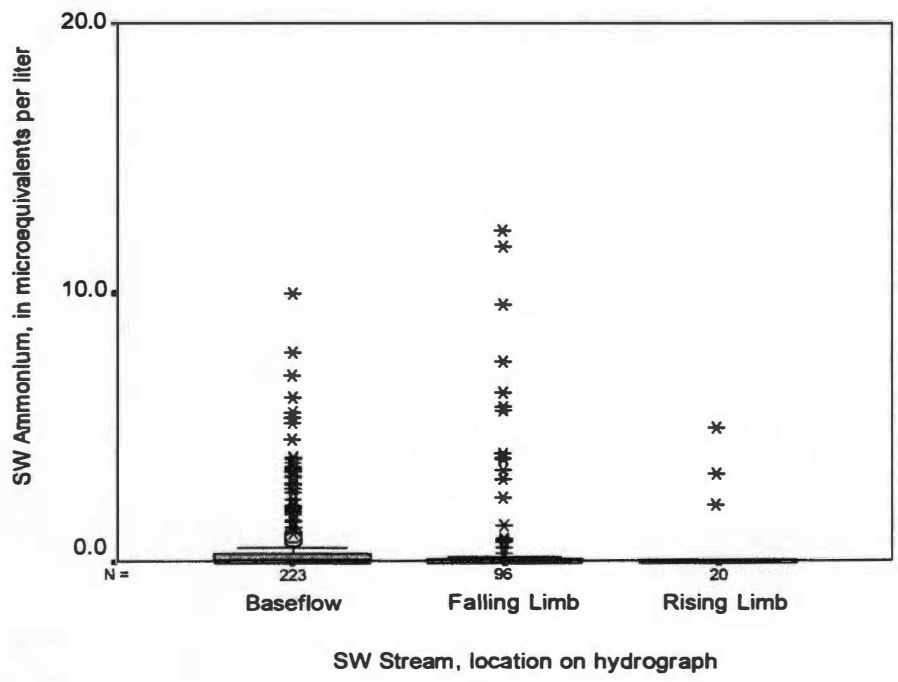
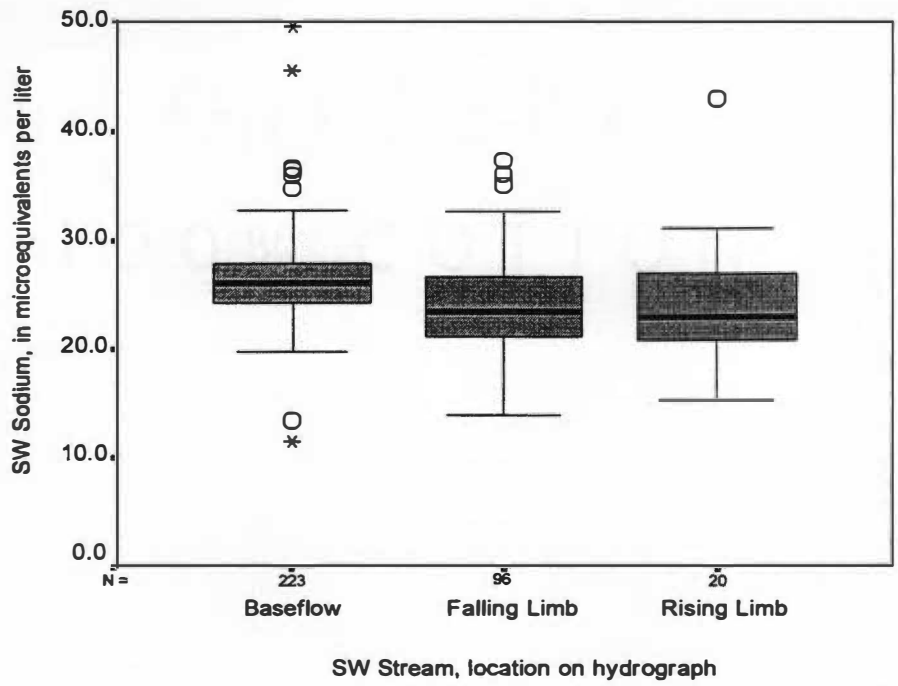


Figure 5-1 (continued). Distributions of weekly sample constituent concentrations by location on the hydrograph for the SW streamlet, 1991-1998.

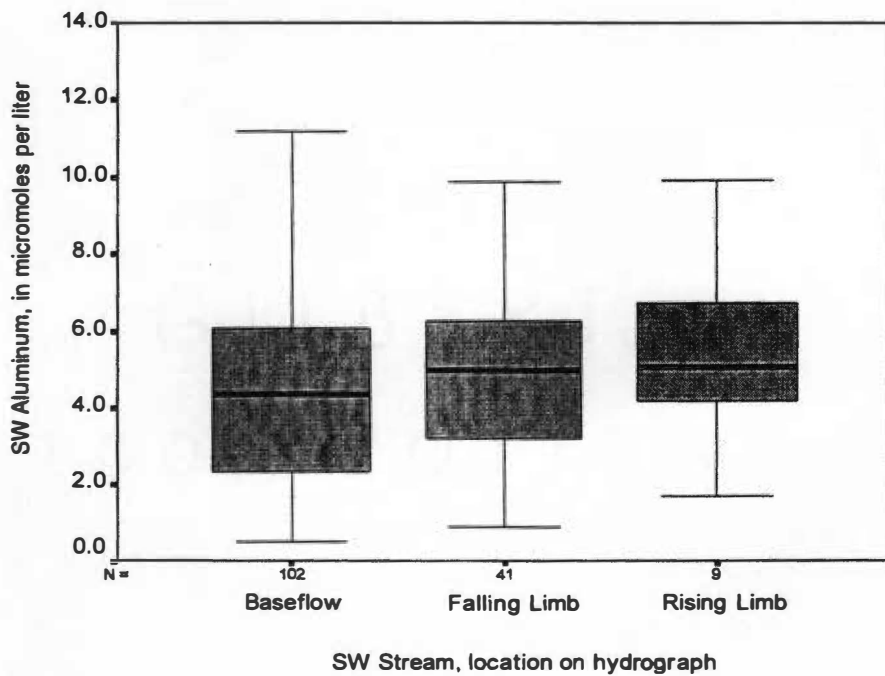
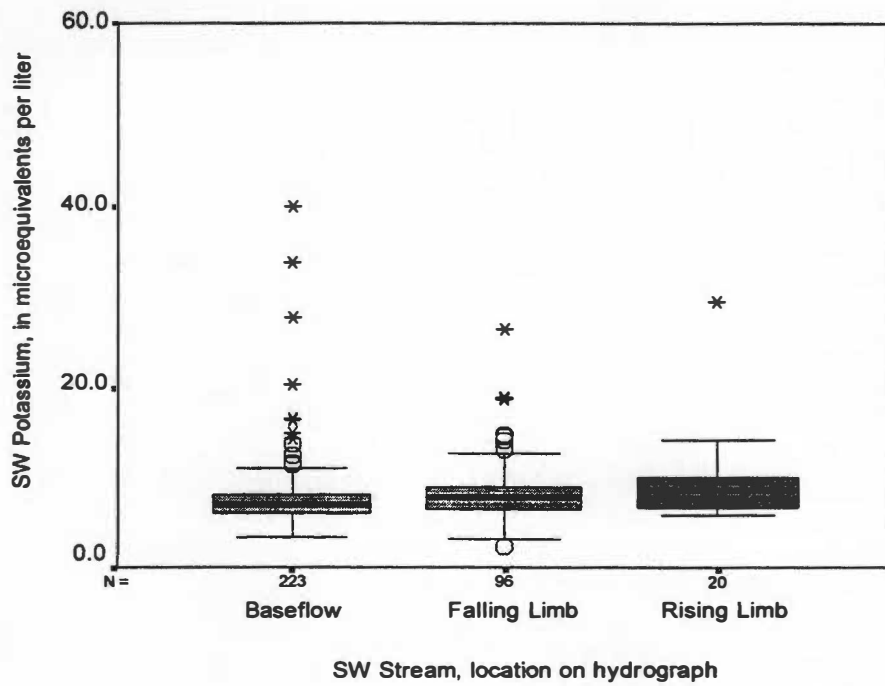


Figure 5-1 (continued). Distributions of weekly sample constituent concentrations by location on the hydrograph for the SW streamlet, 1991-1998.

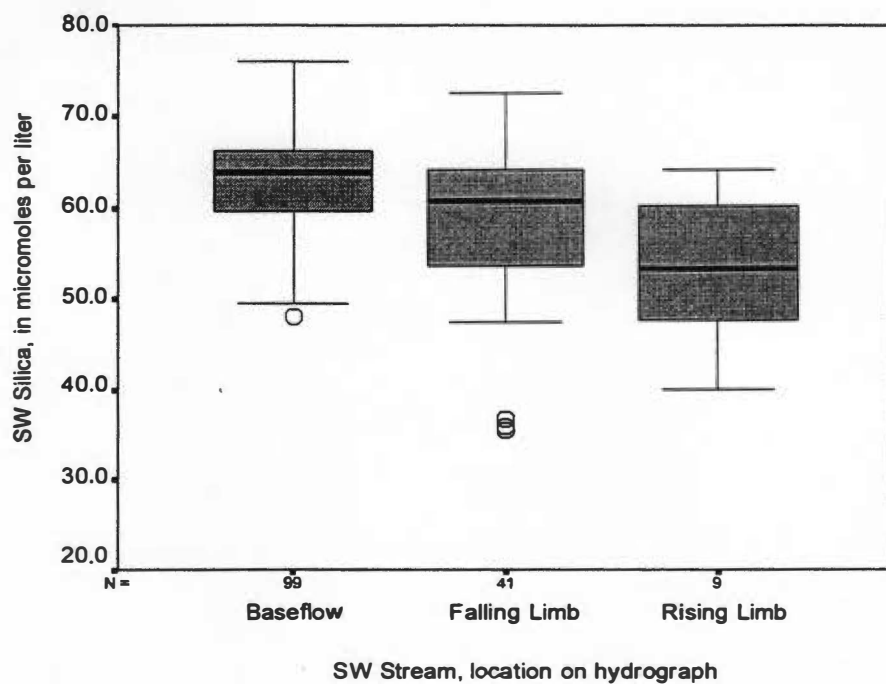


Figure 5-1 (continued). Distributions of weekly sample constituent concentrations by location on the hydrograph for the SW streamlet, 1991-1998.

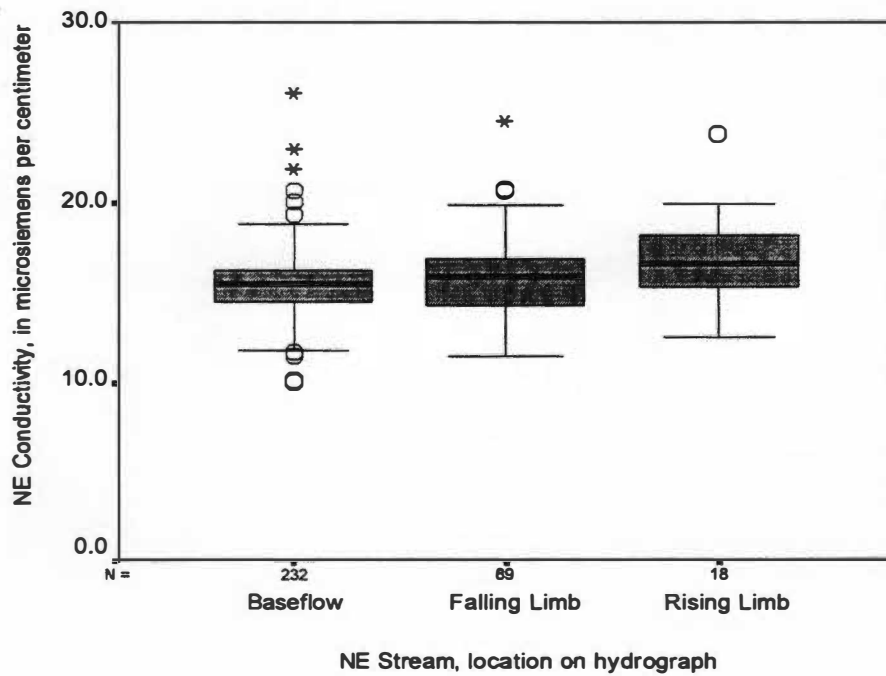
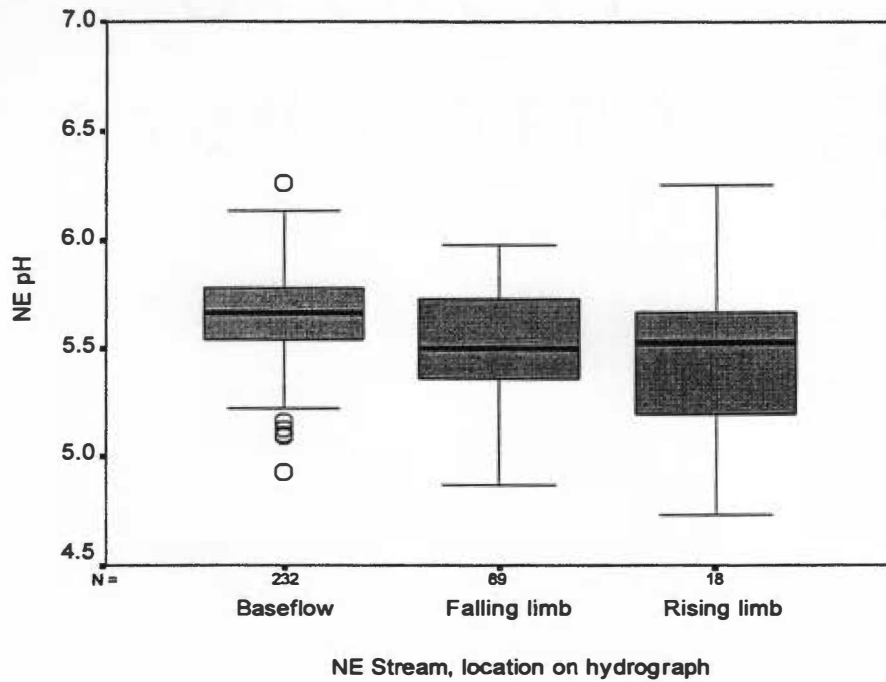


Figure 5-2. Distributions of weekly sample constituent concentrations by location on the hydrograph for the NE streamlet, 1991-1998.

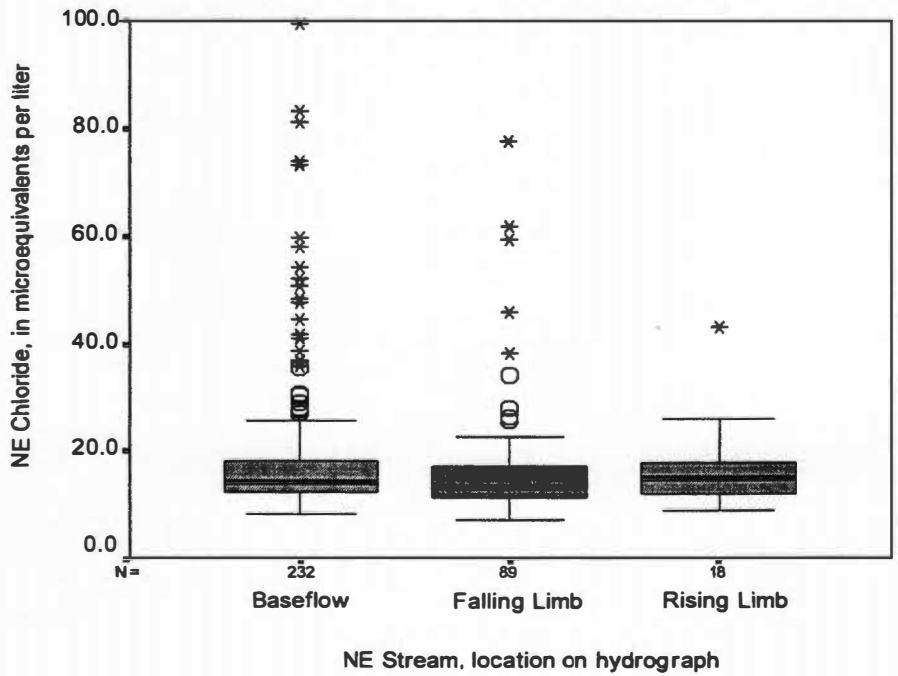
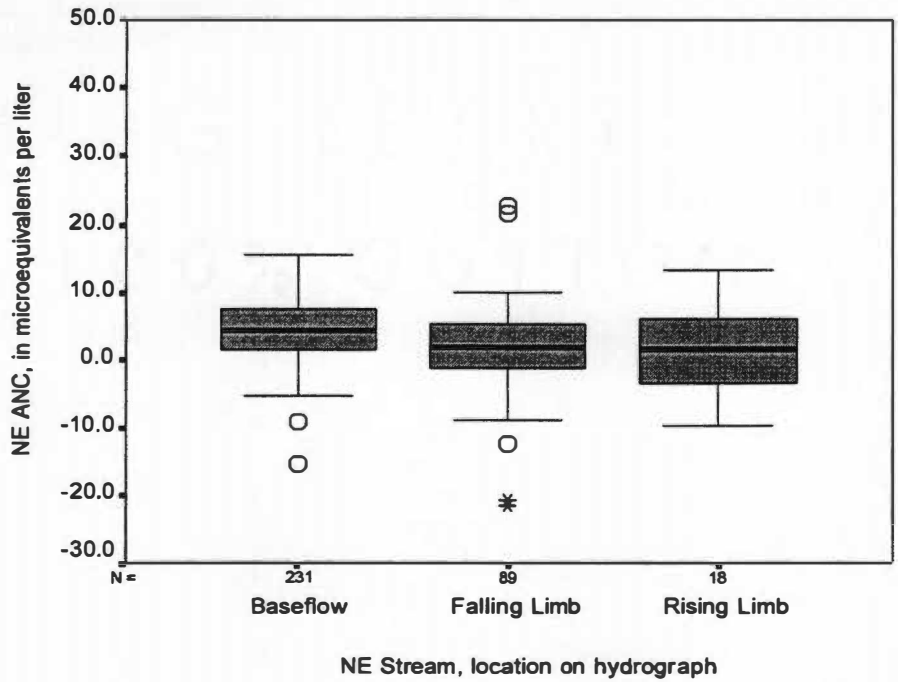


Figure 5-2 (continued). Distributions of weekly sample constituent concentrations by location on the hydrograph for the NE streamlet, 1991-1998.

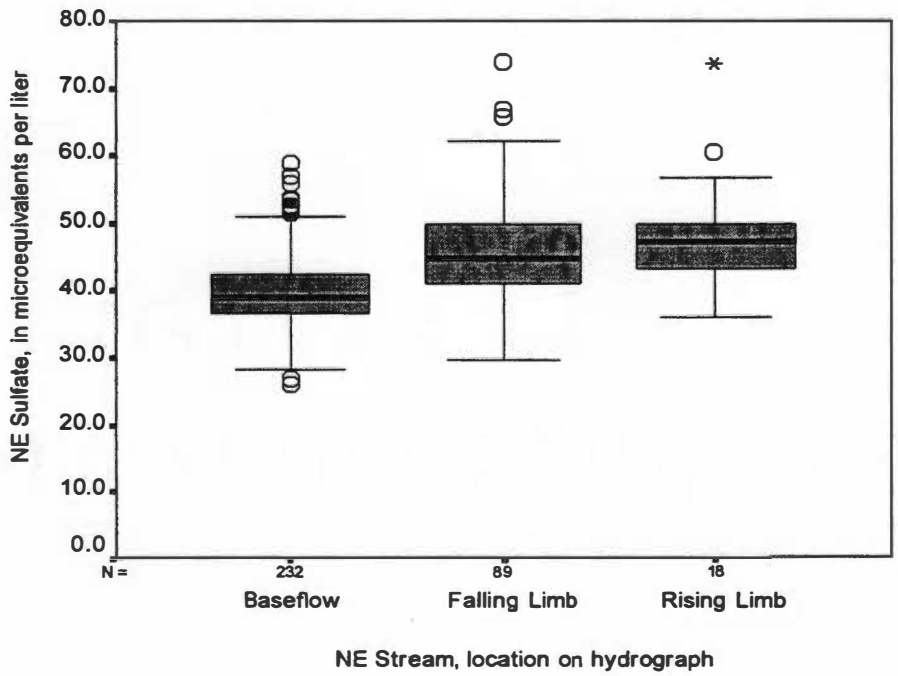
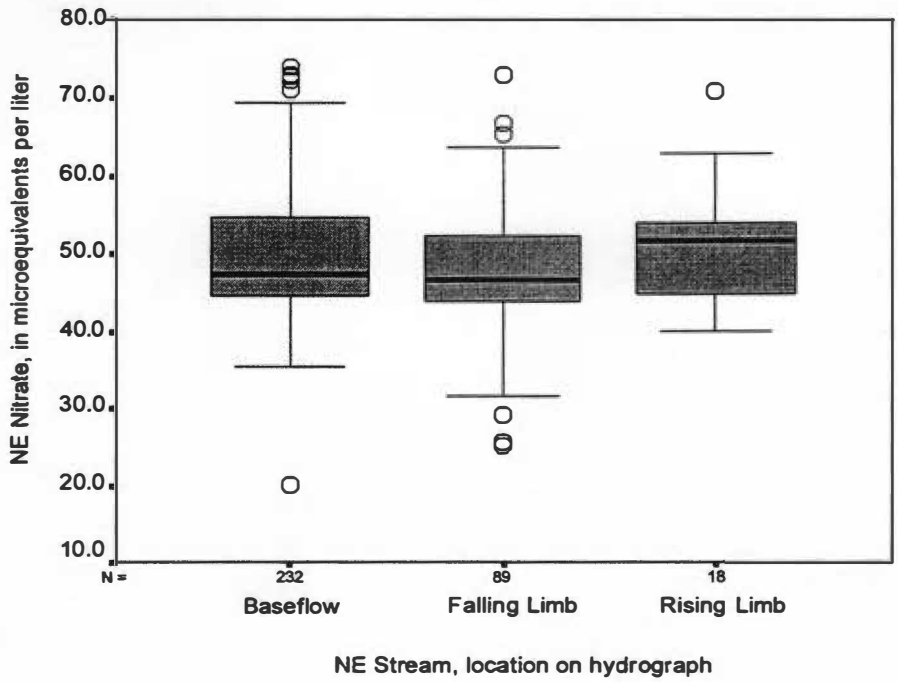


Figure 5-2 (continued). Distributions of weekly sample constituent concentrations by location on the hydrograph for the NE streamlet, 1991-1998.

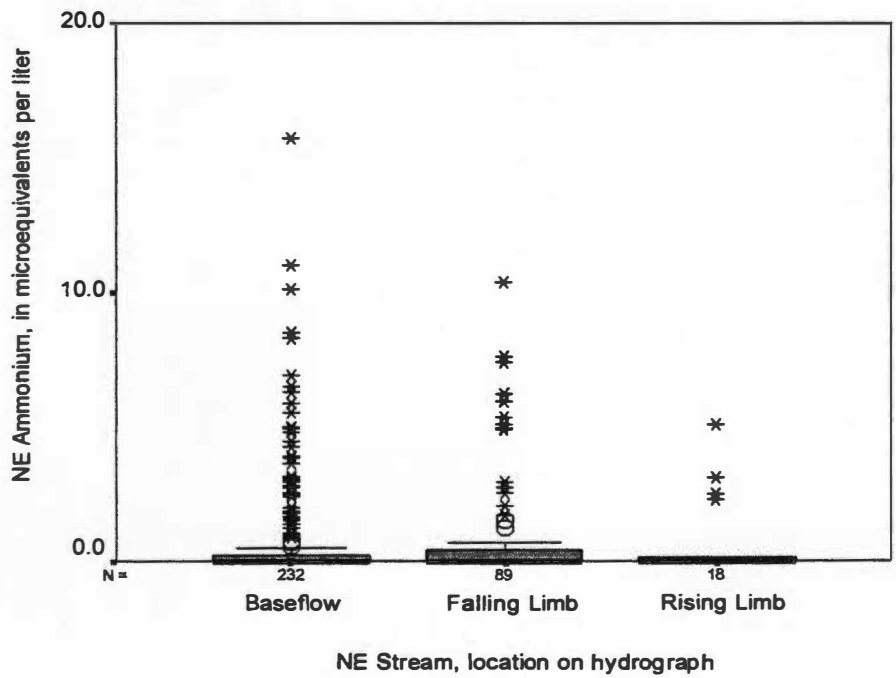
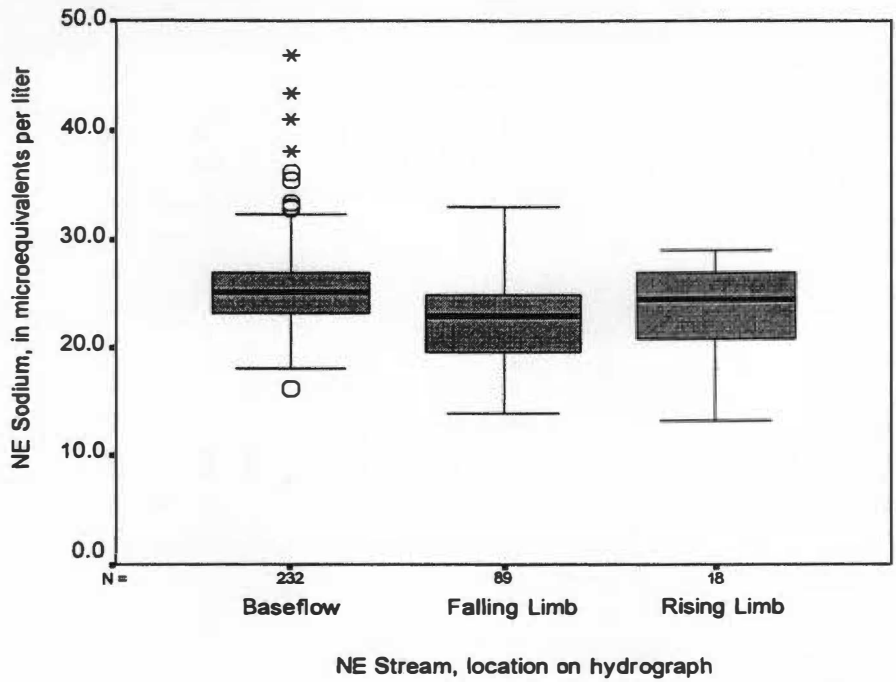


Figure 5-2 (continued). Distributions of weekly sample constituent concentrations by location on the hydrograph for the NE streamlet, 1991-1998.

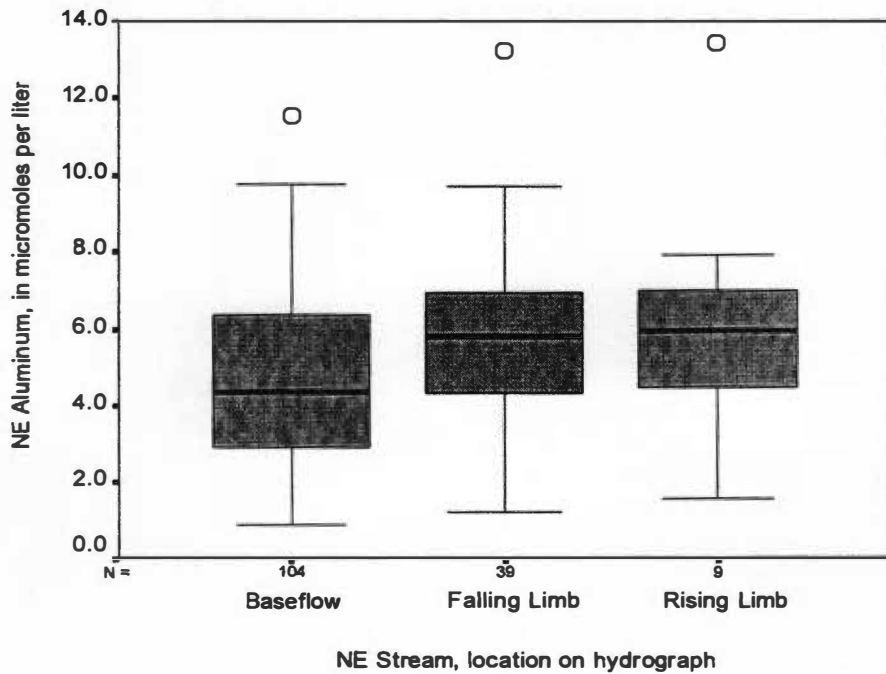
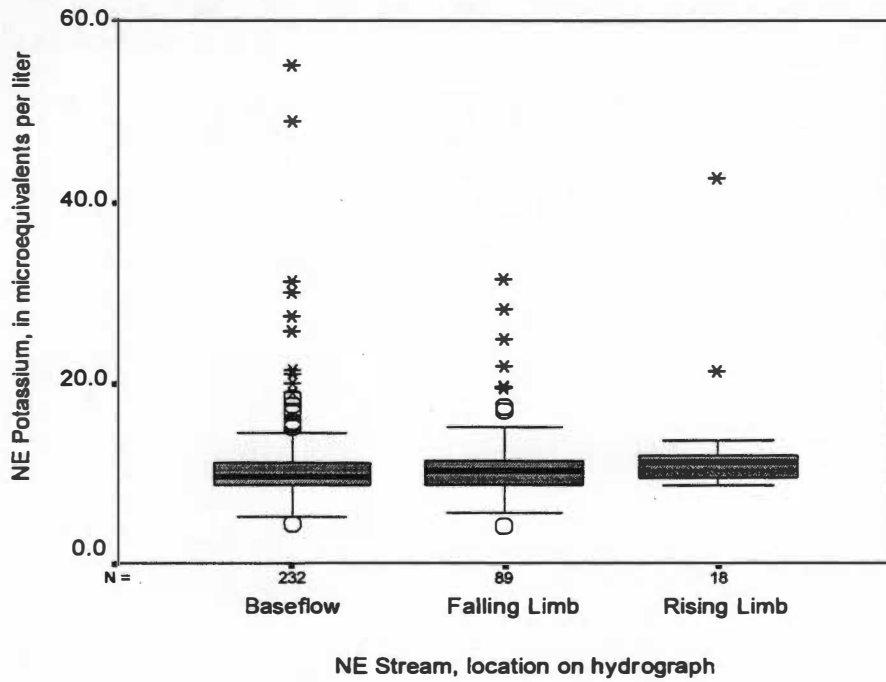


Figure 5-2 (continued). Distributions of weekly sample constituent concentrations by location on the hydrograph for the NE streamlet, 1991-1998.

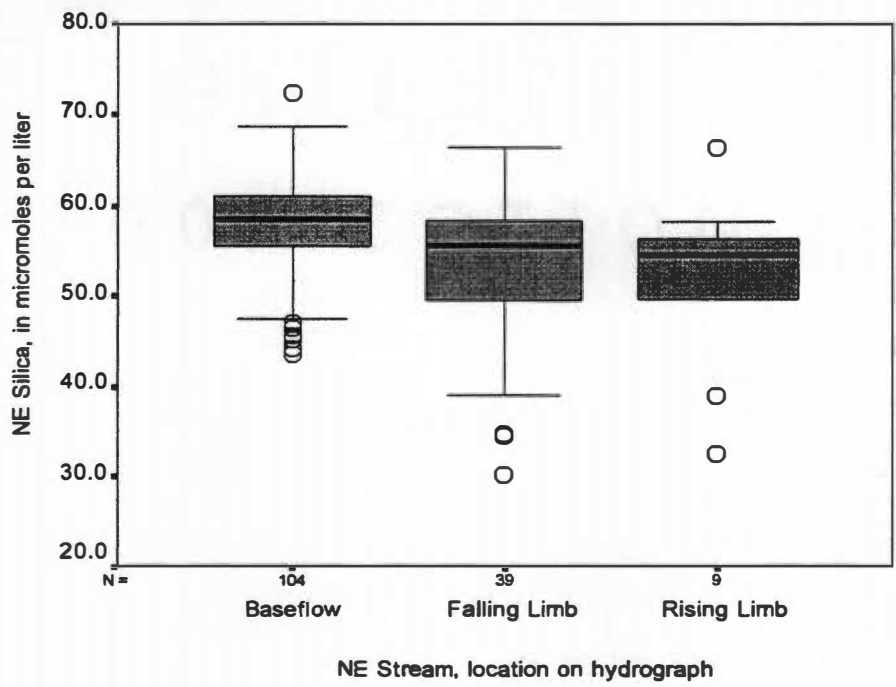


Figure 5-2 (continued). Distributions of weekly sample constituent concentrations by location on the hydrograph for the NE streamlet, 1991-1998.

Table 5-1. Statistical differences in weekly sample analytes by location on the hydrograph for the SW stream.

| Stream | Constituent (concentration) | Location on Hydrograph Combination | | |
|--------|--------------------------------|------------------------------------|---------------------------|------------------------------|
| | | Baseflow- Rising Limb | Baseflow- Falling Limb | Rising Limb- Falling Limb |
| SW | Flow | p = 0.000 | p = 0.000 | p = 0.344 |
| | pH | p = 0.000 | p = 0.000 | p = 0.138 |
| | Conductivity | p = 0.034 | p = 0.211 | p = 0.176 |
| | ANC | p = 0.029 | p = 0.000 | p = 0.664 |
| | Chloride | p = 0.503 | p = 0.138 | p = 0.157 |
| | Nitrate | p = 0.480 | p = 0.161 | p = 0.214 |
| | Sulfate | p = 0.000 | p = 0.000 | p = 0.913 |
| | Sodium | p = 0.012 | p = 0.000 | p = 0.821 |
| | Ammonium | p = 0.343 | p = 0.964 | p = 0.354 |
| | Potassium | p = 0.007 | p = 0.001 | p = 0.183 |
| | Hydrogen Ion | p = 0.000 | p = 0.000 | p = 0.142 |
| | Aluminum | p = 0.297 | p = 0.179 | p = 0.640 |
| | Silica | p = 0.001 | p = 0.005 | p = 0.098 |

Note: P-values are bolded and boxes are shaded if the constituent distributions are statistically equal for the two hydrograph components listed

Table 5-2. Statistical differences in weekly sample analytes by location on the hydrograph for the NE stream.

| Stream | Constituent (concentration) | Location on Hydrograph Combination | | |
|--------|--------------------------------|------------------------------------|---------------------------|------------------------------|
| | | Baseflow- Rising Limb | Baseflow- Falling Limb | Rising Limb- Falling Limb |
| NE | Flow | p = 0.007 | p = 0.000 | p = 0.977 |
| | pH | p = 0.003 | p = 0.000 | p = 0.330 |
| | Conductivity | p = 0.030 | p = 0.087 | p = 0.194 |
| | ANC | p = 0.035 | p = 0.000 | p = 0.825 |
| | Chloride | p = 0.925 | p = 0.018 | p = 0.272 |
| | Nitrate | p = 0.550 | p = 0.050 | p = 0.118 |
| | Sulfate | p = 0.000 | p = 0.000 | p = 0.324 |
| | Sodium | p = 0.251 | p = 0.000 | p = 0.172 |
| | Ammonium | p = 0.846 | p = 0.709 | p = 0.987 |
| | Potassium | p = 0.015 | p = 0.313 | p = 0.069 |
| | Hydrogen Ion | p = 0.031 | p = 0.038 | p = 0.362 |
| | Aluminum | p = 0.136 | p = 0.012 | p = 0.792 |
| | Silica | p = 0.027 | p = 0.008 | p = 0.535 |

Note: P-values are bolded and boxes are shaded if the constituent distributions are statistically equal for the two hydrograph components listed

analytes are included in Figures 5-1 and 5-2 and Tables 5-1 and 5-2. For all analytes, distributions are statistically similar between the rising and falling limbs of the hydrograph. It should be noted here that the strength of the statistical comparisons presented in Tables 5-1 and 5-2 is limited by the fact that only 6% of the weekly samples were taken on the rising limb of the hydrograph.

In order to detect flowpaths of runoff in the watershed and associated chemical signals, soil lysimeter data from 1992 - 1998 were summarized and examined. The mean and median constituent concentrations in soil water data at the three monitored soil horizons are presented in Table 5-3. Median concentration values will be discussed here, given that concentration data are generally not normally distributed. Median nitrate concentrations are highest in the upper soil zone, while median sulfate concentrations are highest in the middle soil zone. Sulfate concentrations are higher than nitrate concentrations in all layers except the uppermost zone. Median potassium and chloride concentrations and conductivity are highest in the upper zone. Median ammonium concentrations are detected only in the upper zone. Higher median sodium concentrations are found in streamwater than in the soil; this supports the conclusion that sodium is observed primarily in groundwater. Study of flowpaths would benefit greatly by having calcium and magnesium data, as they are primary base cations found in the soil and bedrock, yet again, these data are not included due to current QA/QC problems.

Analyte Responses During a Storm Event, October 31 - November 5, 1995

As was mentioned in Chapter IV, while temporal trends in constituents may be apparent by collection of weekly samples, behavior of these constituents during high-flow periods and storm events has not been fully characterized. Therefore, it is important to examine how each constituent

Table 5-3. Soil solution water quality data from 1992 - 1998 for three soil horizons.

| Constituent | Units | A Horizon (10 cm) | | Bw Horizon (20 cm) | | CB Horizon (50 cm) | |
|--------------|-------|-------------------|--------|--------------------|--------|--------------------|--------|
| | | Mean | Median | Mean | Median | Mean | Median |
| pH | | 4.02 | 4.03 | 4.49 | 4.44 | 4.50 | 4.48 |
| Conductivity | μS/cm | 69.85 | 59.10 | 35.42 | 33.55 | 33.38 | 33.50 |
| Chloride | μeq/L | 28.33 | 19.70 | 30.40 | 19.14 | 23.22 | 15.42 |
| Nitrate | μeq/L | 134.53 | 97.73 | 71.40 | 60.55 | 79.30 | 71.34 |
| Sulfate | μeq/L | 104.23 | 92.62 | 109.46 | 99.23 | 100.55 | 95.55 |
| Sodium | μeq/L | 21.78 | 18.55 | 22.07 | 18.15 | 19.84 | 16.54 |
| Ammonium | μeq/L | 2.24 | 0.45 | 2.23 | 0.00 | 0.83 | 0.00 |
| Potassium | μeq/L | 22.30 | 18.84 | 11.08 | 5.92 | 11.30 | 8.54 |

concentration responds as the hydrograph rises and falls. Episodic extremes in concentrations may in fact control which fish and benthic species can survive in this watershed. To examine the behavior of analytes during high flow periods, a storm event study was conducted from October 31 through November 5, 1995.

Figures 5-3 - 5-9 show the analyte concentrations, in addition to temperature and precipitation, over time during the storm event. Three distinct peaks in flow occurred; for both streams, the last peak was the largest, yet unfortunately, a sample was not collected for the apex of this portion of the hydrograph. The flow is noticeably higher (5.8 cfs vs. 2.7 cfs) and the watershed response is much more dramatic for the NE stream than for the SW stream. pH decreases dramatically in both streams as the hydrograph rises, dropping a whole pH unit in the NE stream to a minimum of 4.9. ANC also follows this trend; median ANC in the NE stream is negative and decreases to a minimum of -7.6 $\mu\text{eq/L}$. Therefore, the stream's buffering capacity is reduced as acidic rainfall and runoff enter the streams. Baseline conductivity in both streams is already low, due to the sandstone bedrock's resistance to weathering and therefore low dissolved mineral content in the groundwater. During the storm, the conductivity rises most notably during the first peak of the hydrograph, then returns to baseline levels soon after the storm. It appears that the rise in conductivity is due to flushing of dissolved constituents from the vadose zone. In the NE stream, nitrate and sulfate exhibit interesting behavior. Nitrate levels rise during the first peak of the hydrograph, then decrease and then level off over the remaining peaks of the hydrograph. This "dilutional effect" shows that nitrate is very mobile in the watershed and gets flushed into the stream in the early portions of runoff. Overall, nitrate concentrations rise 25.7 $\mu\text{eq/L}$ during the storm

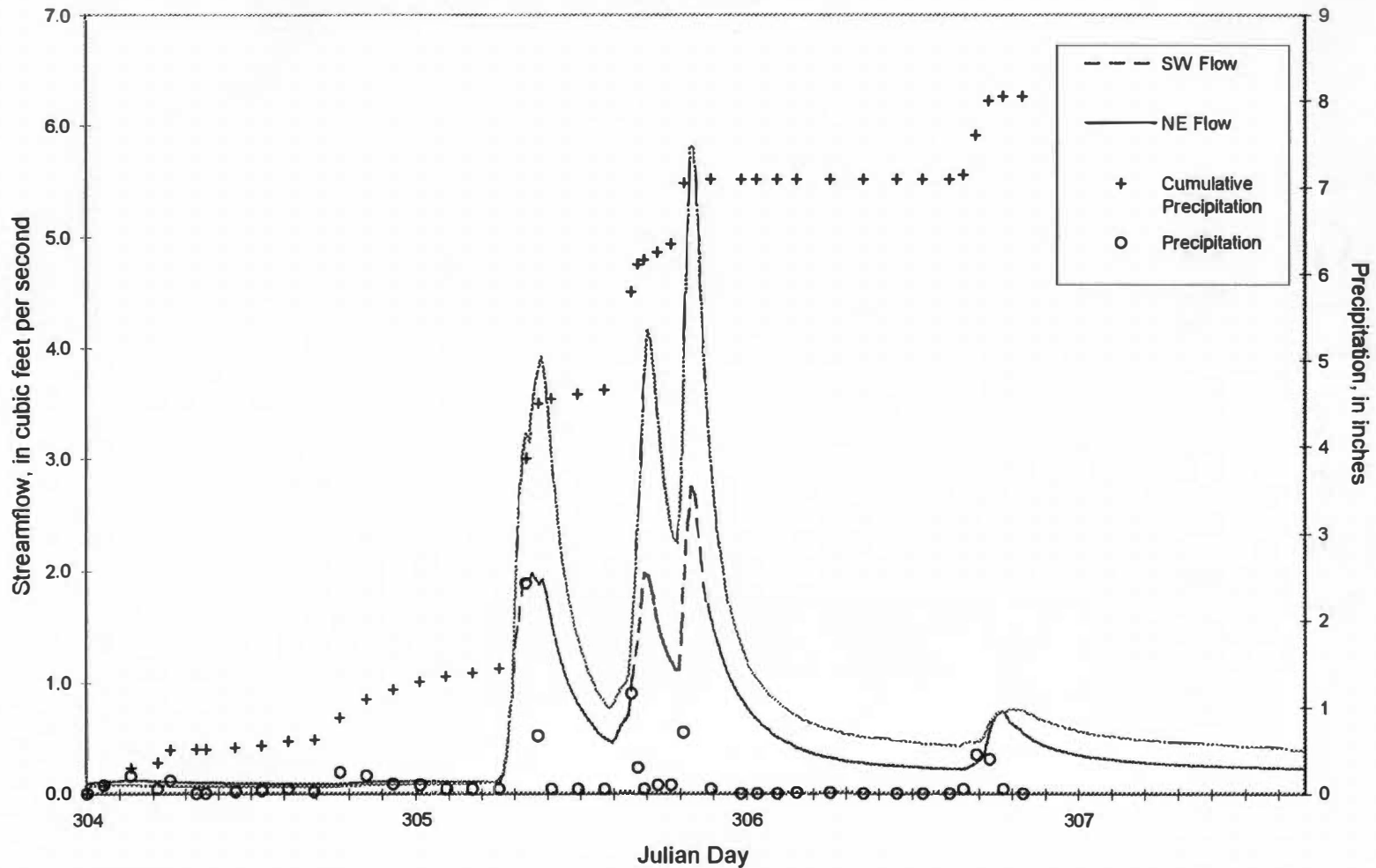


Figure 5-3. Precipitation and streamflow response during a storm event, October 31 - November 5, 1995, for the SW and NE streamlets.

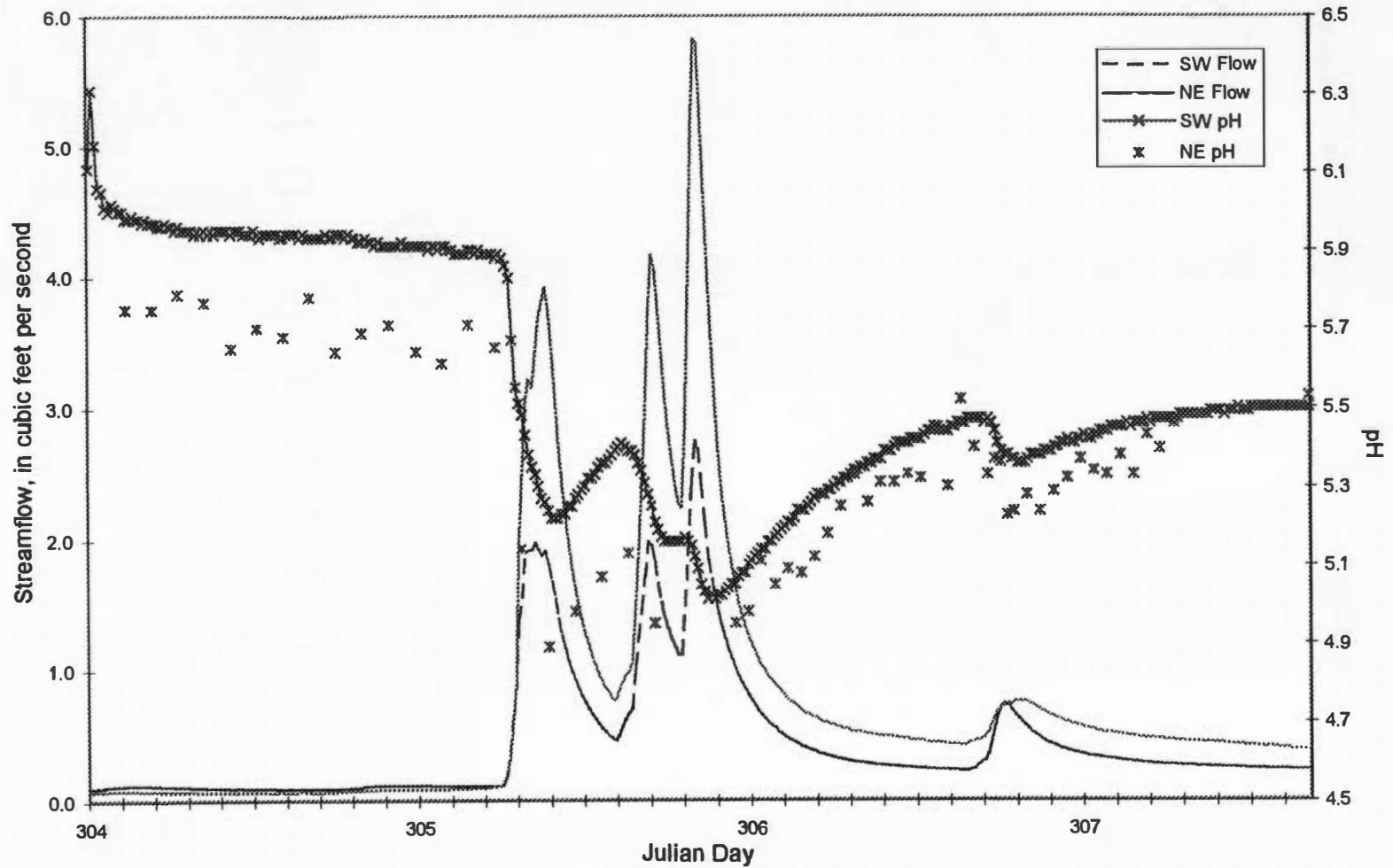


Figure 5-4. pH and streamflow response during a storm event, October 31- November 5, 1995, for the SW and NE streamlets.

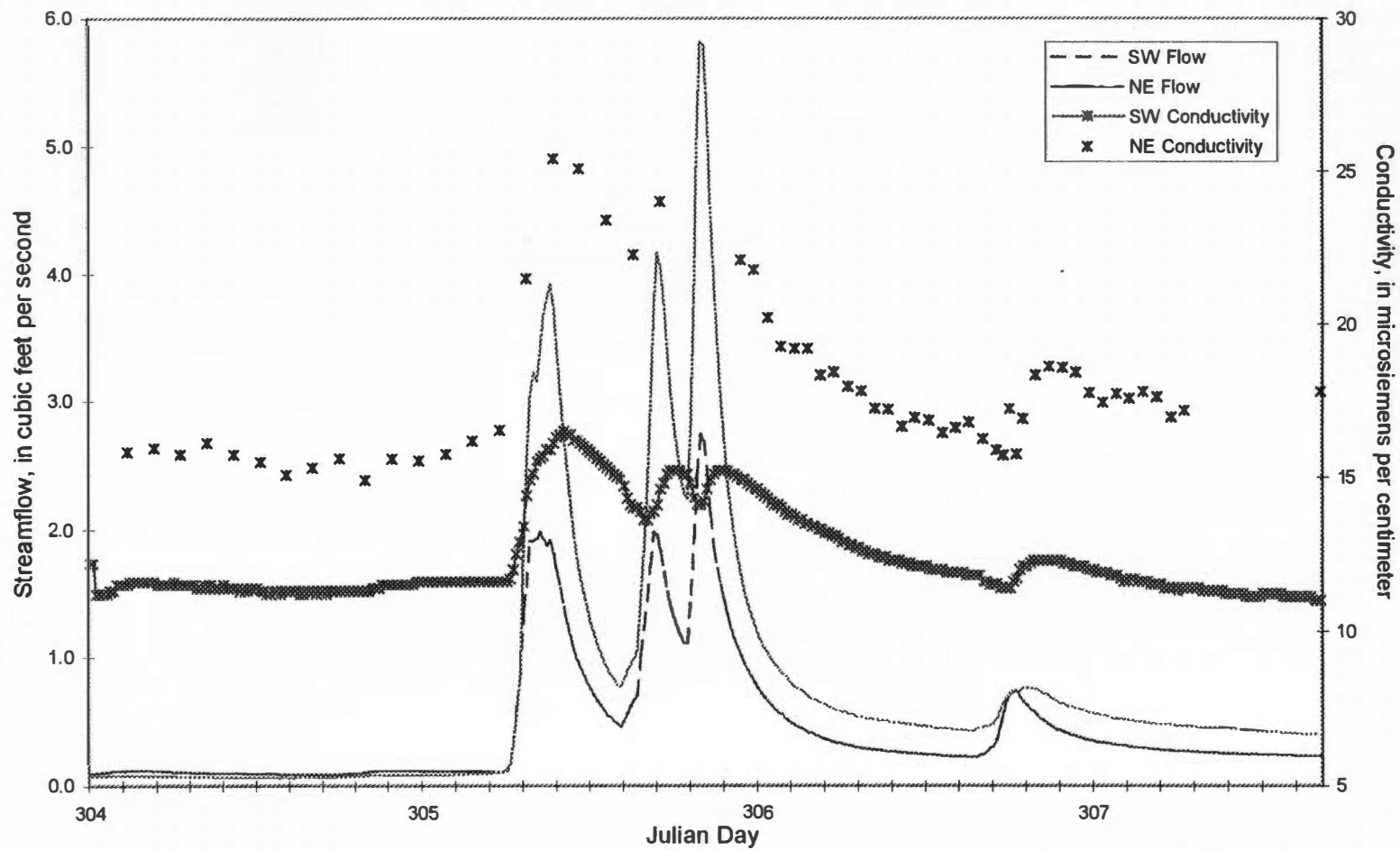


Figure 5-5. Conductivity and streamflow response during a storm event, October 31 - November 5, 1995, for the SW and NE streamlets.

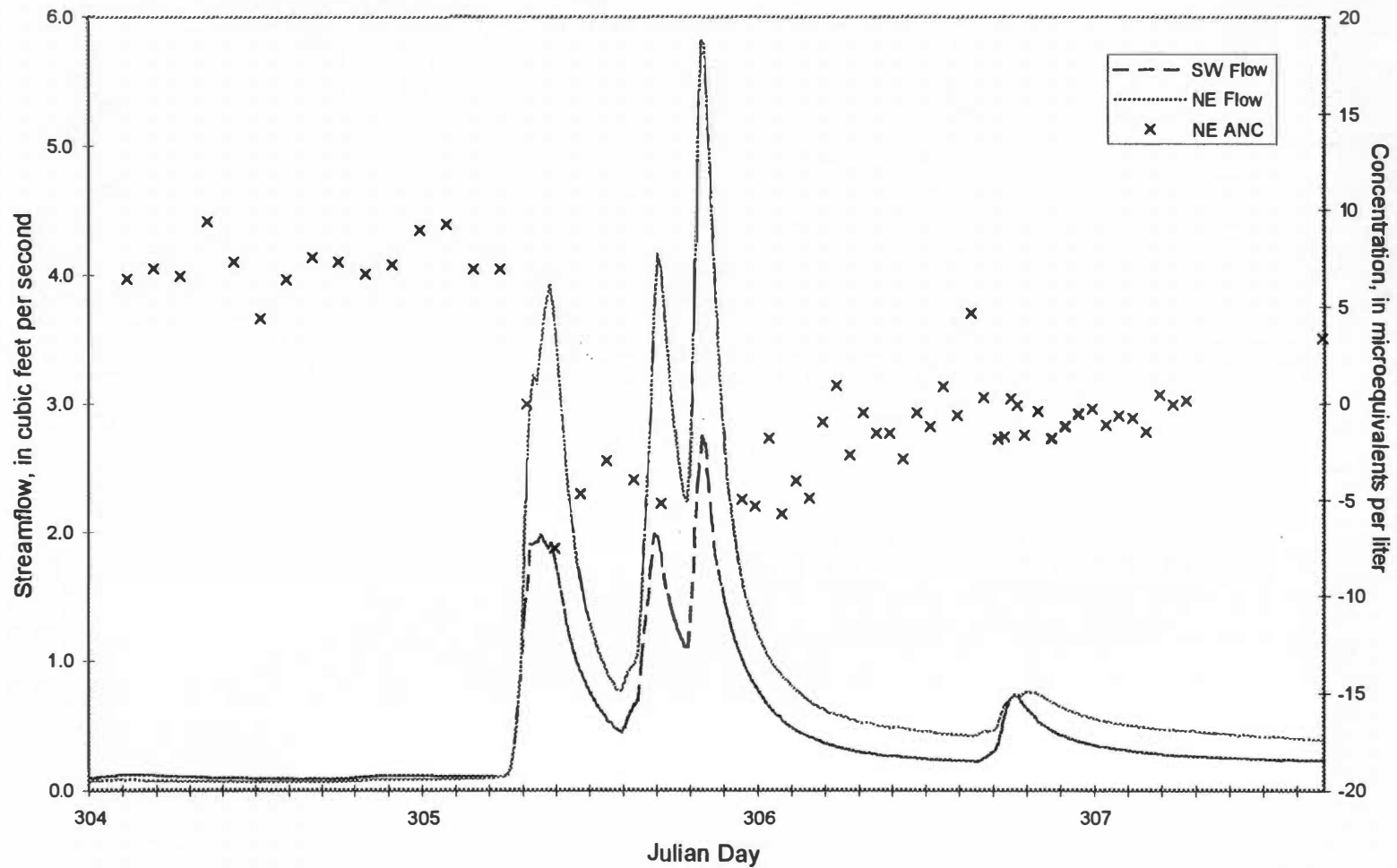


Figure 5-6. Acid neutralization capacity response during a storm event, October 31 - November 5, 1995, for the NE streamlet.

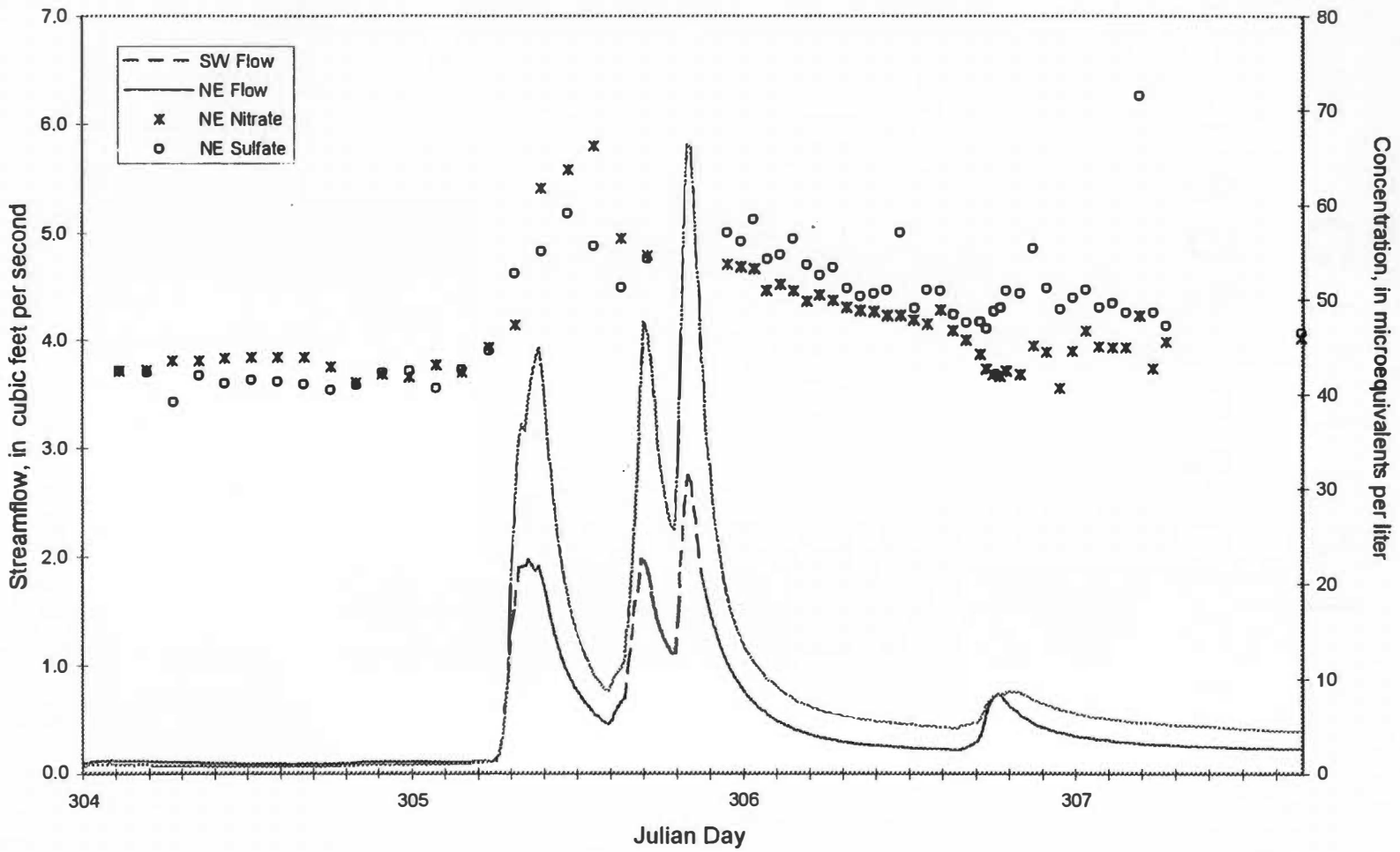


Figure 5-7. Nitrate and sulfate response during a storm event, October 31 - November 5, 1995, for the NE streamlet.

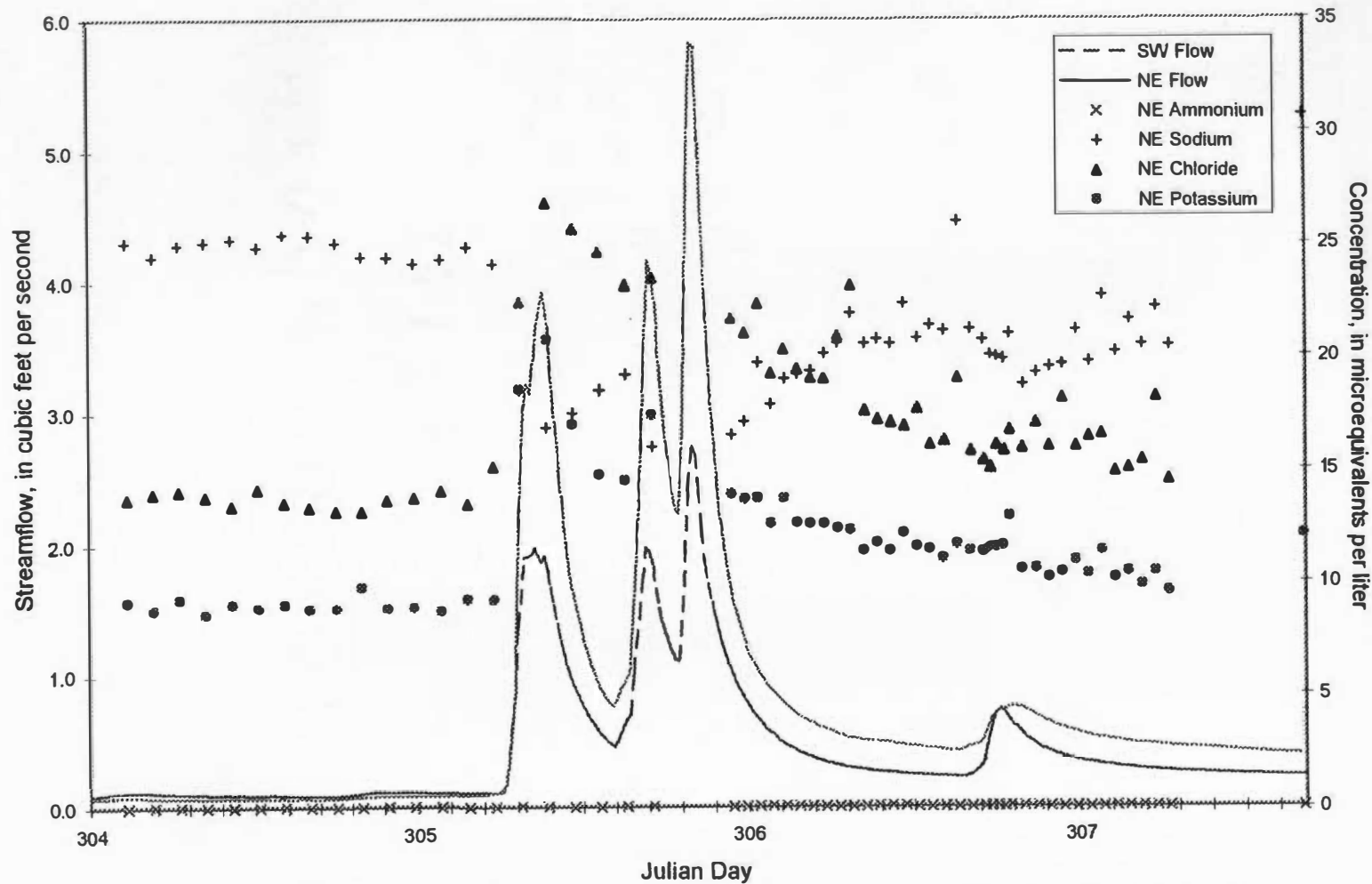


Figure 5-8. Ammonium, sodium, chloride, and potassium response during a storm event, October 31 - November 5, 1995, for the NE streamlet.

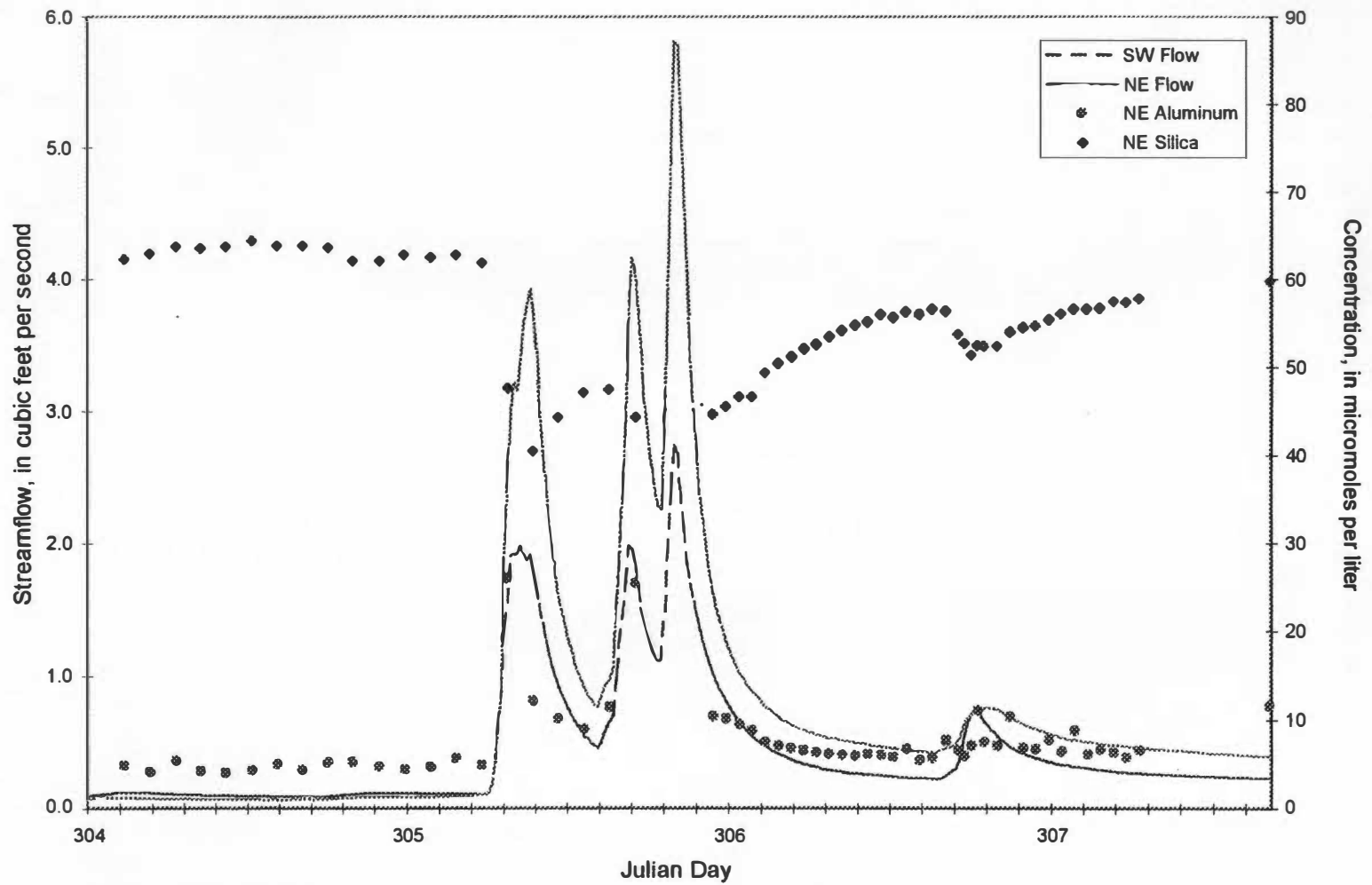


Figure 5-9. Aluminum and silica response during a storm event, October 31 - November 5, 1995, for the NE streamlet.

event. Sulfate levels rise with each peak of the hydrograph, and there appears to be no dilutional effect. Sulfate is less mobile than nitrate, and is released and flushed into the stream at a more controlled rate. Overall, sulfate concentrations rise 32.5 $\mu\text{eq/L}$ during the storm event. Sodium decreases sharply as the hydrograph rises; it is most likely a major component of groundwater and is not present in significant amounts in the vadose zone. Chloride and potassium exhibit similar behavior; both increase as the hydrograph rises, for all peaks. Aluminum concentrations also increase as the hydrograph rises, for all peaks, but silica decreases as the hydrograph rises. This is to be expected given that silica is released into the stream as the bedrock is weathered, and therefore should be present only in the baseflow component of the hydrograph. Aluminum concentrations rise 22.0 $\mu\text{mol/L}$ during the storm event, reaching a maximum of 25.9 $\mu\text{mol/L}$, which is 12.5 $\mu\text{mol/L}$ above the maximum aluminum concentration observed in the weekly samples. Ammonium levels are constant at below the detection limit and do not seem to be influenced by flow.

Descriptive statistics for each constituent during the period studied are listed in Table 5-4 for the NE stream and in Table 5-5 for the SW stream. Perhaps the most important statistics listed are minimum, maximum, and range, for they show how much a particular constituent concentration can change during a storm. A statistic for measuring relative variability, and for determining which constituents experience the greatest relative changes during a storm, is the coefficient of variation, which is simply the sample standard deviation divided by the sample mean. From this statistic, it appears that chloride and potassium concentrations show the greatest relative change in response to increased flow, for constituents measured in $\mu\text{eq/L}$. For the two constituents

Table 5-4. Descriptive statistics for constituents in the NE streamlet during a storm event, October 31 - November 5, 1995.

| Constituent | Units | Median | Mean | Standard Deviation | Minimum | Maximum | Coefficient of Variation |
|--------------|-------------------|--------|-------|--------------------|---------|---------|--------------------------|
| Flow | cfs | 0.46 | 0.75 | 1.03 | 0.06 | 5.82 | 1.37 |
| pH | | 5.33 | 5.37 | 0.24 | 4.89 | 5.79 | 0.04 |
| Conductivity | $\mu\text{S/cm}$ | 17.20 | 17.84 | 2.51 | 14.88 | 25.40 | 0.14 |
| ANC | $\mu\text{eq/L}$ | -0.52 | 0.71 | 4.41 | -7.55 | 9.37 | 6.24 |
| Chloride | $\mu\text{eq/L}$ | 16.37 | 17.35 | 3.50 | 13.15 | 26.85 | 0.20 |
| Nitrate | $\mu\text{eq/L}$ | 45.22 | 47.07 | 5.50 | 40.55 | 66.24 | 0.12 |
| Sulfate | $\mu\text{eq/L}$ | 49.84 | 49.41 | 6.11 | 39.11 | 71.57 | 0.12 |
| Sodium | $\mu\text{eq/L}$ | 20.73 | 21.42 | 2.92 | 16.01 | 30.67 | 0.14 |
| Ammonium | $\mu\text{eq/L}$ | 0.00 | 0.00 | 0.00 | 0.00 | 0.00 | N/A |
| Potassium | $\mu\text{eq/L}$ | 11.36 | 11.51 | 2.52 | 8.59 | 20.76 | 0.22 |
| Aluminum | $\mu\text{mol/L}$ | 6.47 | 7.47 | 4.02 | 3.93 | 25.94 | 0.54 |
| Silica | $\mu\text{mol/L}$ | 55.42 | 55.13 | 6.10 | 40.42 | 64.35 | 0.11 |

Table 5-5. Descriptive statistics for constituents in the SW streamlet during a storm event, October 31 - November 5, 1995.

| Constituent | Units | Median | Mean | Standard Deviation | Minimum | Maximum | Coefficient of Variation |
|--------------|------------------|--------|-------|--------------------|---------|---------|--------------------------|
| Flow | cfs | 0.26 | 0.44 | 0.51 | 0.09 | 2.74 | 1.14 |
| pH | | 5.47 | 5.56 | 0.30 | 5.01 | 6.31 | 0.05 |
| Conductivity | $\mu\text{S/cm}$ | 11.60 | 12.42 | 1.47 | 11.00 | 16.50 | 0.12 |

measured in $\mu\text{mol/L}$, silica and aluminum, aluminum exhibits a much higher relative change. Nitrate, sulfate, and sodium have similar, yet lower, coefficients of variation, and therefore probably exhibit similar relative changes in response to flow.

Analysis of Relationships between Sulfate and Nitrate Concentrations and Precipitation

A test study was conducted using weekly sample data for sulfate and nitrate along with daily precipitation readings from 1991 to 1995. The purpose of this study was to identify relationships, if any, between these analyte concentrations and rainfall and number of consecutive dry days (CDD) prior to sampling.

Sulfate and nitrate concentrations were plotted against inches of rainfall that fell since the last sampling visit (see Figures 5-10 and 5-11) in order to determine if either analyte concentration was significantly higher or lower depending on the amount of rainfall that occurred. From these figures, it is apparent that for each additional 1" of precipitation that falls since the last sampling visit, there is a $1.08 \mu\text{eq/L}$ significant increase in sulfate concentration for the SW stream and a $1.32 \mu\text{eq/L}$ significant increase for the NE stream. Relationships between nitrate and precipitation are not statistically significant; therefore, concentrations are not influenced by changing amounts of rainfall.

Weekly samples were also divided into categories based on the number of CDD before sampling; the distributions of sulfate and nitrate concentrations were then represented in box plots for each CDD category in Figures 5-12 and 5-13, respectively. Regression equations for relationships between sulfate and nitrate and #CDD are included in these figures. It is apparent that for each additional consecutive dry day prior to sampling, there is an $0.65 \mu\text{eq/L}$ significant

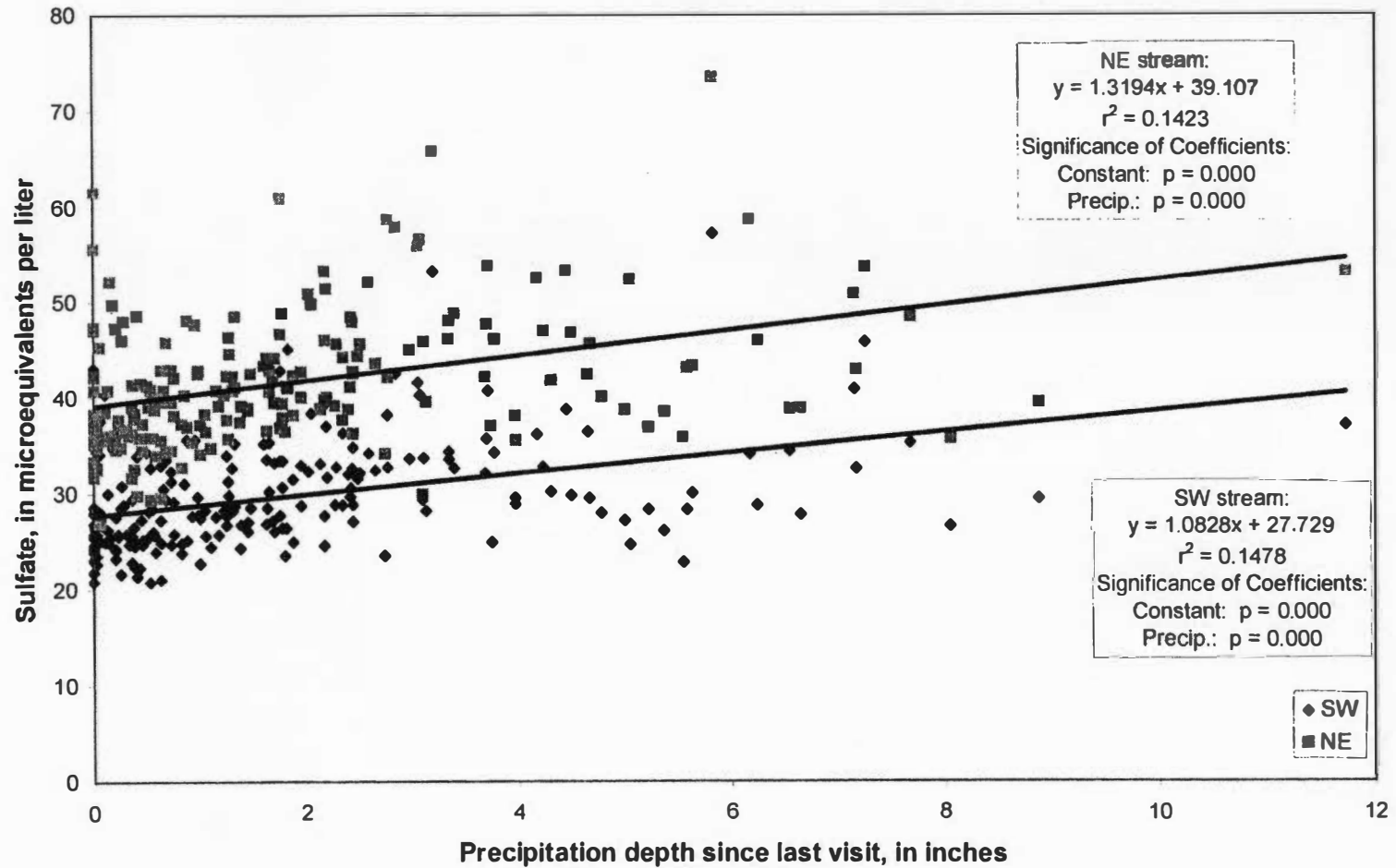


Figure 5-10. Relationship between weekly sample sulfate concentrations and precipitation since last sampling period for the SW and NE streams, 1991-1995.

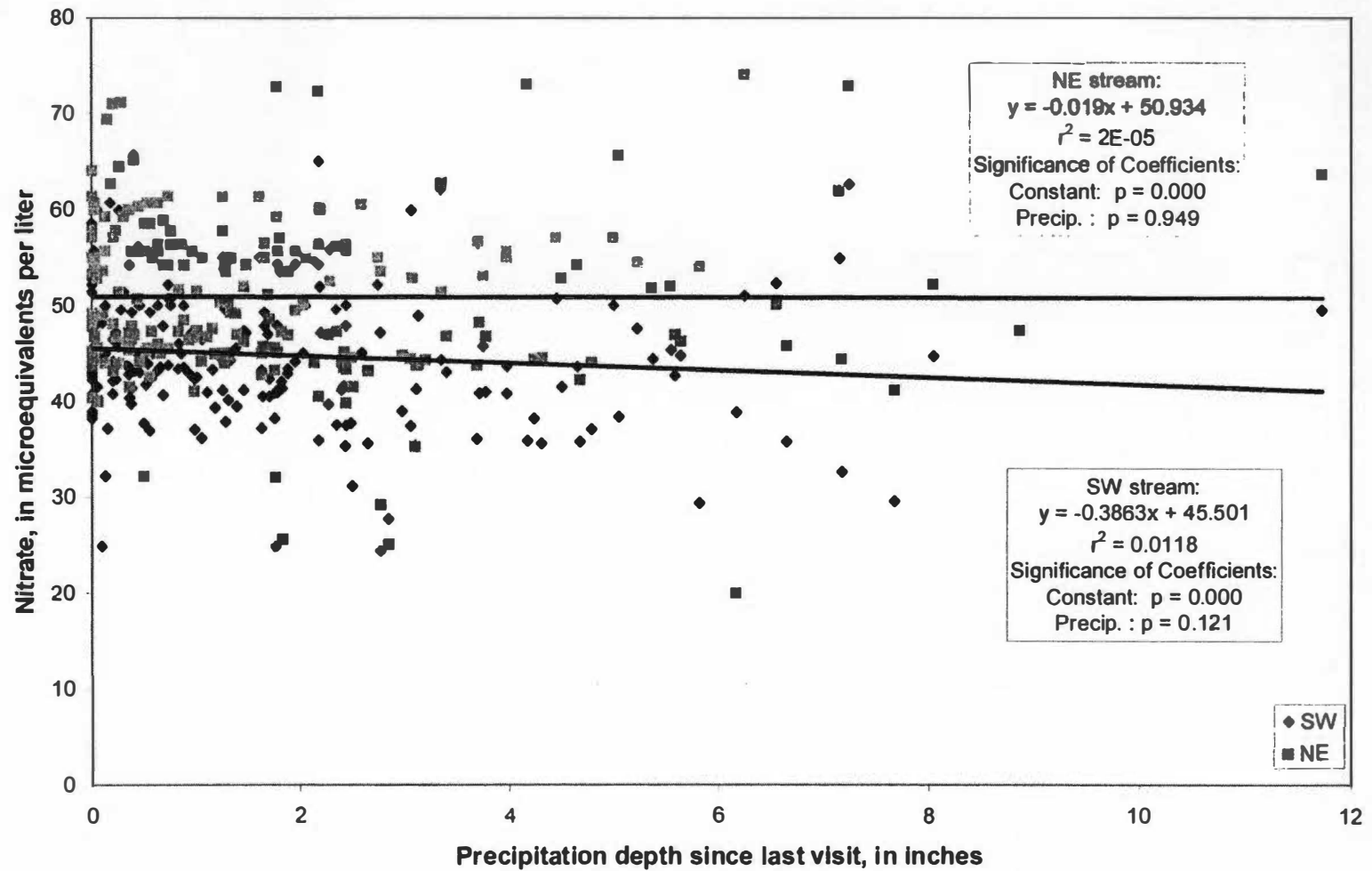
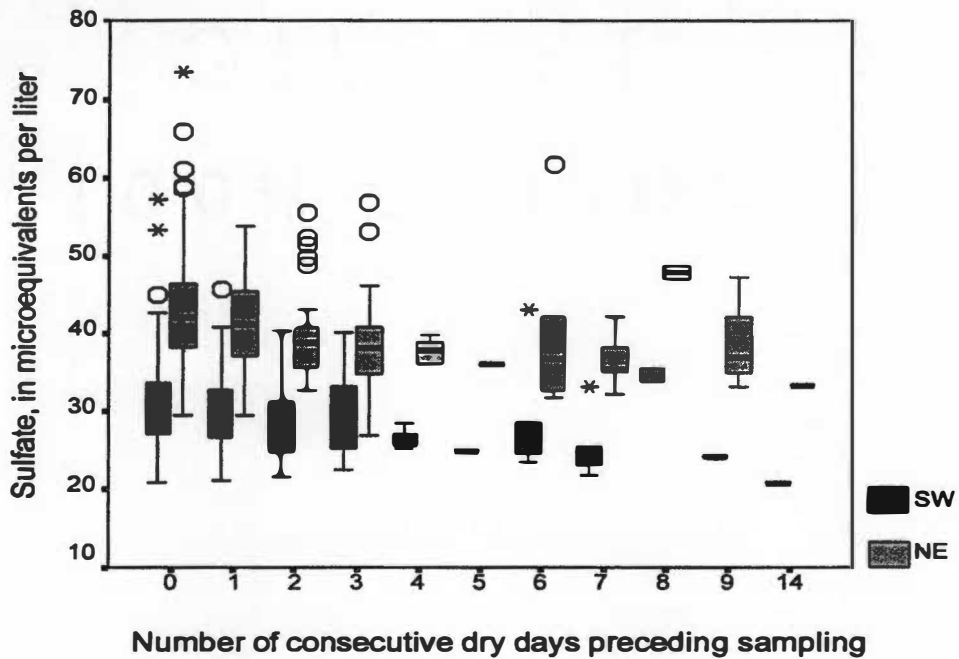


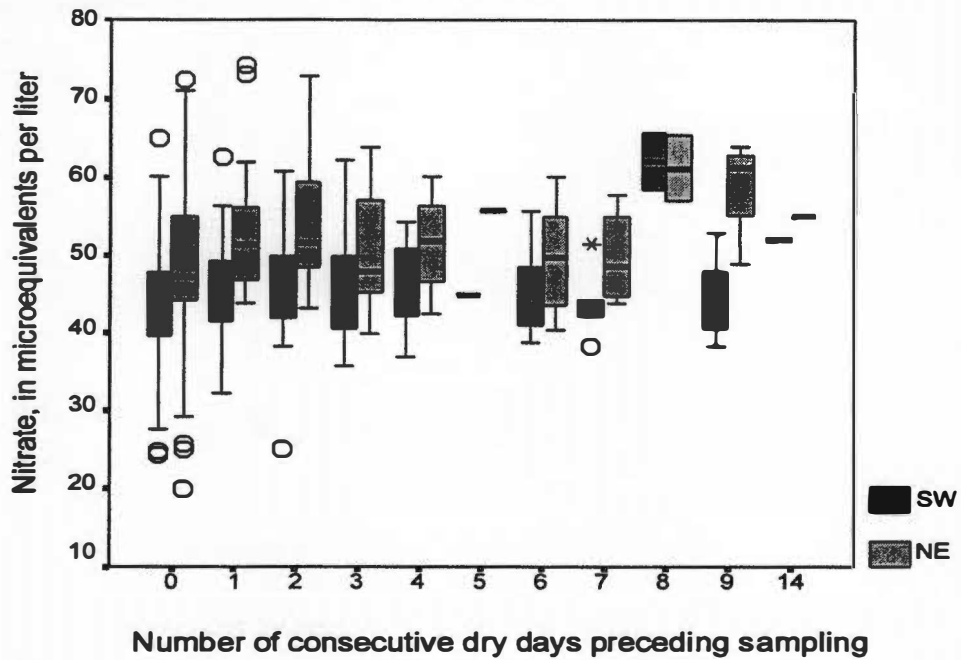
Figure 5-11. Relationship between weekly sample nitrate concentrations and precipitation since last sampling period for the SW and NE streams, 1991-1995.



Regression Equations:

| | |
|--------------------------------------|--------------------------------------|
| <u>SW:</u> | <u>NE:</u> |
| $SO_4 = 30.823 - 0.646 (\#CDD)$ | $SO_4 = 42.685 - 0.674 (\#CDD)$ |
| $r^2 = 0.064$ | $r^2 = 0.045$ |
| Coefficient on constant: $p = 0.000$ | Coefficient on constant: $p = 0.000$ |

Figure 5-12. Distributions of weekly sample sulfate concentrations and associated regression equations for the SW and NE streamlets based on number of consecutive dry days preceding sampling.



| Regression Equations: | |
|--|--|
| <u>SW:</u> | <u>NE:</u> |
| $\text{NO}_3 = 44.076 - 0.495 (\#CDD)$ | $\text{NO}_3 = 50.068 - 0.545 (\#CDD)$ |
| $r^2 = 0.025$ | $r^2 = 0.021$ |
| Coefficient on constant: $p = 0.000$ | Coefficient on constant: $p = 0.000$ |

Figure 5-13. Distributions of weekly sample nitrate concentrations and associated regression equations for the SW and NE streamlets based on number of consecutive dry days preceding sampling.

decrease in sulfate concentration for the SW stream and an 0.67 $\mu\text{eq/L}$ significant decrease for the NE stream. For the same unit increase in #CDD, there is an 0.50 $\mu\text{eq/L}$ significant decrease in nitrate concentration for the SW stream and an 0.54 $\mu\text{eq/L}$ significant decrease for the NE stream. Though all relationships between nitrate/sulfate and #CDD are statistically significant ($p < 0.05$), low r^2 values indicate that only a small percentage of the variability in nitrate and sulfate concentrations is explained by changes in #CDD. In addition, data for some of the CDD categories are limited and trends are more difficult to characterize for the higher CDD categories. Therefore, it would be useful to continue this study with more years of rainfall and concentration data.

Discussion

From the results of the analyses presented in this chapter, it is concluded that the majority of sodium and silica found in the streams is observed in the groundwater component of the hydrograph, and the majority of nitrate, sulfate, conductivity, potassium, chloride, and aluminum found in the streams is observed in the vadose and/or saturated soil zones components. These relationships are supported by the Pearson correlation coefficients in Tables 4-8 and 4-9. Significant ($p < 0.05$) positive correlations with flow exist for conductivity, sulfate, and potassium in both streams and for aluminum in the NE stream. Significant ($p < 0.05$) negative correlations with flow exist for pH, ANC, chloride, nitrate, sodium, and silica for both streams. The relationships between flow and nitrate and chloride may seem to contradict hypothesized behavior; however, it is believed that the negative correlations are due to the “dilutional” effect on nitrate and chloride during storm events. Swistock *et al.* (1989) hypothesized that there should be a significant

difference in constituent concentrations for the same flow on the rising and falling limbs of the hydrograph; however, this analysis shows there is no significant difference for any analyte between the rising and falling limbs. This result is influenced by the small number of weekly samples collected on the rising limb of the hydrograph; therefore, clearer trends may be detected with a larger data set for the rising limb.

The results of the storm event study support results found in the analysis of weekly sample constituents by flow regimes. Again, however, only a relatively small portion of the entire flow spectrum of the watershed is captured by the weekly samples, so the full spectrum of constituent concentrations cannot be represented by weekly samples alone. Episodic changes in constituents such as pH, ANC, and nitrate may in fact be of greater influence on aquatic life than chronic or long-term trends. It is known from continuous flow data that the maximum flow has been 26.8 cfs in the NE stream and 7.8 cfs in the SW stream. Since maximum flow during the storm event reaches only 5.8 cfs in the NE stream and 2.7 cfs in the SW stream, it is evident that larger storms and perhaps greater episodic changes in water quality constituents occur at NDW. This particular storm event may be considered an “average” event. During this event, median ANC is negative (-0.52 meq/L) and pH drops to below 5.0, the level at which streams are considered “acidic” according to Drever (1988). In addition, median pH is below 5.5, the level at which toxic forms of aluminum are solubilized and mobilized (Stumm and Morgan, 1981), hence the 22 $\mu\text{eq/L}$ increase in aluminum during the storm event.

Studies in other watersheds have shown that chemical signals of specific flow paths of runoff can be detected and isolated. Available data from streams at NDW are sufficient only for

limited detection of flowpaths; future research should include the collection of water samples from groundwater, deep saturated soil zones, and shallow soil zones during a storm event. Mulholland *et al.* (1990) observed that water from the vadose zone dominates stormflow early in the event and at peak flow, and water from the deep saturated soil zone dominates later in the storm. This produced chemical signals like elevated sulfate and decreased calcium early in the event, decreased sulfate and calcium later in the event, and decreased sulfate and elevated calcium once the stream returned to baseflow conditions. However, the storm event study at NDW showed no dilution of sulfate concentrations. Studies in other watersheds show that on steeper headwater streams, the vast majority of stormflow is generated by pre-event water in the upper soil zones (Swistock *et al.*, 1989). This could explain the elevated levels of sulfate, nitrate, and other constituents found at highest concentrations in the upper soil zones and the decreased levels of constituents found at highest concentrations in the deep soil zones and in groundwater.

From average nitrate concentrations observed from all three monitored soil layers, it is apparent that the median soil nitrate concentration is 1.7 times larger than the median SW stream nitrate concentration and 1.5 times larger than the NE stream nitrate concentration. Likewise, the median soil sulfate concentration is 3.4 times larger than the median SW stream sulfate concentration and 2.4 times larger than the SW stream nitrate concentration. Therefore, sulfate is retained in the watershed more than nitrate. These results may also mean that a significant amount of sulfate and nitrate may enter the streams from precipitation directly on the channel and/or soil water from deeper zones, and perhaps some is contributed by groundwater.

Results of the analysis of relationships between precipitation and sulfate and between

#CDD and sulfate agree with hypothesized behavior. Studies by Lynch and Corbett (1989), Mulholland *et al.* (1990), Swistock *et al.* (1989), and Collins *et al.* (2000) have shown that greater AMC causes greater sulfate export, primarily from water in the upper soil zones. Increased sulfate concentrations with increased rainfall prior to sampling could also be explained by sulfate in the rainfall itself. Results observed for nitrate and #CDD agree with hypothesized behavior, as it would seem logical that a dry antecedent period would cause a decrease in nitrate concentrations, since contribution of water from the soil zone would decrease. However, the relationship between nitrate and precipitation does not necessarily agree with hypothesized behavior. Though no studies have focused on the use of nitrate as a tracer to detect flow paths due to the complex interactions with which nitrate is involved, it would seem logical that greater amounts of rainfall prior to sampling would contribute more nitrate to the stream, both from the rainfall itself and from water in the upper soil zones. One possible reason that the relationship between nitrate and precipitation is not significant is that if precipitation did occur in the past week, nitrate would have been mobilized and flushed from the watershed very quickly. Sulfate appears to be retained and flushed at a more controlled rate; therefore, trends would be detected over the week.

CHAPTER VI. PARAMETRIC MODELING OF WATER QUALITY

CONSTITUENT CONCENTRATIONS AND LOADS

The weekly sample data was used to calculate loads, or the total number of units flushed out of the watershed over a time period, of each constituent. This information can be used to assess how constituents are retained in or released from the watershed and to assess downstream impacts of these loads. Loads were previously calculated using an “average” method, yet it is believed that a newly proposed method, a multiple linear regression-based model, is superior to the previous method. It is believed that the regression-based model provides greater accuracy because it considers the effect of several variables when making constituent load predictions. In the following sections, the procedures and comparison of results for both methods will be outlined and discussed.

Data Sources

The load and concentration regression models were formed from weekly sample concentration data (chloride, nitrate, sulfate, sodium, ammonium, potassium, hydrogen ion, aluminum, silica) and corresponding flow, pH, and conductivity data for the SW stream. The corresponding flow, pH, and conductivity point values were read from the 15-minute Hydrolab data at the time when each weekly sample was collected. When calculating loads, the regression equations were applied to the 15-minute continuous data (flow, pH, conductivity, time, and seasonality) to calculate loads every 15 minutes.

Methods of Analysis

Previous Load Calculation Method

Previous load estimates were determined by applying what will be termed a flow-weighted “average” method. Load estimates are calculated from weekly sample data, by computing the average analyte concentration between two consecutive weekly samples and multiplying that average concentration by the total volume of flow that occurred in the previous week. The total volume of flow is computed by summing the flows from the 15-minute continuous data and multiplying by the time (usually 7 days) elapsed since the last sample was collected. Each weekly load is calculated based on the following equation:

$$\text{Weekly Load (eq/ha)} = \frac{C_1 + C_2}{2} * V_f * \frac{1 \text{ eq}}{10^6 \mu\text{eq}} * \frac{1}{A_w} \quad (6-1)$$

Where:

- C_1 = Concentration of analyte in previous week’s sample ($\mu\text{eq/L}$)
- C_2 = Concentration of analyte in current week’s sample ($\mu\text{eq/L}$)
- V_f = Total volume of streamflow in previous week (L)
- A_w = Area of the watershed = 17.4 hectares

These flow-weighted mean loads are then summed per month to determine a flow-weighted mean load in eq/ha/month. In the past, further calculations have been made to convert this load into a monthly and yearly flow-weighted concentration for each analyte, according to the following equations:

$$\text{Monthly Mean Concentration } (\mu\text{eq/L}) = \frac{\sum \text{Weekly Loads (eq/ha)} * 10^6 \mu\text{eq}}{\sum \text{Weekly Vf (L)}} * A_w \text{ (ha)} \quad (6-2)$$

$$\text{Yearly Mean Concentration } (\mu\text{eq/L}) = \sum \text{Monthly Mean Concentrations } (\mu\text{eq/L}) \quad (6-3)$$

This section, however, deals only with comparison of loads calculated from two methods; therefore, equations for monthly and yearly mean concentrations are provided only as supplemental information.

Inherent problems with this “average” method are that variations in flow and other watershed influences are not considered, as the average analyte concentration is attributed uniformly to the streams for the previous week. It is evident from the storm event study in the previous section that analyte concentrations can vary dramatically during storm events; resolution in concentration changes is lost when the concentration is multiplied by a total volume of flow.

In order to gain greater resolution and make more precise load calculations, a multiple linear regression-based model was formed from weekly data and applied to 15-minute data. This procedure required that the model have fairly strong predictive power, so several independent variables were tested in the regression model to try to explain variability in each analyte load.

Multiple Linear Regression Method, Load Model

1st Trial:

Each constituent load, which served as the independent variable, was determined by multiplying constituent concentrations by the corresponding streamflow, as follows:

$$\text{Flow (L/s)} * \text{Concentration } (\mu\text{eq/L}) * 1\text{eq}/10^6 \mu\text{eq} = \text{Instantaneous Load (eq/sec)} \quad (6-4)$$

Log transformations were then made on all variables in the regression (load of each constituent, flow, conductivity). The transformed weekly sample data were input into SPSS, in which a multiple linear regression analysis was performed to obtain equations in the following form:

$$\ln(QC) = a + b \ln(Q) + c \ln(\text{cond.}) \quad (6-5)$$

which when de-transformed is in the form:

$$(QC) = e^a Q^b \text{cond}^c \quad (6-6)$$

For each constituent regression model, r^2 values and statistical significance ($p < .10$) of the independent variables were noted. The regression equations for each constituent were then used with 15-minute flow and conductivity data to obtain loads at every 15-minute interval, with the following conversion:

$$\begin{aligned} &\text{Instantaneous Load (eq/sec)} * 60 \text{ sec}/1 \text{ min} * 15 \text{ min} = \\ &\text{Load (eq during 15-minute interval)} \end{aligned} \quad (6-7)$$

These 15-minute loads were then summed by month and divided by the watershed area to obtain load in eq/ha/month.

In some cases, 15-minute conductivity was unavailable due to malfunction of the datalogger. In such cases, regression analysis was conducted for each constituent load based on flow only. These equations were used to obtain a 15-minute load only when no conductivity data were present.

2nd Trial:

It was determined that a more accurate model might be formed by including variables to represent seasonality, time, and point-value pH. Therefore, the weekly sample data and corresponding flow and conductivity were again used to form the regression model as above in the 1st trial, but with additional independent variables included. The load of each constituent was again determined by multiplying concentration by corresponding streamflow, as follows:

$$\text{Flow (L/s)} * \text{Concentration } (\mu\text{eq/L}) * 1\text{eq}/10^6 \mu\text{eq} = \text{Instantaneous Load (eq/sec)} \quad (6-8)$$

The regression variables of load, flow, conductivity, and pH were transformed by calculating their natural log. An independent variable to represent long-term trends with time was introduced by determining the Julian day, cumulative, on which each sample was taken. The Julian day sequence begins with time = 0 on December 31, 1990, at 2400 hrs (t = 1 on January 1, 1991). This variable is cumulative in that it is not re-set to 0 at the end of each year.

A seasonality component was also introduced by determining the fractional part of the year in which each sample was taken. For example, if a sample was taken on May 1, 1995 (Julian day = 121), the fractional part of the year that had elapsed so far is $121/365 = 0.3315$. This value is

then multiplied by 2π to convert it to radians; this term is called θ . The seasonality variable is then introduced into the regression as $(b \sin \theta + c \cos \theta)$.

The transformed weekly sample data and additional variables were input into SPSS, in which a multiple linear regression analysis was performed to obtain equations in the following form:

$$\ln(QC) = I + a t + b(\sin \theta) + c(\cos \theta) + d \ln(Q) + f \ln(\text{cond.}) + g \ln(\text{pH}) \quad (6-9)$$

where:

- C is the concentration in eq/L
- Q is the streamflow in L/s
- cond. is the conductivity in $\mu\text{S}/\text{cm}$
- pH is the sample pH
- I is the regression intercept
- ln is the natural logarithm
- t is the time, in cumulative Julian days (t = 0 is December 31, 1990, at 2400 hrs)
- θ is the fractional part of the year, in radians
- a,b,c,d,f,g are the regression coefficients

Specific regression equations are not listed because this trial was used to form the next set of regression equations, for which non-significant variables are removed.

The 2nd trial regression model was checked for multicollinearity problems by examining residuals plots, correlation coefficients among independent variables, the variance inflation factor, and condition indices.

3rd Trial:

Using the results of 2nd trial, the multiple regression analysis was re-performed for each analyte load with only significant ($p < 0.10$) variables included for each respective load.

Temperature was considered as a possible independent variable, but it was not included due to

gaps in the continuous record of temperature data and because it is believed that seasonal changes are adequately represented by $\sin/\cos \theta$ and flow. Because temperature data are usually missing for the winter record (due to datalogger malfunction), using the temperature record in only spring, summer, and fall could bias the regression.

After the regression models were re-run in SPSS, they were checked to be sure that the remaining variables were still statistically significant with respect to each load. Successive regression iterations were made until models included only variables that were significant. Multicollinearity problems were again assessed by examining correlation coefficients among independent variables, the variance inflation factor, and condition indices.

Multiple Linear Regression Method, Concentration Model

After the load regression model was created, it was thought that a similar model for predicting constituent concentrations would be useful, since aquatic life are probably most influenced by changes in concentrations.

The procedures outlined for the 2nd and 3rd trials in the load regression model were repeated and adjusted to create a regression model based on concentration only. That is, the dependent variable was concentration, and possible independent variables were time, seasonality, flow, conductivity, and pH.

Multicollinearity problems were again assessed by examining correlation coefficients among independent variables, the variance inflation factor, and condition indices. Residual plots were examined to note any further multicollinearity problems and to discover possible reasons for low r^2 values; however, no significant trends or problems were observed.

Results

Load Regression Model

Table 6-1 shows the first trial regression equations for each constituent load, and Table 6-2 shows regression equations based on flow only. Possible multicollinearity problems associated with the third trial regression models are noted in Table 6-3, and full regression equations for the third model are listed in Table 6-4. The independent variables and their coefficients provide insight into the relative behavior of loads and concentrations with changes in those variables. Some inferences about long-term time trends of constituents were made in Chapter IV; the regression equations in this chapter statistically prove these time trends. The load regression equations listed in Table 6-4 show that holding all other variables constant, the natural log of chloride load is increasing overtime at a rate of $2.6E-4$ units per day, and that as flow and pH increase, chloride loads also increase. The natural log of nitrate load is in fact decreasing overtime and a rate of $7.9E-5$ units per day and increases with increasing flow and conductivity. Sulfate loads follow the same patterns as nitrate, though sulfate loads decrease with increasing pH and there are no significant changes over time. The natural log of sodium loads is increasing over time at a rate of $3.6E-5$ units per day and increases with increasing flow, conductivity, and pH. The natural log of ammonium load also is increasing with time at a rate of $7.4E-4$ units per day and increases with increasing flow. Similar to sulfate, potassium loads show no significant changes over time and increase with increasing flow and conductivity, yet potassium loads have no significant relationship with pH. Hydrogen ion loads follow the same pattern as potassium loads. The natural log of aluminum load is increasing over time at a rate of $1.3E-3$ units per day, increases with increasing flow, and decreases with increasing

Table 6-1. 1st trial de-transformed regression equations for the SW streamlet based on flow and conductivity.

| | | |
|---------------|---|---------------|
| Chloride: | $QC = (3.1315E-6 * Q^{0.915} * cond^{0.598})$ | $r^2 = 0.795$ |
| Nitrate: | $QC = (3.0463E-5 * Q^{0.963} * cond^{0.148})$ | $r^2 = 0.970$ |
| Sulfate: | $QC = (1.5557E-5 * Q^{1.125} * cond^{0.186})$ | $r^2 = 0.984$ |
| Sodium: | $QC = (1.7107E-5 * Q^{0.903} * cond^{0.195})$ | $r^2 = 0.970$ |
| Ammonium: | $QC = (5.964E-3 * Q^{0.906} * cond^{-3.045})$ | $r^2 = 0.355$ |
| Potassium: | $QC = (4.665E-7 * Q^{1.025} * cond^{1.066})$ | $r^2 = 0.892$ |
| Hydrogen Ion: | $QC = (1.155E-7 * Q^{1.285} * cond^{0.838})$ | $r^2 = 0.895$ |
| Aluminum: | $QC = (3.2406E-3 * Q^{1.03} * cond^{-2.668})$ | $r^2 = 0.566$ |
| Silica: | $QC = (5.4571E-5 * Q^{0.913} * cond^{0.08072})$ | $r^2 = 0.978$ |

Key: (QC = load (eq/sec), Q = flow(L/s), cond = conductivity (μS/cm))

Table 6-2. 1st trial de-transformed regression equations for the SW streamlet based on flow only.

| | | |
|---------------|--------------------------------|---------------|
| Chloride: | $QC = (1.4404E-5 * Q^{0.927})$ | $r^2 = 0.787$ |
| Nitrate: | $QC = (4.4368E-5 * Q^{0.966})$ | $r^2 = 0.970$ |
| Sulfate: | $QC = (2.5016E-5 * Q^{1.129})$ | $r^2 = 0.984$ |
| Sodium: | $QC = (2.8149E-5 * Q^{0.907})$ | $r^2 = 0.969$ |
| Ammonium: | $QC = (2.4559E-6 * Q^{0.821})$ | $r^2 = 0.306$ |
| Potassium: | $QC = (7.0605E-6 * Q^{1.047})$ | $r^2 = 0.872$ |
| Hydrogen Ion: | $QC = (9.7874E-7 * Q^{1.303})$ | $r^2 = 0.887$ |
| Aluminum: | $QC = (3.6675E-6 * Q^{0.981})$ | $r^2 = 0.510$ |
| Silica: | $QC = (6.6988E-5 * Q^{0.915})$ | $r^2 = 0.978$ |

Key: (QC = load (eq/sec), Q = flow(L/s))

Table 6-3. Summary of 3rd trial load regression model for the SW streamlet.

| Constituent (Load) | Variables Det. to be Significant ($p < .10$) | r^2 | Multicollinearity Problems? |
|---------------------------|---|-------------------------|---|
| Chloride | t, θ , Q, pH | 0.839 | Correlation b/t independent variables VIF okay One high CI (202.5) |
| Nitrate | t, θ , Q, Cond | 0.984 | Correlation b/t independent variables VIF okay One high CI (202.5) |
| Sulfate | θ , Q, Cond, pH | 0.986 | Correlation b/t independent variables VIF okay One high CI (182.77) |
| Sodium | t, θ , Q, Cond, pH | 0.973 | Correlation b/t independent variables VIF okay One high CI (182.77) |
| Ammonium | t, θ , Q | 0.622 | Correlation b/t independent variables VIF okay One high CI (208.89) |
| Potassium | θ , Q, Cond | 0.902 | Correlation b/t independent variables VIF okay One high CI (182.77) |
| H+ Ion | θ , Q, Cond | 0.906 | Correlation b/t independent variables VIF okay CI okay |
| Aluminum | t, θ , Q, Cond | 0.694 | Correlation b/t independent variables VIF okay One high CI (231.25) |
| Silica | t, Q, pH | 0.983 | Correlation b/t independent variables VIF okay One high CI (244.33) |

Key: t = time (cumulative Julian days), θ = seasonality terms, Q = flow (L/s), Cond = conductivity (uS/cm), pH = pH, VIF = variance inflation factor, CI = condition index

Table 6-4. 3rd model load regression equations for the SW streamlet.

| | |
|-------------------|--|
| Chloride: | $\ln(QC) = -13.706 + 2.576E-4 t - 5.44E-2 \sin \theta + 0.18 \cos \theta + 0.936 \ln Q + 1.225 \ln \text{pH}$ |
| De-transformed: | $QC = 1.1157E-6 * e^{2.576E-4 t} * e^{-5.44E-2 \sin \theta} * e^{0.18 \cos \theta} * Q^{0.936} * \text{pH}^{1.225}$ |
| | $r^2 = 0.839$ |
| <hr/> | |
| Nitrate: | $\ln(QC) = -10.232 - 7.912E-5 t + 5.422E-5 \sin \theta + 0.106 \cos \theta + 0.931 \ln Q + 0.148 \ln \text{cond.}$ |
| De-transformed: | $QC = 3.60E-5 * e^{-7.912E-5 t} * e^{5.422E-5 \sin \theta} * e^{0.106 \cos \theta} * Q^{0.931} * \text{cond}^{0.148}$ |
| | $r^2 = 0.984$ |
| <hr/> | |
| Sulfate: | $\ln(QC) = -8.611 - 3.488E-2 \sin \theta - 2.889E-2 \cos \theta + 1.112 \ln Q + 9.089E-2 \ln \text{cond} - 1.246 \ln \text{pH}$ |
| De-transformed: | $QC = 1.8209E-4 * e^{-3.488E-2 \sin \theta} * e^{-2.889E-2 \cos \theta} * Q^{1.112} * \text{cond}^{0.09089} * \text{pH}^{-1.246}$ |
| | $r^2 = 0.986$ |
| <hr/> | |
| Sodium: | $\ln(QC) = -13.05 + 3.552E-5 t - 1.936E-2 \sin \theta + 2.888E-2 \cos \theta + 0.928 \ln Q + 0.18 \ln \text{cond.} + 1.15 \ln \text{pH}$ |
| De-transformed: | $QC = 2.1501E-6 * e^{3.552E-5 t} * e^{-1.936E-2 \sin \theta} * e^{2.888E-2 \cos \theta} * Q^{0.928} * \text{cond}^{0.18} * \text{pH}^{1.15}$ |
| | $r^2 = 0.973$ |
| <hr/> | |
| Ammonium: | $\ln(QC) = -13.973 + 7.353E-4 t + 0.481 \sin \theta - 0.341 \cos \theta + 0.806 \ln Q$ |
| De-transformed: | $QC = 8.5428E-7 * e^{7.353E-4 t} * e^{0.481 \sin \theta} * e^{-0.341 \cos \theta} * Q^{0.806}$ |
| | $r^2 = 0.622$ |
| <hr/> | |
| Potassium: | $\ln(QC) = -13.98 - 0.02635 \sin \theta + 0.143 \cos \theta + 1.008 \ln Q + 0.845 \ln \text{cond.} - 0.225 \ln \text{pH}$ |
| De-transformed: | $QC = 8.4833E-7 * e^{-0.02635 \sin \theta} * e^{0.143 \cos \theta} * Q^{1.008} * \text{cond}^{0.845}$ |
| | $r^2 = 0.902$ |
| <hr/> | |
| H+ ion: | $\ln(QC) = -15.837 + 0.113 \sin \theta + 0.153 \cos \theta + 1.233 \ln Q + 0.814 \ln \text{cond.}$ |
| De-transformed: | $QC = 1.3246E-7 * e^{0.113 \sin \theta} * e^{0.153 \cos \theta} * Q^{1.233} * \text{cond}^{0.814}$ |
| | $r^2 = 0.906$ |
| <hr/> | |
| Aluminum: | $\ln(QC) = -11.287 + 1.346E-3 t + 7.658E-2 \sin \theta - 0.212 \cos \theta + 1.001 \ln Q - 1.066 \ln \text{cond}$ |
| De-transformed: | $QC = 1.2535E-5 * e^{1.346E-3 t} * e^{0.07658 \sin \theta} * e^{-0.212 \cos \theta} * Q^{1.001} * \text{cond}^{-1.066}$ |
| | $r^2 = 0.694$ |
| <hr/> | |
| Silica: | $\ln(QC) = -11.628 - 1.543E-4 t + 0.947 \ln Q + 1.211 \ln \text{pH}$ |
| De-transformed: | $QC = 8.913E-6 * e^{-1.543E-4 t} * Q^{0.947} * \text{pH}^{1.211}$ |
| | $r^2 = 0.980$ |

conductivity. Aluminum loads show no significant relationship with pH; again, this is particularly surprising, as increasing acidity in the watershed is believed to mobilize aluminum from the soil into the stream. The natural log of silica load is increasing over time at a rate of $1.5E-4$ units per day and increases with increasing flow and pH. Silica is the only constituent that shows no significant seasonal trends in the presence of the other independent variables.

Load calculations made from the average and regression methods and summed per month for 1993 and 1994 are shown in Table 6-5. For this test period and in comparison with the regression-based model, the “average” method produced higher estimates of chloride, nitrate, sodium, aluminum, and silica, and lower estimates of sulfate, ammonium, hydrogen ion, and potassium.

Concentration Regression Model

Possible multicollinearity problems for the final concentration regression model are noted in Table 6-6, and full regression equations are listed in Table 6-7. The concentration regression equations in Table 6-7 show that holding all other variables constant, the natural log of chloride concentration is increasing over time at a rate of $2.6E-4$ units per day and that it decreases with increasing flow and increases with increasing pH. The natural log of nitrate concentration is decreasing over time at a rate of $7.9E-5$ units per day, increases with increasing conductivity, and decreases with increasing flow. Sulfate concentrations show no significant changes overtime, but they increase with increasing flow and conductivity and decrease with increasing pH. The natural log of sodium concentration is increasing over time at a rate of $3.6E-5$ units per day, increases with increasing pH and conductivity, and decreases with increasing flow. The natural log of ammonium

Table 6-5. Comparison of mass transport results* from the regression and "average" methods for 1993 and 1994.

| DATE | Reg Chloride | Avg Chloride | % diff | Reg Nitrate | Avg Nitrate | % diff | Reg Sulfate | Avg Sulfate | % diff | Reg Sodium | Avg Sodium | % diff | Reg Ammonium | Avg Ammonium | % diff |
|---------|--------------|--------------|---------|-------------|-------------|--------|-------------|-------------|--------|------------|------------|---------|--------------|--------------|---------|
| Jan-93 | 14.89 | 13.51 | 9.74 | 62.29 | 65.59 | -5.16 | 45.05 | 41.61 | 7.95 | 29.39 | 31.03 | -5.45 | 1.02 | 0.28 | 113.97 |
| Feb-93 | 5.52 | 4.82 | 13.56 | 22.68 | 25.33 | -11.03 | 15.07 | 12.61 | 17.75 | 11.27 | 11.44 | -1.54 | 0.65 | 0.28 | 79.48 |
| Mar-93 | 12.44 | 9.02 | 31.86 | 58.20 | 55.06 | 5.55 | 47.68 | 33.29 | 35.54 | 27.78 | 25.14 | 9.96 | 1.88 | 1.21 | 43.37 |
| Apr-93 | 10.47 | 11.88 | -12.58 | 46.35 | 51.94 | -11.37 | 33.54 | 34.98 | -4.20 | 24.41 | 28.05 | -13.88 | 1.94 | 2.66 | -31.26 |
| May-93 | 4.08 | 5.13 | -22.83 | 17.75 | 18.42 | -3.70 | 11.61 | 14.69 | -23.39 | 10.13 | 10.78 | -6.26 | 0.94 | 2.13 | -77.58 |
| Jun-93 | 2.39 | 2.47 | -3.38 | 9.01 | 8.24 | 8.90 | 5.44 | 5.30 | 2.60 | 5.55 | 5.47 | 1.42 | 0.50 | 0.75 | -40.80 |
| Jul-93 | 1.30 | 1.44 | -10.08 | 5.15 | 5.16 | -0.18 | 3.04 | 3.08 | -1.32 | 3.23 | 3.10 | 3.97 | 0.26 | 0.37 | -35.90 |
| Aug-93 | 5.02 | 7.17 | -35.24 | 20.12 | 23.84 | -16.91 | 19.20 | 14.24 | 29.67 | 12.01 | 13.70 | -13.15 | 0.59 | 0.10 | 142.05 |
| Sep-93 | 5.80 | 5.20 | 10.87 | 19.84 | 19.68 | 0.83 | 14.71 | 13.17 | 11.05 | 12.46 | 13.49 | -7.90 | 0.47 | 0.00 | 200.00 |
| Oct-93 | 2.79 | 3.03 | -8.28 | 9.06 | 8.87 | 2.08 | 5.19 | 5.00 | 3.73 | 5.56 | 6.88 | -21.21 | 0.20 | 0.04 | 131.92 |
| Nov-93 | 10.57 | 12.25 | -14.74 | 36.11 | 38.91 | -7.45 | 29.57 | 22.03 | 29.22 | 19.75 | 21.72 | -9.52 | 0.79 | 0.28 | 95.71 |
| Dec-93 | 12.37 | 9.65 | 24.74 | 44.08 | 38.78 | 12.78 | 36.68 | 27.14 | 29.90 | 22.14 | 18.09 | 20.14 | 0.75 | 0.91 | -18.98 |
| Average | 7.30 | 7.13 | -1.36 | 29.22 | 29.99 | -2.14 | 22.23 | 18.93 | 11.54 | 15.30 | 15.74 | -3.62 | 0.83 | 0.75 | 50.16 |
| Sum | | | -16.36 | | | -25.66 | | | 138.50 | | | -43.42 | | | 601.97 |
| Jan-94 | 20.43 | 23.20 | -12.71 | 75.09 | 58.97 | 24.05 | 61.23 | 52.06 | 16.18 | 36.58 | 35.66 | 2.54 | 1.63 | 0.86 | 61.86 |
| Feb-94 | 17.95 | 23.36 | -26.22 | 71.45 | 80.82 | -12.31 | 61.24 | 52.43 | 15.51 | 33.16 | 47.11 | -34.75 | 2.08 | 0.61 | 109.26 |
| Mar-94 | 15.69 | 20.30 | -25.59 | 66.39 | 74.93 | -12.08 | 60.17 | 45.88 | 26.95 | 31.03 | 43.39 | -33.22 | 2.71 | 1.44 | 61.21 |
| Apr-94 | 10.44 | 20.75 | -66.13 | 42.09 | 40.66 | 3.45 | 35.81 | 30.66 | 15.49 | 21.44 | 24.84 | -14.72 | 2.29 | 1.22 | 60.79 |
| May-94 | 3.68 | 3.86 | -4.89 | 14.54 | 14.74 | -1.38 | 9.79 | 9.60 | 1.96 | 8.20 | 8.61 | -4.93 | 1.08 | 0.00 | 200.00 |
| Jun-94 | 9.17 | 11.68 | -24.07 | 36.67 | 33.90 | 7.86 | 38.09 | 32.63 | 15.45 | 20.61 | 22.19 | -7.37 | 2.18 | 0.00 | 200.00 |
| Jul-94 | 9.26 | 11.45 | -21.17 | 33.17 | 34.51 | -3.95 | 33.47 | 30.57 | 9.05 | 19.97 | 23.63 | -16.79 | 1.67 | 0.00 | 200.00 |
| Aug-94 | 11.23 | 10.54 | 6.37 | 37.39 | 34.84 | 7.05 | 39.30 | 37.20 | 5.49 | 22.77 | 26.50 | -15.16 | 1.41 | 0.00 | 200.00 |
| Sep-94 | 8.23 | 7.37 | 10.97 | 24.67 | 24.05 | 2.54 | 20.33 | 19.75 | 2.88 | 15.50 | 16.69 | -7.40 | 0.75 | 0.00 | 200.00 |
| Oct-94 | 7.47 | 9.39 | -22.80 | 22.97 | 26.59 | -14.63 | 16.85 | 18.07 | -7.01 | 13.52 | 15.03 | -10.57 | 0.74 | 0.36 | 68.54 |
| Nov-94 | 7.29 | 6.06 | 18.37 | 21.78 | 21.55 | 1.05 | 16.37 | 13.39 | 20.05 | 12.17 | 13.06 | -7.03 | 0.51 | 0.00 | 200.00 |
| Dec-94 | 10.27 | 9.66 | 6.13 | 30.54 | 35.55 | -15.18 | 22.12 | 23.35 | -5.40 | 16.50 | 17.82 | -7.69 | 0.75 | 0.00 | 200.00 |
| Average | 10.92 | 13.14 | -13.48 | 39.73 | 40.09 | -1.13 | 34.56 | 30.47 | 9.72 | 20.95 | 24.54 | -13.09 | 1.48 | 0.37 | 146.80 |
| Sum | | | -161.75 | | | -13.52 | | | 116.59 | | | -157.08 | | | 1761.65 |

*All analyte loads are reported in eq/ha/month, unless otherwise noted

Table 6-5 (cont'd). Comparison of mass transport results* from the regression and "average" methods for 1993 and 1994.

| DATE | Reg Potassium | Avg Potassium | % diff | Reg Hyd. Ion | Avg Hyd. Ion | % diff | Reg Aluminum' | Avg Aluminum' | % diff | Reg Silica' | Avg Silica' | % diff |
|---------|------------------|------------------|-----------|-----------------|-----------------|-----------|------------------|------------------|-----------|----------------|----------------|-----------|
| Jan-93 | 10.88 | 11.12 | -2.16 | 2.83 | 2.47 | 13.63 | 2.63 | 1.42 | 59.60 | 74.76 | 78.59 | -5.00 |
| Feb-93 | 3.85 | 3.43 | 11.50 | 0.99 | 0.91 | 8.10 | 1.15 | 0.32 | 112.69 | 28.15 | 29.04 | -3.11 |
| Mar-93 | 9.39 | 9.61 | -2.29 | 2.85 | 3.09 | -8.01 | 3.67 | 1.62 | 77.45 | 72.65 | 64.93 | 11.22 |
| Apr-93 | 6.86 | 9.31 | -30.25 | 1.87 | 2.72 | -36.96 | 3.58 | 7.65 | -72.58 | 64.92 | 65.30 | -0.59 |
| May-93 | 2.47 | 3.03 | -20.24 | 0.53 | 0.57 | -7.67 | 1.53 | 3.96 | -88.78 | 26.50 | 26.39 | 0.41 |
| Jun-93 | 1.31 | 1.14 | 14.19 | 0.22 | 0.20 | 9.07 | 0.78 | 1.51 | -63.29 | 13.90 | 13.99 | -0.62 |
| Jul-93 | 0.74 | 0.69 | 7.13 | 0.10 | 0.10 | 3.07 | 0.43 | 1.03 | -81.83 | 7.90 | 8.72 | -9.88 |
| Aug-93 | 3.71 | 2.84 | 26.57 | 0.83 | 0.46 | 56.98 | 1.72 | 2.71 | -44.93 | 29.49 | 33.93 | -13.99 |
| Sep-93 | 3.38 | 2.95 | 13.44 | 0.59 | 0.42 | 33.08 | 1.64 | 1.54 | 6.54 | 30.49 | 32.17 | -5.35 |
| Oct-93 | 1.51 | 1.59 | -5.08 | 0.21 | 0.17 | 22.36 | 0.61 | 1.20 | -65.64 | 13.07 | 13.77 | -5.22 |
| Nov-93 | 7.62 | 5.67 | 29.34 | 1.96 | 0.91 | 73.38 | 2.30 | 5.13 | -76.08 | 46.35 | 54.37 | -15.92 |
| Dec-93 | 8.52 | 5.75 | 38.85 | 2.21 | 1.14 | 63.80 | 2.88 | 4.28 | -39.03 | 52.71 | 38.43 | 31.34 |
| Average | 5.02 | 4.76 | 6.75 | 1.27 | 1.10 | 19.24 | 1.91 | 2.70 | -22.99 | 38.41 | 38.30 | -1.39 |
| Sum | | | 80.99 | | | 230.84 | | | -275.89 | | | -16.696 |
| Jan-94 | 14.29 | 10.79 | 27.89 | 4.39 | 2.38 | 59.33 | 5.48 | 9.28 | -51.45 | 89.48 | 74.44 | 18.35 |
| Feb-94 | 12.45 | 12.79 | -2.65 | 3.98 | 2.80 | 34.90 | 6.37 | 11.09 | -54.11 | 82.56 | 97.80 | -16.90 |
| Mar-94 | 11.08 | 12.13 | -9.06 | 3.66 | 2.49 | 38.10 | 7.20 | 11.10 | -42.68 | 78.16 | 98.74 | -23.27 |
| Apr-94 | 6.34 | 6.42 | -1.21 | 1.85 | 1.50 | 20.85 | 5.88 | 7.24 | -20.73 | 54.91 | 64.79 | -16.51 |
| May-94 | 1.99 | 2.05 | -2.83 | 0.41 | 0.38 | 7.03 | 2.18 | 1.53 | 35.05 | 20.51 | 17.88 | 13.71 |
| Jun-94 | 5.77 | 4.27 | 29.81 | 1.55 | 1.25 | 21.13 | 6.95 | 5.34 | 26.24 | 52.42 | 60.58 | -14.45 |
| Jul-94 | 5.10 | 6.02 | -16.58 | 1.21 | 1.04 | 15.28 | 6.94 | 5.53 | 22.59 | 50.54 | 56.59 | -11.30 |
| Aug-94 | 6.02 | 6.19 | -2.81 | 1.41 | 1.47 | -4.19 | 7.73 | 6.82 | 12.49 | 56.79 | 63.83 | -11.67 |
| Sep-94 | 4.08 | 3.87 | 5.29 | 0.76 | 0.55 | 32.03 | 4.04 | 2.87 | 33.77 | 36.90 | 37.52 | -1.67 |
| Oct-94 | 4.08 | 3.82 | 6.58 | 0.76 | 0.55 | 32.66 | 2.56 | 2.33 | 9.43 | 31.40 | 29.04 | 7.81 |
| Nov-94 | 4.12 | 3.77 | 8.99 | 0.88 | 0.53 | 50.11 | 2.40 | 2.09 | 13.70 | 27.24 | 26.20 | 3.90 |
| Dec-94 | 5.42 | 5.28 | 2.53 | 1.20 | 1.03 | 15.46 | 3.64 | 3.21 | 12.49 | 37.43 | 39.06 | -4.27 |
| Average | 6.73 | 6.45 | 3.83 | 1.84 | 1.33 | 26.89 | 5.11 | 5.70 | -0.27 | 51.53 | 55.54 | -4.69 |
| Sum | | | 45.95 | | | 322.70 | | | -3.22 | | | -56.26 |

*All analyte loads are reported in eq/ha/month, unless otherwise noted

'Aluminum and silica loads reported in mol/ha/month

Table 6-6. Summary of concentration regression model for the SW streamlet.

| Constituent (Concentration) | Variables Det. To Be Significant (p < .10) | r² | Multicollinearity Problems? |
|--|--|----------------------|--|
| Chloride | t, θ , Q, pH | 0.260 | Correlation b/t independent variables VIF okay CI okay |
| Nitrate | t, θ , Q, Cond | 0.496 | Correlation b/t independent variables VIF okay One high CI (202.5) |
| Sulfate | θ , Q, Cond, pH | 0.518 | Correlation b/t independent variables VIF okay One high CI (182.77) |
| Sodium | t, θ , Q, pH, Cond | 0.343 | Correlation b/t independent variables VIF okay One high CI (163.68) |
| Ammonium | t, θ , Q | 0.466 | Correlation b/t independent variables VIF okay CI okay |
| Potassium | θ , Cond | 0.244 | Correlation b/t independent variables VIF okay One high CI (182.77) |
| H+ Ion | θ , Q, Cond | 0.414 | Correlation b/t independent variables VIF okay CI okay |
| Aluminum | t, θ , Cond | 0.376 | Correlation b/t independent variables VIF okay One high CI (203.55) |
| Silica | t, Q, pH | 0.431 | Correlation b/t independent variables VIF okay One high CI (229.81) |

Key: t = time (cumulative Julian days), θ = seasonality terms, Q = flow (L/s), Cond = conductivity (uS/cm), pH = pH, VIF = variance inflation factor, CI = condition index

Table 6-7. Concentration regression equations for the SW streamlet.

| | |
|-------------------|--|
| Chloride: | $\ln C = 0.109 + 2.576E-4 t - 5.44E-2 \sin \theta + 0.18 \cos \theta - 6.381E-2 \ln Q + 1.225 \ln \text{pH}$ |
| De-transformed: | $C = 1.1152 * e^{2.576E-4 t} * e^{-5.44E-2 \sin \theta} * e^{0.18 \cos \theta} * Q^{-0.06381} * \text{pH}^{1.225}$ |
| | $r^2 = 0.260$ |
| Nitrate: | $\ln C = 3.584 - 7.912E-5 t + 0.05422 \sin \theta + 0.106 \cos \theta - 0.06914 \ln Q + 0.148 \ln \text{cond.}$ |
| De-transformed: | $C = 36.0173 * e^{-7.912E-5 t} * e^{0.05422 \sin \theta} * e^{0.106 \cos \theta} * Q^{-0.06914} * \text{cond}^{0.148}$ |
| | $r^2 = 0.496$ |
| Sulfate: | $\ln C = 5.205 - 3.488E-2 \sin \theta - 2.889E-2 \cos \theta + 0.112 \ln Q + 9.089E-2 \ln \text{cond} - 1.246 \ln \text{pH}$ |
| De-transformed: | $C = 182.1809 * e^{-3.488E-2 \sin \theta} * e^{-2.889E-2 \cos \theta} * Q^{0.112} * \text{cond}^{0.09089} * \text{pH}^{-1.246}$ |
| | $r^2 = 0.518$ |
| Sodium: | $\ln C = 0.765 + 3.552E-5 t - 1.936E-2 \sin \theta + 2.888E-2 \cos \theta - 7.153E-2 \ln Q + 0.18 \ln \text{cond} + 1.15 \ln \text{pH}$ |
| De-transformed: | $C = 2.1490 * e^{3.552E-5 t} * e^{-1.936E-2 \sin \theta} * e^{2.888E-2 \cos \theta} * Q^{-0.07153} * \text{cond}^{0.180} * \text{pH}^{1.15}$ |
| | $r^2 = 0.343$ |
| Ammonium: | $\ln C = -0.157 + 7.353E-4 t + 0.481 \sin \theta - 0.341 \cos \theta - 0.194 \ln Q$ |
| De-transformed: | $C = 0.8547 * e^{7.353E-4 t} * e^{0.481 \sin \theta} * e^{-0.341 \cos \theta} * Q^{-0.194}$ |
| | $r^2 = 0.466$ |
| Potassium: | $\ln C = -0.176 - 0.02319 \sin \theta + 0.146 \cos \theta + 0.853 \ln \text{cond.}$ |
| De-transformed: | $C = 0.8386 * e^{-0.02319 \sin \theta} * e^{0.146 \cos \theta} * \text{cond}^{0.853}$ |
| | $r^2 = 0.244$ |
| H+ ion: | $\ln C = -2.021 + 0.113 \sin \theta + 0.153 \cos \theta + 0.233 \ln Q + 0.814 \ln \text{cond.}$ |
| De-transformed: | $C = 0.1325 * e^{0.113 \sin \theta} * e^{0.153 \cos \theta} * Q^{0.233} * \text{cond}^{0.814}$ |
| | $r^2 = 0.414$ |
| Aluminum: | $\ln C = 2.528 + 1.346E-3 t + 0.07678 \sin \theta - 0.212 \cos \theta - 1.066 \ln \text{cond}$ |
| De-transformed: | $C = 12.5284 * e^{1.346E-3 t} * e^{0.07678 \sin \theta} * e^{-0.212 \cos \theta} * \text{cond}^{-1.066}$ |
| | $r^2 = 0.376$ |
| Silica: | $\ln C = 2.187 - 1.543E-4 t - 5.256E-2 \ln Q + 1.211 \ln \text{pH}$ |
| De-transformed: | $C = 8.9084 * e^{-1.543E-4 t} * Q^{-5.256E-2} * \text{pH}^{1.211}$ |
| | $r^2 = 0.431$ |

concentration also is increasing over time, at a rate of $7.4E-4$ units per day, but decreases with increasing flow. Potassium concentrations show no significant change over time but do increase with increasing conductivity. Hydrogen ion concentrations also show no long-term time trend but exhibit increases with increasing flow and conductivity. The natural log of aluminum concentration, on the other hand, is increasing over time, at a rate of $1.3E-3$ units per day, and decreases with increasing conductivity. Again, the absence of a relationship between aluminum and pH is surprising. The natural log of silica concentration is decreasing over time at a rate of $1.5E-4$ units per day, decreases with increasing flow, and increases with increasing pH. As in the case with loads, silica is the only constituent to show no significant seasonal trends in the presence of other independent variables.

Discussion

Regression models were used to characterize constituent loads and concentrations because the influence of several independent variables could be tested and there were strong relationships between flow and nearly all constituents, a condition that, according to Preston *et al.* (1989), is more accurately and precisely represented if regression methods are used. The multiple linear regression-based models may provide greater accuracy in mass transport calculations in comparison to the previous “average” method, but because “true” load values are not known, a full analysis of the errors associated with both methods is not possible.

The regression models showed no significant long-term trend in sulfate loads or concentrations; research conducted on throughfall deposition quality at NDW shows that sulfate concentrations are significantly decreasing over time in throughfall, but loads are not changing.

Throughfall has been shown to be very representative of total sulfate deposited to a watershed (Shubzda *et al.*, 1995; Nodvin *et al.*, 1995). Research at the Hubbard Brook watershed and at several other sites in the Northeast U.S. has shown decreasing streamwater sulfate concentrations, as well as decreased concentrations in precipitation and throughfall due to decreases in atmospheric deposition of sulfur compounds (Likens and Bormann, 1995; Clow and Mast, 1999). However, in Shenandoah National Park, increasing streamwater sulfate concentrations have been observed over time (Ryan *et al.*, 1989). One possible reason for trends observed at NDW is that atmospheric deposition of sulfur has decreased, but the watershed has not yet begun to rebound or respond as have streams in the Northeast U.S. Research in other watersheds has shown that there is a “lag time” in watershed response to decreased atmospheric deposition of acidic compounds (Likens and Bormann, 1995; Clow and Mast, 1999).

Regression models show that nitrate concentrations and loads have significantly decreased over time; this can be explained by changes in the watershed due to infestation by the balsam woody adelgid, which was discussed in Chapter IV. Research at the Hubbard Brook Watershed showed no significant change in nitrate concentration (Likens and Bormann, 1995), yet research at Biscuit Brook and the Fernow Experimental Watershed showed significant increases in nitrate concentration (Stoddard, 1994). Reasons for these trends are unclear. Research at Hubbard Brook has also shown no significant change in pH over time, which is in agreement with findings at NDW. It appears that stream acidification status at NDW may not be changing; however, aluminum concentrations and loads are increasing, which itself contributes to degradation of the watershed.

CHAPTER VII. SAMPLING STRATEGY TESTING

Data Sources

This analysis was conducted using the same data as in Chapter VI, Parametric Modeling; weekly grab sample data were used to form the load and concentration regression models, and the load regression equations were again applied to the 15-minute continuous data to obtain load estimates every 15 minutes.

Methods of Analysis

The multiple linear regression-based model concept discussed in the previous chapter was used to test several sampling schemes or frequencies to determine whether less frequent grab samples would be just as statistically adequate in representing water quality at NDW as the current weekly grab samples. The sampling strategies tested were bi-weekly samples, tri-weekly samples, and monthly samples, which were all compared to the current weekly sample frequency. The sampling strategy data subsets were all taken from the full set of weekly grab sample data during 1991 to 1998. The bi-weekly subset was formed by retaining one observation every other week, the tri-weekly subset was formed by retaining one observation every three weeks, and the monthly subset was formed by retaining one observation every month. Multiple linear regressions were then performed for each subset for each constituent load, according to the steps outlined in the previous chapter. Independent variables were retained in each equation if significant at $\alpha = 0.10$. All of the load equations were then applied to the continuous 15-minute data (flow, conductivity, pH, time, and seasonality) during a test period, calendar years 1993 and 1994, and instantaneous loads were summed to determine loads per month for each constituent for each sampling strategy. Calendar

years 1993 and 1994 were chosen for the test period because they represented years of streamflow extremes during the full period of record. In other words, the lowest mean and median annual streamflow occurred in 1993 and the highest mean and median annual streamflow occurred in 1994. The summed loads were then compared to loads obtained from equations formed from the full set of weekly grab sample data. All loads, except for ammonium in the monthly model, were determined to be normally distributed from the Kolmogorov-Smirnov test. The loads were compared as paired values and as independent samples to note both differences in monthly values and differences in long-term distributions. To test statistical differences between individual monthly values, a paired t-test was performed on load results from each sampling strategy in comparison with load results from the current weekly scheme. Since ammonium was the only constituent that did not exhibit normality, pairs of ammonium loads were compared using the non-parametric Wilcoxon signed rank test. To test differences in load distributions among sampling strategies, a t-test was performed on all loads except ammonium, which was tested using the non-parametric Mann-Whitney U test.

To compare constituent concentrations, the distributions of the actual concentrations in each sampling strategy data subset were plotted and tested for differences. These values could not be compared as paired values, so data for each sampling scheme were treated as independent samples. In addition, none of the constituent concentrations were normally distributed. Therefore, the non-parametric Mann-Whitney U test was performed on the concentration data to determine which sampling strategies produced statistically different concentration distributions.

Results

Loads Comparison

Figures 7-1 - 7-9 show comparisons of constituent loads based on the sampling strategies tested. For each load calculated, the percent difference in relation to the load obtained from the weekly dataset was also calculated; distributions of these percent differences are shown in Figures 7-1 - 7-9. In general, tighter percent difference distributions that center around zero indicate sampling strategies that produce similar results to the weekly scheme. Table 7-1 shows the results of the paired-t and Wilcoxon signed ranks tests that were performed on each constituent load pair. The null hypothesis in these tests is that any two sampling strategies produce results that are the same in location (mean or median); therefore, if the p-value is greater than the chosen α level of 0.05, the null hypothesis should be accepted, and the two strategies can be considered to produce similar results. In Table 7-1, boxes for strategies that produce statistically similar results to the weekly scheme are shaded and corresponding p-values are bolded. These tests show that the bi-weekly model for chloride produces statistically similar load results to the weekly model. The tri-weekly model for sodium also produces statistically similar load results to the weekly model, as does the bi-weekly model for ammonium. The tests used indicate that no other models produce statistically similar individual load results to the weekly model. However, Table 7-2 shows the results of the independent samples t- and Mann-Whitney U tests; these tests show that all the sampling strategies produce statistically similar distributions to the weekly strategy, except for aluminum in the monthly model. That is, all load distributions, except for monthly model aluminum, produced by the weekly, bi-weekly, tri-weekly, and monthly strategies are statistically the same

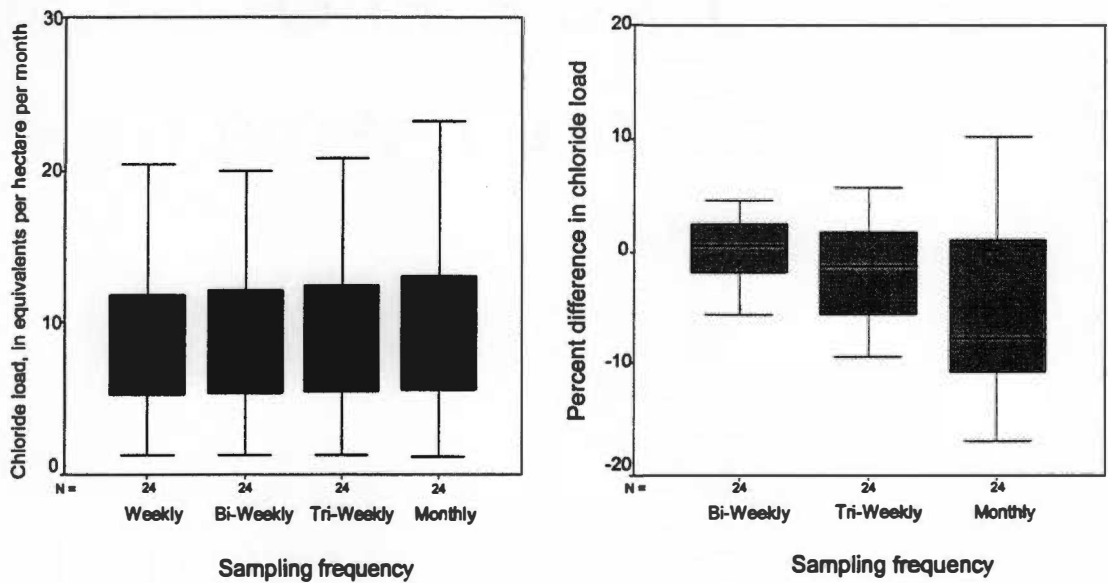


Figure 7-1. Comparison of monthly chloride loads during a test period (1993-1994) based on weekly, bi-weekly, tri-weekly, and monthly sampling schemes.

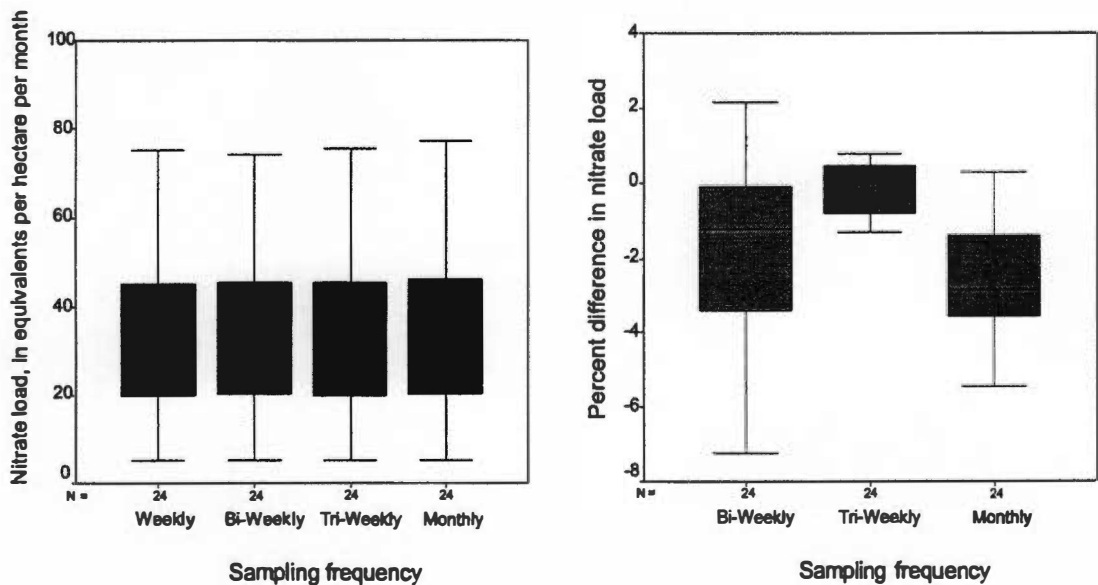


Figure 7-2. Comparison of monthly nitrate loads during a test period (1993-1994) based on weekly, bi-weekly, tri-weekly, and monthly sampling schemes.

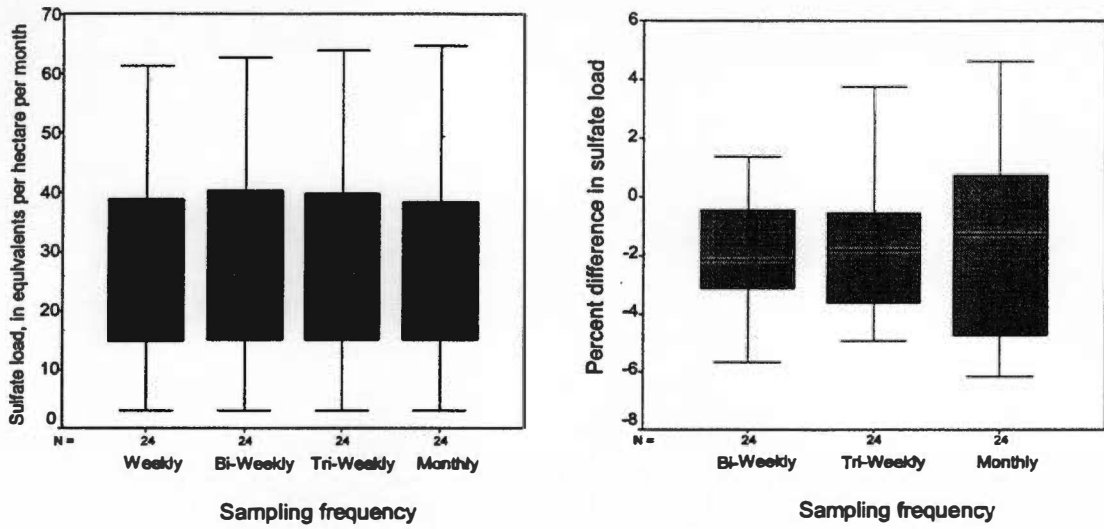


Figure 7-3. Comparison of monthly sulfate loads during a test period (1993-1994) based on weekly, bi-weekly, tri-weekly, and monthly sampling schemes.

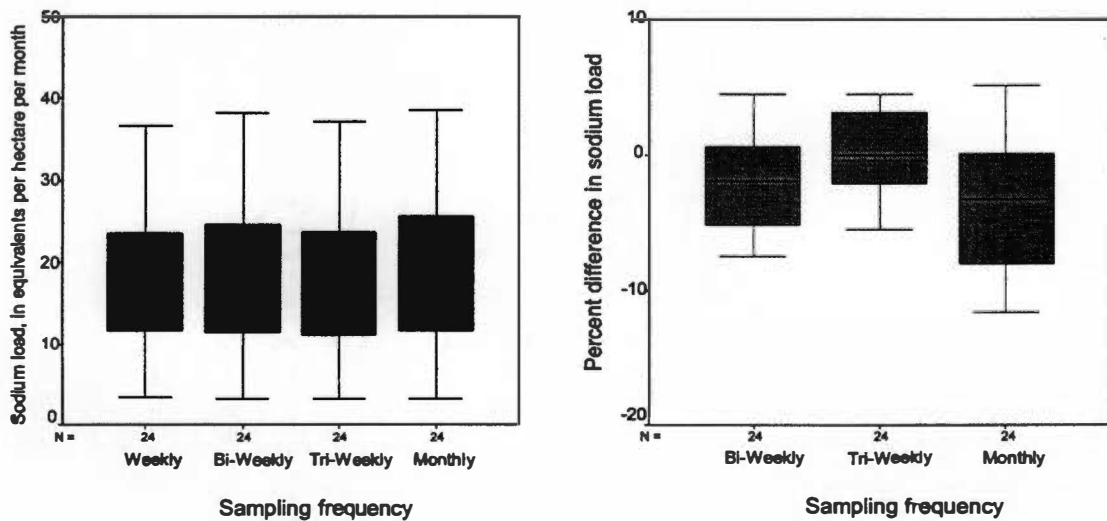


Figure 7-4. Comparison of monthly sodium loads during a test period (1993-1994) based on weekly, bi-weekly, tri-weekly, and monthly sampling schemes.

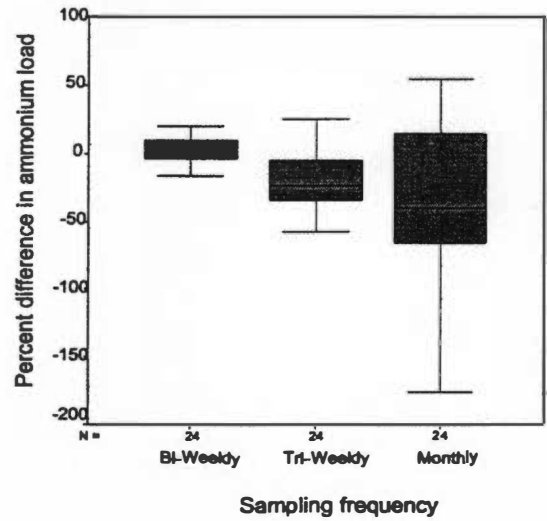
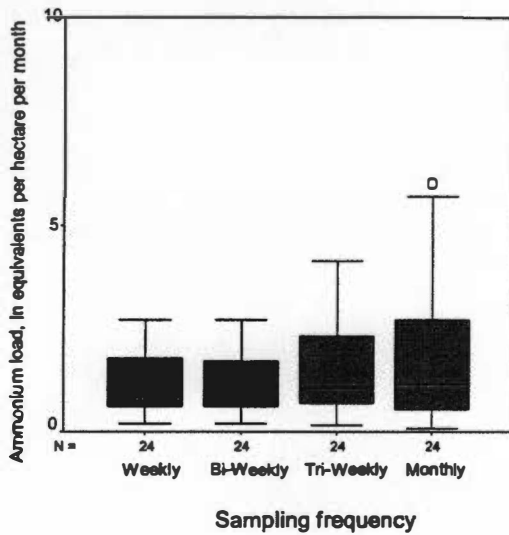


Figure 7-5. Comparison of monthly ammonium loads during a test period (1993-1994) based on weekly, bi-weekly, tri-weekly, and monthly sampling schemes.

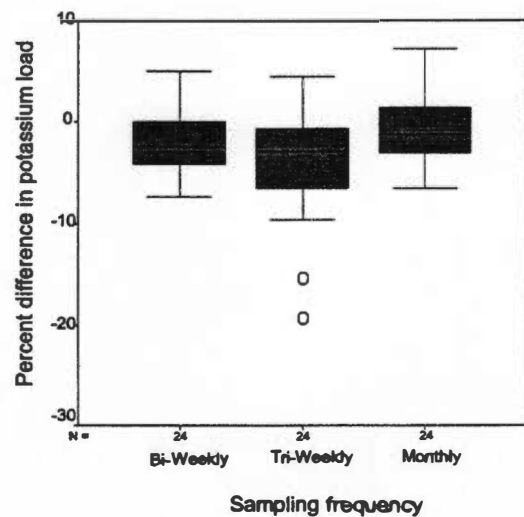
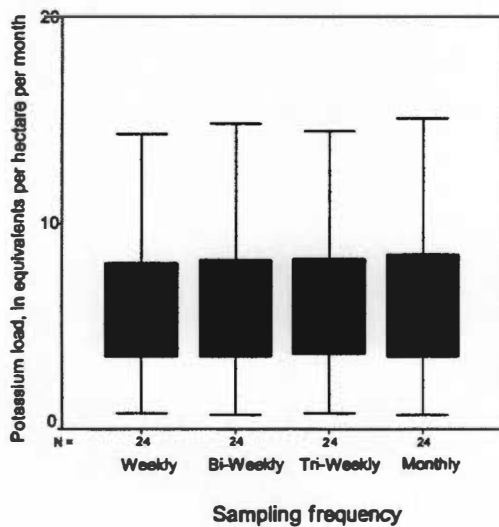


Figure 7-6. Comparison of monthly potassium loads during a test period (1993-1994) based on weekly, bi-weekly, tri-weekly, and monthly sampling schemes.

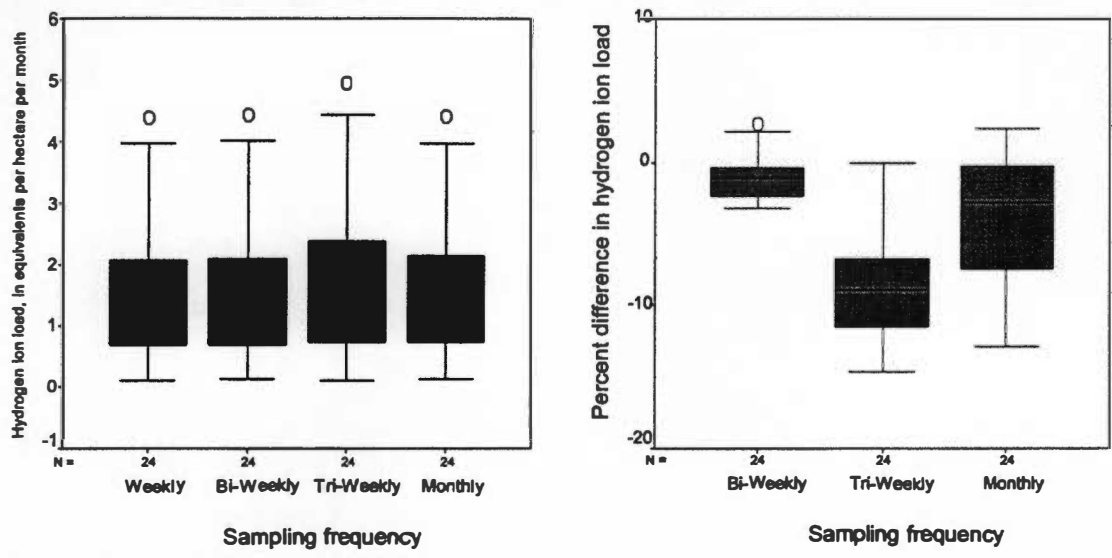


Figure 7-7. Comparison of monthly hydrogen ion loads during a test period (1993-1994) based on weekly, bi-weekly, tri-weekly, and monthly sampling schemes.

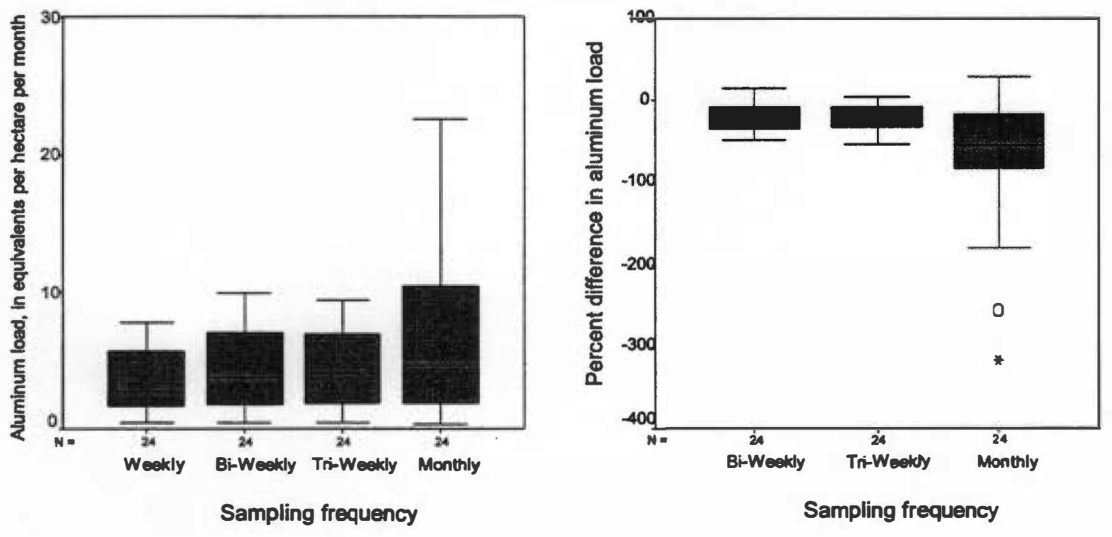


Figure 7-8. Comparison of monthly aluminum loads during a test period (1993-1994) based on weekly, bi-weekly, tri-weekly, and monthly sampling schemes.

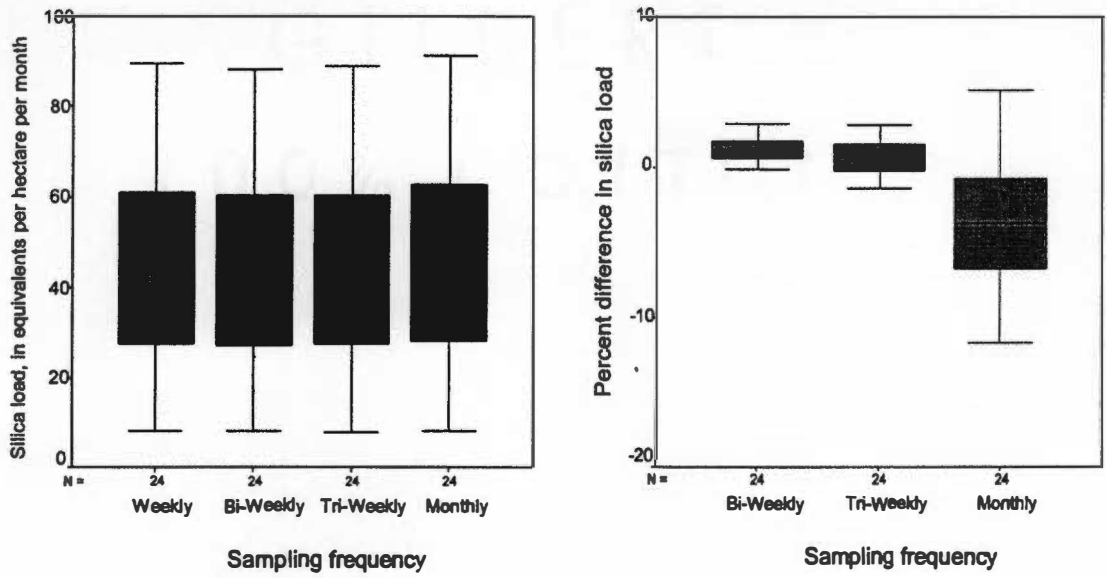


Figure 7-9. Comparison of monthly silica loads during a test period (1993-1994) based on weekly, bi-weekly, tri-weekly, and monthly sampling schemes.

Table 7-1. Statistical differences in load results obtained from different sampling schemes in comparison with the weekly scheme, assuming related samples.

| Constituent (load) | Sampling Scheme Category | | |
|--------------------|--------------------------|------------------|---------------|
| | Bi-Weekly Model | Tri-Weekly Model | Monthly Model |
| Chloride | p = 0.616 | p = 0.003 | p = 0.000 |
| Nitrate | p = 0.003 | p = 0.026 | p = 0.000 |
| Sulfate | p = 0.000 | p = 0.000 | p = 0.006 |
| Sodium | p = 0.001 | p = 0.587 | p = 0.000 |
| Ammonium | p = 0.208 | p = 0.000 | p = 0.003* |
| Potassium | p = 0.000 | p = 0.001 | p = 0.006 |
| Hydrogen Ion | p = 0.018 | p = 0.000 | p = 0.009 |
| Aluminum | p = 0.000 | p = 0.000 | p = 0.001 |
| Silica | p = 0.000 | p = 0.019 | p = 0.001 |

*p-values for ammonium (weekly-monthly model comparison) were generated using the non-parametric Wilcoxon signed ranks test; all others were generated using the parametric paired t test.

Note: P-values are bolded and shaded if the sampling scheme is statistically similar ($p > 0.05$) to the weekly scheme.

Table 7-2. Statistical differences in load results obtained from different sampling schemes in comparison with the weekly scheme, assuming independent samples.

| Constituent (load) | Sampling Scheme Category | | |
|--------------------|--------------------------|------------------|-------------------|
| | Bi-Weekly Model | Tri-Weekly Model | Monthly Model |
| Chloride | p = 0.984 | p = 0.857 | p = 0.605 |
| Nitrate | p = 0.901 | p = 0.979 | p = 0.864 |
| Sulfate | p = 0.903 | p = 0.901 | p = 0.882 |
| Sodium | p = 0.833 | p = 0.982 | p = 0.731 |
| Ammonium | p = 0.894 | p = 0.202 | p = 0.458* |
| Potassium | p = 0.877 | p = 0.822 | p = 0.895 |
| Hydrogen Ion | p = 0.973 | p = 0.675 | p = 0.927 |
| Aluminum | p = 0.300 | p = 0.287 | p = 0.016 |
| Silica | p = 0.915 | p = 0.961 | p = 0.789 |

*p-values for ammonium (weekly-monthly model comparison) were generated using the non-parametric Mann-Whitney U test; all others were generated using the parametric t test.

Note: P-values are bolded and shaded if the sampling scheme is statistically similar ($p > 0.05$) to the weekly scheme.

in location (mean or median) and variance. An obvious discrepancy exists between the results of the two tests assuming dependent and independent samples. After reflection, it was determined that examining and representing loads long-term is of greater importance than examining the accuracy of load calculations per month. Thus, treating the data sets as independent samples rather than paired sets would be more appropriate for the purposes of this study. In addition, some load distributions produced by certain sampling strategies are nearly identical to the weekly model distributions and show relatively small percent differences (see Figures 7-1 - 7-9). On average, sampling on a bi-weekly basis would produce loads within 1% of weekly sample loads, except for aluminum, which would be within 25%. Tri-weekly sampling would produce loads within 2.5% of weekly sample loads, except for ammonium and aluminum, which again would be within 25%. Monthly sampling would produce loads within 4% of weekly sample loads, except for ammonium and aluminum, which would be within 50% and 60%, respectively.

In general, the percent difference plots in Figures 7-1 - 7-9 show a negative bias; in other words, most of the loads calculated under the bi-, tri-, and monthly schemes are higher than loads calculated under the weekly scheme. This could be due to outliers in the weekly data set that were coincidentally retained when forming the bi-, tri-, and monthly data subsets.

For further reference, load regression equations for each sampling strategy are provided in the Appendix, Tables A-2 - A-4.

Concentrations Comparison

Figure 7-10 shows comparisons of constituent concentration distributions based on the sampling strategies tested. Because the concentration data sets for each sampling scheme are

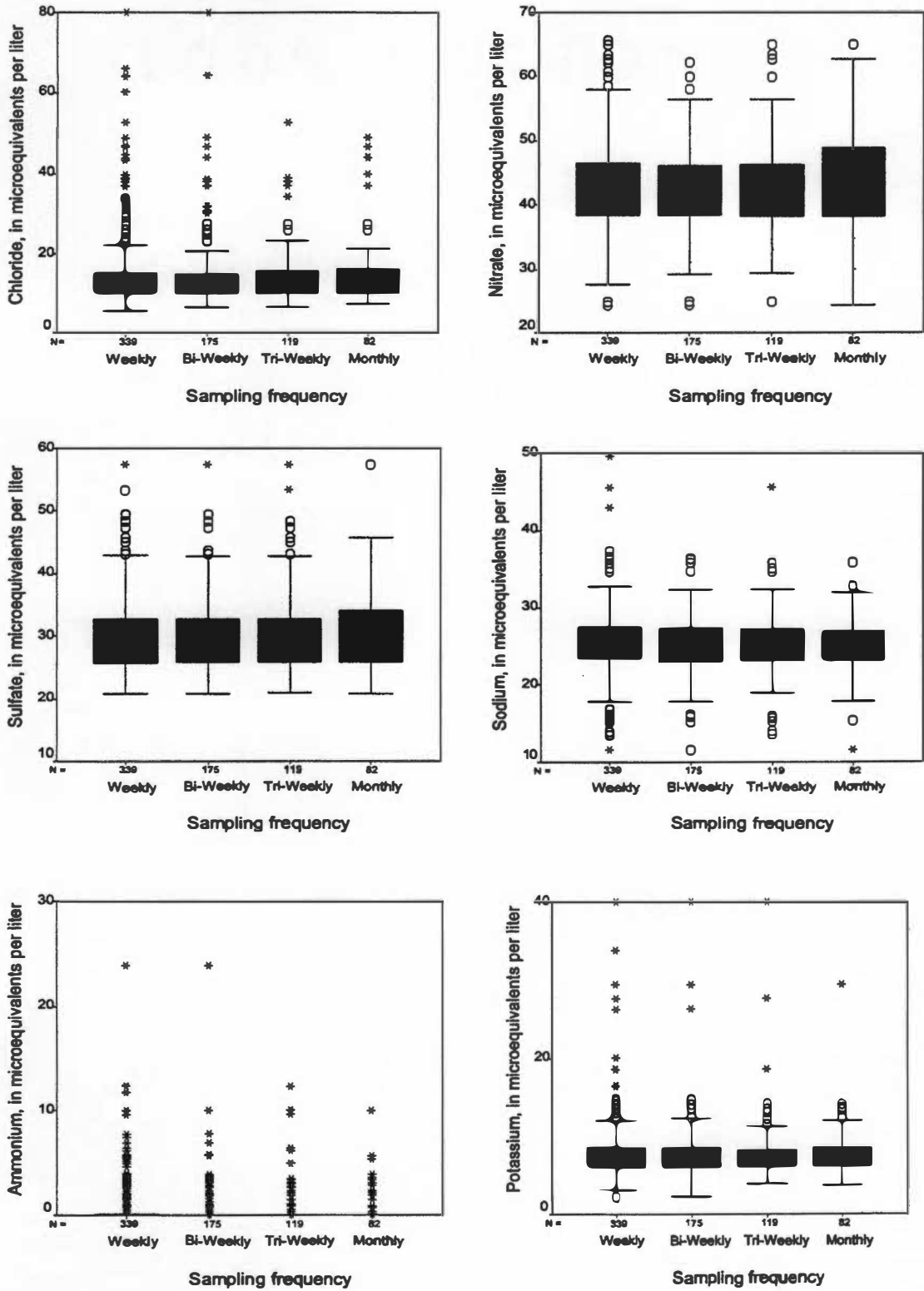


Figure 7-10. Comparison of constituent concentration distributions based on weekly, bi-weekly, tri-weekly, and monthly sampling schemes.

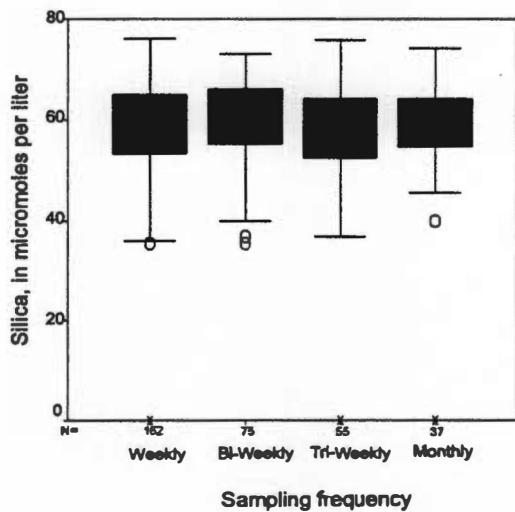
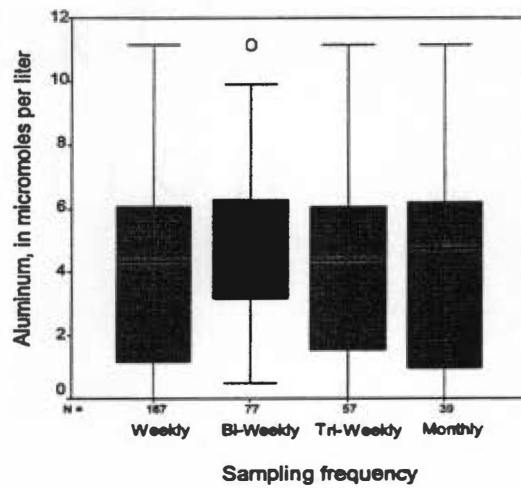
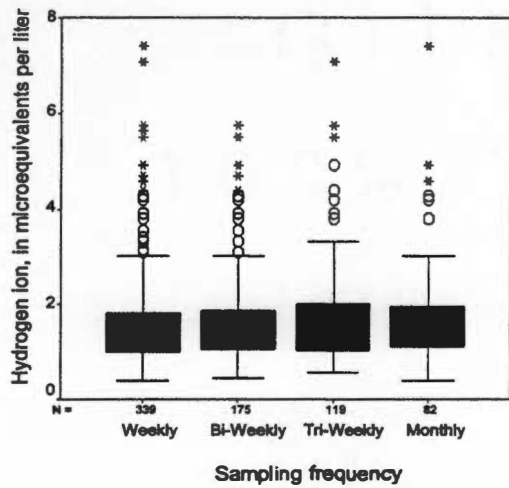


Figure 7-10 (continued). Comparison of constituent concentration distributions based on weekly, bi-weekly, tri-weekly, and monthly sampling schemes.

subsets of the original weekly data set, the data sets cannot be paired and thus percent differences cannot be computed. Table 7-3 shows the results of the Mann-Whitney U tests performed on each sampling strategy subset of concentration data. All boxes are shaded and all p-values are bolded; thus these tests show that all of the sampling strategies produce statistically similar ($p > 0.05$) concentration distributions to the weekly strategy distribution.

The suggestion that outliers were retained when forming each sampling strategy data subset is supported by Figure 7-10, which shows that for many analytes, the number of outliers in the distributions for each sampling strategy is similar. With any particular analyte, the number of outliers in the weekly data distribution should ideally be three times the number of outliers in the tri-weekly data distribution. This does not necessarily signal an error in procedure, but it does serve to explain the negative bias in loads predicted, which was discussed in the previous section.

Though they were not used to determine concentration distributions, concentration regression equations for each sampling strategy are provided in the Appendix, Tables A-5 - A-7, for further reference on which variables influence constituent concentrations under different sampling strategies.

Discussion

Overall, sampling on a bi-weekly or tri-weekly basis at NDW would be just as adequate in representing loads and concentrations as sampling on a weekly basis. On average, most load calculations would be within 1 - 2.5 % of results obtained from weekly samples, and both models produce load and concentration distributions that are statistically equal in location (mean or median) and variance to those produced by the weekly model. Statistical analysis of sampling strategies

Table 7-3. Statistical differences in concentration distributions based on sampling scheme in comparison with the weekly scheme.

| Constituent (concentration) | Sampling Scheme Category | | |
|--------------------------------|--------------------------|---------------------|------------------|
| | Bi-Weekly Model | Tri-Weekly Model | Monthly Model |
| Chloride* | p = 0.741 | p = 0.886 | p = 0.610 |
| Nitrate | p = 0.957 | p = 0.948 | p = 0.600 |
| Sulfate | p = 0.738 | p = 0.894 | p = 0.668 |
| Sodium | p = 0.429 | p = 0.396 | p = 0.634 |
| Ammonium | p = 0.870 | p = 0.940 | p = 0.695 |
| Potassium | p = 0.892 | p = 0.760 | p = 0.868 |
| Hydrogen Ion | p = 0.240 | p = 0.188 | p = 0.379 |
| Aluminum | p = 0.253 | p = 0.923 | p = 0.864 |
| Silica | p = 0.475 | p = 0.442 | p = 0.738 |

*p-values for all constituents were generated using the non-parametric Mann-Whitney U test
 Note: P-values are bolded and shaded if the sampling scheme is statistically similar ($p > 0.05$) to the weekly scheme.

conducted by Robertson and Roerish (1999) supports this; they found that for long-term monitoring studies, sampling on either a monthly or semimonthly basis would be statistically adequate. However, for NDW, the monthly sampling strategy, although statistically similar to the weekly scheme when considering concentrations and most loads, does not represent aluminum loads well and produces some erratic load distributions and high percent differences. Therefore, it may not be as reliable for representing all analytes as the other sampling strategies.

CHAPTER VIII. SUMMARY OF MAJOR CONCLUSIONS

From the results of the water quality monitoring research presented in this section, the following major conclusions and observations were made:

1. Based on stream flow frequency curves compared to actual sampled flows, high flow events are under-represented; thus, stream water quality during high flow events is under-represented by current sampling schemes.
2. In general, flow in the SW stream is higher than flow in the NE stream during baseflow conditions. During major and minor rainfall events, however, flow is consistently higher in the NE stream than in the SW stream. Flow and water quality in the SW stream are apparently more dependent upon groundwater inputs, while flow and water quality in the NE stream are apparently more dependent upon vadose zone flow and cross-over tributaries from the SW stream during storm events.
3. The NE and SW streams are statistically different ($p < 0.05$) with respect to all analyte concentrations except ammonium. Most analyte concentrations are higher and show greater fluctuations in the NE stream than in the SW stream.
4. From results of a storm event study on October 31 - November 5, 1995, and studies in similar watersheds, most runoff entering streams during storms appears to be pre-event water generated in the vadose zone or upper soil layers. In addition, hydrologic response to storms at NDW is rapid.

5. Higher sulfate concentrations are observed in the streams when more rainfall has occurred since the previous visit. In the SW stream, an increase of one inch of rainfall produces a significant ($p < 0.05$) increase in sulfate concentration of $1.08 \mu\text{eq/L}$. In the NE stream, an increase of one inch of rainfall produces a significant increase in sulfate concentration of $1.32 \mu\text{eq/L}$.
6. Lower sulfate concentrations are observed in the streams when the dry period prior to sampling has been longer. In the SW stream, an increase in one consecutive dry day prior to sampling produces a significant decrease in sulfate concentration of $0.65 \mu\text{eq/L}$. In the NE stream, an increase in one consecutive dry day prior to sampling produces a significant decrease in sulfate concentration of $0.67 \mu\text{eq/L}$.
7. Nitrate concentrations observed in the streams are not significantly influenced by precipitation prior to sampling.
8. Lower nitrate concentrations are observed in the streams when the dry period prior to sampling has been longer. In the SW stream, an increase in one consecutive dry day prior to sampling produces a significant decrease in nitrate concentration of $0.50 \mu\text{eq/L}$. In the NE stream, an increase in one consecutive dry day prior to sampling produces a significant decrease in nitrate concentration of $0.54 \mu\text{eq/L}$.
9. The multiple linear regression-based models may provide greater accuracy in mass transport calculations in comparison to the previous “average” method,

because it accounts for several possible influences on analyte loads and concentrations. Because “true” load values are not known, a full analysis of the errors associated with both methods is not possible.

10. The load regression model shows the following significant ($p < 0.10$) time trends for water quality in the SW stream:

- The natural log of chloride load is increasing at a rate of $2.6E-4$ units per day.
- The natural log of sodium load is increasing at a rate of $3.6E-5$ units per day.
- The natural log of aluminum load is increasing at a rate of $1.3E-3$ units per day.
- The natural log of ammonium load is increasing at a rate of $7.4E-4$ units per day.
- The natural log of nitrate load is decreasing at a rate of $7.9E-5$ units per day.
- The natural log of silica load is decreasing at a rate of $1.5E-4$ units per day.
- Sulfate, potassium, and hydrogen ion loads are not changing over time.
- All analyte loads except silica are influenced by seasonality, in the presence of other variables.

11. The load regression model based on seasonality terms only shows the following significant ($p < 0.10$) patterns:

- Chloride loads reach a maximum around January 31 and a minimum around August 1. Seasonality explains 12.7% of the variability in instantaneous chloride load, or a range of $4.42E-5$ eq/sec.
- Nitrate loads reach a maximum around February 10 and a minimum around August 11. Seasonality explains 19.3% of the variability in instantaneous nitrate load, or a range of $1.68E-4$ eq/sec.
- Sulfate loads reach a maximum around February 17 and a minimum around August 17. Seasonality explains 11.5% of the variability in instantaneous sulfate load, or a range of $1.00E-4$ eq/sec.
- Sodium loads reach a maximum around February 12 and a minimum around August 14. Seasonality explains 11.7% of the variability in instantaneous sodium load, or a range of $7.01E-5$ eq/sec.
- Ammonium loads reach a maximum around April 12 and a minimum around October 12. Seasonality explains 17.1% of the variability in instantaneous ammonium load, or a range of $9.40E-6$ eq/sec.
- Potassium loads reach a maximum around January 29 and a minimum around July 31. Seasonality explains 15.8% of the variability in instantaneous potassium load, or a range of $3.06E-5$ eq/sec.
- Hydrogen ion loads reach a maximum around February 12 and a minimum

around August 12. Seasonality explains 18.5% of the variability in instantaneous hydrogen ion load, or a range of $8.06\text{E-}6$ eq/sec.

- Aluminum loads reach a maximum around April 1 and a minimum around October 2. Seasonality explains 7.7% of the variability in instantaneous aluminum load, or a range of $1.11\text{E-}5$.

12. The concentration regression model shows the following significant ($p < 0.10$)

time trends for the SW stream:

- The natural log of chloride concentration is increasing at a rate of $2.6\text{E-}4$ units per day.
- The natural log of sodium concentration is increasing at a rate of $3.6\text{E-}5$ units per day.
- The natural log of aluminum concentration is increasing at a rate of $1.3\text{E-}3$ units per day.
- The natural log of ammonium concentration is increasing at a rate of $7.4\text{E-}4$ units per day.
- The natural log of nitrate concentration is decreasing at a rate of $7.9\text{E-}5$ units per day.
- The natural log of silica concentration is decreasing at a rate of $1.5\text{E-}4$ units per day.
- Sulfate, potassium, and hydrogen ion concentrations are not changing over time.

- All analyte concentrations except silica are influenced by seasonality, in the presence of other variables.

13. The concentration regression model based on seasonality terms only shows the following significant ($p < 0.10$) patterns:

- Chloride concentrations reach a maximum around November 16 and a minimum around May 18. Seasonality explains 5.4% of the variability in chloride concentration, or a range of 3.72 $\mu\text{eq/L}$.
- Nitrate concentrations reach a maximum around January 15 and a minimum around July 17. Seasonality explains 23.3% of the variability in nitrate concentration, or a range of 9.15 $\mu\text{eq/L}$.
- Sulfate concentrations reach a maximum around January 22 and a minimum around July 21. Seasonality explains 2.3% of the variability in sulfate concentration, or a range of 2.17 $\mu\text{eq/L}$.
- Sodium concentrations reach a maximum around September 21 and a minimum around March 21. Seasonality explains 8% of the variability in sodium concentration, or a range of 3.35 $\mu\text{eq/L}$.
- Ammonium concentrations reach a maximum around May 14 and a minimum around November 11. Seasonality explains 23.4% of the variability in ammonium concentration, or a range of 2.78 $\mu\text{eq/L}$.
- Potassium concentrations reach a maximum around December 13 and a minimum around June 13. Seasonality explains 15.4% of the variability in

potassium concentration, or a range of 3.03 $\mu\text{eq/L}$.

- Hydrogen ion concentrations reach a maximum around January 31 and a minimum around August 1. Seasonality explains 19.1% of the variability in hydrogen ion concentration, or a range of 0.90 $\mu\text{eq/L}$.
- Aluminum concentrations reach a maximum around May 23 and a minimum around November 22. Seasonality explains 10% of the variability in aluminum concentration, or a range of 2.74 $\mu\text{mol/L}$.

14. Based on test period results and in comparison with the load regression model, the previous load “average” model produced the following :

- Higher estimates of nitrate, chloride, sodium, aluminum, and silica.
- Lower estimates of sulfate, ammonium, hydrogen ion, and potassium.

15. Grab samples collected from the streams on a bi-weekly or tri-weekly frequency would be as statistically adequate for characterizing water quality as are samples collected on a weekly basis.

CHAPTER IX. RECOMMENDATIONS FOR FUTURE RESEARCH

Based on the conclusions stated in Chapter VIII and others provided in the text, the following recommendations are made for gaining better understanding of water quality characteristics and relationships in the Noland Divide Watershed:

Sampling:

1. Perform storm event sampling more frequently.
2. Sample vadose zone, overland flow, and groundwater during storm events to further identify sources of streamflow and related chemical “signals.”
3. For the fall season, consider sampling at other times of the day, particular in the afternoon, in order to better represent the streamflow parent distribution.

Equipment:

1. Use automated pumping samplers or passive samplers to capture streamwater samples during storm events
2. Install solar panels at the stream datalogger to avoid loss of data due to battery depletion.
3. Install storage modules at the stream datalogger that would periodically download and store continuous data; this would also help to avoid loss of data due to battery depletion or environmental factors.

Analysis/Research:

1. Obtain more powerful statistical software and/or computers that could accommodate and perform complete statistical and graphical analyses on the full set of continuous data.
2. Continue analysis of the NE stream continuous (15-minute) data to further analyze differences between the two streams.
3. To further understand relationships between antecedent moisture condition and sulfate/nitrate, consider recording the approximate AMC every time a weekly grab sample is obtained.
4. To further understand relationships between precipitation and sulfate, it would be useful to measure rainfall intensity for several storm events during a test period.
5. To further understand streamflow source inputs and related chemical signals, flowpath tracer studies should be conducted using conservative and/or naturally-occurring tracers, such as aluminum, oxygen-18, or calcium and sulfate. If possible, these experiments should be conducted under varying antecedent moisture conditions.
6. To support the use of the multiple linear regression-based models for loads and concentrations, a full analysis of errors associated with this method and the “average” method should be performed, perhaps by performing Monte Carlo simulations.

REFERENCES

REFERENCES

- Albek, E., Identification of the different sources of chlorides in streams by regression analysis using chloride-discharge relationships, *Water Environment Research*, 71(7), 1310-1319, 1999.
- Baker, J.P., and C.L. Schofield, Aluminum toxicity to fish in acidic waters, *Water, Air and Soil Pollution*, 18, 289-309, 1982.
- Baker, J.P., J. Van Sickle, C.J. Gagen, D.R. DeWalle, W.E. Sharpe, R.F. Carline, B.P. Baldigo, P.S. Murdoch, D.W. Bath, W.A. Krester, H.A. Simonin, and P.J. Wightingon, Jr., Episodic acidification of small streams in the northeastern United States: effects on fish populations, *Ecological Applications*, 6, 422-437, 1996.
- Campbell, D.H., J.S. Baron, K.A. Tonnessen, P.D. Brooks, and P.F. Schuster, Controls on nitrogen flux in alpine/subalpine watersheds of Colorado, *Water Resources Research*, 36(1), 37-47, 2000.
- Church, M.R., Hydrochemistry of forested catchments, *Annual Review of Earth and Planetary Science*, 25, 23-59, 1997.
- Clow, D.W., and M.A. Mast, Long-term trends in stream water and precipitation chemistry at five headwater basins in the northeastern United States, *Water Resources Research*, 35(2), 541-554, 1999.
- Cochran, W.G., *Sampling Techniques*, 3rd ed., John Wiley and Sons, New York, 1977.
- Cohn, T.A., L.L. DeLong, E.J. Gilroy, R.M. Hirsch, and D.K. Wells, Estimating constituent loads, *Water Resources Research*, 25(5), 937-942, 1989.
- Collins, R., A. Jenkins, and M. Harrow, The contribution of old and new water to a storm hydrograph determined by tracer addition to a whole catchment, *Hydrological Processes*, 14, 701-711, 2000.
- Cosby, B.J., G.M. Hornberger, J.N. Galloway, and R.F. Wright, Time scales of catchment acidification: a quantitative model for estimating freshwater acidification, *Environmental Science and Technology*, 19(12), 1144-1149, 1985.
- Creed, I.F., L.E. Band, N.W. Foster, I.K. Morrison, J.A. Nicolson, R.S. Semkin, and D.S. Jeffries, Regulation of nitrate-N release from temperate forests: a test of the N flushing hypothesis, *Water Resources Research*, 32(11), 3337-3354, 1996.

- Delcourt, H.R., and P.A. Delcourt, *Quaternary Ecology*, Chapman and Hall, New York, 1991.
- Drever, J.I., *The Geochemistry of Natural Waters*, 2nd ed., Prentice Hall, New Jersey, 1988.
- Eshleman, K.N., L.M. Miller-Marshall, and J.R. Webb, Long-term changes in episodic acidification of streams in Shenandoah National Park, Virginia, USA, *Water, Air and Soil Pollution*, 85, 517-522, 1995.
- Ferguson, R.I., Accuracy and precision of methods for estimating river loads, *Earth Surface Processes and Landforms*, 12(1), 95-104, 1987.
- Flum, T., and S.C. Nodvin, Factors affecting streamwater chemistry in the Great Smoky Mountains, USA, *Water, Air and Soil Pollution*, 85, 1707-1712, 1995.
- Genereux, D.P., H.F. Hemond, and P.J. Mulholland, Use of radon-222 and calcium as tracers in a three-end-member mixing model for streamflow generation on the west fork of Walker Branch Watershed, *Journal of Hydrology*, 142, 167-211, 1993.
- Helsel, D.R., and R.M. Hirsch, *Statistical Methods in Water Resources*, Elsevier, New York, 1992.
- Herlihy, A.T., P.R. Kaufmann, and M.E. Mitch, Stream chemistry in the Eastern United States 2. current sources of acidity in acidic and low acid-neutralizing capacity streams, *Water Resources Research*, 27(4), 629-642, 1991.
- Hill, A.R., W.A. Kemp, J.M. Buttle, and D. Goodyear, Nitrogen chemistry of subsurface storm runoff on forested Canadian Shield hillslopes, *Water Resources Research*, 35(3), 811-821, 1999.
- Hyer, K.E., J.R. Webb, and K.N. Eshleman, Episodic acidification of three streams in Shenandoah National Park, Virginia, USA, *Water, Air and Soil Pollution*, 85, 523-528, 1995.
- Johnson, D.W., and S.E. Lindberg, *Atmospheric Deposition and Forest Nutrient Cycling*, Springer-Verlag, New York, 1992.
- Johnson, D.W., H. Van Miegroet, S.E. Lindberg, D.E. Todd, and R.B. Harrison, Nutrient cycling in red spruce forests of the Great Smoky Mountains, *Canadian Journal of Forest Research*, 21, 769-787, 1991.

- King, P.B., R.B. Neuman, and J.B. Hadley, *Geology of the Great Smoky Mountains National Park, Tennessee and North Carolina: U.S. Geological Survey Professional Paper #587*, Washington, D.C., 1968.
- Likens, G.E. and F.H. Bormann, *Biogeochemistry of a Forested Ecosystem*, 2nd ed., Springer-Verlag, New York, 1995.
- Lundin, L., Soil water chemistry dependence on water pathways and turnover, *Water, Air and Soil Pollution*, 85, 1695-1700, 1995.
- Lynch, J.A., and E.S. Corbett, Hydrologic control of sulfate mobility in a forested watershed, *Water Resources Research*, 25(7), 1695-1703, 1989.
- McCann, M., G. Harwell, and J. Shubzda, Assessment of stream water quality and atmospheric deposition rates at selected sites in the Great Smoky Mountains National Park, 1991-1998, Summary report submitted to the National Park Service under contract no. 1443-CA-5460-98-006 (amendment 3), 2000.
- McAvoy, D.C., Episodic response of aluminum chemistry in an acid-sensitive Massachusetts catchment, *Water Resources Research*, 25(2), 233-240, 1989.
- Mulholland, P.J., Hydrometric and stream chemistry evidence of three storm flowpaths in Walker Branch Watershed, *Journal of Hydrology*, 151, 291-316, 1993.
- Mulholland, P.J., G.V. Wilson, and P.M. Jardine, Hydrogeochemical response of a forested watershed to storms: effects of preferential flow along shallow and deep pathways, *Water Resources Research*, 26(12), 3021-3036, 1990.
- Nodvin, S.C., H. Van Miegroet, S.E. Lindberg, N.S. Nicholas, and D.W. Johnson, Acidic deposition, ecosystem processes, and nitrogen saturation in a high elevation southern appalachian watershed, *Water, Air and Soil Pollution*, 85, 1647-1652, 1995.
- Peine, J.D., J.C. Randolph, and J.J. Presswood, Evaluating the effectiveness of air quality management within the Class I area of Great Smoky Mountains National Park, *Environmental Management*, 19, 515-526, 1995.
- Peters, N.E., Water-quality variations in a forested Piedmont catchment, Georgia, USA, *Journal of Hydrology*, 156, 73-90, 1994.
- Preston, S.D., V.J. Bierman, Jr., and S.E. Silliman, An evaluation of methods for the estimation of tributary mass loads, *Water Resources Research*, 25(6), 1379-1389, 1989.

- Richards, R.P., and J. Holloway, Monte Carlo studies of sampling strategies for estimating tributary loads, *Water Resources Research*, 23(10), 1939-1948, 1987.
- Robertson, D.M., and E.D. Roerish, Influence of various water quality sampling strategies on load estimates for small streams, *Water Resources Research*, 35(12), 3747-3759, 1999.
- Ryan, P.F., G.M. Hornberger, B.J. Cosby, J.N. Galloway, J.R. Webb, and E.B. Rastetter, Changes in the chemical composition of stream water in two catchments in the Shenandoah National Park, Virginia, in response to atmospheric deposition of sulfur, *Water Resources Research*, 25(10), 2091-2099, 1989.
- Schlesinger, W.H., *Biogeochemistry: An Analysis of Global Change*, Harcourt Brace Jovanovich, New York, 1991.
- Shubzda, J., S.E. Lindberg, C.T. Garten, and S.C. Nodvin, Elevational trends in the fluxes of sulphur and nitrogen in throughfall in the southern Appalachian mountains: some surprising results, *Water, Air and Soil Pollution*, 85, 2265-2270, 1995.
- Silsbee, D.G., and G.L. Larson, Water quality of streams in the Great Smoky Mountains National Park, *Hydrobiologia*, 89, 97-115, 1982.
- Sklash, M.G., and R.N. Farvolden, The role of groundwater in storm runoff, *Journal of Hydrology*, 43, 45-65, 1979.
- Smoot, J.L., T.D. Liebermann, R.D. Evaldi, and K.D. White, Water-quality assessment of the Kentucky River Basin, Kentucky-analysis of available surface-water-quality data through 1986, *USGS Water-Supply Paper 2351*, US Government, Washington, D.C., 1995.
- Steele, T.D., Computation of major solute concentrations and loads in German rivers using regression analysis, *Catena*, 7, 111-124, 1980.
- Stoddard, J.L., Long-term changes in watershed retention of nitrogen: its causes and aquatic consequences, In: Baker, L.A. (Ed.) *Environmental Chemistry of Lakes and Reservoirs, Advances in Chemistry Series No. 237*, American Chemical Society, Washington, D.C., 1994.
- Stumm, W., and J.J. Morgan, *Aquatic Chemistry*, 3rd ed., Wiley-Interscience, New York, 1981.
- Swistock, B.R., D.R. DeWalle, and W.E. Sharpe, Sources of acidic storm flow in an Appalachian headwater stream, *Water Resources Research*, 25(10), 2139-2147, 1989.

Walling, D.E., Assessing the accuracy of suspended sediment rating curves for a small basin, *Water Resources Research*, 13(3), 531-538, 1977.

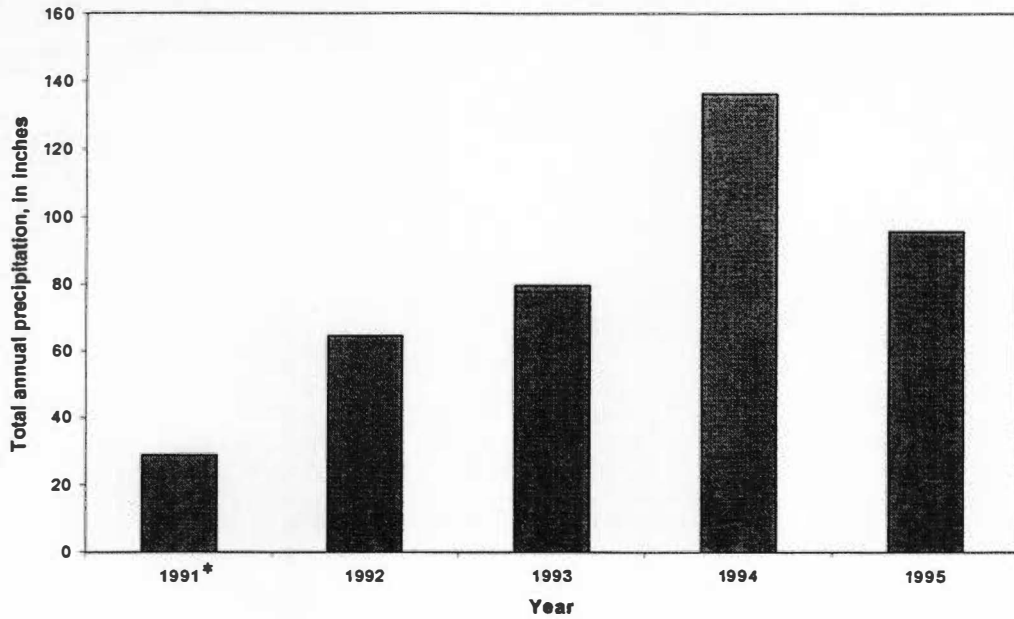
Webb, J.R., B.J. Cosby, J.N. Galloway, and G.M. Hornberger, Acidification of native brook trout streams in Virginia, *Water Resources Research*, 25(6), 1367-1377, 1989.

APPENDIX

Table A-1. Summary of characteristics of the Noland Divide Watershed.

| Category | Characteristic |
|-------------------------------|--|
| Area | 17.4 hectares |
| Elevational Range | 1695 - 1940 meters AMSL |
| SCS Curve Number | 55 |
| Time of Concentration* | ~20 minutes |
| Average Watershed Slope | 0.44 ft/ft |
| Average Stream Channel Slope | SW: 0.35 ft/ft NE: 0.36 ft/ft |
| Watershed/Streams Orientation | Watershed is southeast-facing; streams drain to southeast |
| Geology | Thunderhead Sandstone |
| Soils | Umbric Dystrochrepts (loams, sandy loams, loamy sands - SCS Soil Group B) |
| Forest Types | Old-growth red spruce and mature yellow birch |
| Understory Vegetation Types | Frasier fir, red spruce, blackberry, witch hobble, blueberry, mountain ash, rhododendron |

*Time of concentration determined from the SCS/NRCS equation for overland flow and Manning's equation for open channel flow.



*Indicates partial year

Figure A-1. Total annual precipitation at Noland Divide Watershed, 1991 - 1995.

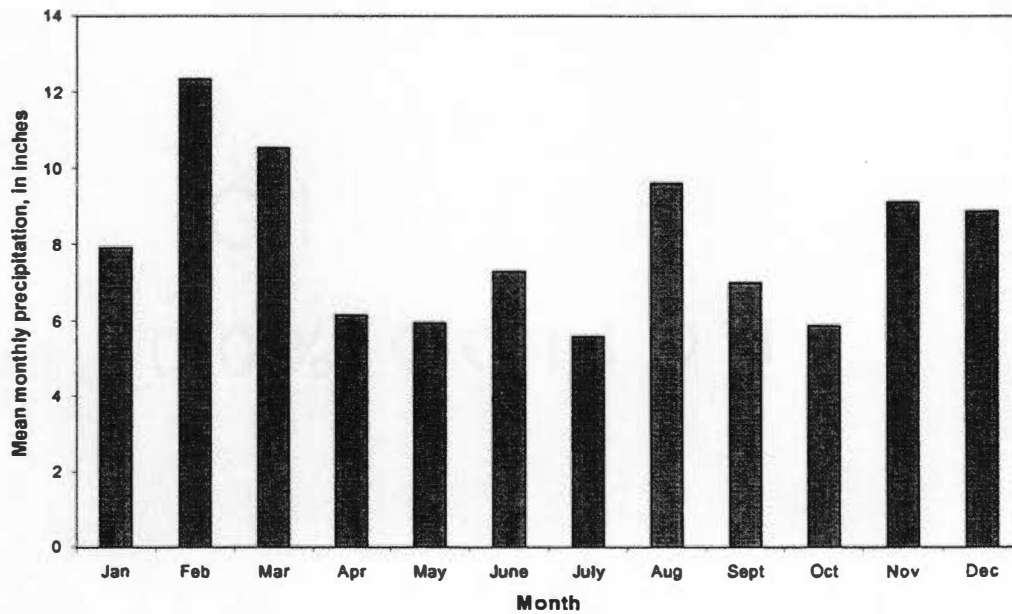


Figure A-2. Mean monthly precipitation at Noland Divide Watershed, 1991 - 1995.

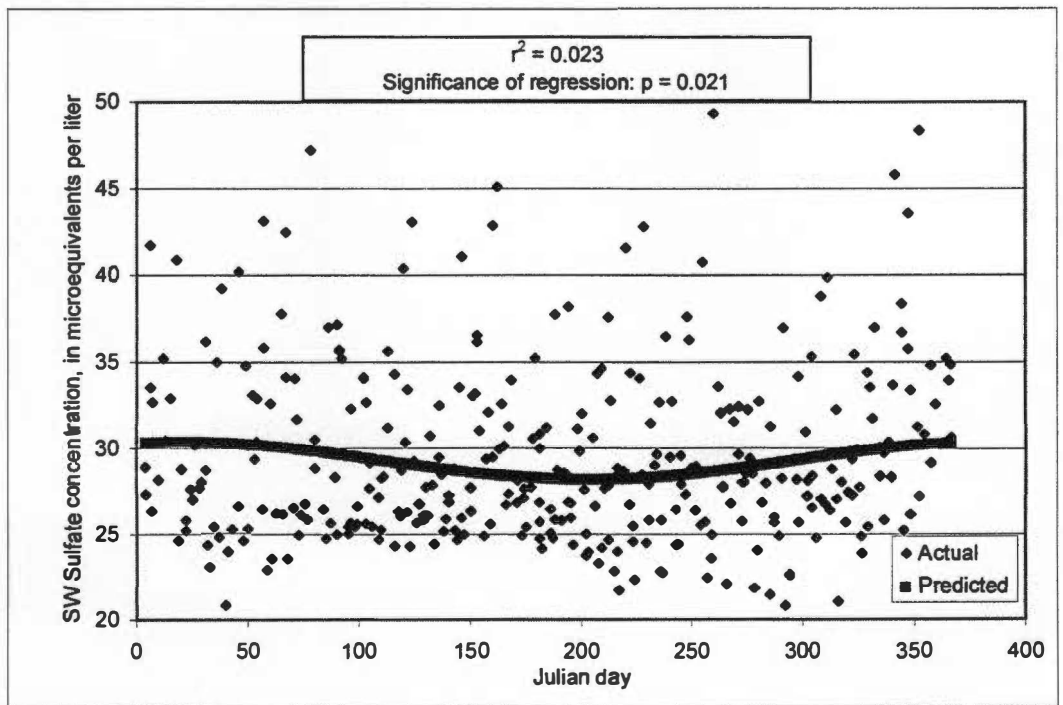
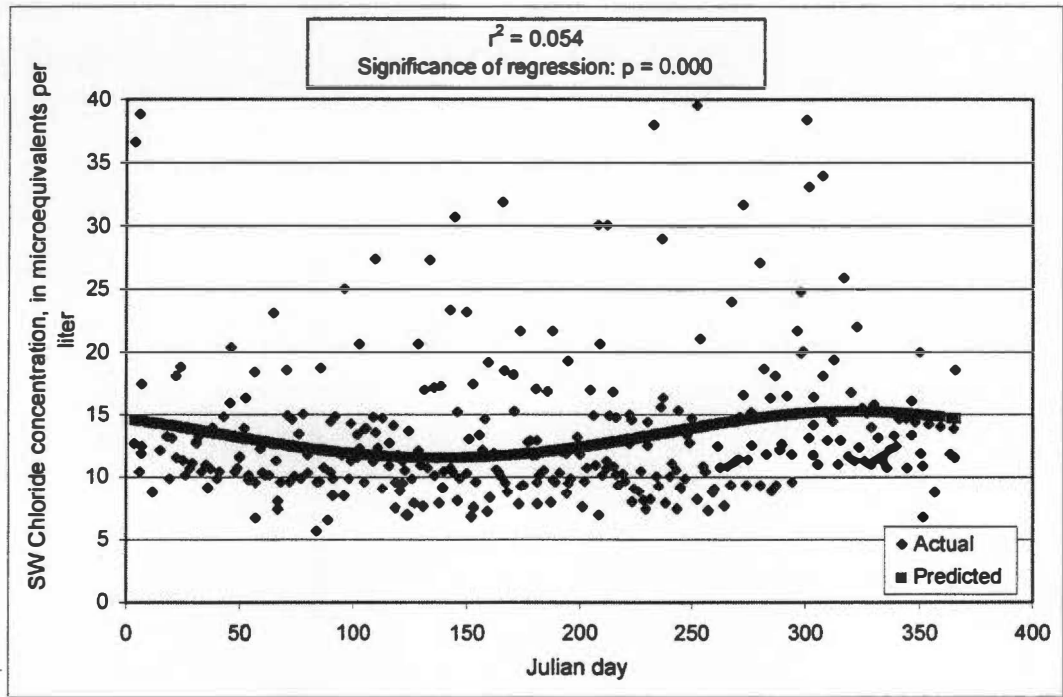


Figure A-3. Seasonal sine/cosine wave functions for analyte concentrations in the SW stream.

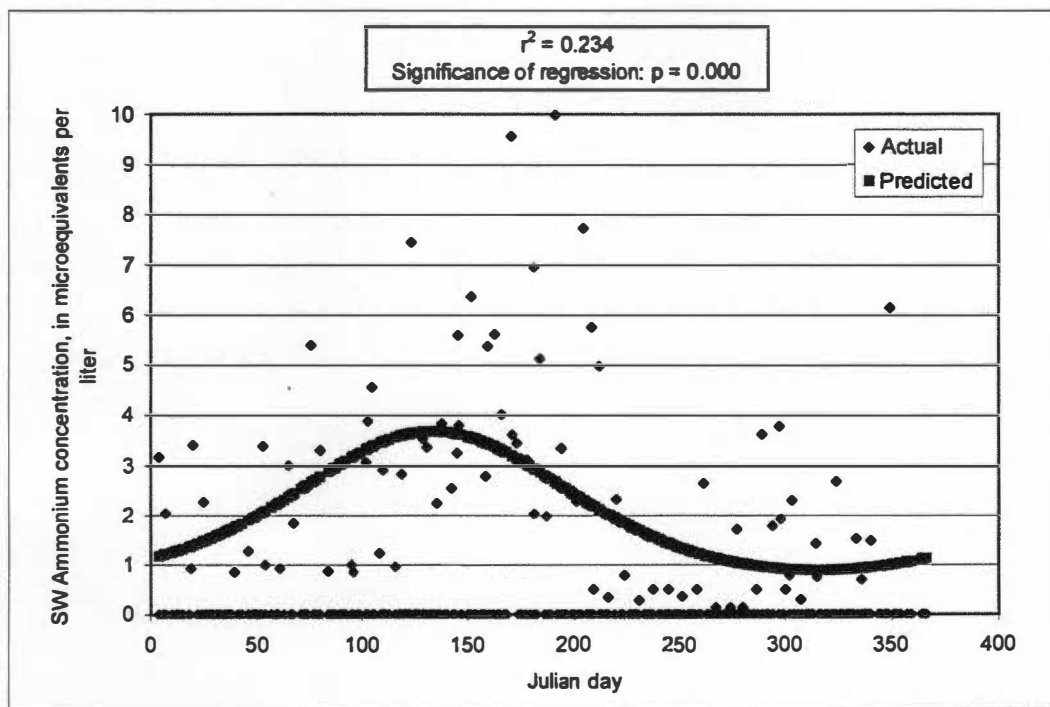
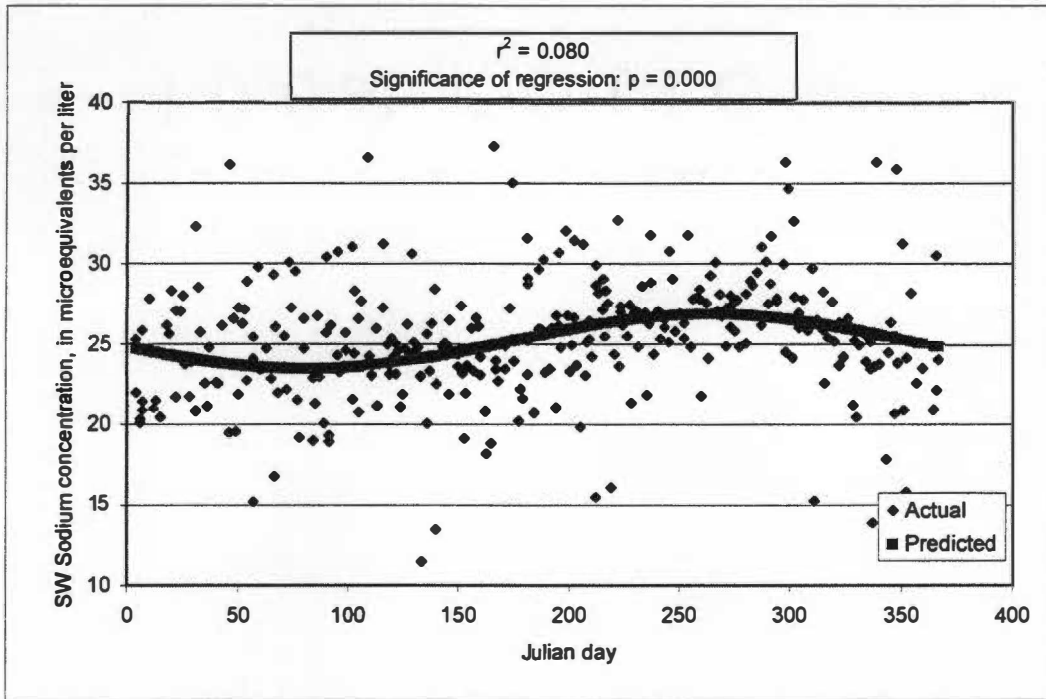


Figure A-3 (continued). Seasonal sine/cosine wave functions for analyte concentrations in the SW stream.

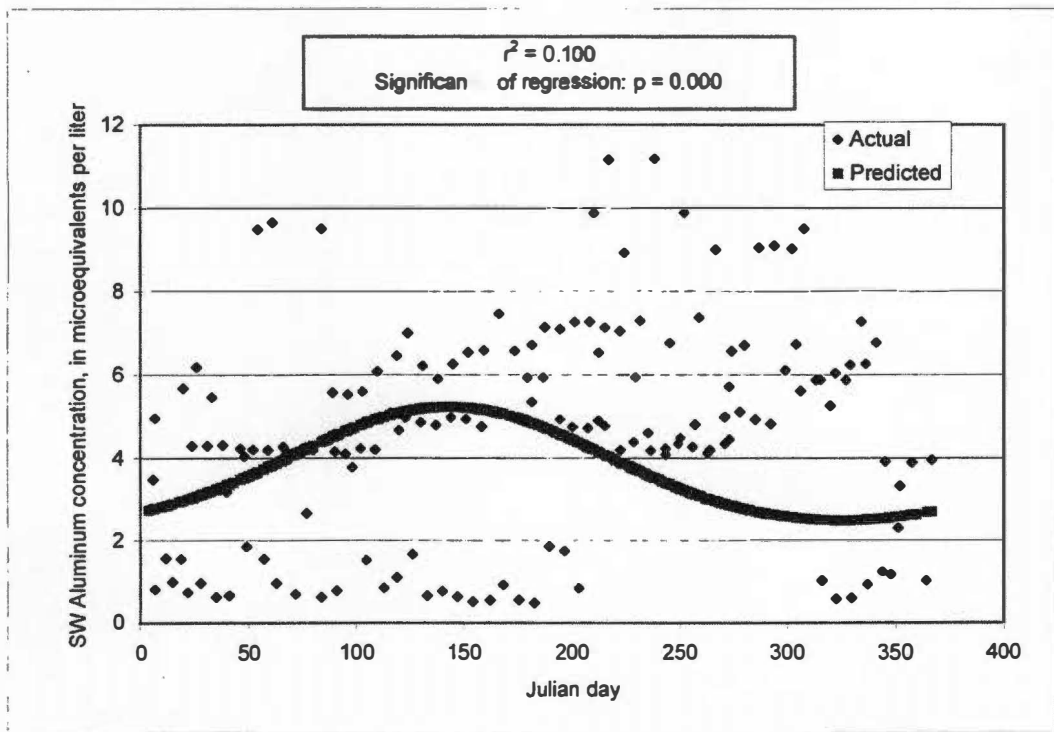
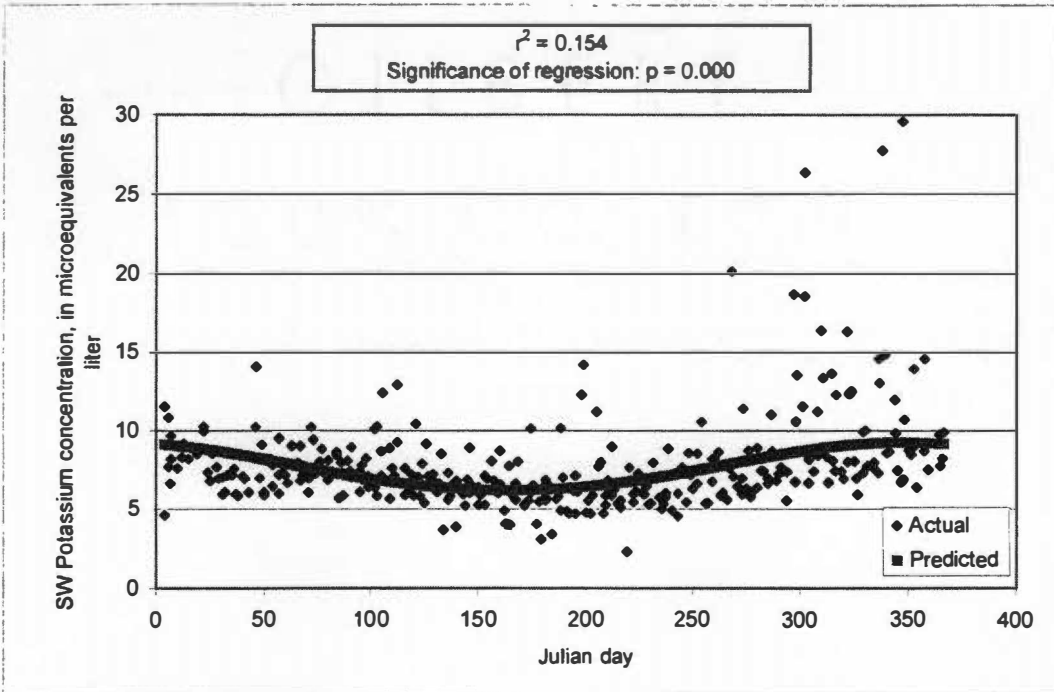


Figure A-3 (continued). Seasonal sine/cosine wave functions for analyte concentrations in the SW stream.

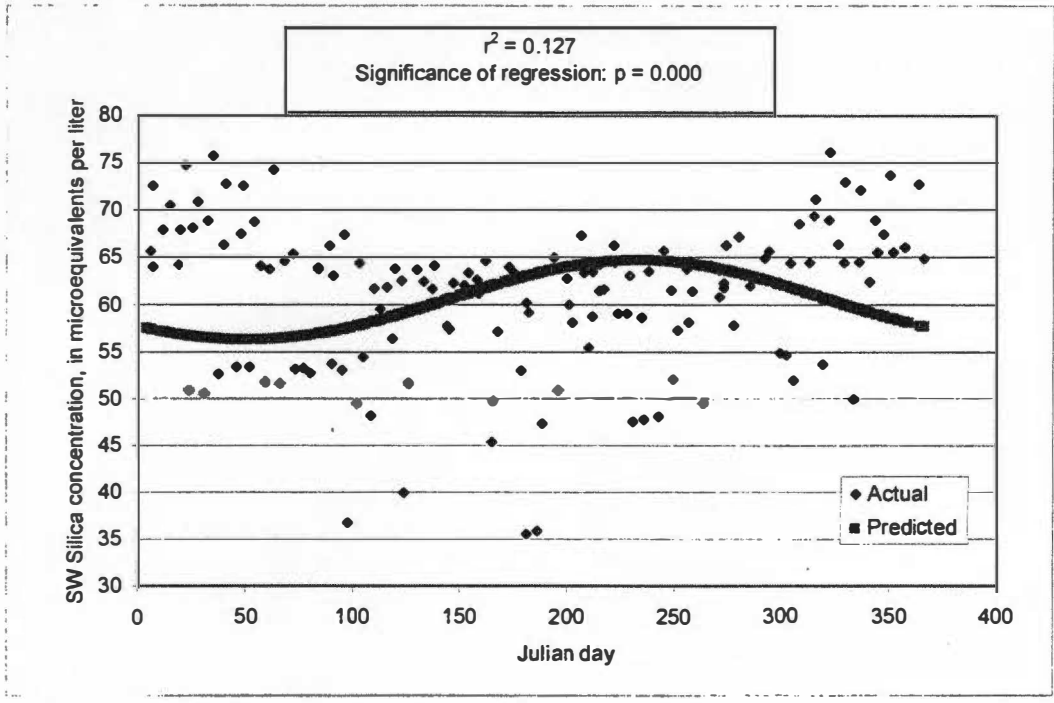


Figure A-3 (continued). Seasonal sine/cosine wave functions for analyte concentrations in the SW stream.

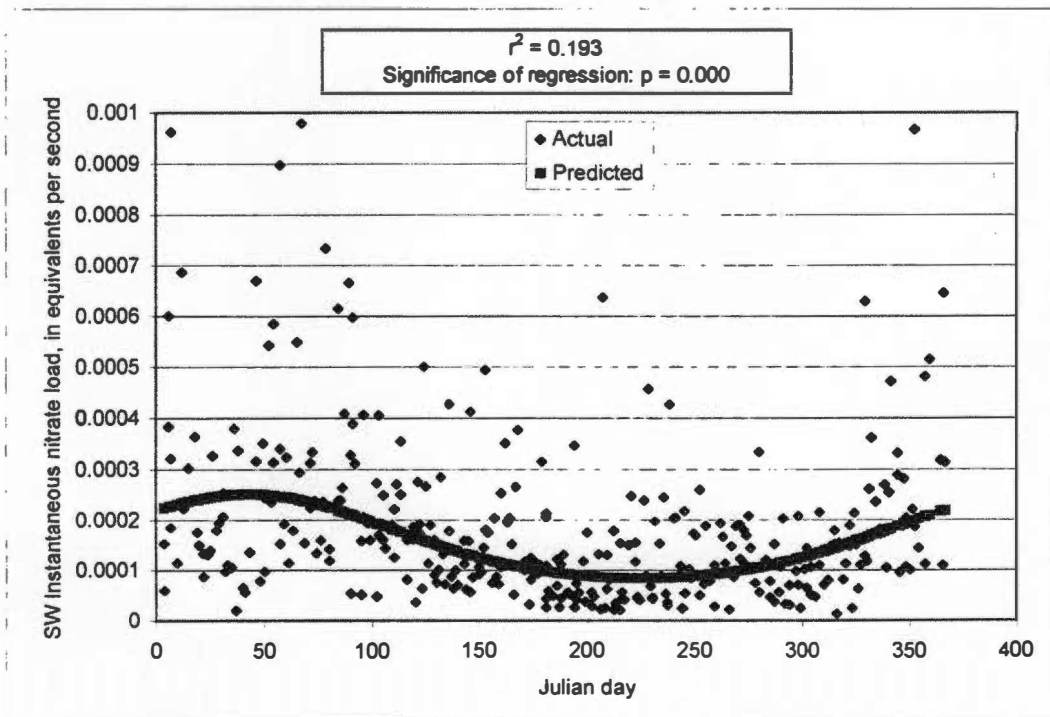
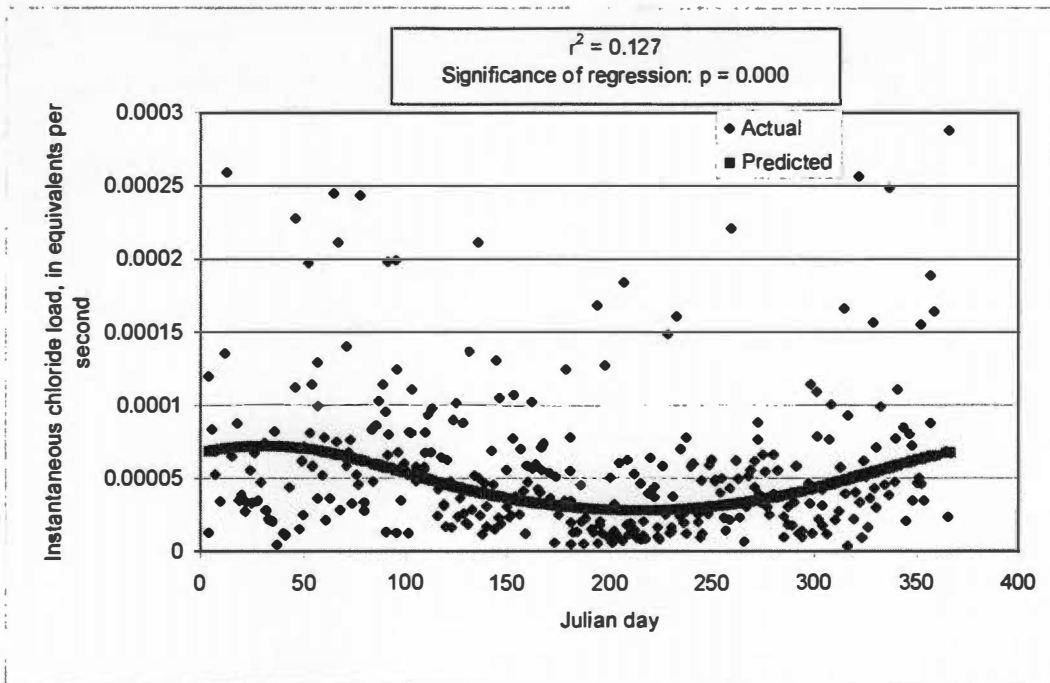


Figure A-4. Seasonal sine/cosine wave functions for analyte instantaneous loads in the SW stream.

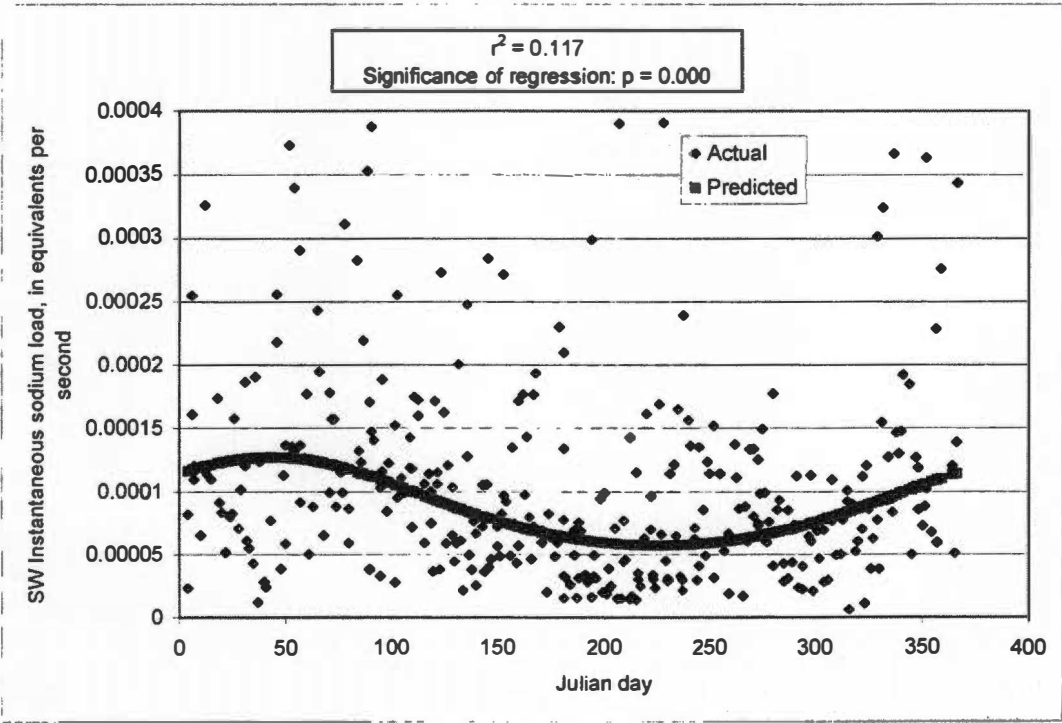
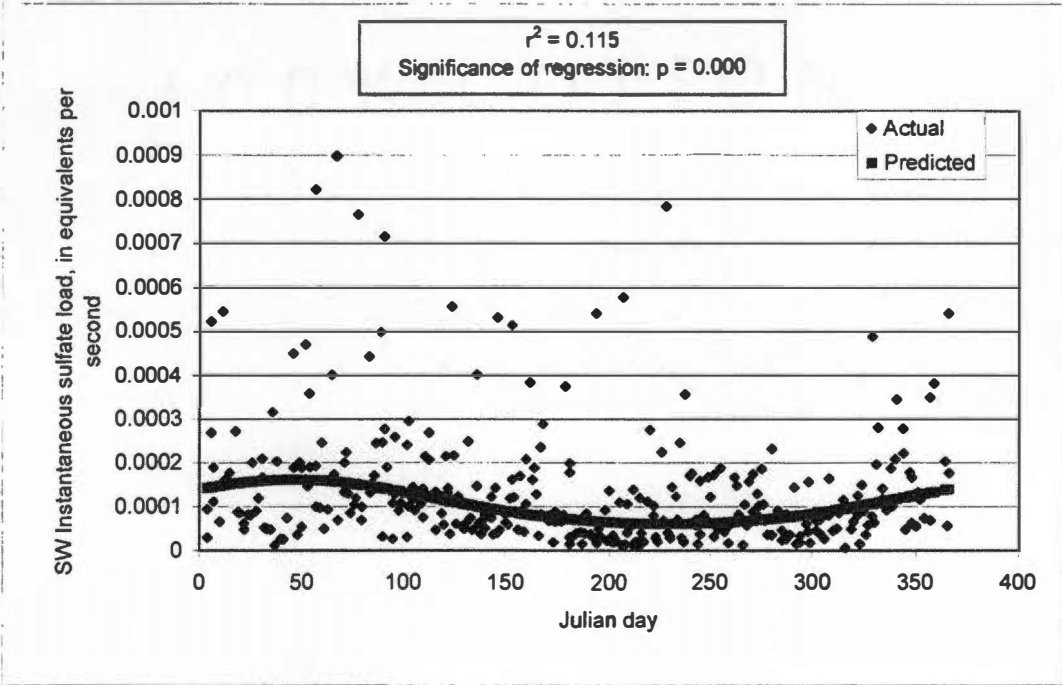


Figure A-4 (continued). Seasonal sine/cosine wave functions for analyte instantaneous loads in the SW stream.

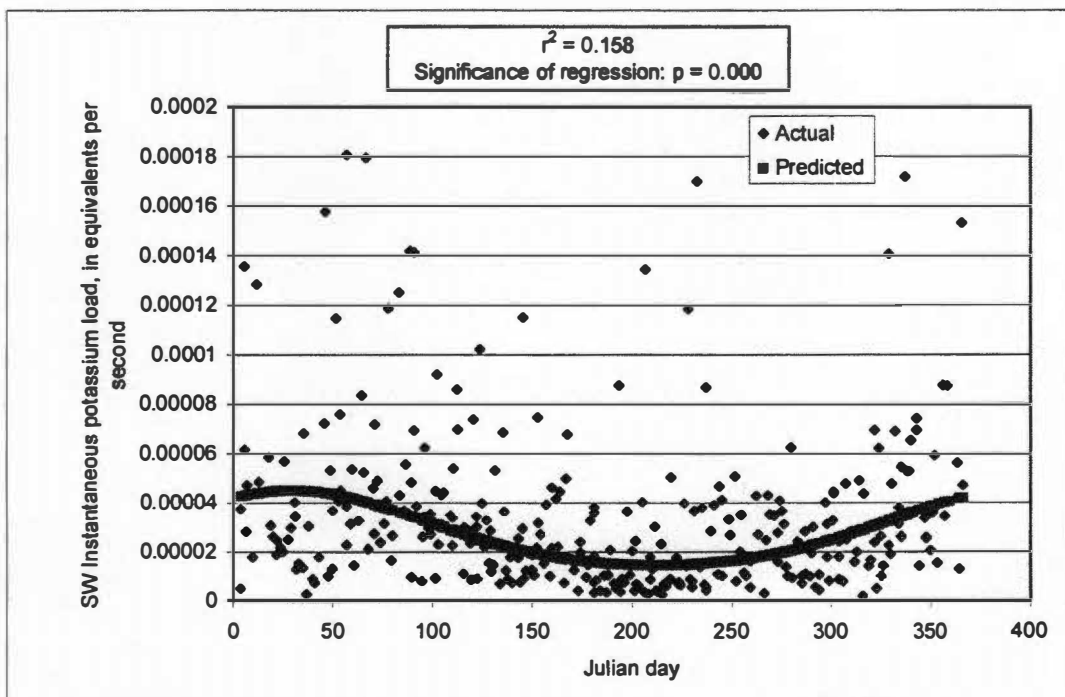
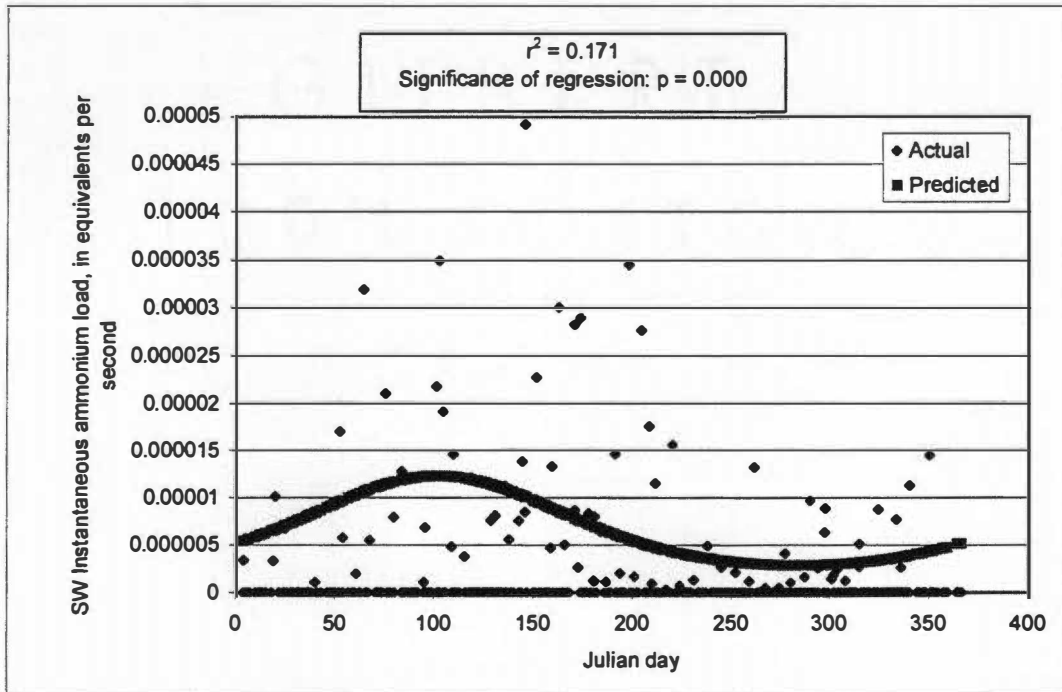


Figure A-4 (continued). Seasonal sine/cosine wave functions for analyte instantaneous loads in the SW stream.

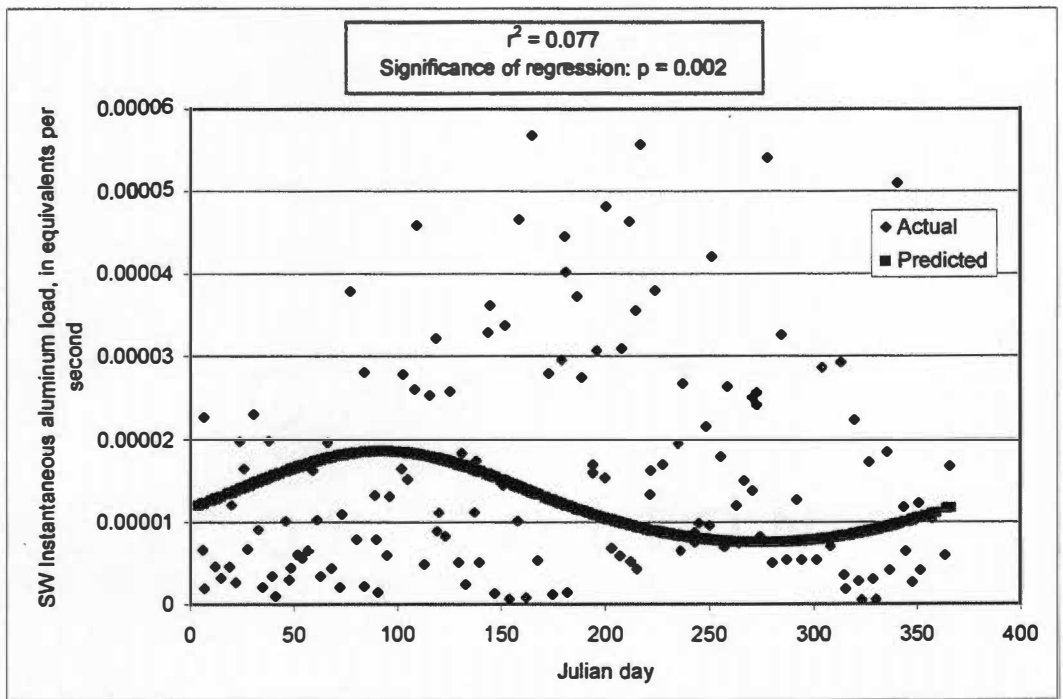
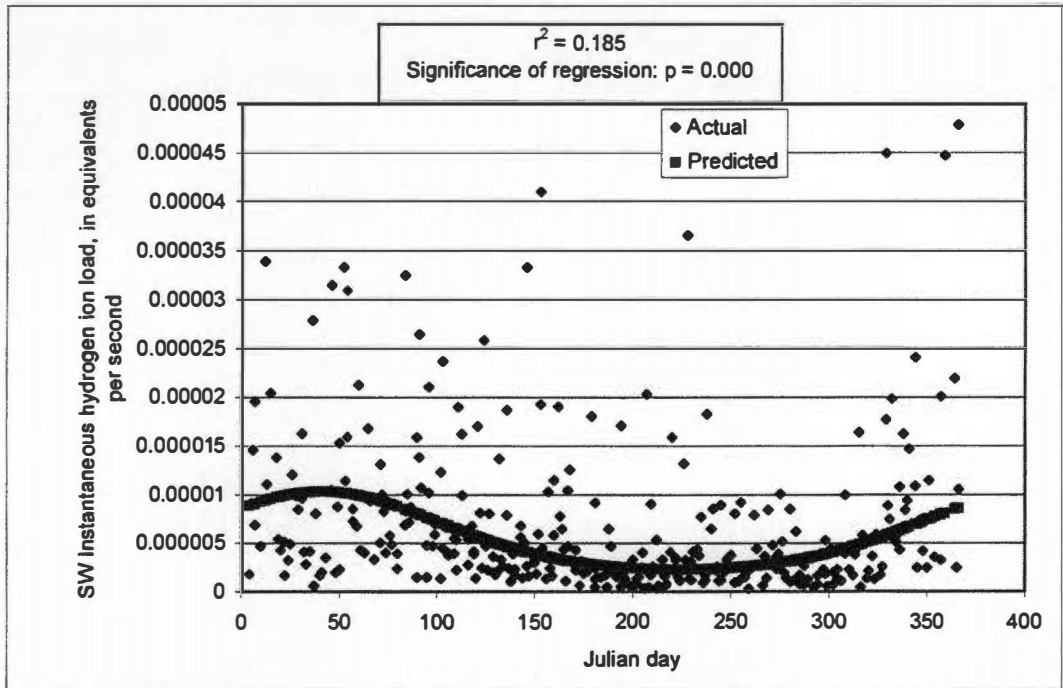


Figure A-4 (continued). Seasonal sine/cosine wave functions for analyte instantaneous loads in the SW stream.

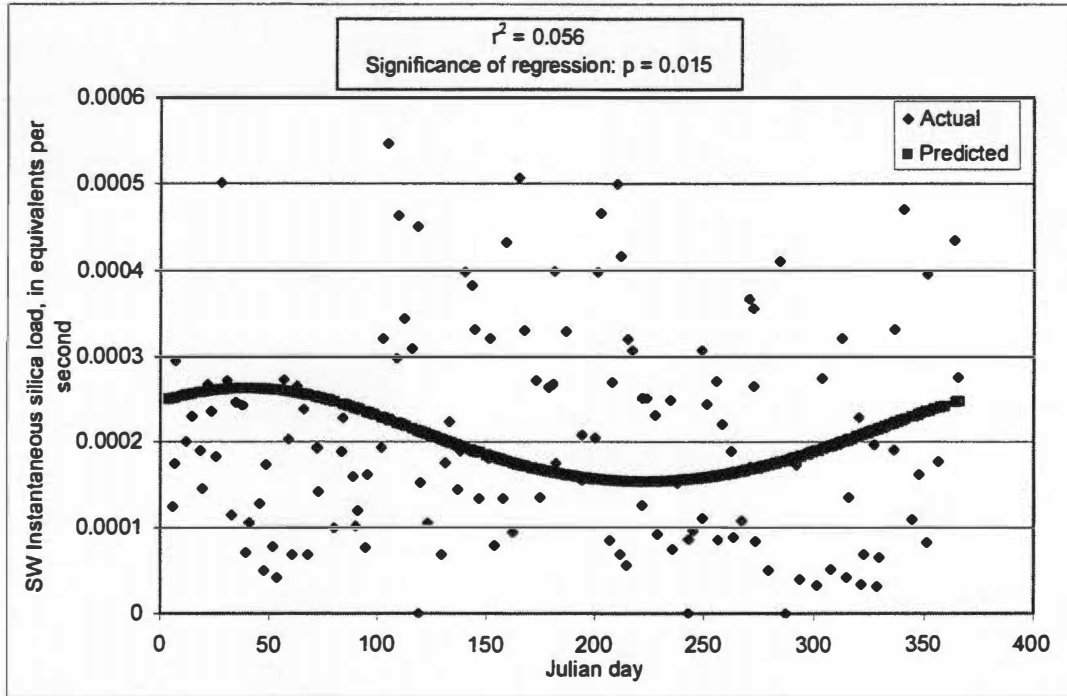
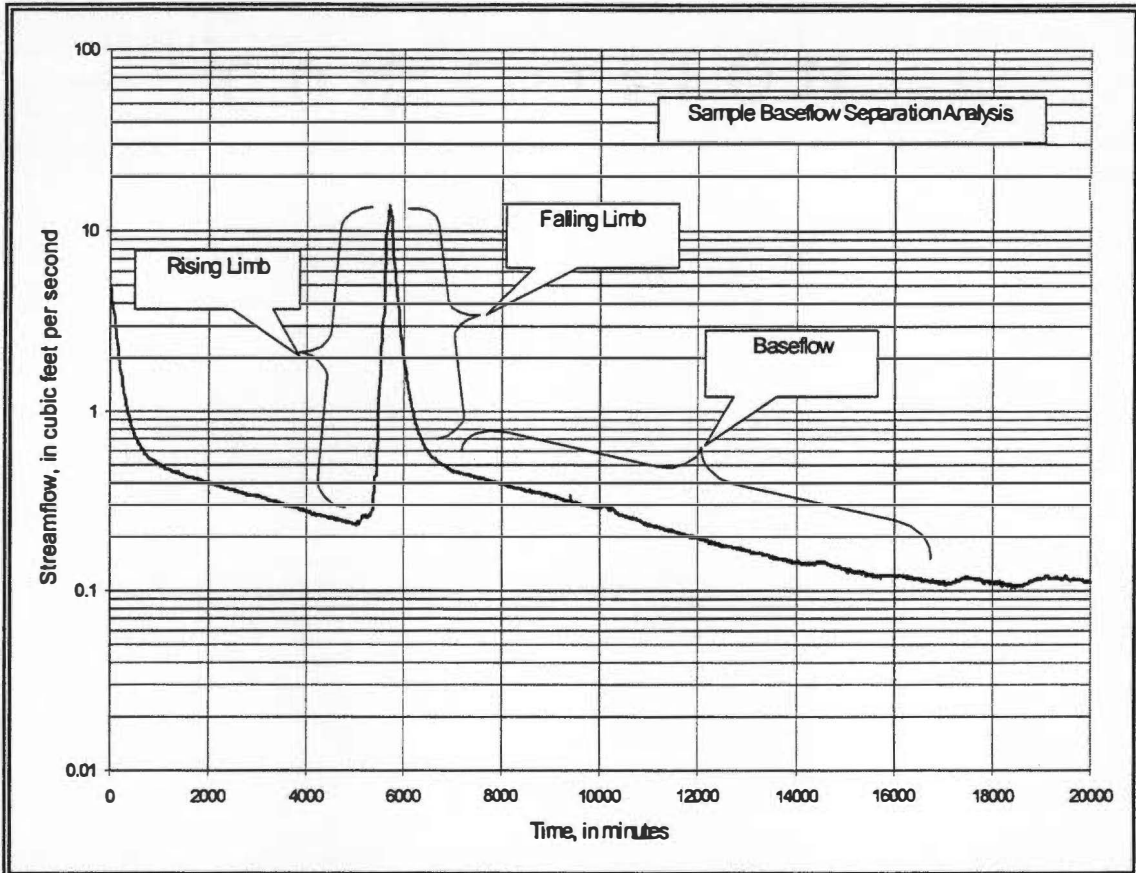


Figure A-4 (continued). Seasonal sine/cosine wave functions for analyte instantaneous loads in the SW stream.



Baseflow Separation Procedure:

1. Plot streamflow (on log scale) versus time (on linear scale).
2. Baseflow component will appear linear, following the falling limb of the hydrograph.
3. Water quality samples are designated "r" if taken on the rising limb of the hydrograph, designated "f" is taken on the falling limb, and designated "b" if taken during baseflow conditions.

Figure A-5. Sample hydrograph and baseflow separation procedure for assigning locations on the hydrograph when weekly samples are taken.

Table A-2. Load regression equations for the SW streamlet, bi-weekly sampling strategy.

| | |
|-------------------|--|
| Chloride: | $\ln(QC) = -11.546 + 2.546E-4 t - 6.755E-2 \sin \theta + 0.157 \cos \theta + 0.926 \ln Q$ |
| De-transformed: | $QC = 9.6747E-6 * e^{2.546E-4 t} * e^{-6.755E-2 \sin \theta} * e^{0.157 \cos \theta} * Q^{0.926}$ |
| | $r^2 = 0.856$ |
| Nitrate: | $\ln(QC) = -8.652 - 7.7E-5 t + 4.861E-2 \sin \theta + 8.653E-2 \cos \theta + 0.925 \ln Q - 0.681 \ln pH$ |
| De-transformed: | $QC = 1.7478E-4 * e^{-7.7E-5 t} * e^{4.861E-2 \sin \theta} * e^{8.653E-2 \cos \theta} * Q^{0.925} * pH^{0.681}$ |
| | $r^2 = 0.985$ |
| Sulfate: | $\ln(QC) = -8.443 - 5.777E-2 \sin \theta - 2.25E-2 \cos \theta + 1.126 \ln Q - 1.219 \ln pH$ |
| De-transformed: | $QC = 2.154E-4 * e^{-5.777E-2 \sin \theta} * e^{-2.25E-2 \cos \theta} * Q^{1.126} * pH^{-1.219}$ |
| | $r^2 = 0.988$ |
| Sodium: | $\ln(QC) = -12.272 + 3.109E-5 t - 2.236E-2 \sin \theta + 3.128E-2 \cos \theta + 0.947 \ln Q + 0.959 \ln pH$ |
| De-transformed: | $QC = 4.681E-6 * e^{3.109E-5 t} * e^{-2.236E-2 \sin \theta} * e^{3.128E-2 \cos \theta} * Q^{0.947} * pH^{0.959}$ |
| | $r^2 = 0.975$ |
| Ammonium: | $\ln(QC) = -13.764 + 7.376E-4 t + 0.618 \sin \theta - 0.291 \cos \theta + 0.668 \ln Q$ |
| De-transformed: | $QC = 1.0529E-6 * e^{7.376E-4 t} * e^{0.618 \sin \theta} * e^{-0.291 \cos \theta} * Q^{0.668}$ |
| | $r^2 = 0.585$ |
| Potassium: | $\ln(QC) = -13.493 - 3.326E-2 \sin \theta + 0.147 \cos \theta + 1.036 \ln Q + 0.633 \ln \text{cond.}$ |
| De-transformed: | $QC = 1.3806E-6 * e^{-3.326E-2 \sin \theta} * e^{0.147 \cos \theta} * Q^{1.036} * \text{cond}^{0.633}$ |
| | $r^2 = 0.924$ |
| H+ ion: | $\ln(QC) = -15.842 + 0.128 \sin \theta + 0.168 \cos \theta + 1.214 \ln Q + 0.836 \ln \text{cond.}$ |
| De-transformed: | $QC = 1.318E-7 * e^{0.128 \sin \theta} * e^{0.168 \cos \theta} * Q^{1.214} * \text{cond}^{0.836}$ |
| | $r^2 = 0.909$ |
| Aluminum: | $\ln(QC) = -8.789 + 1.322E-3 t + 1.05 \ln Q - 2.049 \ln \text{cond}$ |
| De-transformed: | $QC = 1.524E-4 * e^{1.322E-3 t} * Q^{1.05} * \text{cond}^{-2.049}$ |
| | $r^2 = 0.689$ |
| Silica: | $\ln(QC) = -12.114 - 1.614E-4 t + 0.947 \ln Q + 1.486 \ln pH$ |
| De-transformed: | $QC = 5.4822E-6 * e^{-1.614E-4 t} * Q^{0.947} * pH^{1.486}$ |
| | $r^2 = 0.984$ |

Table A-3. Load regression equations for the SW streamlet, tri-weekly sampling strategy.

Chloride: $\ln(QC) = -11.537 + 2.188E-4 t - 8.964E-2 \sin \theta + 0.157 \cos \theta + 0.953 \ln Q$

De-transformed: $QC = 9.7621E-6 * e^{2.188E-4 t} * e^{-8.964E-2 \sin \theta} * e^{0.157 \cos \theta} * Q^{0.953}$

$r^2 = 0.895$

Nitrate: $\ln(QC) = -10.179 - 8.493E-5 t + 6.308E-2 \sin \theta + 0.109 \cos \theta + 0.932 \ln Q + 0.129 \ln \text{cond.}$

De-transformed: $QC = 3.7959E-5 * e^{-8.493E-5 t} * e^{6.308E-2 \sin \theta} * e^{0.109 \cos \theta} * Q^{0.932} * \text{cond}^{0.129}$

$r^2 = 0.988$

Sulfate: $\ln(QC) = -8.851 - 5.632E-2 \sin \theta - 1.203E-2 \cos \theta + 1.136 \ln Q - 0.997 \ln \text{pH}$

De-transformed: $QC = 1.4324E-4 * e^{-5.632E-2 \sin \theta} * e^{-1.203E-2 \cos \theta} * Q^{1.136} * \text{pH}^{-0.997}$

$r^2 = 0.988$

Sodium: $\ln(QC) = -12.7 + 5.29E-5 t - 4.215E-2 \sin \theta + 5.413E-2 \cos \theta + 0.93 \ln Q + 1.196 \ln \text{pH}$

De-transformed: $QC = 3.0511E-6 * e^{5.29E-5 t} * e^{-4.215E-2 \sin \theta} * e^{5.413E-2 \cos \theta} * Q^{0.93} * \text{pH}^{1.196}$

$r^2 = 0.977$

Ammonium: $\ln(QC) = -14.511 + 1.089E-3 t + 0.514 \sin \theta - 0.269 \cos \theta + 0.985 \ln Q$

De-transformed: $QC = 4.9883E-7 * e^{1.089E-3 t} * e^{0.514 \sin \theta} * e^{-0.269 \cos \theta} * Q^{0.985}$

$r^2 = 0.761$

Potassium: $\ln(QC) = -13.087 - 9.084E-2 \sin \theta + 0.13 \cos \theta + 1.032 \ln Q + 0.483 \ln \text{cond.}$

De-transformed: $QC = 2.072E-6 * e^{-9.084E-2 \sin \theta} * e^{0.13 \cos \theta} * Q^{1.032} * \text{cond}^{0.483}$

$r^2 = 0.932$

H+ ion: $\ln(QC) = -15.744 + 8.272E-2 \sin \theta + 0.177 \cos \theta + 1.264 \ln Q + 0.782 \ln \text{cond.}$

De-transformed: $QC = 1.4537E-7 * e^{8.272E-2 \sin \theta} * e^{0.177 \cos \theta} * Q^{1.264} * \text{cond}^{0.782}$

$r^2 = 0.921$

Aluminum: $\ln(QC) = -8.608 + 1.087E-3 t + 1.032 \ln Q - 1.993 \ln \text{cond}$

De-transformed: $QC = 1.8264E-4 * e^{1.087E-3 t} * Q^{1.032} * \text{cond}^{-1.993}$

$r^2 = 0.712$

Silica: $\ln(QC) = -11.855 - 9.667E-5 t + 0.948 \ln Q + 1.3 \ln \text{pH}$

De-transformed: $QC = 7.103E-6 * e^{-9.667E-5 t} * Q^{0.948} * \text{pH}^{1.3}$

$r^2 = 0.984$

Table A-4. Load regression equations for the SW streamlet, monthly sampling strategy.

| | |
|-------------------|--|
| Chloride: | $\ln(QC) = -11.647 + 2.902E-4 t - 7.431E-2 \sin \theta + 0.198 \cos \theta + 0.986 \ln Q$ |
| De-transformed: | $QC = 8.7452E-6 * e^{2.902E-4 t} * e^{-7.431E-2 \sin \theta} * e^{0.198 \cos \theta} * Q^{0.986}$ |
| | $r^2 = 0.905$ |
| Nitrate: | $\ln(QC) = -9.857 - 7.679E-5 t + 4.421E-2 \sin \theta + 0.119 \cos \theta + 0.938 \ln Q$ |
| De-transformed: | $QC = 5.2379E-5 * e^{-7.679E-5 t} * e^{4.421E-2 \sin \theta} * e^{0.119 \cos \theta} * Q^{0.938}$ |
| | $r^2 = 0.984$ |
| Sulfate: | $\ln(QC) = -8.863 + 1.119 \ln Q - 0.970 \ln pH$ |
| De-transformed: | $QC = 1.4153E-4 * Q^{1.119} * pH^{-0.970}$ |
| | $r^2 = 0.985$ |
| Sodium: | $\ln(QC) = -12.421 + 0.963 \ln Q + 1.057 \ln pH$ |
| De-transformed: | $QC = 4.033E-6 * Q^{0.963} * pH^{1.057}$ |
| | $r^2 = 0.975$ |
| Ammonium: | $\ln(QC) = 6.310 + 5.083E-4 t + 0.884 \sin \theta - 0.551 \cos \theta + 0.804 \ln Q - 11.375 \ln pH$ |
| De-transformed: | $QC = 550.0449 * e^{5.083E-4 t} * e^{0.884 \sin \theta} * e^{-0.551 \cos \theta} * Q^{0.804} * pH^{-11.375}$ |
| | $r^2 = 0.834$ |
| Potassium: | $\ln(QC) = -14.267 - 2.888E-2 \sin \theta + 0.141 \cos \theta + 1.05 \ln Q + 0.93 \ln \text{cond.}$ |
| De-transformed: | $QC = 6.3668E-7 * e^{-2.888E-2 \sin \theta} * e^{0.141 \cos \theta} * Q^{1.05} * \text{cond}^{0.93}$ |
| | $r^2 = 0.967$ |
| H+ ion: | $\ln(QC) = -15.211 + 5.3E-2 \sin \theta + 0.161 \cos \theta + 1.229 \ln Q + 0.58 \ln \text{cond.}$ |
| De-transformed: | $QC = 2.4771E-7 * e^{5.3E-2 \sin \theta} * e^{0.161 \cos \theta} * Q^{1.229} * \text{cond}^{0.58}$ |
| | $r^2 = 0.915$ |
| Aluminum: | $\ln(QC) = -6.79 + 1.429E-3 t + 1.209 \ln Q - 2.953 \ln \text{cond}$ |
| De-transformed: | $QC = 1.125E-3 * e^{1.429E-3 t} * Q^{1.209} * \text{cond}^{-2.953}$ |
| | $r^2 = 0.747$ |
| Silica: | $\ln(QC) = -9.53 - 1.164E-4 t - 4.985E-2 \sin \theta - 2.22E-2 \cos \theta + 0.953 \ln Q$ |
| De-transformed: | $QC = 7.264E-5 * e^{-1.164E-4 t} * e^{-4.985E-2 \sin \theta} * e^{-2.22E-2 \cos \theta} * Q^{0.953}$ |
| | $r^2 = 0.984$ |

Table A-5. Concentration regression equations for the SW streamlet, bi-weekly sampling strategy.

| | |
|-------------------|---|
| Chloride: | $\ln C = 2.269 + 2.546E-4 t - 6.755E-2 \sin \theta + 0.157 \cos \theta - 7.404E-2 \ln Q$ De-transformed: $C = 9.6697 * e^{2.546E-4 t} * e^{-6.755E-2 \sin \theta} * e^{0.157 \cos \theta} * Q^{-7.404E-2}$ $r^2 = 0.269$ |
| Nitrate: | $\ln C = 5.164 - 7.7E-5 t + 4.861E-2 \sin \theta + 8.653E-2 \cos \theta - 7.469E-2 \ln Q - 0.681 \ln \text{pH}$ De-transformed: $C = 174.8625 * e^{-7.7E-5 t} * e^{4.861E-2 \sin \theta} * e^{8.653E-2 \cos \theta} * Q^{-7.469E-2} * \text{pH}^{-0.681}$ $r^2 = 0.478$ |
| Sulfate: | $\ln C = 5.372 - 5.777E-2 \sin \theta - 2.25E-2 \cos \theta + 0.126 \ln Q - 1.219 \ln \text{pH}$ De-transformed: $C = 215.293 * e^{-5.777E-2 \sin \theta} * e^{-2.25E-2 \cos \theta} * Q^{0.126} * \text{pH}^{-1.219}$ $r^2 = 0.587$ |
| Sodium: | $\ln C = 1.543 + 3.109E-5 t - 2.2236E-2 \sin \theta + 3.128E-2 \cos \theta - 5.303E-2 \ln Q + 0.959 \ln \text{pH}$ De-transformed: $C = 4.6786 * e^{3.109E-5 t} * e^{-2.236E-2 \sin \theta} * e^{3.128E-2 \cos \theta} * Q^{-5.303E-2} * \text{pH}^{0.959}$ $r^2 = 0.253$ |
| Ammonium: | $\ln C = 5.113E-2 + 7.376E-4 t + 0.618 \sin \theta - 0.291 \cos \theta - 0.332 \ln Q$ De-transformed: $C = 1.0524 * e^{7.376E-4 t} * e^{0.618 \sin \theta} * e^{-0.291 \cos \theta} * Q^{-0.332}$ $r^2 = 0.467$ |
| Potassium: | $\ln C = 0.218 - 1.817E-2 \sin \theta + 0.154 \cos \theta + 0.691 \ln \text{cond.}$ De-transformed: $C = 1.2436 * e^{-1.817E-2 \sin \theta} * e^{0.154 \cos \theta} * \text{cond}^{0.691}$ $r^2 = 0.262$ |
| H+ ion: | $\ln C = -2.026 + 0.128 \sin \theta + 0.168 \cos \theta + 0.214 \ln Q + 0.836 \ln \text{cond.}$ De-transformed: $C = 0.1319 * e^{0.128 \sin \theta} * e^{0.168 \cos \theta} * Q^{0.214} * \text{cond}^{0.836}$ $r^2 = 0.435$ |
| Aluminum: | $\ln C = 4.768 + 1.328E-3 t - 1.927 \ln \text{cond}$ De-transformed: $C = 117.6836 * e^{1.328E-3 t} * \text{cond}^{-1.927}$ $r^2 = 0.334$ |
| Silica: | $\ln C = 1.702 - 1.614E-4 t - 5.267E-2 \ln Q + 1.486 \ln \text{pH}$ De-transformed: $C = 5.4849 * e^{-1.614E-4 t} * Q^{-5.267E-2} * \text{pH}^{1.486}$ $r^2 = 0.467$ |

Table A-6. Concentration regression equations for the SW streamlet, tri-weekly sampling strategy.

| | |
|-------------------|---|
| Chloride: | $\ln C = -0.547 + 2.217E-4 t - 9.138E-2 \sin \theta + 0.180 \cos \theta + 1.569 \ln \text{pH}$ De-transformed: $C = 0.579 * e^{2.217E-4 t} * e^{-9.138E-2 \sin \theta} * e^{0.180 \cos \theta} * \text{pH}^{1.569}$ $r^2 = 0.278$ |
| Nitrate: | $\ln C = 3.637 - 8.493E-5 t + 6.308E-2 \sin \theta + 0.109 \cos \theta - 6.815E-2 \ln Q + 0.129 \ln \text{cond.}$ De-transformed: $C = 37.977 * e^{-8.493E-5 t} * e^{6.308E-2 \sin \theta} * e^{0.109 \cos \theta} * Q^{-6.815E-2} * \text{cond}^{0.129}$ $r^2 = 0.559$ |
| Sulfate: | $\ln C = 4.965 - 5.632E-2 \sin \theta - 1.203E-2 \cos \theta + 0.136 \ln Q - 0.997 \ln \text{pH}$ De-transformed: $C = 143.309 * e^{-5.632E-2 \sin \theta} * e^{-1.203E-2 \cos \theta} * Q^{0.136} * \text{pH}^{-0.997}$ $r^2 = 0.606$ |
| Sodium: | $\ln C = 1.115 + 5.290E-5 t - 4.215E-2 \sin \theta + 5.413E-2 \cos \theta - 7.039E-2 \ln Q + 1.196 \ln \text{pH}$ De-transformed: $C = 3.050 * e^{5.290E-5 t} * e^{-4.215E-2 \sin \theta} * e^{5.413E-2 \cos \theta} * Q^{-7.039E-2} * \text{pH}^{1.196}$ $r^2 = 0.426$ |
| Ammonium: | $\ln C = -0.711 + 1.085E-3 t + 0.516 \sin \theta - 0.275 \cos \theta$ De-transformed: $C = 0.491 * e^{1.085E-3 t} * e^{0.516 \sin \theta} * e^{-0.275 \cos \theta}$ $r^2 = 0.587$ |
| Potassium: | $\ln C = 0.657 - 7.677E-2 \sin \theta + 0.137 \cos \theta + 0.527 \ln \text{cond.}$ De-transformed: $C = 1.929 * e^{-7.677E-2 \sin \theta} * e^{0.137 \cos \theta} * \text{cond}^{0.527}$ $r^2 = 0.247$ |
| H+ ion: | $\ln C = -1.928 + 8.272E-2 \sin \theta + 0.177 \cos \theta + 0.264 \ln Q + 0.782 \ln \text{cond.}$ De-transformed: $C = 0.145 * e^{8.272E-2 \sin \theta} * e^{0.177 \cos \theta} * Q^{0.264} * \text{cond}^{0.782}$ $r^2 = 0.482$ |
| Aluminum: | $\ln C = 5.059 + 1.096E-3 t - 1.923 \ln \text{cond}$ De-transformed: $C = 157.433 * e^{1.096E-3 t} * \text{cond}^{-1.923}$ $r^2 = 0.333$ |
| Silica: | $\ln C = 1.961 - 9.667E-5 t - 5.237E-2 \ln Q + 1.300 \ln \text{pH}$ De-transformed: $C = 7.106 * e^{-9.667E-5 t} * Q^{-5.237E-2} * \text{pH}^{1.300}$ $r^2 = 0.415$ |

Table A-7. Concentration regression equations for the SW streamlet, monthly sampling strategy.

| | |
|-------------------|---|
| Chloride: | $\ln C = 2.153 + 2.895E-4 t - 7.747E-2 \sin \theta + 0.193 \cos \theta$ |
| De-transformed: | $C = 8.611 * e^{2.895E-4 t} * e^{-7.747E-2 \sin \theta} * e^{0.193 \cos \theta}$ |
| | $r^2 = 0.352$ |
| Nitrate: | $\ln C = 3.959 - 7.679E-5 t + 4.421E-2 \sin \theta + 0.119 \cos \theta - 6.214E-2 \ln Q$ |
| De-transformed: | $C = 52.405 * e^{-7.679E-5 t} * e^{4.421E-2 \sin \theta} * e^{0.119 \cos \theta} * Q^{-6.214E-2}$ |
| | $r^2 = 0.469$ |
| Sulfate: | $\ln C = 4.952 + 0.119 \ln Q - 0.970 \ln \text{pH}$ |
| De-transformed: | $C = 141.458 * Q^{0.119} * \text{pH}^{-0.970}$ |
| | $r^2 = 0.516$ |
| Sodium: | $\ln C = 1.394 - 3.711E-2 \ln Q + 1.057 \ln \text{pH}$ |
| De-transformed: | $C = 4.031 * Q^{-3.711E-2} * \text{pH}^{1.057}$ |
| | $r^2 = 0.175$ |
| Ammonium: | $\ln C = 15.472 + 4.942E-4 t + 0.864 \sin \theta - 0.629 \cos \theta - 8.868 \ln \text{pH}$ |
| De-transformed: | $C = 5.240E6 * e^{4.942E-4 t} * e^{0.864 \sin \theta} * e^{-0.629 \cos \theta} * \text{pH}^{-8.868}$ |
| | $r^2 = 0.721$ |
| Potassium: | $\ln C = -0.451 - 2.888E-2 \sin \theta + 0.141 \cos \theta + 4.987E-2 \ln Q + 0.930 \ln \text{cond.}$ |
| De-transformed: | $C = 0.637 * e^{-2.888E-2 \sin \theta} * e^{0.141 \cos \theta} * Q^{4.987E-2} * \text{cond}^{0.930}$ |
| | $r^2 = 0.540$ |
| H+ ion: | $\ln C = -1.396 + 0.053 \sin \theta + 0.161 \cos \theta + 0.229 \ln Q + 0.580 \ln \text{cond.}$ |
| De-transformed: | $C = 0.248 * e^{0.053 \sin \theta} * e^{0.161 \cos \theta} * Q^{0.229} * \text{cond}^{0.580}$ |
| | $r^2 = 0.412$ |
| Aluminum: | $\ln C = 6.460 + 1.447E-3 t - 2.640 \ln \text{cond}$ |
| De-transformed: | $C = 639.061 * e^{1.447E-3 t} * \text{cond}^{-2.640}$ |
| | $r^2 = 0.384$ |
| Silica: | $\ln C = 4.286 - 1.164E-4 t - 4.985E-2 \sin \theta - 2.220E-2 \cos \theta - 4.668E-2 \ln Q$ |
| De-transformed: | $C = 72.675 * e^{-1.164E-4 t} * e^{-4.985E-2 \sin \theta} * e^{-2.22E-2 \cos \theta} * Q^{-4.668E-2}$ |
| | $r^2 = 0.346$ |

VITA

Molly S. McCann was born in Nashville, Tennessee on April 14, 1975. She was raised in Mount Juliet, Tennessee, where she graduated with honors from Mount Juliet High School in May, 1993. She then entered the University of Tennessee, Knoxville, to study Civil Engineering. During fall 1996 and spring 1997, she spent a year abroad, traveling extensively through Chilean Patagonia with the National Outdoor Leadership School and then attending the Royal Melbourne Institute of Technology in Melbourne, Australia. She returned to the University of Tennessee, Knoxville, and graduated with a Bachelor of Science degree in Civil Engineering (summa cum laude) with a minor in Spanish in December, 1998. She then entered the graduate program in Environmental Engineering at the University of Tennessee, Knoxville, and received her Master of Science degree in August, 2000.